University of Cincinnati

Date: 9/20/2021

I, Rand Issa Talib, hereby submit this original work as part of the requirements for the degree of Doctor of Philosophy in Civil Engineering.

It is entitled:

Novel Integrated Modeling and Optimization Technique for Better Commercial Buildings HVAC Systems Operation

Student's name: **Rand Issa Talib**

This work and its defense approved by:

Committee chair: Nabil Nassif

Committee member: Hazem Elzarka, Ph.D.

Committee member: Raj Manglik, Ph.D.

Committee member: Munir Nazzal, Ph.D.

Committee member: Amanda Webb, Ph.D.

UNIVERSITY OF Cincinnati

40499

Novel Integrated Modeling and Optimization Technique for Better Commercial Buildings HVAC Systems Operation

A Dissertation Submitted to the Graduate School of
the University of Cincinnati

In Partial Fulfillment of the Requirement for the Degree of
DOCTOR OF PHILOSOPHY
in Civil Engineering

in the Department of Civil and Architectural Engineering and
Construction Management, College of Engineering and Applied Science

by
Rand Issa Talib

2021

Committee Chair: Dr. Nabil Nassif

Committee Member: Dr. Hazem Elzarka
Committee Member: Dr. Raj M. Manglik
Committee Member: Dr. Amanda Webb
Committee Member: Dr. Munir D. Nazzal

Abstract

The primary energy sources in commercial buildings are electricity that accounts for 61%, followed by 32% for natural gas. According to EIA, the heating, ventilation, and air condition systems account for about 25% of the total commercial building's energy use in the US. Therefore, advanced modeling and optimization methods of the system components and operation offer great ways to reduce energy consumption.

Since HVAC systems modeling is a characteristic and challenging process thus, while developing an HVAC system and component model, close attention should be given to the accuracy of the model structure, model parameters, and constraints. So, the final selected model can accurately deal with constraints, uncertainties, control the time-varying applications and handle a broad range of operating conditions.

Also, the use of the optimization process to automate selecting the best model structure is crucial. Because every component is different, we cannot propose one model to fit that specified component in all systems. Choosing the best model structure is a time-consuming process. Here comes the optimization process role in automating the process of selecting the optimal model structure for each application.

This research will introduce an innovative method of modeling and optimizing HVAC system operation to reduce the total energy consumption while improving the indoor thermal comfort level. The data-driven two-level optimization technique introduced in this research will utilize the use of real system performance data collected from the building automation systems (BAS) to create accurate component modeling and optimization process as the first level of optimization (MLO). Accurate component modeling techniques are crucial for the results accuracy of the process of optimization the HVAC systems performance. Lastly, artificial neural network (ANN) was chosen as the component modeling tool.

The second level of optimization utilizes the whole system-level optimization (SLO). Genetic algorithm was selected as the optimization learning algorithm. Later, the two optimization levels will be integrated together to optimize the HVAC system operation.

The proposed two-levels optimization technique has contributed to the field of modeling and optimization of HVAC systems through several new contributions.

- Optimize multiple system setpoints. The system setpoints that will be optimized are the supply air temperature (T_s), duct static pressure (P_s), minimum zone airflow rates (Q_z), and minimum outdoor air ventilation rate (Q_v).
- Implement the demand control methodology with the optimization process to modify the electricity consumption power profile when the demand response signal is received.
- Implement the occupancy schedule inputs into the optimization process to account for the number of occupants and optimize the zone level ventilation ratio.
- Implement the real-time zones occupancy sensor readings. This approach will crucially affect the zones' ventilation flow rates and zones minimum flowrates.
- Lastly, implement the method of zone minimum airflow rates setpoint rests. This method will balance between ventilation requirements and reheat energy consumption.

The proposed optimization process was tested and validated, and savings were calculated. This research has validated the use of the proposed optimization technique in improving the energy efficiency of exciting systems.

Dedication

I dedicate this to my little boy, Rayan, for all these times you woke up in the middle of the night looking for Mommy, as I was still up working on this dissertation and asked if I wanted some water while offering your little sippy cup to comfort me. You always said to me, “Mommy, you can do this!.” This is for you, baby boy. Without your unconditional love, none of this would have been possible.

I also dedicate this paper to my Mom and Dad, my dear husband, Ali, and my brother Samer, for your continued emotional support and for always believing in me to achieve my goal through the darkest moments.

Acknowledgment

I would like to express my sincere gratitude to my advisor in my master's and Ph.D. degrees, Dr. Nabil Nassif. He invested his time in me, believed in my potentials, gave me his educational and financial support. I consider myself lucky to have him as my advisor. He guided me from my first steps in understanding the HVAC system until this point. In addition, he taught me everything I know about research work. This work would have never been possible without his knowledge, patience, constant review, and guidance.

I would like to thank my committee members, Dr. Raj M. Manglik, Dr. Hazem Elzarka, Dr. Munir D. Nazzal, and Dr. Amanda Webb, for giving me their time and expertise to improve my work.

A special thank you to Dr. Amanda Webb, who has invested lots of hours to improve my writing skills and research structure. She has been one of the most challenging yet most kind professors I ever had. She always empowered me as a woman in engineering and saw the potential in me. She left a mark on my path, and I learned a lot from her work ethic. I thank her for all her genuine contributions to my work and me as a person.

I also want to thank the University of Cincinnati, civil and architectural engineering department for their financial support. Without that, I would not be able to achieve the honor of obtaining a Ph.D. in civil engineering.

I would also like to thank my family and friends for their unconditional love and support at all times.

Contents

List of Figures

List of Tables

List of Symbols

Symbols	Description	Units
ΔT	temperature difference	F^o
A	Area	ft^2
C°	Celsius	C°
CFM	Cubic feet per minute	cfm
CH_{vlv}	Chilled water valve position	_
Cp	Specific heat of air	Btu/lb. F°
E_v	system efficiency	_
FPM	Foot per minute	fpm
Fs	Fan speed	fpm
ft^3	cubic feet	ft^3
H	Enthalpy	Btu
Hr	Hour	hr
in. w.g	inch of water gage	in. w.g
ma	Dry air mass flow rate	lb/h
^oF	Fahrenheit	^oF
P	Power	kWh
P_s	Duct static pressure	in.w.g
PSI	Pounds per square inch	Psi
q_l	Latent load	Btu/h
Q_o	Outside airflow rate	CFM
q_s	Sensible load	Btu/h

Q_{sys}	System airflow rate	CFM
q_t	Total load	Btu/h
Q_v	Ventilation airflow rate	CFM
RH%	Relative humidity	%
S	Seconds	s
T	Temperature	F^o
T_{cW}	Chilled water temperature	F^o
T_{cWm}	Chilled water mixed temperature	F^o
T_{cWr}	Chilled water return temperature	F^o
T_{cWs}	Chilled water supply temperature	F^o
T_{hW}	Hot water temperature	F^o
T_{hWm}	Hot water mixed temperature	F^o
T_{hWr}	Hot water return temperature	F^o
T_{hWs}	Hot water supply temperature	F^o
T_m	Mixed air temperature	F^o
T_o	Outside air temperature	F^o
T_r	Return air temperature	F^o
T_s	Supply air temperature	F^o
T_z	Zone temperature	F^o
V	Specific volume	ft^3 /lb
VLV	Valve	_
W	humidity ratio of moist air	lb(water)/lb(dry air)
W_m	Mixed air humidity ratio	_

W_r	Return air humidity ratio	_
W_s	Supply air humidity ratio	_

List of Abbreviations and Definitions

AHU	- Air Handling Unit
ANN	- Artificial Neural Network
ASHRAE	- American Society of Heating Refrigeration and Air Conditioning Engineers
AVG	- Average
BAS	- Building Automation System
BSA	- Bootstrap Aggregation
BTU	- British Thermal Unit
CV%	- coefficient of variation
DC	- Demand Control
DOE	- Department of Energy
DS	- Demand Signal
DX	- Direct Expansion
EIA	- Energy Information Administration
GA	- Genetic algorithm
HVAC	- Heating, Ventilation and Air Conditioning
IAQP	- Indoor Air Quality Procedure
IBP	- Incentive-based programs
Max	- Maximum
Min	- Minimum
MLO	- Model Level Optimization Process
MSE	- Mean square error
OA	- Outside Air

OAT - Outside Air Temperature

PBP -price-based programs

R^2 - Coefficient of determination

SLO - System Level Optimization Process

SVM - Support Vector Machine

VAV - Variable Air Volume

Chapter 1

Introduction

1.1 Background

In 2017, about 39% (or about 38 quadrillion British thermal units) of total US energy consumption was consumed by the residential and commercial sectors, according to EIA (EIA, 2017). It was found that in 2012 the space heating consumes most of the commercial buildings' overall energy (EIA, 2017). The advanced global revenue will also grow from $7.0 billion in 2014 to $12.7 billion in 2023. Besides the electricity prices that are rapidly increasing and the increasing cost of operating the HVAC systems in the buildings, the buildings are responsible for 44.6% of the total CO_2 emissions, which is the most considerable portion compared to 34.3% for transportation and 21.1% for the industry sector. Thus, the need for a better operation mechanism of those existing systems becomes more crucial (Talib et al., 2018). HVAC systems are heating ventilation and air conditioning systems responsible for heating and cooling the space and ventilation to maintain the inhabitant's comfort levels. HVAC systems are complex nonlinear systems that have different variables as the parameters of that systems. Many studies have been done to fully understand those systems and reduce their energy (ASHRAE, 2011). Even though the HVAC systems operate using the same thermodynamics principles, they still have different applications depending on the building type.

Chilled water HVAC systems are one of the most popular HVAC systems. They are sized for numerous building types where careful consideration must be taken in the design process. They are widely used in commercial, industrial, and institutional applications. And they come in all shapes, sizes, and patterns. They are responsible for cooling the water as well as the process of dehumidification. The chilled water system is one of the most widely used systems in the United States commercial buildings. Figure 1 below shows a typical chilled water system.

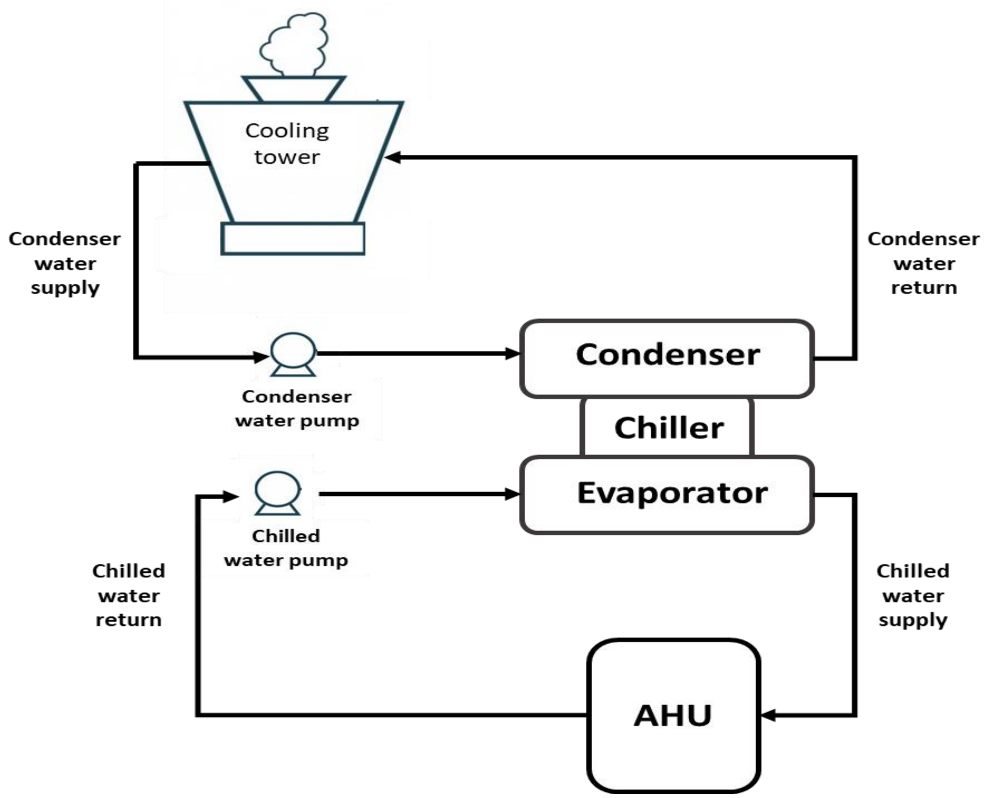

Figure 1. Schematic of a chilled water system.

The chilled water systems consist of the waterside as well as the airside. The chilled water systems' waterside consists of the cooling tower, the chiller, pumps, pipes, and valves. The waterside is responsible for cooling the water and send it to the airside. Simultaneously, the airside that is used to condition and circulate the air is represented by the Air Handling Unit (AHU). The AHU usually consists of the cooling and heating coil, fans/ blowers, dampers, and filters. The AHU can be located outside the building on the ground or roof, inside the attics, mechanical rooms, etc.

Another popular HVAC system popularly used in commercial buildings in the US is the packaged direct expansion system (DX). Those systems are responsible for about 0.74 quads or 54% of the cooling primary energy consumption for commercial buildings and are used to cool nearly half of all commercial spaces (Wiley and Sons, 2016). A Dx system consists of two central devices. The condenser is located outdoor, and the evaporator is located indoors. A conduit connects the two for refrigerant lines and wiring. The spilt systems can include one condenser connected to multiple evaporator units to serve single or multiple zones under the same or different environmental conditions (Seyam, S, 2018). Figure 2 shows a typical DX system schematic.

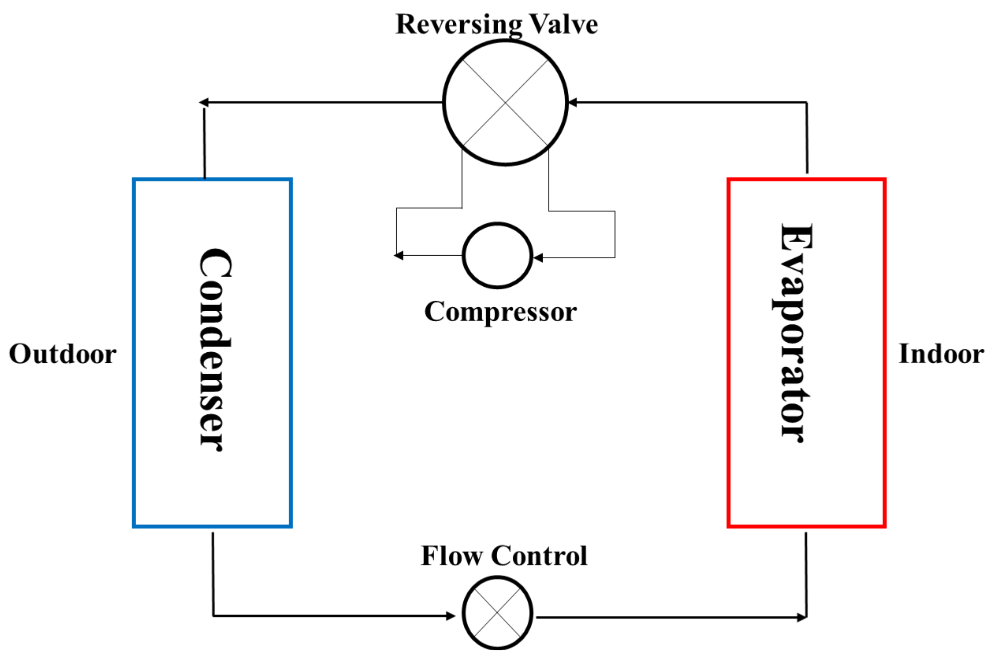

Figure 2. Schematic showing the layout of a typical split DX system.

Since HVAC systems are a complex structure that consists of heat and mass transfer equipment, they also consist of sensors and controllers that control several system variables. Those variables are supply air temperature, supply air fan speed, duct static pressure, chilled water valve position, and chilled water temperature. Thus, to predict the energy consumed by those systems, we need to measure and model the system's components from either measured data or from the knowledge of previous physical laws and methods (Afram et al., 2014).

Nowadays, many resources show the process of designing the HVAC systems, especially the chilled water systems for new buildings. (Bell et al., 2016, Olama A., 2017, Stanford et al., 2011:2012, Khazaii et al., 2014, and Janis et al., 2014). Are some of the books that are available now with dedicated chapters for the chilled water design. Those chapters specify the equation, data, and rule of thumb methods with all the minimum and maximum values for the design process. All those methods and equations can be used in the design process. This process is called a "physical model" or a "forward model" to design the HVAC system in newly constructed buildings.

Forward models are based on engineering principles and usually required detailed physical information. However, using physical models in actual system operations requires detailed physical information that may not always be available. In addition, it requires longer time to complete the calculations that may exceed the optimization period. Therefore, the forward physical models are rarely used for the applications such as real-time building energy system operations.

On the other hand, the "data-based models" do not need any information on the system. They can simply be used for such real-time applications as real-time performance data are available in most modern building automation systems BASs. Therefore, data-enabled model-based techniques may be the most effective way to achieve optimally secured and demand flexible building energy system operations (Afram et al., 2015 and Nassif et al., 2018).

Today, modeling and simulation are recognized techniques for solving energy consumption and cost issues in several engineering fields. For example, machine learning techniques were used as tools to predict the performance of HVAC systems. One of the machine learning tools that are widely used nowadays is ANN (artificial neural networks). The current search for new models of computing using neural networks is motivated by our desire to solve natural, intelligent tasks by taking advantage of computer technology developments. Artificial Neural Networks (ANNs) are nonlinear mapping structures based on the human brain's principal functions. They are potent tools for modeling, especially when a given data's mathematical relationship is unknown or not easily discerned. Over the years, they have become the focus of attention, mainly due to their wide range of applicability and the ease of working with complicated problems. Since McCulloch and Pitts' first neural model, hundreds of different models were developed that are considered ANNs (McCulloch and Pitts 1943).

While another popularly used modeling technique called support vector machine (SVM) was also used to model HVAC systems' performance for multiple purposes. SVM is one of the methods that use supervised learning used for classification and clustering purposes. In general, SVM is also extended to solve regression problems and thus support vector regression. A study conducted by (Liang et al., 2007) presented a model-based fault detection and diagnosis method using SVM. It was found that this method can help reduce the energy consumption of the system and the maintenance cost. Moreover, maintain the health of the HVAC systems.

However, multiple data-based models have been developed and are now published. Thus, an optimization process must be implemented to choose the best model and select between several models to reduce energy consumption. Optimization is a process in mathematics that is used to maximize and minimize a specific function. One of the most popular optimization methods is the genetic algorithm (GA). GA is an optimization technique that is based on the theory of natural selection. This process simply means considering a set of solutions to a problem and selecting the best fitting solution. GA is implemented to minimize the cost and maximize efficiency (Arabali et al., 2013). Previous studies proved GA to be an efficient tool for optimizing the HVAC modeling process when implemented on a whole system and component levels. GA can provide up to 11% of cooling energy savings. This value may vary depending on the systems and building type, location, use, and current control methods (Nassif, 2014).

From this background, the overall idea of modeling, simulation, and optimization of HVAC was discussed. It is clear that there have been lots of efforts in the field of modeling and optimizing HVAC systems to reduce the energy consumed by those systems. There have been numerous data-driven models and techniques designed to predict the performance of the HVAC component and attempts to optimize its performance. However, there have been some shortcomings that are associated with the previous studies. Some of those shortcomings are that the models were developed on assumptions and metrics that needed to be justified. Some of the modeling techniques used need to be further discussed and justify selecting this modeling technique and not others. Some of those studies can also be marked incomplete because they focused on few aspects of the systems and not the whole system level, affecting the results' accuracy since the HVAC systems are integrated entities. Moreover, some of those models are not flexible enough to be used in other HVAC systems other than those specified.

Therefore, the use of the optimization process to automate selecting the best model structure became crucial. Because every component is different, we cannot propose one model to fit that specified component in all systems. Choosing the best model structure is a time-consuming process. Here comes the optimization process role in automating the process of selecting the optimal model structure for each application.

Thus, in this research, the gap in previous studies will be discussed and addressed. Moreover, an overall integrated system-level performance modeling and optimization technique will be proposed.

1.2 Objective

This research aims to develop a new integrated data-driven modeling and optimization technique for better building HVAC efficiency. This goal will be achieved through three main objectives that will address the primary goal by serving as pieces of the whole picture of an integrated, optimized system.

1. Selecting the best modeling tool from multiple proposed ones
2. Create an accurate modeling and optimization technique to accurately predict the performance of the HVAC system components. This is the first level of optimization (MLO). The MLO process consists of two calculations loops. The inner loop is used for the model parameter tuning and another outer loop for the proposed optimization process, as shown in figure 3.

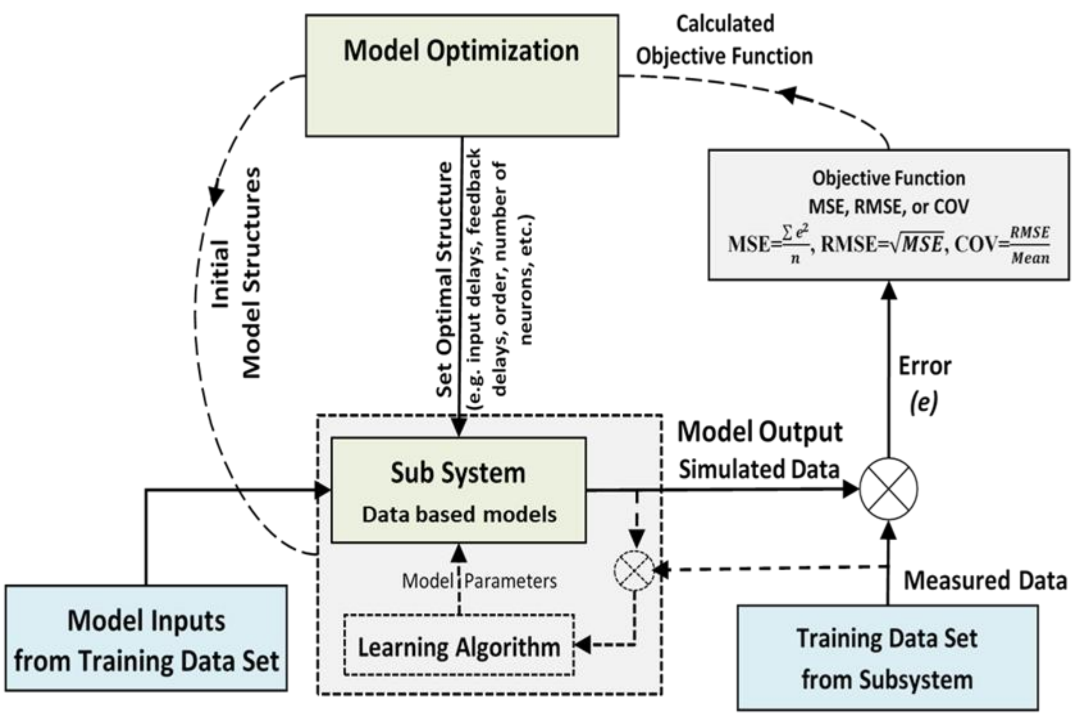

Figure 3. Schematic of the proposed component model optimization process

A typical learning algorithm was used in the inner loop where the model's parameters are tuned. For this purpose, artificial neural networks were selected. And the variables that were adjusted in the process are (1) input time delays, (2) feedback time delays, and (3) the number of neurons (hidden layer size). At the same time, the model parameters are the weight and bias. The tuning of the parameters will be completed on the whole testing data set.

The outer loop is the proposed calculation to determine the optimal model structure. A high-level optimization will be performed in this loop to select the best model structure that produces the minimum error values in model prediction. This process will not replace the typical learning algorithm. Instead, it will automate the process to deliver more accurate predictions with lower processing time.

3. Propose an integrated two levels optimization technique for better HVAC system performance. The process will include integrating the first level of optimization (MLO) and the second level of optimization, a whole system performance optimization (SLO). The proposed optimization technique will reduce the systems' energy consumption while improving the thermal comfort levels of the zones. The optimization tool that was selected to achieve this goal is the genetic algorithm (GA). Figure 4 below shows a schematic for the proposed integrated whole system model optimization process.

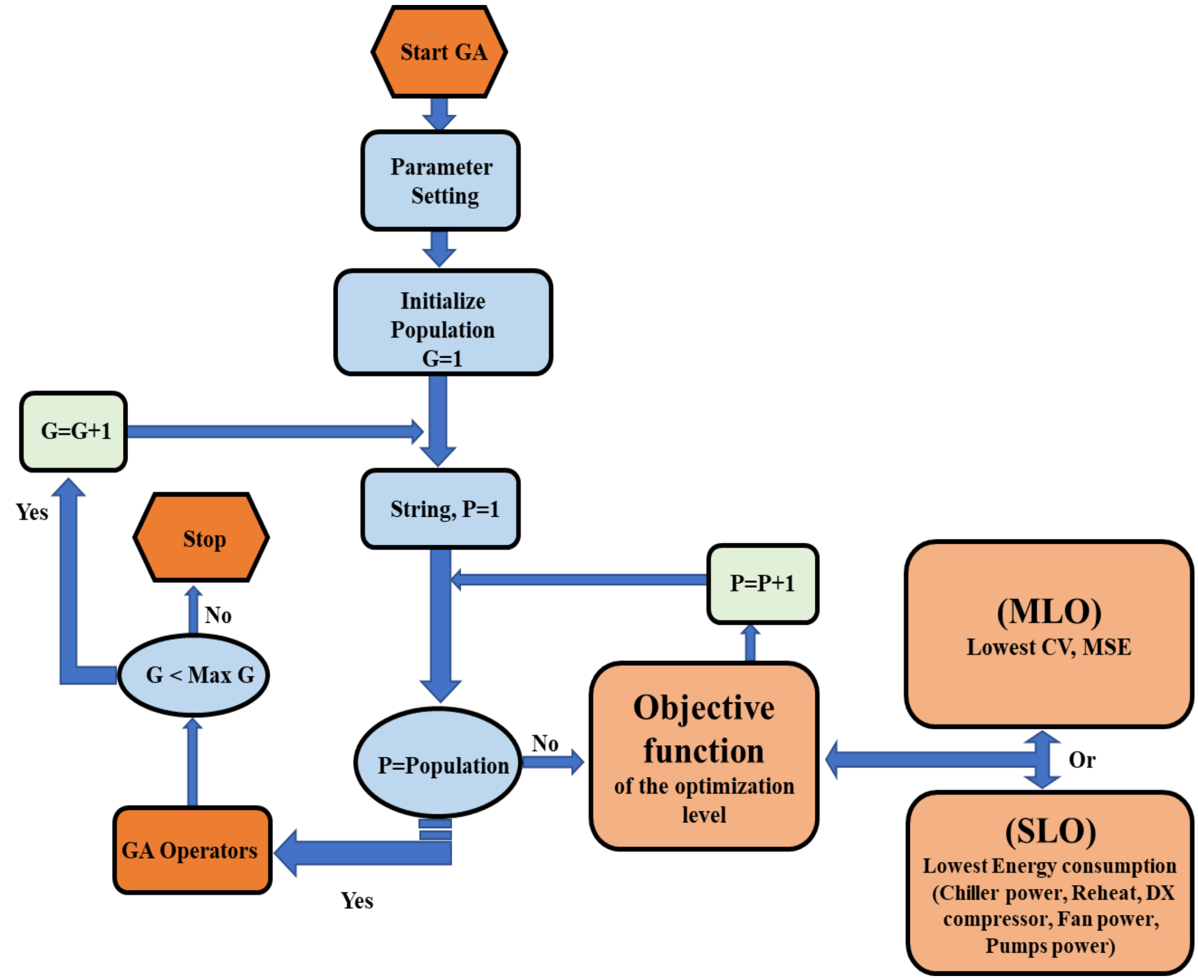

Figure 4. A schematic of the integrated optimization process.

1.3 Research gap

This section will discuss the gaps in previous studies that need to be addressed or better examined.

1.3.1 Using rule-based control strategies (engineering physical-based data) vs. model-based approaches (actual performance and simulation data)

Modeling and simulation of building system performance have a significant impact on energy savings. One drawback of component performance predictions that are being used now is using physical-based estimated data. Estimated data does not correctly evaluate the component performance because it does not account for many factors like building occupants. Therefore, using actual performance data or simulation data for component modeling approaches will give more accurate results. It will account for occupant behavior, operational inefficiencies, and interactive effects that are difficult or costly to account for in building energy models (Mathew et al., 2015).

A study compared the design stage estimated data vs. the building's actual performance using NBI's (new buildings institute) database of LEED-certified buildings. The study has found that measured EUIs for 50% of the buildings deviated by about 25% from the projected performance, with 30% significantly better and 25% significantly worse (Turner et al., 2008)

The simulated data or actual performance data can be used to develop data-driven algorithms that can be used for more accurate and flexible predictions than the physical model's estimation data. Most of the buildings are now equipped with BAS (building automation system) to provide us with an outstanding amount of actual building operation data (Xiao et al., 2014). However, most of the researchers do not use those data for modeling systems' energy consumption. Instead, they tend to use estimation data based on physical models and estimations, resulting in less accurate models. Therefore, this research will focus on using existing building data to create accurate data-driven models instead of using the rule method of operation (Sequences of Operation for HVAC System) stated by ASHRAE guideline 36 (ASHRAE 36, 2018).

1.3.2 Accuracy of data-driven models and optimization technique significance

An adequately identified model can provide accurate or close to accurate results and, at the same time, may require minimum calculations time (Afroz et al., 2018). Therefore, creating an accurate model through accurately identifying their parameters became crucial. Parameter identification, influenced by input data, excitation signals, and model structure, is essential in system identification accuracy and efficiency (Agbi et al., 2012). Even though parametric testing methods are crucial to determine the system order, there is still a lack of a methodical approach for the model structure selection, order determination, and parameter identification (Li et al., 2014). Most existing studies nowadays use the trial-and-error approach to decide on the model structure, order, and parameters (Afroz et al., 2018). While the HVAC system, like many other types of process controls in certain features like nonlinearity, time-dependent, time-varying system dynamics, insufficient data, complex interactions between the components, and limited supervisory controls. Therefore, the HVAC system's modeling is a very characteristic challenging process (Afram et al., 2014). Thus, developing models that can accurately deal with constraints, and uncertainties, control the time-varying applications and time delays, and handle a broad range of operating conditions became crucial.

As previously stated, the HVAC components are complex nonlinear components. And every component is different. Therefore, we cannot propose one model to fit that specified component in all systems. Choosing the best model structure is a time-consuming process. Thus, an optimization process needs to be implemented to select the best model and choose between several models to reduce energy consumption (Kusiak et al., 2010).

1.3.3 Considering the whole building as one zone

Most of the available studies nowadays in the modeling and optimization of HVAC systems consider the whole space as a single zone or use a single room to carry out the experiment (Afroz et al., 2018). However, only a few studies have considered the multi-zone. There are essential factors that are hardly being addressed when using the whole building as a single zone. One of them is the effects of thermal interactions, like convective heat transfer, between the zones. Therefore, a study was conducted to examine an ANN multi-zone-based model created to evaluate the non-residential buildings' thermal comfort index. The study has found that considering the heat transfer between zones has increased the energy efficiency and thermal comfort (Garnier et al., 2014). Another study using an ANN multi-zone-based model examined factors like mechanical cooling, ventilation, weather conditions, and heat in a multi-zone building. The study also discussed the importance of heat transfer between the zones by comparing the single zone's accuracy to a multi-zone model. The study has found that the multi-zone-based model is more accurate than the single zone (Huang et al., 2015).

Therefore, this research will use a multi-zone experiment to consider the zones' thermal interactions and get more accurate results.

1.3.4 Not implementing the occupancy schedule

Most researchers nowadays are utilizing models in their simulated work. However, this approach's drawback is when implementing a created model to simulated work does not account for occupants' influence, time, schedule, and interaction with the indoor environment. The occupant's presence can be used as an input in most models and directly influences the building's energy consumption. (Page et al., 2008) have conducted a study showing the influence of occupants on the buildings by stochastic models that emphasize the occupants. Also, (Sun et al., 2014) have developed models for overtime occupancy based on measured occupancy data from an office building. The study shows that the presented model can be used to generate occupant schedules to be used as an input for building energy simulations. Therefore, it is recommended to use actual buildings for this type of application.

Therefore, this research will address the occupancy schedule approach implemented in the optimization technique proposed in this research. Also, the proposed tool in this research is designed to be implemented in real commercial buildings. Therefore, a real building will be sought to test the proposed tool and examine the energy-saving. If accessing an actual building with real-time data was not available, then a simulation building will be used to test the proposed methodology. An existing building implementation will be addressed in future work.

1.3.5 Developing the models using a short period

Very few models have used real performance data collected over a long performance span (Frausto et al., 2003). Instead, some researchers have trained their models using simulation data or a limited set of data collected in a short period (Ríos-Moreno et al., 2007).

For example, a study conducted by (Kulkarni et al., 2004) modeled the building systems using MATLAB. However, the study considered the building as one thermal network also only one season of data was used. Therefore, the model can be considered incomplete because it covered only the winter season, so only the heating system was considered. Moreover, developing models using a limited range of data (less than one month) is not accurate for predicting indoor temperature and relative humidity, unlike other studies that developed models using more extended periods. For example, a study conducted by (Mustafaraj et al., 2010) developed models using an extended period (nine months). However, the study has found that no model can predict the indoor temperature and humidity levels. This conclusion contradicts (Patil et al., 2007), who used a shorter period.

Thus, depending on the complexity, type of application, and previous knowledge of the topic being modeled, the duration of the data collection period is specified. But based on the previous studies, a data span of a week or two resulted in less accurate models. Therefore, a more extensive data span will be gathered from an actual system performance in our study.

1.3.6 lack of integration between system-level and zone-level

There have been lots of physical models predicting the ventilation airflow rate. For example, the ASHRAE standard (ASHRAE 62.1) has described the method for calculating the ventilation needed for each zone. In addition, there have been numerous studies in the area of control strategies in VAV systems. These strategies are based on maintaining a constant static pressure set point in the main duct without considering the actual pressure-demand (system level). Those strategies are summarized by (Pang et al., 2017) as follows:

- Occupied zone setpoint temperatures and night set back
- VAV box minimum flow (typically 30%)
- Optimum start
- Supply air temperature reset
- Economizer and minimum outdoor air intake

Those strategies consider only the zone level without integrating the system level. This research proposes a method to integrate the minimum zone airflow rate setpoint with the outside airflow rate to optimize the zone ventilation rate.

1.3.7 Not implementing the minimum zone airflow rate, minimum ventilation requirements, occupancy schedule, and demand control (DC) in the optimization process

There have been some studies that implemented the whole system optimization technique in the past. Those studies used the approach of resetting the system set points to reduce the total system energy consumption. A dissertation work conducted by a fellow Ph.D. student (Tesiero, R. C., III., 2014) proposed an integrated optimization technique to reduce the energy consumed by chilled water VAV systems. The study has utilized the use of both physical models and data-driven models to model the system component. Later, the optimization process was implemented to optimize two system setpoints the supply air temperature and duct static pressure. The work was established on the assumption of a fixed minimum zone airflow rate of 20% of the design flow, fixed occupancy schedule that is assumed to be the maximum number of design people. Also, the work has not accounted for the occupancy sensors reading. The study has found that this approach can reduce the total system energy consumption by at least 13%.

Therefore, this research will address the previous study's gap by creating a modeling and optimization technique that utilizes all data-driven models instead of hybrid modeling. That will ease the optimal structure models finding using the optimization process in a sufficiently timely manner. Therefore, reduce the time required to select the optimal model structure to predict the component performance and eventually predict the actual total system energy consumption.

Also, this research will propose implementing the occupancy schedule inputs into the optimization process to account for the actual number of occupants at each time step and reduce the ventilation flowrates to the exact required amounts. The occupancy schedule can be updated based on real-time knowledge of the occupant's count, zones type of use, and schedule. For example, in conference rooms and when there are meetings times in the schedule or lecture rooms and when there are lectures in the schedule against when it is empty. And the occupant behaviors such as lunchtimes and breaks, etc. Another method to get an accurate occupant count is CO2. This approach will enhance the sustainability goals of ASHRAE 62.1 by optimizing the zone level ventilation ratio and fulfilling the gap in this related code, as well as reducing the total system energy consumption. Also, this research will implement the real-time zones occupancy sensor readings. This approach will crucially affect the zones' ventilation flowrates and zones minimum flowrates. Lastly, this research will implement the method of zone minimum air flowrates setpoint reset. This approach will allow this setpoint to be adjusted over the operation time instead of using the constant design minimum values. This method is crucial to reduce reheat energy consumption.

Finally, a new approach that was rarely introduced in any previous work will be implemented in this research, which is the demand-control method. Implementing the demand control methodology with the optimization process in response to the demand response signal received from the utility companies to modify the electricity consumption power profile by alleviating the peak load demand when the demand response signal is received.

1.3 Research contribution and structure

This research aims to develop an accurate data-driven modeling and optimization technique for HVAC systems that are commonly used in commercial buildings in the US. Those systems are chilled-water variable air volume (VAV) systems and direct expansion (DX) systems. The data-driven models will duplicate the real systems as close as possible. The models created based on actual data gathered from an existing physical system will be later optimized to automate the process of selecting the best model structure. This optimization process reflects the first level of optimization (MLO)

The second level of optimization is the system optimization process (SLO) for prediction and performance optimization. The optimization process of the system setpoints will be implemented to minimize the energy consumption and the cost of operation under normal conditions and demand control. For more accurate calculations, the final results will be measured in terms of power and energy consumption savings (kWh and BTU) and cost of operation savings (US dollars).

This novel optimization approach will be achieved through load prediction of the next time step while including the minimum zone airflow rate technique proposed by ASHRAE as well as accounting for the occupancy factor through the CO_2 concentration level readings and or occupancy schedule. At the same time, while developing this approach, we will consider an essential factor that was neglected in the previous studies, which is the demand response to the grid needs, as shown later.

This proposed integrated two-level optimization approach is flexible and can be adjusted to any HVAC system type with an online operation.

Like previously stated, in this research, two types of systems were chosen to be examined, the chilled water VAV system and the DX system. Both systems were modeled in this research. The first optimization level was created for both systems to automate the modeling process, and the results were discussed. In contrast, the integrated two-level optimization process was implemented in only the chilled water system. The DX system was modeled but will be tested in future work due to the shortage of resources and time. The final results of implementing the proposed methods savings and challenges were discussed

The goal of this research will be accomplished through three main steps that will be treated as different objectives or chapters.

1. Compare multiple proposed artificial intelligence modeling techniques and choose the most suitable technique for modeling HVAC systems' performance.
2. Develop an accurate data-driven model of the chilled water VAV systems and DX split systems. As well as implementing a model-level optimization technique that will help automate the process of the parametric study.
3. Develop a whole integrated system performance optimization process that includes both the component and system levels to reduce the total energy consumption and improve the indoor thermal comfort levels.

This research is constructed of six chapters.

Chapter 1 As shown above. Summarize the background of this research. Also, it discusses the gap in the previous studies that led to the idea behind this research.

Chapter 2 shows the literature review on the previous studies conducted in modeling and optimizing HVAC systems.

Chapters 3, 4, 5 will show each phase of this research and the methodology to reach that goal of that phase. Finally, the results and main findings were discussed.

Chapter 6 will conclude this research and prominent findings regarding energy, cost savings, and future work that will help improve the results.

The intention behind having this research structure of having separate phases as separate chapters instead of one extensive methodology was to make this document more accessible and more time-efficient for the reader. Therefore, if one is interested in one objective of this research, one can navigate that chapter without reading through the whole document.

Figure 5 below shows the overview diagram with research phases and how they fall into the final prescribed goal.

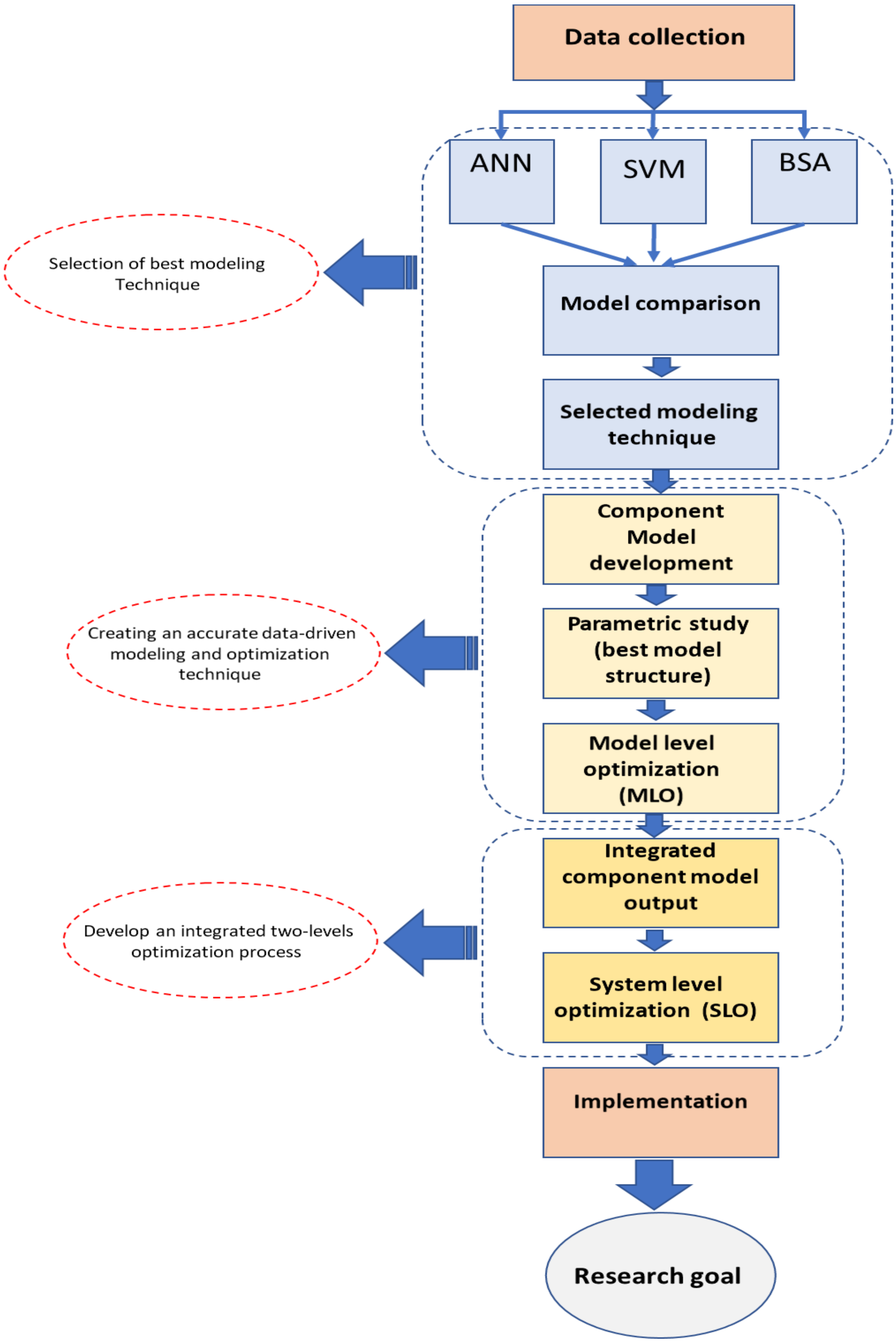

Figure 5. The research structure.

Chapter 2

Literature review

2.1 Introduction

Today, modeling and simulation are recognized techniques for solving energy cost issues in several engineering fields. This chapter shows the literature review and previous studies that were done in the field of modeling and optimization of HVAC systems. This chapter summarizes the state-of-the-art findings in modeling the components of HVAC systems aiming to reduce energy consumption. The most common artificial intelligence tools used for that purpose and how they were implemented. The optimization techniques were previously researched at both the component level and system level.

2.2 HVAC Modeling and simulation

Building energy performance problems arise from the infinite architectural and mechanical building designs and multiple energy analysis methods and tools available. Energy efficiency is achieved through properly functioning equipment and control systems, whereas building controls and operation problems are the primary causes of inefficient energy usage. Collected and maintained building data sets are an adequate opportunity to build databases and data-driven algorithms that can be utilized to evaluate the building performance and energy savings that are related to retrofits projects (Mathew et al., 2015). Lacking the historical data has limited the ability to validate the engineering-based models intended to predict energy consumption. Thus, the recent increase in the number of buildings that benchmark their energy use on public resources has increased the amount of available data that can be used (ENERGY STAR, 2018). The recent availability of more data to use has made modeling the buildings' energy performance more accurate. And the building performance data has become less isolated from public use. With the recent efforts to collect buildings data for modeling, benchmarking, and retrofits projects. There has been an emphasis on managing the building data that sits in the utility sheets or in building automation systems (BAS) not used.

2.2.1 Building automation systems (BAS)

Most buildings now are equipped with BAS systems. With those systems, we can easily access the building's real-time performance data that can be used to model the HVAC system performance accurately. Those data can be a massive benefit for the new revolution in the modeling and simulation of building systems' performance, leading to energy savings. Thus, one of the main achievable goals of the effective use of BASs is to improve the building's energy efficiency, lowering costs, and providing better performance (Wang, S. et al., 2008a).

Building automation system (BAS) consists of sensors, controllers, actuators, and software. An operator interfaces with the system via a central workstation or web browser, as shown in figure 6. In addition, the BAS provides users with as-built drawings, floor plans, and specific graphics of HVAC systems.

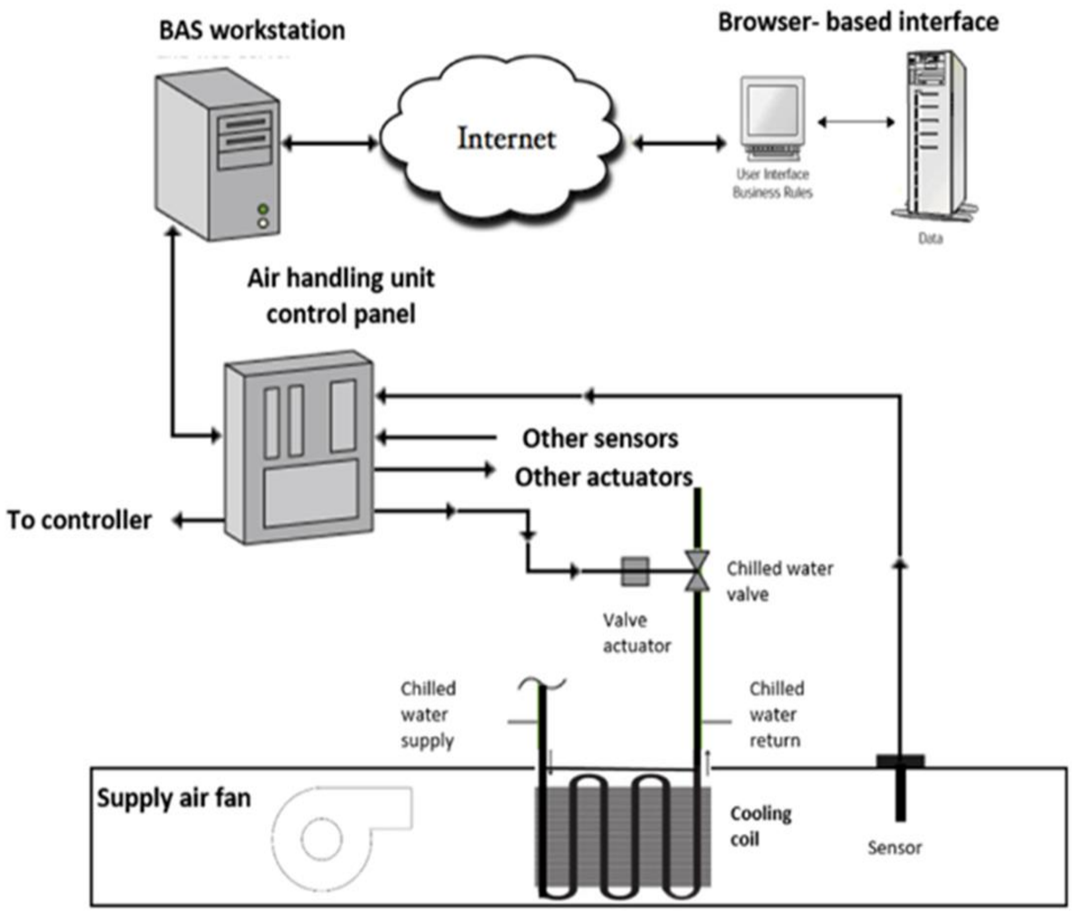

Figure 6. Building Automation System (BAS) component

The BAS presents operators with a graphical user interface (GUI) illustration of the whole HVAC system. In addition, the BAS displays several system measurements such as Supply and return air temperature, static duct pressure, damper positions, fan power, fan pressure, etc. Figure 7 shows the BAS schematic and how it is connected to the controllers of a chilled water system to record the performance data.

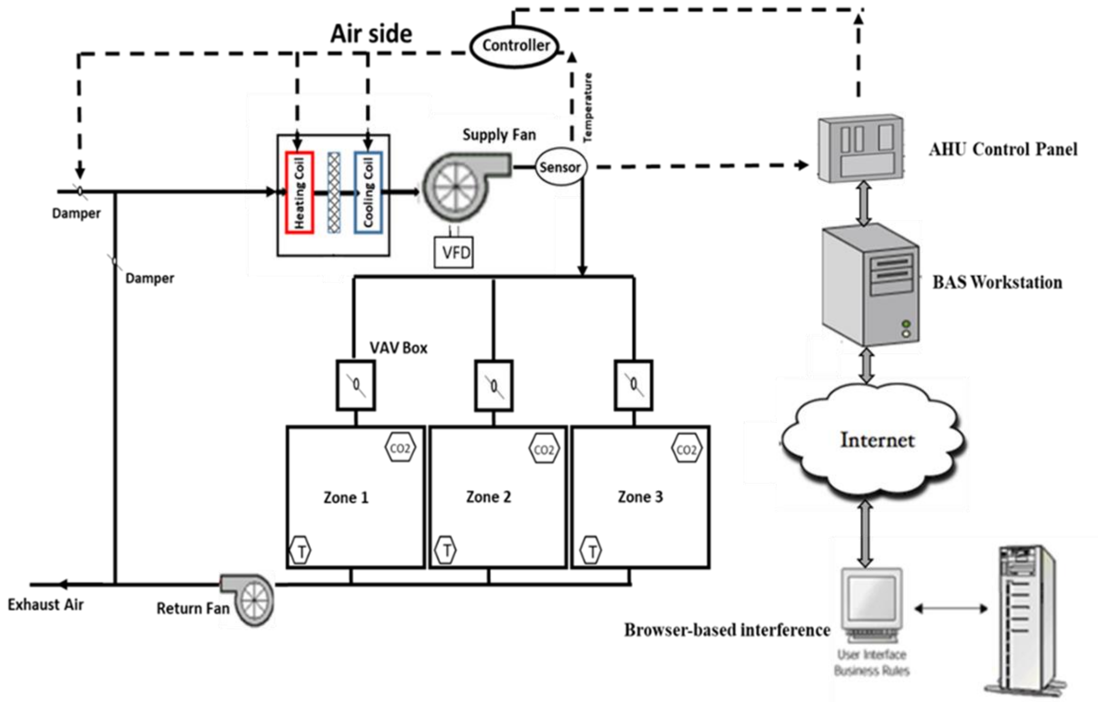

Figure 7 A schematic of a typical chilled water VAV system and its connection to the BAS

2.2.2 HVAC systems model types and evolution

HVAC systems are complex nonlinear systems. Therefore, no one model can be comprehensive enough to satisfy all system types and conditions. The first building performance model was introduced in the late 70s when its IT controlling systems were introduced (Caffrey, R., 1998). HVAC models can be divided into three types, Black box, white box, and gray box model (Homod, R. Z., 2013) as shown in figure 8.

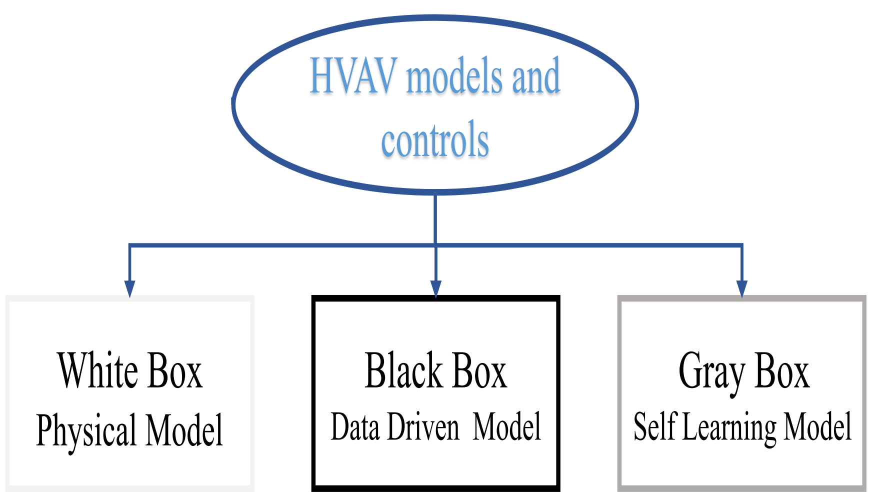

Figure 8. HVAC system models' types

2.2.2.1 White box model

White box models are also known as forward physical or Mathematical models. There are two types of white-box models: Lumped and distributed parameters. This modeling type is famous for modeling the HVAC system process based on physical and chemical conservation laws such as mass, momentum, and energy conservation. Those models describe the links between the inputs and outputs in the form of mathematical equations (Homod, R. Z., 2013). Forward models need detailed physical information, and they are used to predict output based on known structure and variable inputs (Hyvikinen, J., 1996).

(Ghiaus et al., 2010) used a forward control algorithm using feed-forward to balance the weather conditions and model predictive programing for set-points tracking to estimate the heating loads. The study has assumed that the thermal model of the building is linear. The study has inflicted many assumptions, such as that the thermal capacity of the wall and indoor is lumped and that the weather and internal loads are known since they used predictive models for that. This probably causes lower accuracy of the load predictions for the study.

(Wang et al., 2008) have proposed a theoretical forward model for VAV air conditioning systems. The study has assumed that the supply air temperature is equal to the coil's surface temperature and that there is no internal latent load by neglecting the moisture content of the supply air.

The use of such models in existing buildings and real-time system operations may not be available. It will require instant tuning and elevated time to process the calculation that might surpass the optimization period. (Nassif, 2018). Furthermore, the information needed to create those models is not limited to the building structure and the internal loads, the number of people, zone activity type, and lighting heat gain. Therefore, such models are rarely used in real-time operations.

2.2.2.2 Black box models

Black-box models are also called data-driven models or backward models. Those models fit the transfer function model to the data's input and outputs and do not reflect the actual model's specific physical information (Homod, R. Z., 2013). Such models' mathematical representation can be in terms of regression, neural networks, fuzzy models, etc.

Those models can operate on real-time applications when they are highly adaptive and reproducible. On the other hand, data-driven models, are much simpler and used for cases when system-specific component models are required or for fault detection and diagnosis (Hyvikinen, J., 1996).

Many studies have implemented the black box models in modeling and simulation of HVAC systems aiming to improve the control system of thermal performance. For example, a study by (Mustafaraj et al., 2010) has implemented a black box model using the autoregressive with external inputs (ARX), autoregressive moving average with external inputs (ARMAX), Box-Jenkins (BJ), and output error (OE) models to examine the thermal performance of a commercial building. The models have predicted the room's temperature and relative humidity for different time scales. The study found that all the models have accurately predicted the rooms' thermal performance, with the BJ model being the most accurate. Furthermore, since those models are adaptive, they can be applied to control by changing their parameters. Therefore, those models can be used for online control of HVAC systems for commercial buildings and could be extended to other types of buildings.

However, since those models depend on the systems' actual performance data, they must be updated regularly and can not be used outside the training set range. Also, the data-driven approaches for energy savings purposes benefit from giving the results as a probabilistic distribution of energy savings. With increasing energy savings, companies and techniques understanding the uncertainty in energy savings became crucial (Mills E., 2011).

2.2.2.3 Gray box models

Gray box models are also called semi-physical or hybrid models. Those models are a combination of black box and white box models. In some cases where some HVAC processes are physically described but are less clearly described, the physical model can be combined with the white box model to improve those models and vice versa, resulting in gray box models (Homod, R. Z., 2013).

(Leephakpreeda, T., 2008) have implemented this type of modeling to determine the indoor thermal comfort of HVAC systems under a dynamic environment. Since, the temperature setpoints of fresh air supplied to the system are dynamically changed in time and not known previously. The study has proposed a gray box adaptive control theory (ACT) technique to capture the relationship between indoor thermal comfort and outdoor temperature. The research has validated using such models in HVAC control systems based on the actual occupants' survey data on thermal comfort.

In gray box models, the physical model part is derived from the thermodynamics principle while the parameters are determined from Catalogs, actual performance data, and or commissioning and survey data (Homod, R. Z., 2013). Also, (Wang et al., 2004) have proposed an accurate gray box model predicting cooling coil units' performance. The technique was developed based on energy balance and heat transfer laws. Commissioning information is then used to determine at least three model parameters. The study has validated the use of such models and found that this method gave better results in predicting the actual coil performance than other conventional prediction methods.

2.3 Artificial intelligence tools used in modeling and simulation of HVAC systems.

Artificial intelligence (AI) is an advanced area of computational science and engineering. Artificial intelligence was first invented in the 1950s. The first attempts have failed due to a lack of automated means of training. The attempts to implement nonlinear artificial intelligence methods have kept failing until 1990 when those attempts have a chance of success (Livshin, I., 2019). With the increase in computer computing powers and the need for artificial methods capable of solving complex problems that exceed human capabilities, there were numerous efforts to develop artificial intelligence methods. One of the many industries that have witnessed a significant evolution in deploying AI methods is the HVAC system industry. Many AI studies have been conducted aiming to understand the performance of those systems and analyze the relationship between their components to operate those systems better and eventually reduce their energy consumption. AI has many tools that are widely used now like, Artificial Neural Networks (ANN), Support Vector Machine (SVM), Aggregated Bootstrapping (ABS), Transfer Function (TF), State-Space (SS), and Autoregressive Exogenous (ARX). This research will focus on only ANN, SVM, and ABS and discuss the literature review behind it.

2.3.1 Artificial Neural Networks (ANN)

Artificial intelligence neural network (ANN) architecture mimics the neurological human brain network. They consist of multiple layers of neurons that are directly connected to each other's (Livshin, I., 2019). Figure 9 shows a schematic of the human brain neuron.

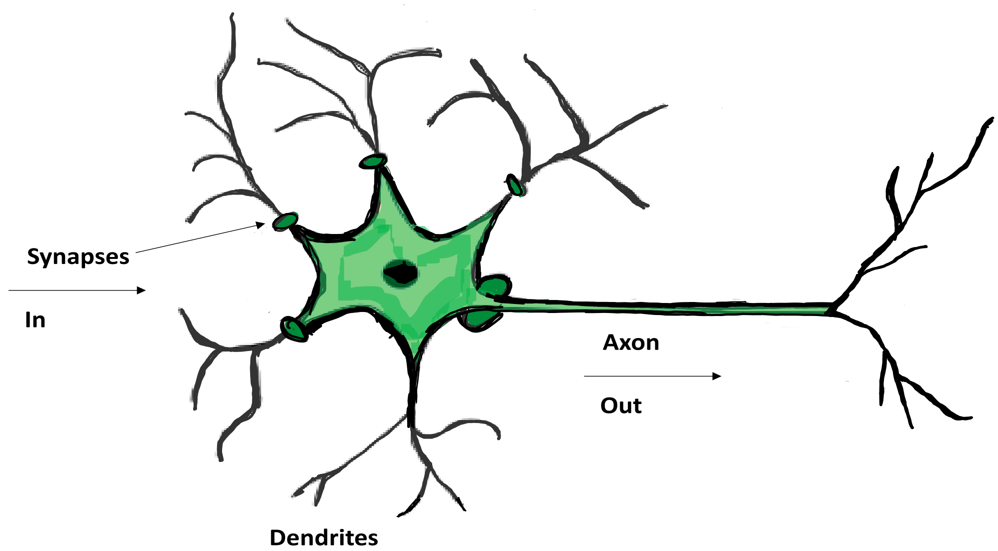

Figure 9. Human brain neurons

Every biological neuron consists of a cell body with a nucleus, Axon, Dendrites, and Synapses. In the biological neurons, the synapses receive an impulse that is transferred to be processed by the cell body. Then the response is sent out through the axon then to the synapses connected to other neurons.

Mimicking that structure, the artificial neural networks are constructed of a neuron body, and it has a connection to the other neurons, as shown in figure 10.

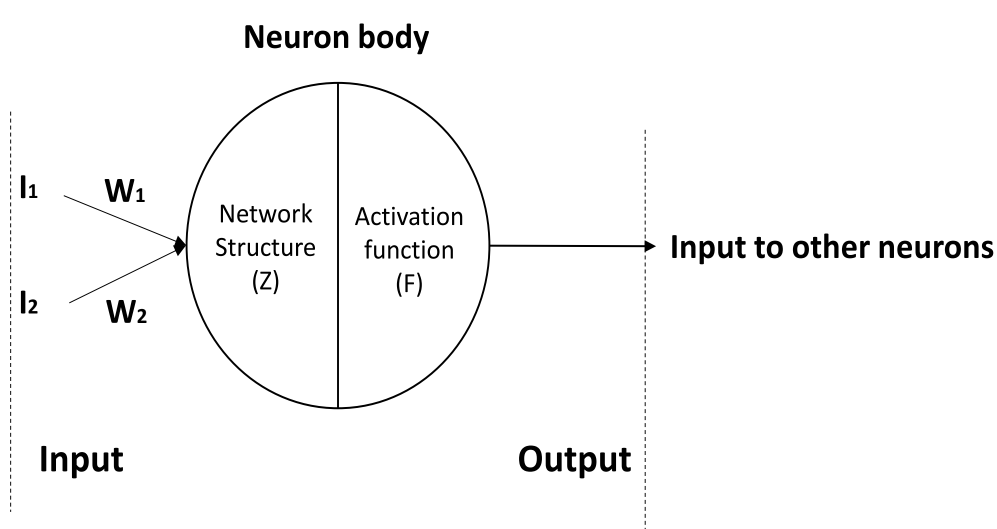

Figure 10. Artificial neuron structure

Each input to the neuron body is assigned a weight (W). The weight of the input dictates its impact on the output. For example, if the weight assigned to the first input neuron is greater than the weight of the second input neuron in the neuron body, then the first neuron's impact on the output is more significant than the second neuron (Livshin, I., 2019). In other words, the output is dominated by the first output. The body of the neuron is usually represented by a circle that is consisted of two parts. One is called the network input or sum of the network that is represented by (Z). This section shows the calculation that the neuron body performs (equation 1).

$$\mathrm{Z} = W_1 * I_1 + W_2 * I_2 + B \ldots(1)$$

And the second part is the output neuron we call it here (F). F can be calculated by applying the activation function. The activation function is a special nonlinear function applied to the linear part of the Z function (equation 2).

$$F = \sigma(Z) \ldots\ldots\ldots\ldots\ldots\ldots\ldots(2)$$

One of the most frequently used activation functions is called sigmoid (equation 3). The sigmoid function is a well-behaved function on an interval of [-1, 1]. Also, it saturates fast outside of its interval range, meaning that its value is less likely to change with the change of its argument (Livshin, I., 2019).

$$\sigma(Z) = \frac{1}{1+e^{-z}} \ldots\ldots\ldots\ldots\ldots(3)$$

When multiple layers of neurons connect together, they form the neuron network. In general, a neuron network is constructed of an input layer to start and an output layer. In the middle of those two layers, there are one or more hidden layers. The input layers receive the input from the outside, transferring it to the hidden layer where most of the calculations are performed. When the output is reached, it is carried away by the output layer, this is called a feed-forward network (Cunningham et al., 2008). Figure 11 below shows a neuron network layout.

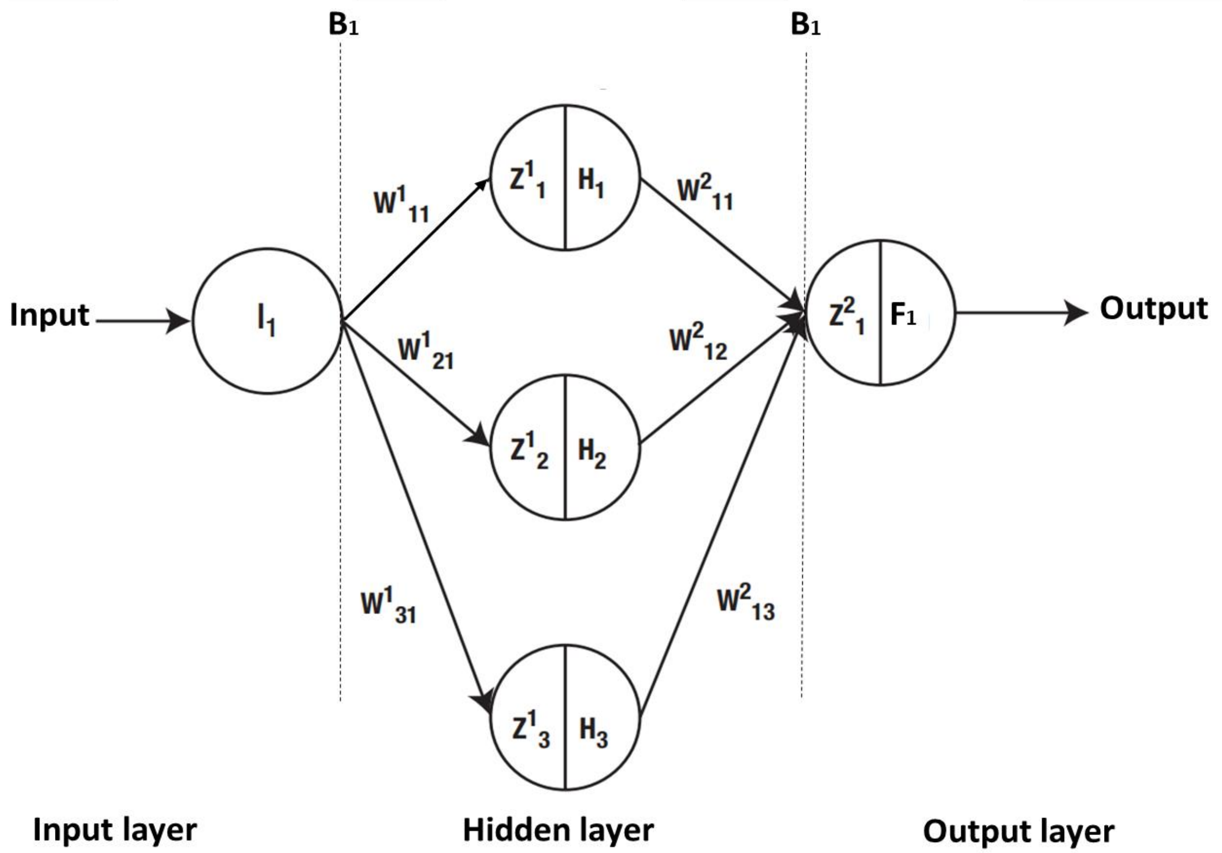

Figure 11. Neuron network layout

Each neuron in every layer is connected to all the neurons in the following layer. This connection carries a weight (W). the weight of the connection determines the effect of this input on the final output. Each weight is numbered with two indexes, as shown in figure 11. The first index represents the number of neurons in the receiving layer, while the second index represents the number of neurons in the sending layer. In addition, each layer is assigned a bias (B). the bias carries weight as well, and it is helping in making the calculation more flexible when matching the targeted output (Werbos, 1974).

When training the network, the weights and the bias are initially assigned randomly based on previous studies and recommendations, knowledge of the studied subject, and experimenting. Also, the number of the network's hidden layers depends on the complexity of the function being estimated. The more complex the process is, the more layers are needed to lead to the best approximation results.

An essential character of the neural networks is their adaptivity, where they learn by example rather than by the traditional methods. Therefore, these models can be used to virtually model any part of any system as long as the model can be trained by receiving sample data and a teaching mechanism. Therefore, the ANNs are considered a valuable tool in modeling the HVAC system components. Eventually, this will provide researchers and designers with a powerful, simple method to address the HVAC system's needs and create a more energy-efficient HVAC system.

2.3.2 Supply Vector Machine (SVM)

Support Vector Machine (SVM) is one method that uses supervised learning for classification and clustering purposes. For example, machine learning with maximizing (support) of the separating margin (vector) is called support vector machine (SVM) (Huang et al., 2018). SVM was first introduced by (V. N. Vapnik1995) in 1995. Afterward, SVM was largely developed by Vapnik and co-workers at the AT&T Bell Laboratories. In general, SVM is also extended to solve regression problems and thus support vector regression. The basic idea behind the SVM is to reduce the dimensionality of a data set consisting of many variables that correlate with each other and retain the variation present in the dataset up to the maximum extent.

According to (Vapnik, 1995) the goal of SVM is finding the function $f(x)$ at most error deviation from the actual targets (Y) for all input training data (X) and at the same time aiming for the results that are as flat as possible. Meaning that any error (ε)that is less than the error (ε)deviation of the targets is acceptable, but anything that falls outside of that deviation margin is not. Figure 12 below shows this concept where only the points outside the deviation margin are not acceptable, and they have most of the effect on the output target (Schölkopf et al., 2002 and Smola et al., 2004). In SVMs, the input space is mapped into a higher dimensional dot-product space called a feature space (Xuemei et al., 2009).

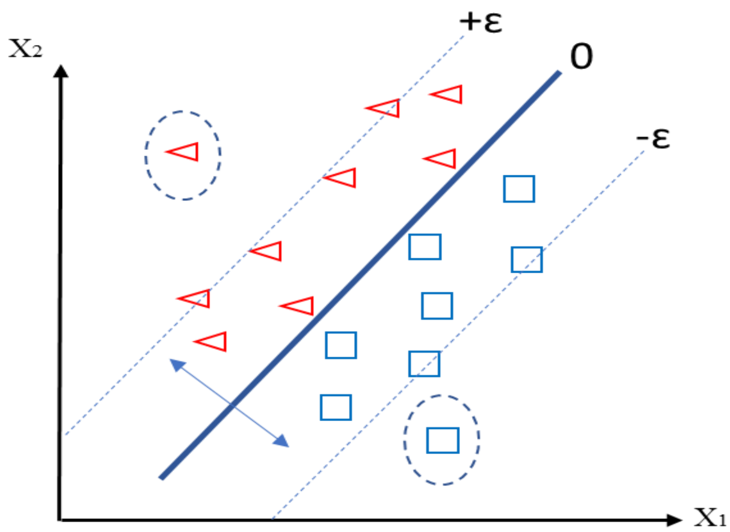

Figure 12. The soft deviation setting for a linear SVM.

Then the main objective is to find an optimal hyperplane 0 in the feature space. The hyperplane is the decision boundary that clearly classifies the data points. Because to separate between any two data sets, we can have multiple hyperplanes. Therefore, the SVM objective is to find the hyperplane with a maximum deviation (margin) distance between the data points to utilize future data points confidently. The data that is closer to the hyperplane are called support vectors, as shown in figure 13.

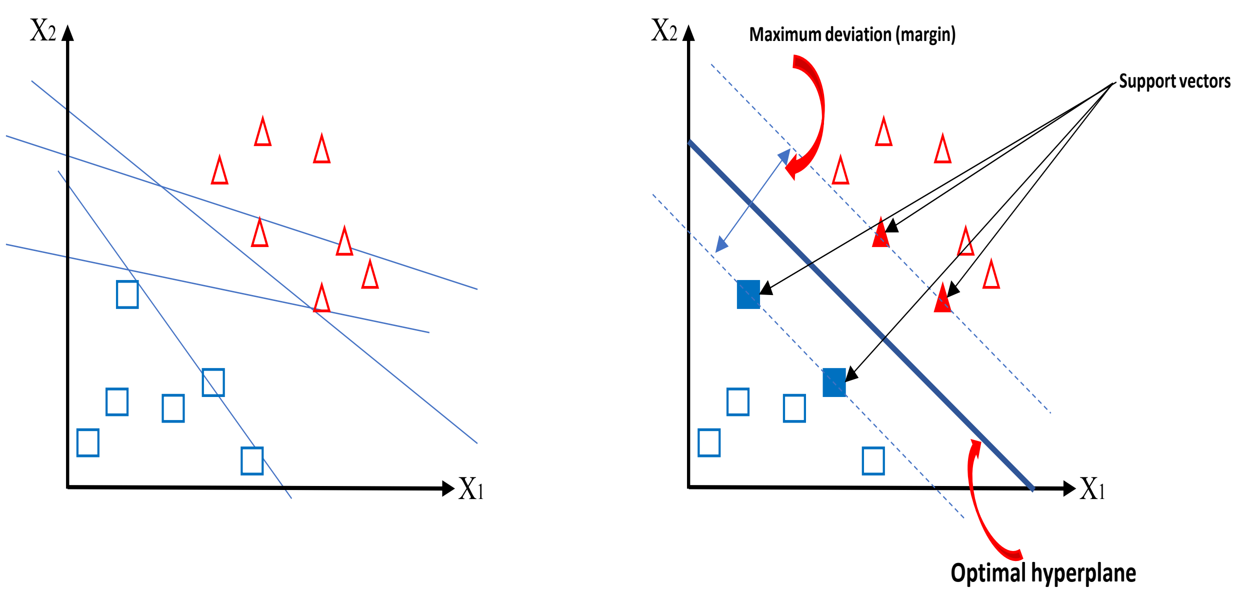

Figure 13. Possible hyperplane and the optimal hyperplane

By using the SVM, we are trying to maximize the margin. The margin boundaries are those support vectors, and by deleting them, we can change the hyperplane position and increase the margin (Gandhi, 2018).

A hyperplane in n-dimensional space is generally a line in two dimensions. In three dimensions, it is a plane, and in more dimensions, it is a hyperplane with n being the number of features. In two dimensions, the function of the line is given by equation 4.

$$AX1 - \mathrm{X2} + \mathrm{b} = 0 \ldots\ldots\ldots\ldots\ldots\ldots (4)$$

The equation is derived from equation 5 for two-dimensional vectors.

$$a\mathrm{X} + \mathrm{bY} = \mathrm{Y} \ldots\ldots\ldots\ldots\ldots\ldots\ldots\ldots (5)$$

Following the same derivative, the equation for the hyperplane can be represented in equation 6.

$$W^T Xi + b = Y^{\wedge} i \ldots\ldots\ldots\ldots\ldots\ldots (6)$$

SVM is a novel network algorithm that is adaptive, fast, and has good learning abilities for small and large sample data. SVM has been developed to be a powerful tool in data analysis and machine learning algorithms. SVM obtains its structure from the concept of structural risk minimization through the within-class distance, which makes up for the shortcomings of other learning methods. Therefore, SVM can find an optimal solution by solving a quadratic problem and having good learning abilities (Xuemei et al., 2009).

2.3.3 Bootstrap Aggregation (BSA)

Multiple classifier systems, also called ensemble systems, have recently grown more attention within computational data science and machine learning. We use the concept of ensemble learning and decision-making on a daily basis in our lives. We often seek expert opinions on different problems in life, like consulting with various doctors before deciding on a major medical operation and seeking multiple design options and cost estimates before deciding on a major HVAC installation or system update, etc. This utilizes the concept of ensemble learning, which is selecting the best option between multiple suited ones where no decision has a nonzero variability. In other words, create several classifiers with similar bias and then combining the outputs to reduce their variance (Zhang et al., 2012;2015)

Breiman's bagging algorithm is short for Bootstrap Aggregation, is one of the earliest and influential types of ensemble learning. Bootstrapping is simply the method of random sampling with replacement. Such a sample is referred to as a resampling. Bagging is most suitable for small training data sets (Zhang et al., 2012;2015). However, it has been used for more extensive data sets through breaking down the more comprehensive data sets into smaller sets called "bites." The individual bites are trained using the individual classifiers and then combined. The prediction is then made by aggregating or averaging the predictions of the ensemble. This method shown in figure 14 is called Random Forest (Svetnik et al., 2003). Random Forest was proven to be a powerful tool that can deliver a performance with high accuracy compared to others.

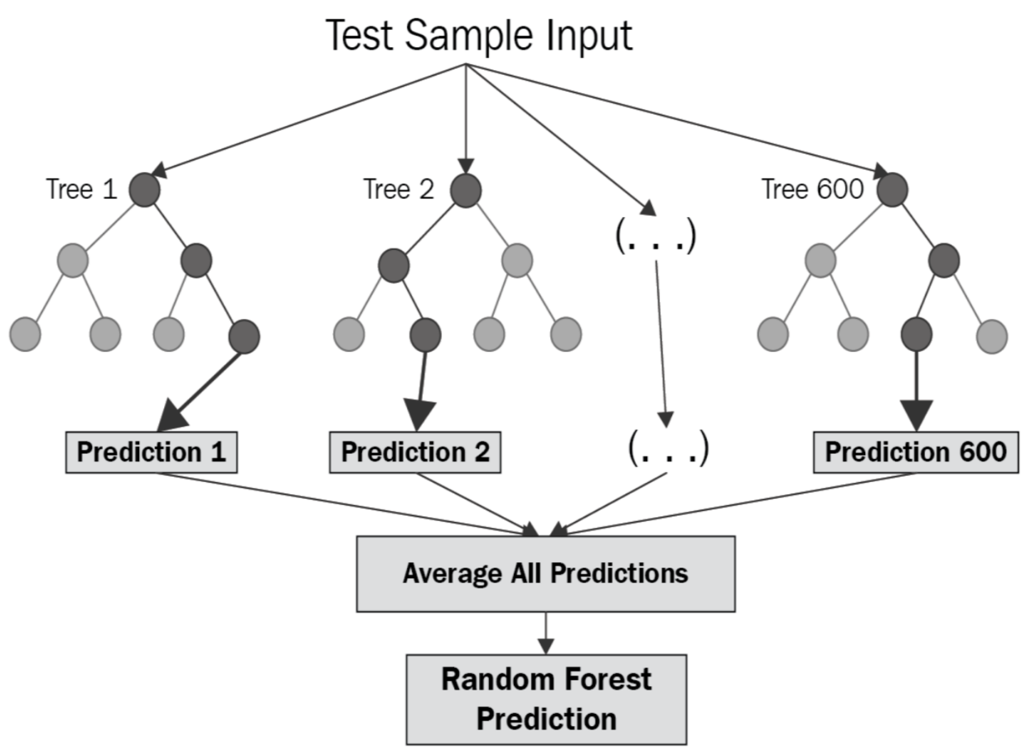

Figure 14. Random Forest structure (source: https://medium.com/swlh/random-forest-and-its-implementation-71824ced454f).

When using Random Forest to solve regression algorithms, the mean square error is used to decide how the data branches (Schott. 2019), (equation 7).

$$\mathrm{MSE} = 1/N \ \sum_{i=1}^{n} (\mathbf{F}_{\mathrm{i}} - \mathbf{Y}_{\mathrm{i}})^2 \ldots\ldots\ldots\ldots\ldots\ldots\ldots \text{(7)}$$

Also, it was described by (Zhang et al., 2012;2015) in the supervised learning algorithm based classifier as in (equation 8)

$$\mathrm{V}_c = \sum_{t=1}^{T} \mathrm{V}_{t,c}\,, \quad C = 1, \ldots\ldots, C \ldots\ldots\ldots\ldots\ldots\ldots \text{(8)}$$

Where (T) is an integer specifying ensemble sizes from an R% to create the training data.

Also, some redundancy may occur in features that will later cause errors because high dimension data cost both speed and accuracy of the classification algorithms. Since learning algorithms data are measured in very short intervals of time, the data set is extensive. So, converting these high-dimensional data into lower space is needed to achieve better speed and accuracy (Khan et al., 2019). To stop overfitting from happening, bootstrapping will be implemented.

Ensemble learning is a way of achieving better simplification performance of learning algorithms. Those ensemble systems have proven themselves to be effective and adaptable in a broad spectrum of problems in real-world applications. And this method has generally improved the performance of created models by 40% by decreasing the models' generalization error (Arsov et al., 2017).

2.4 Modeling evaluation metrics

The selection of variables in multiple regression is a problem that needs to be given great attention (Allen, 1971). In modeling the HVAC systems, the model's performance evaluation depends on operational evaluation by examining its parameters' variability and associativity. Therefore, distinguishing between the modeled and observed data is called the error value, which has great importance.

The error can be explained in terms of many statistical measures like MSE (mean square error), RMSE (root mean square error), MBE (mean bias error), NMBE (normalized mean bias error), CV% (coefficient of variance), R^2 (coefficient of determination), F-Score (harmonic mean of precision), and CVRMSE (coefficient of variance of root mean squared error), etc. (Ruiz et al., 2017).

Instead of one, some studies have examined the error as two structures, bias and variance. The bias measures the accuracy of the models and refers to an error or poor representation of the data. And the variance measures the precision of the performance of the modeling results compared to the observed (Solazzo et al., 2016).

When evaluating different model's sensitivity using a single statistical measure, the difference in the error distribution is crucial. Therefore, using more than one statistical method is vital to deliver a complete understanding of the model's error variation (Chai et al., 2014).

2.4.1 Mean Square Error (MSE)

Mean square error (MSE) is one of the most common statistical criteria used in measuring the performance of computational models and the selection of variables. MSE is claimed to be more meaningful than most other selection criteria like the residual sum of squares (Allen, 1971). MSE is a single reliability measure. The objective of MSE is to compare two individual measures through the degree of similarity or distortion between them. Therefore, if we have two measures, X and Y, where X is a known matrix variable, and Y is a vector response. And x = {xi |i = 1, 2,…,N} and y = {yi |i = 1,2,…,N}. N is the number of signal samples, and xi and yi are the values of the I sample in x and y, respectively. The MSE between the signals is calculated with equation nine below (Buford, 2016).

$$MSE(x, y) = \frac{1}{N}\sum_{i=1}^{N} (x_i - y_i)^2 \ldots\ldots\ldots\ldots\ldots\ldots\ldots(9)$$

In MSE, the error value is usually calculated as the difference between the original values (data) and the undistinguished values; in this case, it is $\in_i = X_i - Y_i$.

When performing this statistical method or prediction, the lower the MSE value means, the more accurate the results are. An MSE of zero indicated perfect accuracy, which is usually not feasible in everyday practice.

2.4.2 Root Mean Square Error (RMSE)

Root Mean Square Error (RMSE) is adapted in average model performance error evaluation. RMSE that is also called root mean square deviation (RMSD), is a statistical method used to distinguish between the estimated values and the actual observed values. The difference or deviation between the two values is referred to as residuals. RMSE mathematically is represented by equation ten below.

$$RMSE = \sqrt{MSE} = \sqrt{\frac{1}{N}\sum_{i=1}^{N} (\in i)^2}, \ldots\ldots \in i = (x_i - y_i)^2 \ldots\ldots\ldots\ldots\ldots (10)$$

When using RMSE, the assumption is that the error is unbiased and follows a normal distribution. Therefore, using RMSE should give a better understanding of the error distribution (Chai et al., 2014).

However, it is claimed by few studies that the RMSE is not a good predictor of the average model performance and might be misleading. Since it is a function of three characteristics of a set of errors instead of the average error, few concerns were raised by (Willmott et al., 2005). However, when evaluating one model, using only RMSE detailed interpretation is not critical to the accuracy of the results since the variation of the same model will have similar error distribution, unlike when evaluating different models (Chai et al., 2014).

2.4.3 Coefficient of Variation (CV%)

The coefficient of variation is a statistical method that is also known as the relative standard deviation. It is a measure of the frequency distribution of a random variable, and it is widely used in engineering and data science studies. CV is unit-free and is represented as a percentage of the observed standard deviation to the observed mean. Thus, monitoring the CV is essential in process control when the variables have a clear mean value, and their variance is a function of the mean. In addition, because the CV is a unit-free measure, it is commonly used to compare the variability among data sets of different units or mean values (Teoh et al., 2017;2016).

Since implementing the CV% as a statistical measuring method in many disciplines, monitoring the CV% is receiving significant attention among researchers lately. To better understand the CV% mathematically, suppose that ($X_{i,1}$, $X_{i,2}$…., $X_{i,n}$) is a group of data samples with the (n) size at time i= 1, 2, …. Let the mean (μ_i) of the set is >0, (σ_i) is the standard deviation of it, and (Y_0) is the population CV when the process is in control. Here (Y_0) is the control process target value, then the CV (Y_i) can be represented in equation 11 below.

$$Y_0 = Y_i = \left(\frac{\sigma_0}{\mu_0}\right) \ldots\ldots\ldots\ldots\ldots\ldots\ldots\ldots (11)$$

And the sample mean $\bar{X}_i$, and variance S_i are expressed by equations 12 and 13, respectively.

$$\bar{X}_i = \sum_{j=1}^{n} X_{i,j} \ /n \ldots\ldots\ldots\ldots\ldots\ldots\ldots\ldots (12)$$

$$S_i = \sqrt{\sum_{j=1}^{n}(X_{i,j}} - \bar{X}_i)^2 \ / \ (n-1) \ldots\ldots\ldots (13)$$

This shows that that the variables (μ_i) and (σ_i) may change from one subgroup to another while the CV (Y_i) must be equal to the predefined target Y_0 that is common for all the subgroups (Teoh et al., 2017;2016).

CV% of a value less than one (zero or negative) refers to perfect accuracy and zero error value, which is not feasible. Therefore, the CV%, in this case, is meaningless and will lead to the wrong assumption about the process being examined. Thus, the CV is used strictly to compare the dispersion of positive random variables (Curto et al., 2009).

2.4.4 Coefficient of Determination (R^2)

The coefficient of determination $R^{2,}$ also known as the adjusted R^2, explains the total variation in a sample data. In other words, it is defined as the proportion of the corrected sum of squares that is explained by the model (Piepho, 2019). R^2 is one of the most popular measures for the goodness of fit for the linear models. And it ranges from 0 to 1. The R^2 value of 1 indicated the nonappearance of residual variation. To better understand the structure of R^2 for sample data for linear models, we need to know the difference between linear models and the extended version of it. The linear models can be expressed as in equation 14 below.

$$Y = X\beta + e \dots\dots\dots\dots\dots\dots (14)$$

Where Y is the response vector for a design matrix of X. While e represents the residual error vector and β is a set effect vector (Piepho, 2019).

However, linear models can be extended to linear mixed models, allowing for random effects. In those models, R^2 will have the same form as linear models. Extended linear mixed models can be represented as in equation 15.

$$Y = X\beta + Zu + e \dots\dots\dots\dots\dots\dots (15)$$

Where (u) is a random-effects vector with for Z design matrix. And u and e are assumed to be independent (Piepho, 2019).

Finally, R^2 gives you the percentage of variation in Y that is explained by x. Thus, R^2 can be represented mathematically as in equation 16 below (Tjur, 2009).

$$R^2 = \left(\frac{\sum(Yi-\bar{Y})(\hat{\mu}i-\bar{y})}{\sqrt{\sum(Yi-\bar{Y})^2\sum(\hat{\mu}i-\bar{y})^2}}\right) \dots\dots\dots\dots\dots\dots (16)$$

Many studies have been conducted aiming to reduce the R^2 value to result in a better fit model. This may be important but not always sufficient since R^2 is mostly dependent on the x-values of the set of samples. Therefore when sampling the data with the intention of having a well-explained slop will result in an R^2 close to 1(Draper et al., 1981).

After discussing the types of machine learning model types, tools used, and types of statistical measures to select the best model structure as well as the best modeling tool among the others. The following section will examine how those were previously implemented in modeling the HVAC systems components and operation.

2.5 HVAC computational models' implementation and development

Data-driven models based on real systems data are proven to help understand HVAC systems' performance and explain the relationship's system components (Talib et al., 2019). Those data-based modeling techniques aim to improve the building's indoor air quality (IAQ), causing concern in the overall human health and comfort levels (ASHRAE, 62.1). HVAC systems are nonlinear systems, and it makes it hard to maintain thermal comfort. To better understand the performance of the HVAC system and optimize its operation, many studies have been conducted over the years. Either using a white box, black box, and or gray-box models.

A study by (Xia et al., 2020) developed a white box-based modeling approach to predict the transient responses and steady-state operation performance of a direct expansion (DX) HVAC system. The study has developed five lumped models based on a partial lumped parameter strategy, one for each main component of the condenser, compressor, evaporator, expansion valve, and space conditions. Each model was created through mass and energy balance equations. The numerical models were then validated by comparing their predicted results with measured data from an experimental real DX system. The results of the predicted performance had a high accuracy when compared against the experimental ones. The study claims this approach can be helpful for energy-efficient DX HVAC system design and controller development.

Another study by (Afram et al., 2015) has used a black box models technique using artificial neural network (ANN), transfer function (TF) process, state-space (SS), and autoregressive exogenous (ARX) models that are built-in functions in Matlab. The models were used to simulate the energy recovery ventilator's performance, air handling unit, buffer tank, radiant floor heating, and ground source heat pump. A comparison was made between the models to select the best modeling technique that meets most of the selection criteria of predicting the output of the outlet water temperature and the outlet air temperature. The study has found the ANN has performed the overall best in terms of predicting the outputs. Another study conducted by the same researchers examined the same experiment set up using a gray-box model and process models. The study has found that the ANN and ARX could predict both outputs better than the gray box and process models (Afram et al., 2015).

Another used black-box model to model the HVAC loads during peak hours and their effect on the whole grid power. The study has justified using gray-box models instead of a white physical model due to the HVAC system's complexity. And the HVAC systems are dynamic systems where the white-box models are hard to adapt to the load change over time, unlike the black box models. The study has used historical forecasting weather data as inputs and the building power consumption as output to train the models. Then the models will be tested to predict the HVAC performance loads and eventually the energy consumption based on current weather forecast information. The models were developed using the ensemble learning methods utilizing four classification methods, Elastic Net MLR, Decision tree, Random Forest, and Gradient Boosted Trees. The mean square error RMSE was used as the evaluation metric. The results of the study have found that the Gradient Boosted Trees held the lowest RMSE value close to 0.16 “reading from charts” in predicting the HVAC load prediction (Tian et al., 2018).

Using black box models and gray box models are popular in modeling the HVAC systems performance, load forecasting, and fault detection and diagnosis because of the complexity of the heat and mass transfer mechanisms which is the basis of HVAC system design. Therefore, in the following sections and after recognizing the modeling tools, a background of how the modeling tools served in constructing the black, gray box models, and sometimes white-box model helped predict the HVAC systems performance. As well as load forecasting, and fault detection, and diagnosis will be examined.

A study was conducted by (Lee et al., 2019) to optimize the air handling unit discharge air temperature to reduce the total energy consumption. The study has used co-simulation between EnergyPlus software and MATLAB via BCVTB (Building Control virtual Test Bed). The study has used simulated data created with EnergyPlus. The data are used to train the model that was created using the ANN toolbox built-in MATLAB. The model structure had multiple input layers like outdoor temperature, outdoor relative humidity, diffuse solar radiation rate, direct solar radiation rate, AHU supply air temp, and cooling coil cooling rate. In contrast, the output was the total energy consumption. The study has manually reached the best model structure by changing the model variables and recording the error value changes accordingly. The best model structure is the model that held the lowest error value in terms of CV(RMSE) (coefficient of variation of the root mean square error). The study has found that using ANN models to optimized the performance of the AHU discharge air temperature has resulted in significant energy savings in the total energy consumption of the unit.

A study by (Kim et al., 2015) has used ANN to model the chiller performance in a centralized HVAC system. The study has examined several parameters and their effects on the accuracy of the created model. The parameters were the number of neurons and the amount of training data. The performance data were simulation data that are collected were split into testing and training sets. The model's results were compared to a DOE reference building to test the accuracy of the results. The accuracy was measured in terms of the coefficient of variation of mean square error. The study has found that by increasing the training set, the accuracy of the results has increased. However, that means decreasing the testing set size, which will offset the accuracy of the results. Also, when holding the training set size fixed and changing the number of neurons, it was found that this did not affect the accuracy results. Therefore, it was found that the model structure of 60% training data and 40% testing data and 12 neurons had held the highest accuracy value of 99.1%. (Kim et al., 2015).

Another study was conducted to predict the energy consumption of the AHU and absorption chiller using ANN's. The study has collected data for one month. The study has validated the use of ANN in accurately predicting the performance of the AHU. The error value of the models has ranged between 13.27% to 15.25 and from 19.42% to 19.53% for the training period and testing period, respectively. While, for the chiller absorption performance model, the error values ranged from 24.64 to 25.58% and 7.12 to 29.39% in the training and testing periods, respectively. The models have satisfied the criterion presented by ASHRAE guideline 14. The study has found that despite the fact the models have met the performance criteria. Still, the error values were somewhat higher than what was anticipated, and high accuracy values were not met. The study has concluded that this higher error value was due to a poor data set collected in a short period of time. It is believed that to achieve better prediction results, thorough verification and improvement of the data set is a must to improve the predictive models and avoid overfitting and underfitting (Jee-Heon, 2020).

A study was conducted by (Vakiloroaya et al., 2013) to model an actual air-cooled chiller equipped with a ducted fan coil unit of an office building. Actual performance data were collected in the month of July. The study used a gradient projection-based optimization algorithm to optimize the supply air temperature and flow rate setpoints. The model parameters were achieved through monitoring data and mathematical models to create the model structure. Simultaneously, the actual performance data served as inputs and outputs to train and test the models. The energy usage was calculated for each day by summating the system energy consumption in each working hour. The study results have shown that after implementing the optimization technique, the compressor and condenser fan energy have decreased by 8.8% and 4.6%, respectively. At the same time, the supply fan power energy consumption has increased by 2.3%. However, the overall total energy savings were 11.4% less than when operating under normal control conditions. Also, the results have validated the effectiveness of using such models for online applications.

A data acquisition system using ANN was developed to control the performance of AHU (Tse et al., 2004). Also, a study has been conducted on a baseline case of one zone using ANN. The inputs were weather, occupancy, and indoor temperature. The goal was to minimize energy consumption, and a genetic algorithm engine optimized the model. The study has shown a 25% reduction in energy consumption than the baseline heating strategy (Reynolds et al., 2018).

While for the DX system that was also investigated in previous studies. A model using a combination of fuzzy logic controllers and ANN modeling was implemented to examine the ability to enhance the indoor air temperature and humidity control system for a variable speed DX system. First, the ANN model was tested and trained using previous performance data of the system. After testing and training the ANN model, ANN-aided fuzzy logic controllers were developed. The result of the study has claimed that the proposed controlling strategy properly controlled both the dry and wet bulb temperature. And the developed controller strategy was able to trace the changes in set points with an acceptable range of accuracy and sensitivity (li et al., 2015).

Also, various studies have implemented the SVM modeling tool to better understand the performance of HVAC systems leading to more energy-efficient systems and enhanced thermal comfort levels while reducing the faults of the performance through fault detection and diagnosis.

One study by (Li et al., 2019) has proposed a solution of HVAC systems fault detection by implementing the SVM as a learning algorithm for all types of faults that can occur in HVAC systems. After learning the consistent nature of faults in the HVAC system, the SVM learning method will identify the type of fault in the subsystems using statistical approaches. The learning process speed was enhanced by applying the principal component analysis to compress the training data set size. This process can be later automated to be implemented in multiple HVAC systems to help in identifying several common HVAC air handling units' faults.

A study by (Van Every et al., 2017) implemented the SVM to detect faults in HVAC systems. The study used a Gaussian process regression (GP) regression algorithm to model the system's parameters. The data were fed into the regression model to be tested and trained while the error values were calculated. Then the output was used in the next model using SVM. The data that were tested using the GP is supposed to be the non-faulty performance of the system. When the SVM is trained using those data and then tested, faults are detected when inputs that produce low error in typical situations show a high error. The results show that the method has successfully improved the performance of the systems. Since the systems are trained with non-faulty data that are totally supervised, it is suitable for online operations.

Most of the previous studies have used measured performance data or simulation data to analyze the performance of HVAC systems. In addition, most of the studies have used forecasting weather data as a significant input in their analysis, one of which is a study we mentioned above by (Tian et al., 2018). However, the actual weather conditions are often different from the weather forecast data, which will significantly affect the accuracy of the prediction results. To deal with this uncertainty, a study by (Zhao et al., 2018) has proposed an approach based on the Monte Carlo Method (MCM) to process the weather forecasting data using a 24 hour ahead approach. The SVM was utilized to create the model for load predictions. The study results have shown that using the MCM approach instead of the unadjusted forecasting weather data has resulted in better performance prediction data closer to the actual real load. This was proved through sensitivity analysis, where the mean absolute percentage error (MAPE) was reduced from 11.54% to 10.92%.

The other learning algorithms that will be discussed in this research are bootstrap aggregation (bagging) and the previous studies conducted using that tool. Multiple researchers have implemented this approach in modeling the performance of HVAC systems successfully. One of those was a study conducted by (Manimaran et al., 2015) to predict residential buildings' heating and cooling loads using the bootstrap aggregation ensemble method. The study has used the data collected from 768 residential buildings designed using the Ecotect design from the UCI machine learning repository. Instead of a single model, the learning method will aggregate the predictions of multiple classifiers made by multiple REPTrees as a base classifier. Then, reducing the error to build compact decision trees. The results of this method were compared against a neural network that was used as the base classifier. The study claims the created models can accurately predict the heating and cooling load with a satisfactory R^2 value of 0.9985 and 0.983, respectively. The results have validated the use of such a method and its ability to improve the performance of HVAC systems.

Ensemble learning methods like bagging, boosting, random forest, and conditional forest were valuable methods in studying the HVAC system's performance, load forecasting, fault detection and diagnosis, and many more.

Load forecasting models are essential to understand the system's performance in the building and the electricity market. In this aspect, a study was conducted using the four ensemble methods mentioned above to observe the load forecasting in short terms and evaluate the effectiveness of those models in predicting it. And observe the energy consumption of the building and ways to improve it. A (107639 Ft^2) campus university in Spain was used as the case study where load data were collected. The hourly temperature was data was collected to serve as the forecasting model's input. Also, if it is a working day or a holiday, the type of day was considered since it significantly affects the accuracy of the results. The four methods of ensemble learning were trained and tested using the actual load data. Finally, a way of predicting the load 48 hours ahead of time was applied. The results show all models were good performers, but the random forest was the most accurate method. All methods were validated by implementing them in the same case study building, and the result shows an improvement in the building's performance. When applying those methods to predict the load ahead of time, the building's energy consumption (measured in electricity costs) has dropped by around 11% (Del Carmen Ruiz-Abellon et al., 2018).

fault detection for existing HVAC systems is vital for systems operation, for the systems to be both cost-effective and accurate. (Parzinger et al., 2020) carried a study to examine the faults in HVAC system total heating power. The predictive models in the study were developed using several machine learning tools, one of them was the random forest tool previously described in this chapter. The predicted total heating power was compared against the actual heating power through residual analysis. The algorithm that was developed in this paper has two methods, one is using the grid search to find the fault decision rule when faults are observed, the other is uses the rate of estimated faults to find the fault decision rule when faults are unobserved. The results of the study show that the first method of observed faults has achieved better results. However, the second method is closer to actual practice, where faults are not followed. Still, it came with difficulty finding a threshold value crucial in determining how accurately the faults are predicted. Finally, the study has claimed that using residual analysis for fault detection is beneficial because the results do not depend on the type of prediction models applied. Systems information and parameters are not crucial for the process execution. Therefore, this type of fault detection method can be used for different predictive models and is also suitable for online system fault detection operations.

All the previously discussed studies have proposed methods of implementing the machine learning predictive models in modeling the components and operation of HVAC systems aiming for better systems operation and energy savings. However, most studies have generated several models and then chose the best model's structure and best modeling technique through numerous types of sensitivity analysis, residual analysis, statistical measures, etc. Therefore, to automate this process to be more suitable for online systems operation practices comes the role of "Optimization."

2.6 Optimization

Optimization refers to a process applied in mathematics for minimizing or maximizing a function. Optimization can be explained as seeking improvements. The start of optimization to find a solution for a specific problem in a mathematical term has started with the invention of calculus and the theory of a minimum and maximum function. Since the mathematical solutions for real-world issues are a complex issue, the invention of computers has helped overcome the limits where the golden age of optimization took off in the 1950s (Ho et al., 2007).

Nowadays, many complex problems have evolved with the development of many industries. The solutions include computational modeling and simulation using physical and mathematical rules to find the most feasible solution. However, the answer to those problems' difficulty doesn't stop at modeling them, but also because the modeling and simulation process is often quite time-consuming. Also, the changing nature of the problems that are dependent on time makes the mathematical solution less sufficient.

In many engineering problems, the solution might be choosing the good enough option instead of the best one since the best solution might not be feasible or cost-effective. Many engineers use this estimation approach when solving problems based on their experience in the field. Nowadays, many optimization approaches and theories have been developed to be knowledge-based rather than expertise-based. Therefore, those rules are implemented in most industrial decision-making aspects by adjusting the process to optimize a specific function without violating predefined constraints. The most common goals of the optimization process are to minimize the cost while maximizing efficiency or productivity. Figure 15 shows a general schematic for the optimization process adapted in modeling and simulation.

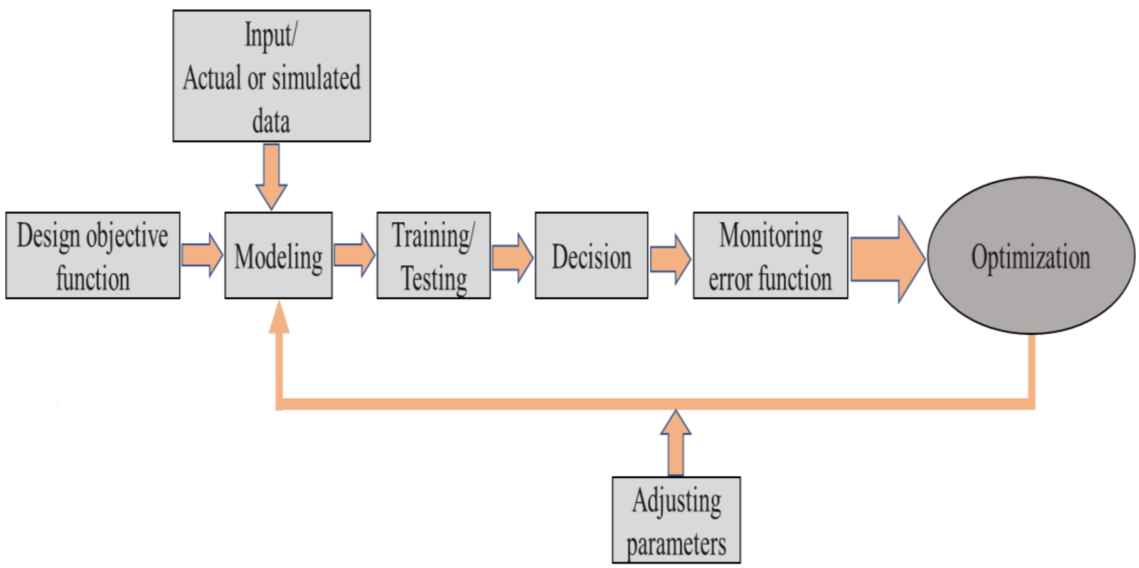

Figure 15. Modeling optimization fundamental.

Over the last two decades, efforts have been made to develop optimal control strategies for building HVAC systems to minimize overall energy and operating costs while maximizing building performance, efficiency, and occupant comfort levels, without violating the operating constraints of each component and without sacrificing indoor environmental air quality. Those cost-efficient strategies have developed due to the growing scale of online data collection and integration of BAS systems in buildings.

Studies have shown that computational intelligence approaches have been developed to optimize energy consumption, improve thermal comfort, indoor air quality, and occupant preferences (Ahmed et al., 2019). Researchers have studied several ways of optimizing HVAC systems. Conventional methods and data-driven methods. (Murphy, J. 2006) have discussed energy savings control strategies and optimization for VAV systems as following.

1. Optimal start/stop: This strategy utilizes the building automation system (BAS) to determine the length of the period required to bring each zone from the current to the optimal temperature. The system waits as long as possible before it starts cooling to make sure that it is ready just in time for occupancy. The same thing with optimal stop strategy, the building uses the BAS to determine how early the system can be shut off for each zone, so the temperature will drift away from the set temperature just in time when the zone is not occupied.
2. Ventilation optimization: In a typical VAV, the rooftop unit delivers fresh air to several individually controlled spaces using the DCV Demand Controller Ventilation strategy. The best approach to optimize ventilation in a multiple zone VAV system is to combine multiple DCV strategies at the zone level. For example, using CO2 sensors in the highest occupied zones like conference rooms and using occupancy sensors in the less densely occupied zones like private offices while using a time-of-day schedule reset in the zones with a predictable occupancy pattern.

While (Strum E. 2016) have studies ways to optimize the right balance for multiple zone VAV energy savings.

1. Fan pressure optimization: This strategy uses communication controllers to optimize the static pressure in the duct. The controllers use the BAS continually to pull information from the VAV terminal with the most open damper. The setpoint of the supply fan is then used to supply just enough pressure so that at least one damper is widely open.
2. Supply- air- temperature reset: this method resets the SA temperature setpoint of the system at part load condition to save the compressor or reheat energy and increase the benefit of an airside economizer. There are several methods used to reset SA temperature.
   A. Reset based on outdoor air temperature.
   B. Reset based upon VAVA damper position.

C. Reset based upon outdoor air temperature and VAV damper position.

However, there have been studies that defeated the previous optimization methods. It was found that all the methods above have their drawbacks. For example, it was found that the fan outlet pressure control is reliable and first-cost effective but cannot minimize operating costs (Stanke, D. 1991). Moreover, the same study has proposed another method called Critical zone reset that has the advantage of being reliable, lower operating costs by keeping the critical zone terminal unit fully open at all load conditions. It was stated that this method has no disadvantages (Stanke, D. 1991).

Optimization techniques were also implemented in measuring the faults in the HVAC system's operation. A study by (DEY et al., 2016) proposed a manual method or a rule of thumb method in detecting the faults of HVAC systems operation that is claimed to be a robust approach in fault detection in real buildings operations. The Expert rules-based fault detection is fast and reliable when applied in building automation systems for commercial buildings. However, this approach has its downfall of having many possibilities of fault to one rule. For example, the supply air temperature sensor fault can be sensed by the rule method. Yet, this fault can be caused by multiple causes like cooling coil fault, fan degradation, or sensor drifting. Therefore, the main cause is hard to determine based on the rule method.

Another study used the same approach on the Air Handling Units and VAV Box operation to classify the main Air handling performance assessment rules (Schein et al., 2003). Based on expert rules that are derived from mass and energy balance, few rules were derived. The proposed rules are evaluated on multiple types of buildings like commercial office buildings, restaurants, and university campuses. Simultaneously, using the control signals to determine the air handling unit's mode of operations identifies which subset of rules will be evaluated. Control strategies are used to measure the VAV boxes and AHU performance, while statistical quality controls are used to assess the process error.

The previous rule of thumb approach in detecting the faults is shown to have multiple likelihoods of faults to one rule. Therefore optimization process becomes necessary to overcome this problem by selecting the most fitted fault among the rest. Then more reliable, fast, and affordable solutions can be reached promptly. (Mirnaghi et al., 202) have extensively reviewed the previous literature on fault detection and diagnosis methods studies on HVAC systems using data-driven and manual approaches. The review has concluded that unsupervised methods are time-consuming, unreliable, and rarely used in online applications. The study showed that implementing optimization algorithms using both supervised and unsupervised learning approaches, also known as hybrid methods, are more accurate, reliable, easily implemented in online operations, and can accurately capture the disruption, especially in large-scale HVAC systems with different types of data features.

Besides the conventional methods of optimization, there have been data-driven approaches. For example, an integrated optimization technique was proposed to predict the air handling unit's supply air temperature and duct static pressure. The optimization technique will integrate four component models of a chiller, pump, fan, and reheat device using MLP (multiple-liner perceptron) method. The results have demonstrated an energy saving of 7% of the total consumption of the unit (Kusiak et al., 2010). In comparison, a study was conducted to optimize the temperature ramp control of a room. The room was computationally modeled. Particle swarm optimization and harmony search algorithms were used for the optimization process. The setting for the supply air static pressure and the discharge air temperature setpoint was optimized. It was found from the study that the mentioned optimization algorithms are suitable for solving the optimization models (He et al., 2014).

Also, instead of only using one optimization technique, many optimization algorithms can be integrated with each other to create an integrated optimization tool. For example, a study has integrated three intelligent algorithms for optimization. The algorithms are Genetic Algorithm (GA), Particle Swarm Optimization (PSO), and Greedy Algorithm (GRA), which were integrated to develop a temperature prediction technique for HVAC units. The tool was found efficient and gave better predictions of the modeling structure being analyzed (Yan et al., 2019).

2.6.1 Genetic algorithm (GA)

The optimization tool that will be used to execute this research is genetic algorithm (GA). Genetic algorithm is one of the most popular optimization techniques based on the natural selection theory. Charles Darwinian developed the natural selection theory in 1859 on the principle of “Survival of the fittest.” This evolutionary principle was the start of the introduction of computation techniques and optimization. Where those principles were translated into algorithms that are used in the search for optimal solutions to the proposed problem

GA can be represented as a tree of evaluation of a single function. Each leaf represents a value from the set of given values, while the internal nodes represent a function. The leaf is evaluated as the corresponding value, while the function is considered an argument resulting from its parents and added to the next generation (Sivanandam et al., 2007;2008).

Generally, there are five phases in considering GA. Those processes are (1) initial population, (2) Evaluation, (3) Selection, (4) Crossover, and (5) Mutation. Figure 16 shows the optimization process using GA and how the five steps were implemented. Step (2) Evaluation was represented as the objective function. While steps 3, 4, and 5 are defined as the GA operator.

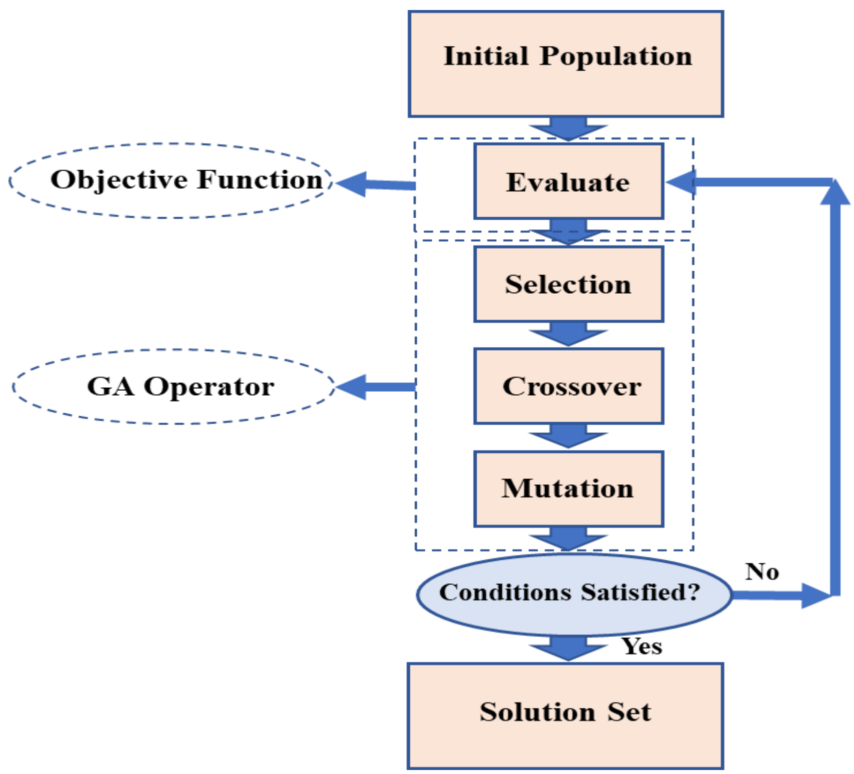

Figure 16. A schematic of general optimization process using GA operator.

Implementing the GA to model the performance of HVAC systems has been getting more and more attention lately. A study was conducted by (Nasruddin et al., 2019) examined the accuracy of implementing the ANN as a modeling tool to simulate the performance of HVAC systems while the multi-objective genetic algorithm was selected as the optimization tool. The case study building is equipped with two chillers, VAV chilled water AHU and dedicated outdoor units. The objective function of the study was to increase the human comfort level in the building while reducing energy consumption. The result of the study has shown that the ANN was able to accurately predict the objective function and its correlation with the input variables chosen for the study. Also, the multi-objective genetic algorithm has proven to be a powerful tool by pointing the optimal possible design that can satisfy both objectives without compromising any other aspects of the system's operation.

Another study has examined the effect of using optimized ANN models with GA on the power consumption of the chiller, the secondary chilled water pump, and the air handling unit. The study has compared the results of implementing those optimized models against the base case of a constant load and set points. The study has resulted in a 20% savings in terms of power consumption. Moreover, it was recorded that the COP (Coefficient of Performance) has increased by 28% compared to the base case scenario (Lee et al., 2014).

Following the same lead, another study by (Reynolds et al., 2018) has used ANN to model a zone-level case study while using the genetic algorithm for those models. The building was a small office building located in the UK. The building consists of six conditioned zones with electric heating and cooling with natural ventilation. The parameters that led the study were weather, occupancy, and indoor set-point temperature serving as inputs. In contrast, the objective function was to reduce energy consumption and cost. It was shown after analyzing the results that these optimization methods have reduced the energy consumption by 25% compared to the baseline case. The study also claimed that this process resulted in a better systems operation by shifting the load to a cheaper price period, resulting in a 27% reduction in energy cost compared to the base case.

While another study (Mtibaa et al., 2021) combined a model predictive control (MPC) strategy with GA, the MPC was utilized using dual-stream neural networks based on multivariate time series of controlled and uncontrolled inputs. The optimization process utilized GA to reduce energy consumption, peak demand, and discomfort during occupied hours under a self-tuned setpoint. The study claims using this approach resulted in 50% savings in energy consumption while reducing the discomfort levels by 80%.

Comping the GA with tools other than ANN has also resulted in significant accomplishments in the field of modeling and simulation of HVAC systems. For example, a study by (Garnier et al., 2015) examined a multizone non-residential building in France. The building HVAC systems have been modeled using the Predicted mean vote index (PMV) as an indicator for thermal comfort, while the GA was used to solve the optimization challenge. The study has determined the optimal time to tune the system on/off in both heating and cooling modes to reduce energy consumption. The research shows that this approach resulted in reducing energy consumption while maintaining thermal comfort levels.

Most of the previous studies have used GA as an optimization tool to automate the process of modeling and simulation. When the GA played an essential role in selecting the optimal model structure that will best predict the objective function, also, some studies used the GA in the data mining before modeling to optimize the training data for network improvement. An exciting study has used the GA to optimize the data used in modeling a power load prediction. The study by (LIN Z. 2019) has collected power load data and utilized the GA five steps shown in Figure 14 to remove the noise from the data sets and select a population of data that meets the selection requirements. The optimal training data sets were later inputted to support vector machine models to be tested and trained to predict the power. The study shows that this method has improved training efficiency, network performance, and prediction capabilities.

Following the same lead, A study by (Han et al., 2011) has investigated the faults in the chiller systems. This study has proposed a method of evaluating small subsets of the feature instead of one large set. The SVM tool was the modeling tool responsible for detecting the faults in the systems and evaluating the potential feature subsets that the GA was responsible for finding.

Chapter 3

Comparing between multiple machine learning algorithms

3.1 Introduction

With the current data availability and the need for more models to predict the HVAC systems' performance, and since buildings in the United States consume about 75% of the annual electricity production and 55% of the natural gas production (EIA, 2017), the most significant portion of that consumption is dedicated to the heating and cooling systems. Therefore, modeling those systems have become crucial. As a result, there have been lots of efforts in the aspect of designing the HVAC systems. Also, tremendous research efforts have been made in the area of modeling and simulation of HVAC systems. Many tools have been thoroughly discussed and evaluated as an artificial intelligence modeling technique that can be used to model the performance of HVAC systems.

A study by (Sakthivel et al., 2010;2009) has compared an artificial neural network, fuzzy logic, roughest-based methods, and support vector machine in capturing the faults in the performance of the Monoblock centrifugal pumps. The results have shown that the ANN-based fault classifier model is challenging to train. Still, it held higher accuracy results than the fuzzy logic and roughest-based methods, which held lower accuracy. However, the study has claimed the SVM to be the best modeling technique among the rest.

Another study followed the same lead of comparing multiple modeling tools and then deciding on the most suitable one serving the specific research need. The study developed fault detection and data analysis technique in AHU steam and chilled water valve leakage. The study was conducted while gathering data from 107 buildings on the campus of the University of Texas at Austin (UT Austin). The data were collected for a 15-minute interval over a span of 400 days. The study has compared multiple artificial intelligence modeling techniques. The models that were investigated were Logistic Regression (Log. Reg.), k-Nearest Neighbors (kNN), Support Vector Machine (SVM), Multi-Layer Perceptron Artificial Neural Network (MLP ANN), Classification and Regression Trees (CART), and Adaptive Boosting (AdaBoost). The models were examined in their ability to distinguish features from noise with minimal classification error quickly. Also, the tool's adaptability to the differences in data, the satisfaction of the modeling requirements, and minimal storage and computation requirements. It was found by this study that most models were able to predict the chilled water and steam leakage accurately. However, the Random Forest model had a slightly higher accuracy among all models but fulfilled one less design criterion. Therefore, the final decision was made to choose the decision tree model as the best modeling technique. It held the highest prediction accuracy value among the rest and fulfilled all the design criteria (McHugh et al., 2019).

Following the same lead, another study has compared the ANN and random forest ensemble learning method to predict hourly HVAC energy consumption in a hotel in Spain. The study has considered the occupancy measure as the primary variable that will affect the accuracy of the results. The study results have found that both modeling techniques are good predictors of HVAC energy consumption. However, when performing sensitivity analysis, the ANN model resulted in an RMSE value of 4.97. at the same time, the Random Forest resulted in a 6.10 RMSE value. Therefore, based on this statement, the ANN can be selected as the best modeling technique. However, the study has disclosed that the random forest model was an easier and faster model to train since it can deal with multi-dimensional complex data and it can perform internal cross-validation, unlike the ANN (Ahmad et al., 2017). Therefore, it is hard to decide which one is the best modeling technique, especially with a closer RMSE value for both models. Therefore, depending on the application, needs, availability of variables, requirements, and previous educated experience, will be the cutting edge in deciding the best modeling technique, whether accuracy, training time, complexity level, availability of the tool, etc.

After discussing the importance of building performance data and the types of modeling tools available nowadays and mentioning the reason behind choosing data-driven models and not physical models, the question now is, what is the most suitable technique for modeling the HVAC component? And why? Generally, no one tool can fit all but a method to decide on the best modeling tool for accurately modeling the components of HVAC systems as part of the purpose of this research will be proposed. Therefore, this chapter will examine the three modeling techniques: artificial neural netwar (ANN), bootstrap aggregation, and support vector machine (SVM), and compare them to decide on the best tool to serve our specific research goal.

3.2 Methodology

The proposed tools were tested and trained using the same data set, predicting the same output for a clear comparison. To accomplish the objective of choosing the best artificial intelligence modeling technique. The supply air temperature was selected to be predicted as a function of (1) chilled water temperature, (2) chilled water valve position, (3) mixed air temperature, (4) supply airflow. Those inputs and outputs are selected based on previous experience, as most cooling coils component's structure.

The available data were limited for this section that was done earlier at the beginning of the research project. So, previously available data from an existing building located in North Carolina was used. Later more recent data from an existing lab became available to finish the remaining objectives of this research. Therefore, those data will be used only in this section.

3.2.1 Building description and data collection

The New Academic Classroom Building is located in North Carolina, A&T State University, Greensboro, NC. This three-story, eighty-eight thousand square foot structure is a multi-use classroom building conditioned by typical VAV systems. The mechanical system for this building consists of six Air Handling Units (AHUs) with variable frequency drives (VFD) and a chilled water central plant with two chillers. The arrangement for each AHU includes supply and return fans, exhaust, return, bypass, and outside air (OA) dampers, and heating and cooling coils. The entire chilled water (CHW) system connects to a global automated system, which supervises the activity of this system, and other HVAC systems throughout North Carolina A&T's campus. In addition, the building is equipped with a BAS system. For this study, the third-floor air handling unit four (AHU-3-4) in the New Academic Classroom Building is selected for examination.

As seen in Figure 17, the BAS displays several system measurements such as damper positions, fan power, fan pressure, and ambient air conditions. Those data were recorded.

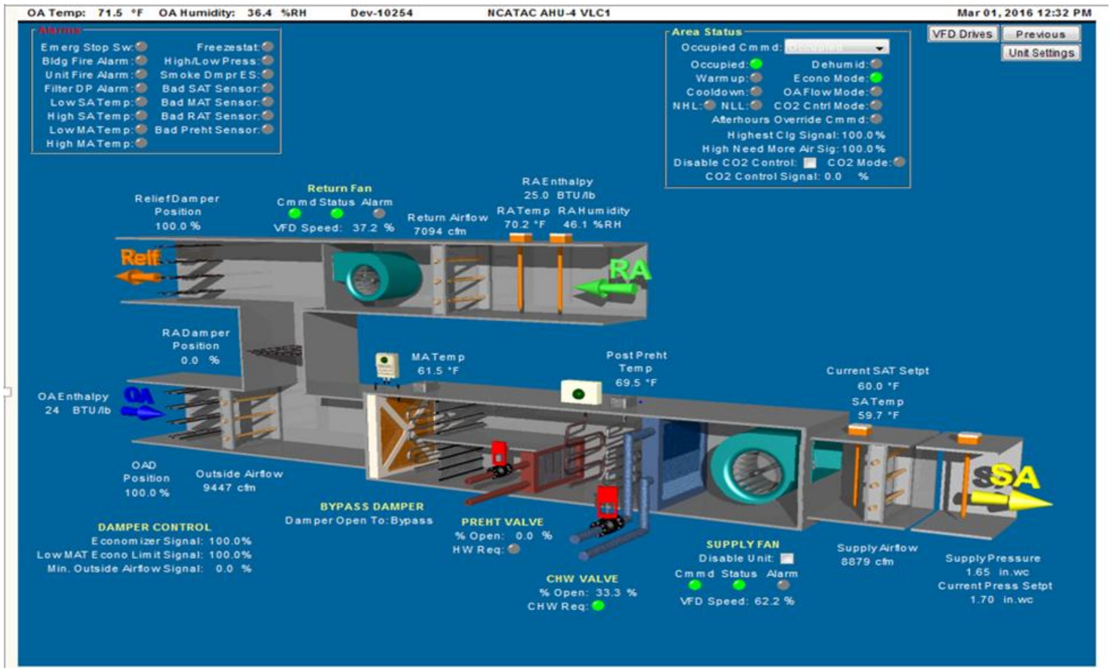

Figure 17. BAS's GUI for the Academic Classroom Building's AHU-4

The observed data from the building automation system were organized into a spreadsheet to prepare the model creation. The CHW system was run at five-minute time intervals from November 2014 to February 2015. In total, 28,767 sample points were collected from the system, representing more than 100 hours of system run time. Table 1 below shows the data that was collected from the BAS system.

Table 1. A sample of the collected data from the BAS system

Abbreviated terms	Description
Qsys	Supply airflow (CFM)
T_{cws}	Chilled water temperature (°F)
CH $_{VLV}$	Chilled water valve position (°F)
T_m	Mixed air temperature (°F)
T_s	Supply air temperature (°F)

After all the measurements have been downloaded into a spreadsheet, it is properly sorted to remove undesirable data. It is important to note that the BAS software continuously records measurements, even if the CHW system is turned off. These points are removed because they are repetitive and won't improve the learning capabilities of the ANN models. Since the scope of this experiment is limited to modeling steady-state performance, and would also not be beneficial to developing the neural network models. Once all the null data points are removed, the total sample data size is reduced to close to 26,789 points.

After the data filtering, the collected data is split into two samples designated for training and testing. This task is performed because it is desired that the models generate reproducible results. Of the data collected, the training set will consist of two months of data, while one month of data is selected to test the models. Now that the data is filtered and organized into two sets developing the models can begin.

3.2.2 Experimental setup and basis of comparison

To evaluate several data-based modeling techniques, we proposed to create different models. Each model will utilize one of those techniques. The models will use the same inputs and output data to be tested and trained. Then the models will be compared, and the best-fitted model will be used selected as the modeling technique for this research. Three predictive modeling techniques were chosen to be evaluated in this research. Those models were:

Model (1): Support Vector Machine (SVM)

Model (2): Artificial Neural Network (ANN)

Model (3): Bootstrap Aggregation (BSA)

After the three models were tested and trained, we examined how well the model fits the data. There is a lot of statistical metrics that are available to test and validate the model performance. Some are discussed in chapter 2. Many recent kinds of research have addressed using such metrics to evaluate the performance of predictive energy models. However, the types of metrics used to assess the performance of energy models have been an argument topic for a while now. And there will always be an argument that there are no conclusive statistical cut-off criteria for model goodness-of-fit directories (Reddy et al., 2000).

A recent study done by (Chakraborty et al., 2018) claimed that RN_RMSE when used in tandem with $R^{2,}$ can provide a more meaningful and accurate representation of the performance of system-level energy models. And R^2 is one of the model performance evaluation tools broadly used for model testing and validation (Van Liew et al., 2003). Therefore, another study was conducted to evaluate the ASHRAE guideline 14 old metrics that used the R^2 and CV(RMSE) as a measure for model accuracy. The study showed that the correlations between input and output error measures were not statistically significant, implying that the metrics put forth in ASHRAE Guideline 14 are as good as any other binary metrics tested (Garrett et al., 2016).

R^2 is better used to compare several models in terms of how well the model fits the data (Ahmed et al. 2014 and Chua Wang et al., 2009). Moreover, both IPMVP (International Performance Measurement and Verification Protocol) and ASHRAE Guideline 14 indicate that R^2 is the most important criterion by which a model's validity and usefulness should be assessed.

Therefore, in this chapter, we used R^2 to examine the fitness of the model. R^2 (coefficient of determination) is the proportion of variation in the outcome values explained by the predictor variables (inputs). R^2 can be represented mathematically by equation 17.

$$R^2 = 1 - \frac{\sum_{k=1}^{n}(Y_K - \widehat{Y_k})^2}{\sum_{k=1}^{n}(Y_K - \mu)^2} \quad \ldots\ldots\ldots\ldots\ldots\ldots \text{(17)}$$

In other words, R^2 tells us how well the model fits the data (goodness of fit). The R^2 value can range from 0-1. The Higher the R^2, the better the model. An R^2 that is close to one refers to a perfect fit, while a value close to Zero or negative indicates a flawed fit model (ASHRAE guideline 14). For example, an R^2 value of 0.9 may be translated as 90% of the variance in the baseline is explained by the modeled values.

3.3 Results

The selected inputs to feed the created models were chilled water temperature, chilled water valve position, mixed air temperature, and supply airflow. At the same time, the output was the supply air temperature. Figure 18 shows that predicting the supply air temperature based on the four inputs chosen to create the model's structure. We notice that all three models held high R^2 values to train the specific dataset provided from the results above. The Bootstrap Aggregation achieved the highest testing R^2 value of 97.3%.

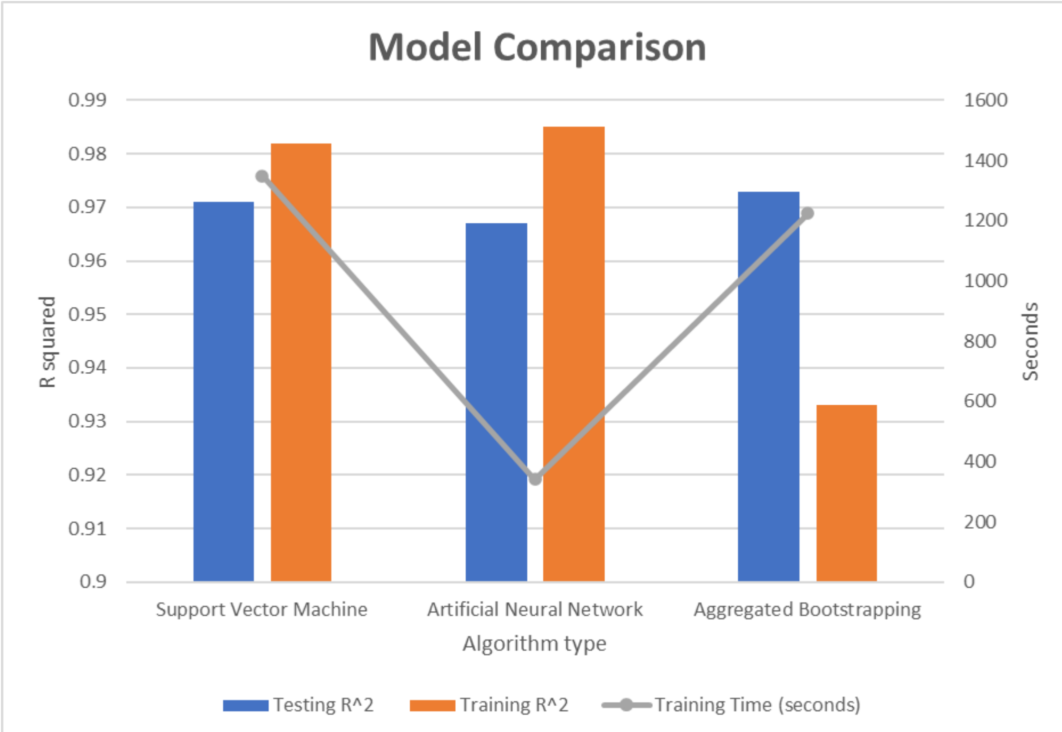

Figure 18. Comparison of model fitness (R^2)

Table 2 shows a comparison in training time between all three models. The Artificial Neural Network had the lowest training time at 341.3 seconds. Therefore, the artificial neural networks tool was selected as the modeling technique.

Table 2. Comparison of Model Training Times

Model	**Training Time (s)**
Support Vector Machine	1349.3
Artificial Neural Network	341.3
Aggregated Bootstrapping	1225.1

3.4 Discussion

By looking at the previous studies, (Ahmad et al., 2017) performed the same concept in a study in Spain to compare between the ANN and BSA. The study has found that both had higher RMSE values. However, the BSA was found to be faster and easier to train. The study claimed that both tools are suitable methods in predicting the HVAC energy consumption. However, the study left the answer vague that it depends on the application type.

Many other previous studies claimed it is hard to decide which one is the best modeling technique, especially with a comparable accuracy value for the selected models. Therefore, depending on the application, needs, availability of variables, requirements, and previous educated experience, will be the cutting edge in deciding the best modeling technique, whether accuracy, training time, complexity level, availability of the tool, etc.

For the bootstrap aggregation model, it is true that it held the highest R^2 value, but its training time was almost four times as much as that for the neural network model. Also, the training time has increased with the increase in training set size. While, the artificial neural networks had the lowest training time for this research, which is less than 6 minutes. However, keep in mind that the training set was a small set, and the training time will be increasing with the increment in the complexity of the model and the training set size.

And this research aims to create an optimization process that will optimize the system setpoints to reduce the energy consumption every 15 minutes. A fast tool that can compute the needed results in less than 10 minutes was required. Meaning, training time was the cutting edge in choosing the most suitable modeling tool due to the complexity of the component being molded. Therefore, the artificial neural networks tool was selected as the modeling technique to carry out this research. Because it held the lowest training time comparing to the other models.

Chapter 4

Develop an accurate component data-driven modeling and optimization technique

4.1 Introduction

This chapter will first examine the inner structure of neural networks and how they were developed to serve our purpose. Later the structure of each component model using ANN will be discussed, showing the inputs and outputs of each model and the created structure. However, to link these data-based component models to obtain the whole system model, some equations (not the data-drive model) were also used. For instance, equations from the ASHRAE standard 62 to calculate the ventilation requirements were used, as will be shown later. Afterward, a model-level optimization process (MLO) using GA will be implemented to automate the process and select the best model structure that holds the lowest error value. GA was chosen to solve the optimization process due to its capability of handling a wide range of variables at one time, the ability to work with complex simulation programs, proven to be effective in solving complex problems that cannot be easily solved with traditional optimization methods, and it is a publicly available user-friendly tool.

The ANN models are a universal approximation mechanism (Livshin, I., 2019). Meaning the built network can predict the value of any function at some arguments (X). The function that will be later used for training the network. But first, the function needs to be approximated using points within the range of the training set. Later this approximated function will be used to find the function values of any point of interest.

As previously discussed in chapter 2. Each artificial neural network consists of input, hidden, and output layers, starting from left to right. Each connection between the layers carries a weight. The initial network will require assigning a random weight to those connections, and this weight will be adjusted in later iterations. The number of hidden layers depends on the complexity of the function. Approximating the initial function will be done through mathematical calculations carried by the hidden layers. The number of hidden layers that lead to the best approximation is usually determined experimentally.

To create HVAC component models using artificial neural networks the network needs to be tested and trained (Mohanraj et al., 2012). Moving from left to right is called a forward pass, where the input layer sends the input for the hidden layer to calculate the output and send it through the output layer. The error value will be calculated, and if not sufficient, the backward pass (backpropagation) will happen from right to left. To adjust the layers' weight to reduce the error between the network output and the desired output. This process is called training the network. The training process is terminated automatically when the error falls below the desired value.

Since the ANNs are adaptive by nature and they learn by example. The trained network includes all the weights and bias parameters that predict a specific function with the desired degree of precision. Later this network structure can be used on a set of input data representing the function to predict an output within predefined error value limits. This process is called testing the network.

As previously mentioned, HVAC systems are complex nonlinear systems. Therefore, detailed information about each component and solid knowledge of the heat and mass transfer laws while defining the variables and parameters of the process becomes crucial. To develop a more accurate model, the variables that can be adjusted to create the model structure chosen for this research are; the number of neurons, time delay, and feedback delay.

Number of Neurons: This factor is one of the most influential parameters in the performance of ANN. Although more neurons require more computation, their implementation might result in more efficiency for solving complex problems. The hidden neuron can influence the error on the nodes to which their output is connected. The stability of the neural network is estimated by error. The minimal error reflects better strength, and the higher error reflects the worst stability. The excessive hidden neurons will cause overfitting; that is, the neural networks have overestimated the complexity of the target problem. The model order is designed to help increase the model's probability of fitting the data, but one must take caution when increasing the order. The increase of order may allow one's model to fit more points, but the addition of parameters may not necessarily represent the system being studies. In this sense, determining the proper number of hidden neurons to prevent overfitting is critical in the prediction problem.

Time delay: A time delay may be defined as the time interval between the start of an event at one point in a system and its resulting action at another point (O'Dwyer, 2003). In the modeling field, delays are also known as the time lag or dead time of a system. For example, a time delay of 3 means a delay of three sampling periods. The Artificial Neural Network process aims to develop several estimation models, all of which its parameters can be varied.

Feedback delay: feedback delay is a system structure that eventually causes output from one node to influence input to that same node. For this investigation, the Feedback delay used ranges from1-3.

Optimization of the ANN network is a significant task. The parameters that affect the structure of the network can be optimized to choose the optimal model structure. Optimization of HVAC systems was analyzed in previous studies. Optimization is vital to overcome the limitation that comes with modeling using ANN. Genetic algorithm (GA) was introduced to optimize the network parameters. The optimal model structure selected using GA will minimize the time and effort. GA is an excellent method to automate the process of trial and error used to manually determine the optimal model structure (Mohebbi et al., 2008).

Genetic algorithm (GA) is a technique used to systemize the searching for an optimal solution. GA considers a solution as an individual, and a population is a group of individuals. The three main genetic operators are reproduction, crossover, and mutation. A genetic algorithm starts by generating several solutions to a problem, evaluates them, and applies the basic genetic operators to that initial population according to the individual fitness of each individual. This process generates a new population with higher average fitness than the previous one, which will be evaluated. This process is repeated for the number of generations set by the user, dependent on problem complexity (Galdas et al., 2003).

4.2 Methodology

After choosing the ANN as the modeling technique, a data-driven model will be developed for each component of the AHU unit using ANN. The inputs and outputs of each model are tuned to create the structure of each model. Later, a parametric study will be conducted to test the performance of each model. The testing results will be compared against the actual system performance data to choose the optimal model structure with the lowest error value.

Moreover, an optimization technique will be used to automate this process and help select the best model structure. Finally, the optimization results will be compared against the parametric study results to validate the results.

An ANN model will be carried out using four steps (Mohanraj et al. 2012): (1) extract the results or data (2) train the network using experimentally or theoretically predicted values (3) test the network with the data that are not used for training (4) identify the best network structure.

The created model's accuracy is tested in terms of MSE (Mean Square Error) and CV% (Coefficient of Variance), representing the error values of the models in predicting the actual performance. The model parameters that were adjusted in each iteration to get the best model structure are:

1. The number of hidden layers of neurons (N). For this investigation, the number of neurons that will be used ranges from 1-100.
2. Feedback delay (FD). The FD in this study is measured by minutes. Each FD period is 5 minutes, and the total feedback delay is fifteen minutes.
3. Time delay (ID). The ID is measured in minutes for this experiment. And to match the FD, the time delay will range from 1-3 intervals of 5 minutes for each interval resulting in a total of 15 minutes of delay.

Figure 19 shows a schematic of the modeling process using ANN.

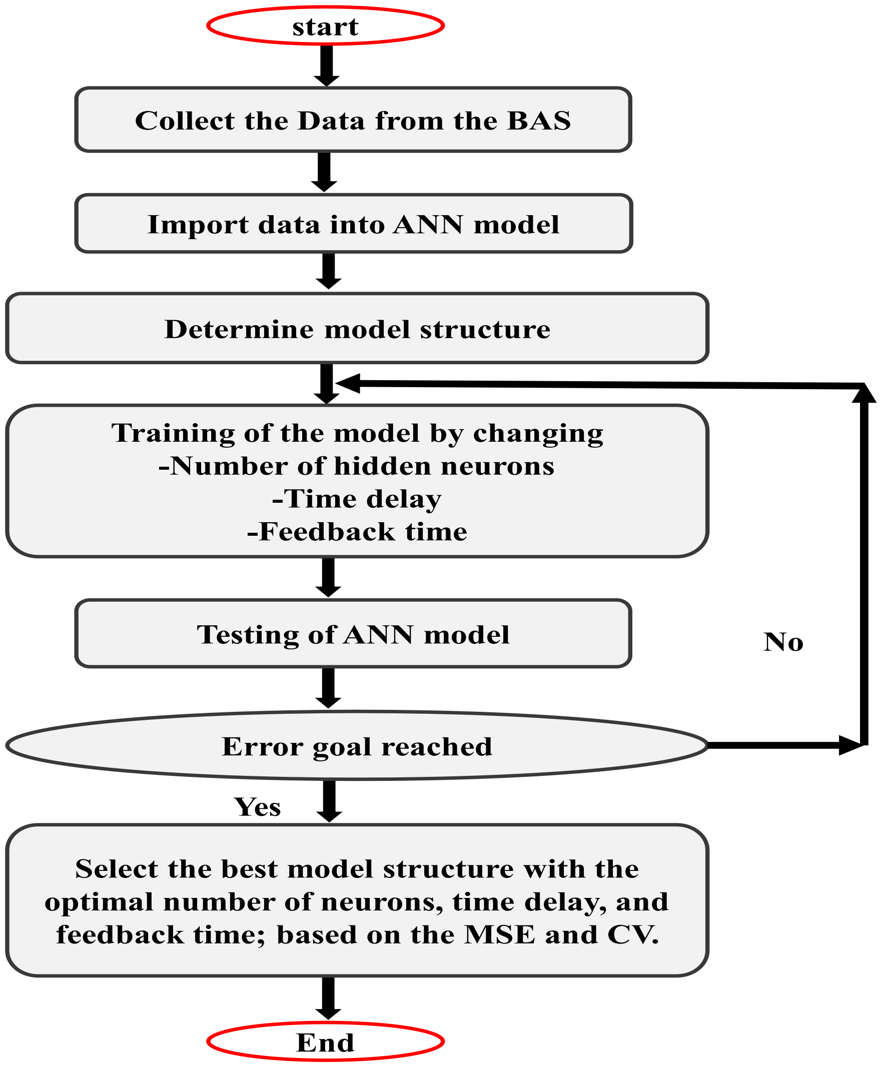

Figure 19. A schematic of the modeling process using ANN.

The two HVAC systems examined in this research are the chilled water VAV system and direct expansion (DX) systems. The chilled water systems consisted of an airside represented by the air handling unit (AHU) and a waterside represented by the chiller and boiler. In contrast, the DX system is an airside only.

To achieve the research objective, the components of the Chilled water VAV system need to be modeled and optimized. The components that will be modeled and optimized are the cooling coil, heating coil, fan power, zone level model, and reheat coils. Figure 20 shows a schematic of the chilled water VAV system airside and its components.

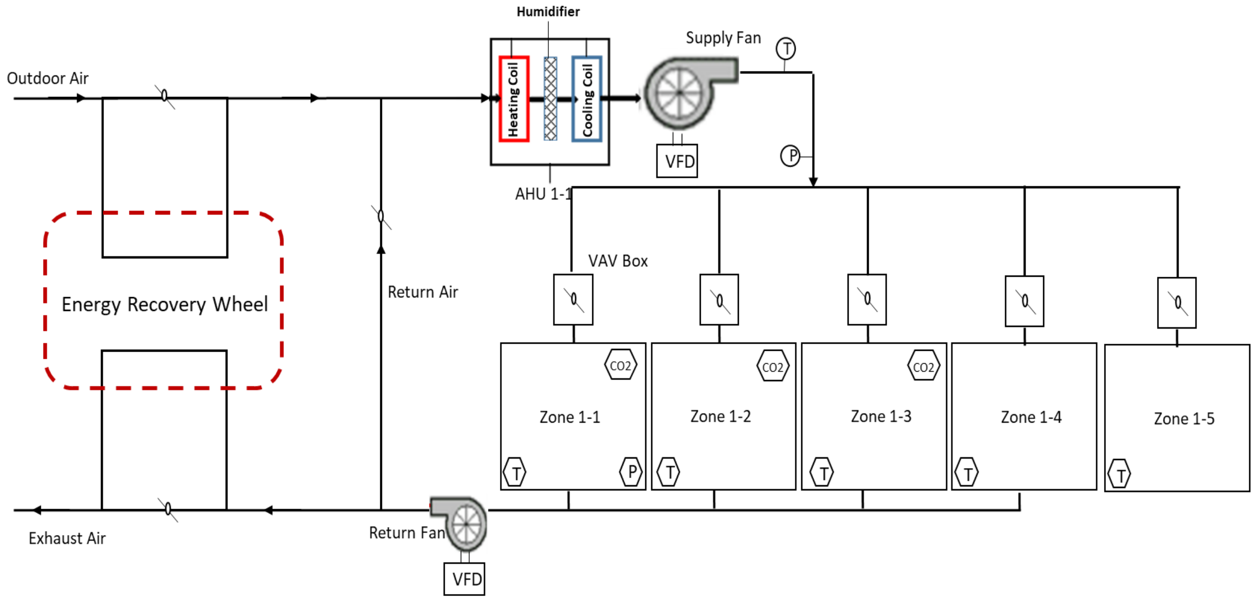

Figure 20. Typical chilled water variable air volume AHU schematic

While for the waterside, the chiller, boiler, chiller pumps, and boiler pumps will be modeled and optimized. Figure 21 shows a schematic of the chilled water variable air volume airside and its connection to the waterside.

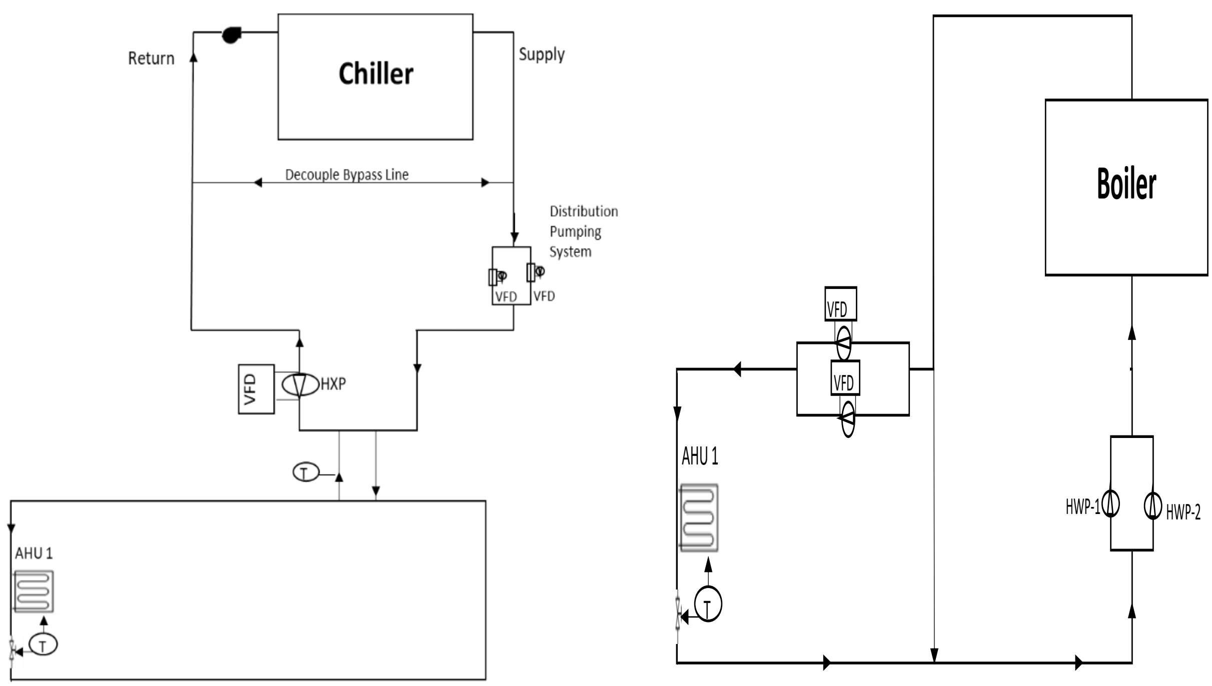

(A) (B)

Figure 21. Chilled water variable air volume system schematic. (A) The chiller and its connection to the AHU, (B) the boiler, and its relationship to the AHU.

While for the Dx system, an air-only system, the components that will be modeled and optimized are the DX cooling coil, DX heating coil, fan power, and zone level model. Figure 22 shows a schematic of the Dx system and its components.

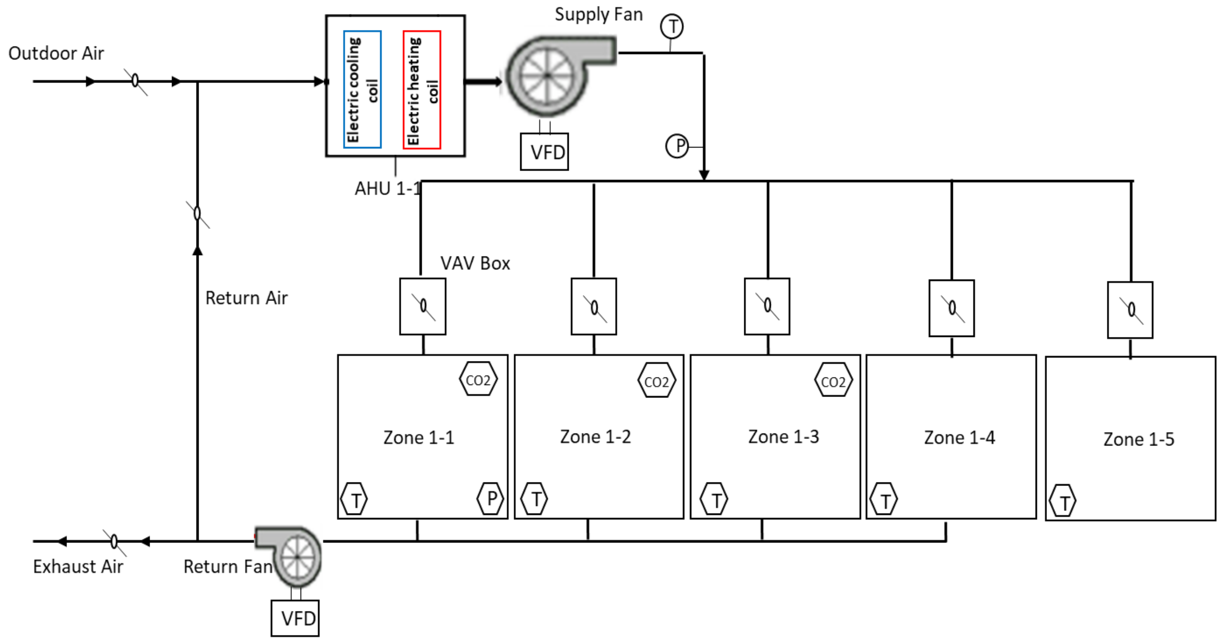

Figure 22. Typical Direct expansion system schematic

After the modeling process is complete and the models' structures are established, a model level optimization (MLO) will be implemented to automate the process. The optimization process will help in selecting the best model structure that holds the lowest error values. GA was chosen to be used to solve the optimization process for this research for multiple reasons.

- Other optimization approaches require substantial alteration, while GA is an easily understood approach that can be used in a wide range of applications.
- The capability of GA to handle a wide range of variables at one time. Without overfitting or requiring an extended period.
- GA has the capability to work with complex simulation programs.
- GA is Proven effective in solving complex problems that cannot be easily solved with other optimization methods.
- GA is publicly available, user-friendly, and easily implemented GA codes.

4.2.1 Data collection

Data were collected from the Building Energy Assessments, Solutions, and Technologies (BEAST) lab to conduct this research. BEAST is a multidisciplinary research lab focusing on building energy solutions and intelligent building technologies. BEAST is 2500 ft^2, room 209 (around 1700 ft^2) and room 203 (about 800 ft^2), located at the University of Cincinnati, Cincinnati, Ohio. The lab is intended to serve as educational and research resources and have the flexibility to address a wide range of research studies and provide training and educational tools. In addition, the lab is a unique facility for research, training, professional certification, outreach activities, and workshops (BEAST lab, 2020).

The lab is equipped with several full-scale multi-zone HVAC systems. The systems are (1) chilled water VAV system, (2) DX VAV system, (3) four-pipe fan coil units, and (4) Variable Refrigerant Flow VRF. The systems serve three 8 by 8 ft.-controlled zones. The chilled water VAV system and DX multi-zone VAV systems share the same air distribution system with three single-duct hot-water reheat VAV boxes, providing cold and warm air to meet the cooling or heating loads in the zones. The heating or cooling loads can be artificially introduced in each zone. At the same time, the chilled and hot water is provided to the terminal units through the chilled water central plant and hot water central plant. Figure 23 shows a layout of the BEAST lab.

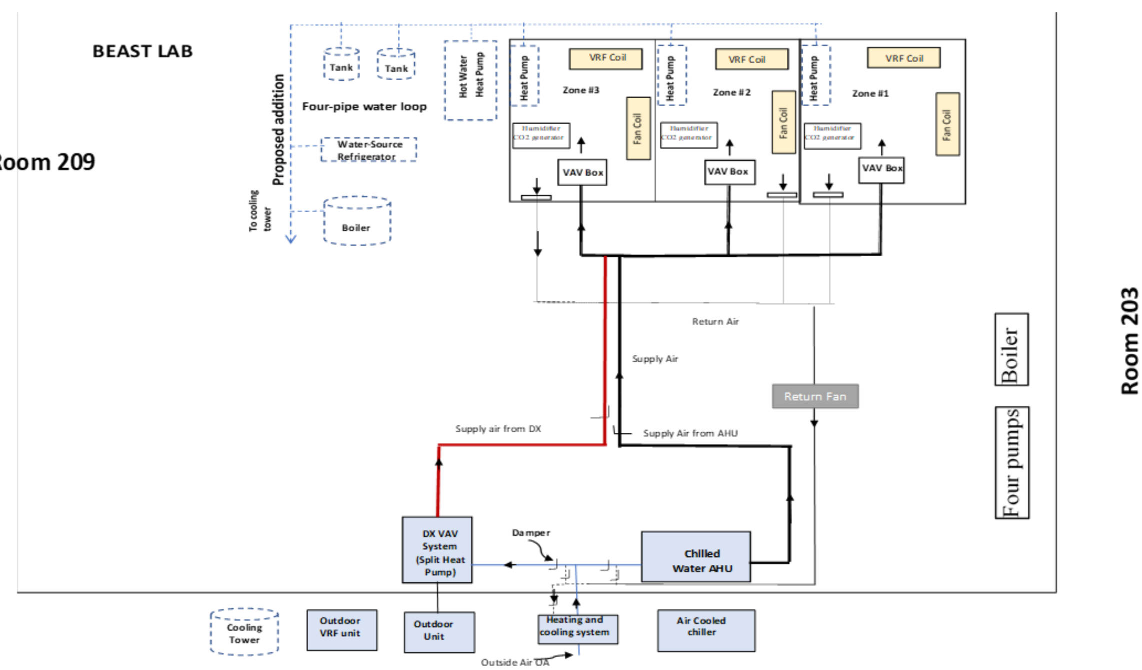

(A)

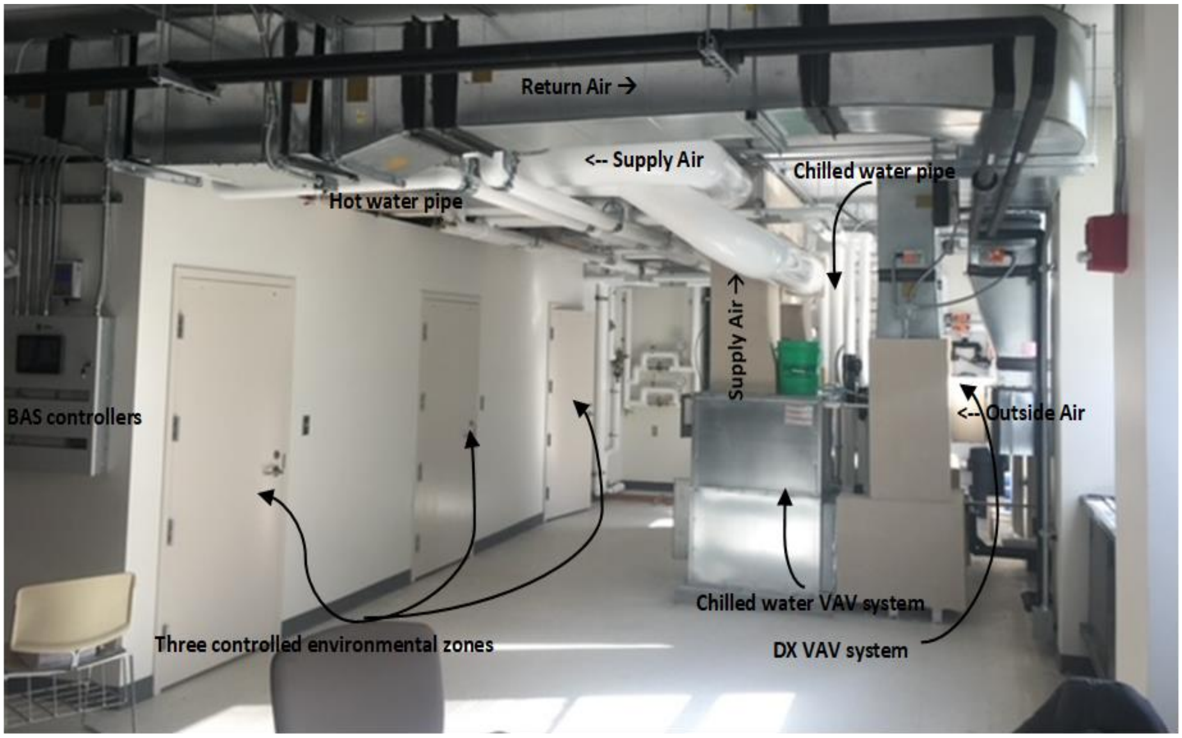

(B)

Figure 23. (A) BEAST schematic layout. (B) BEAST lab after the equipment installation.

The operation and control of all equipment are achieved through a "real" web-based building automation system integrated with MATLAB-based monitoring and many computational energy solution tools.

The chilled water system consists of an AHU equipped with a cooling and heating coil, return and supply fan, dampers, and filters. This system serves the zones with VAV boxes provided with hot water reheat. Figure 24 shows the chilled water VAV system.

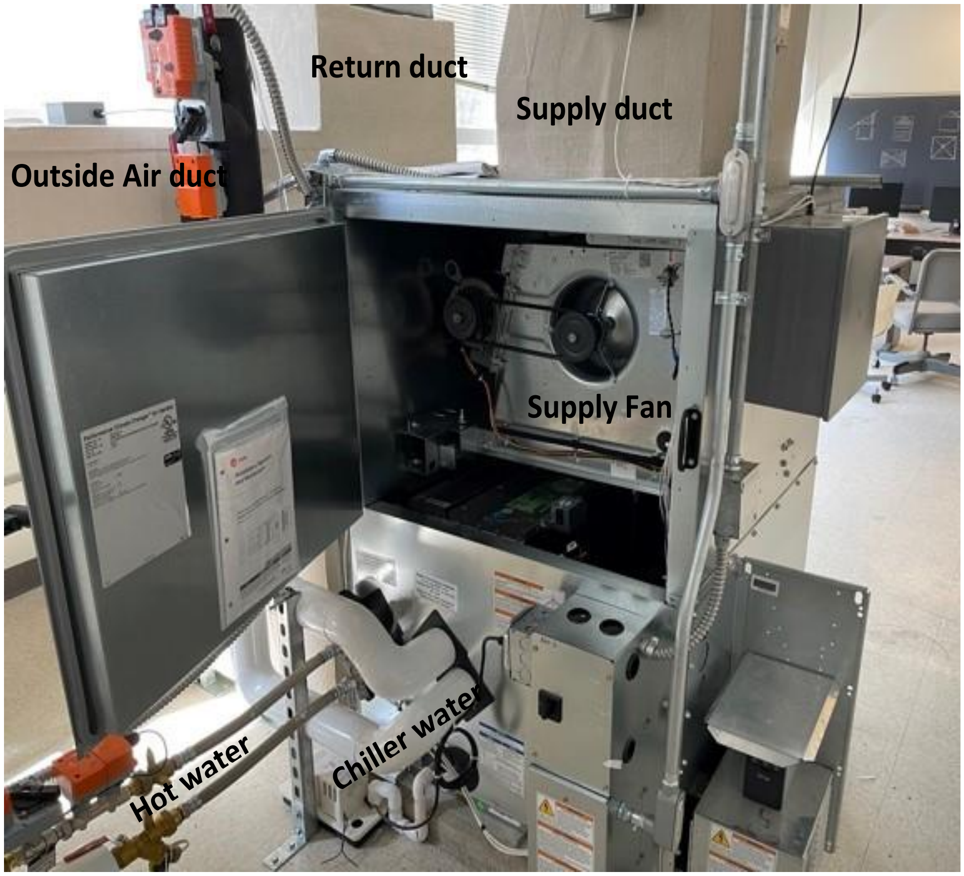

Figure 24. Chilled water VAV system.

The chilled water system has four control loops: space control loops, supply air temperature SAT control loop, duct static pressure control loop, and ventilation control loop. Also, the system utilized the use of the economizer. Therefore, if the outside air temperature is proper, the control strategies activate the economizer to result in free cooling by introducing the appropriate amount of fresh air. Figure 25 shows the control display of the system.

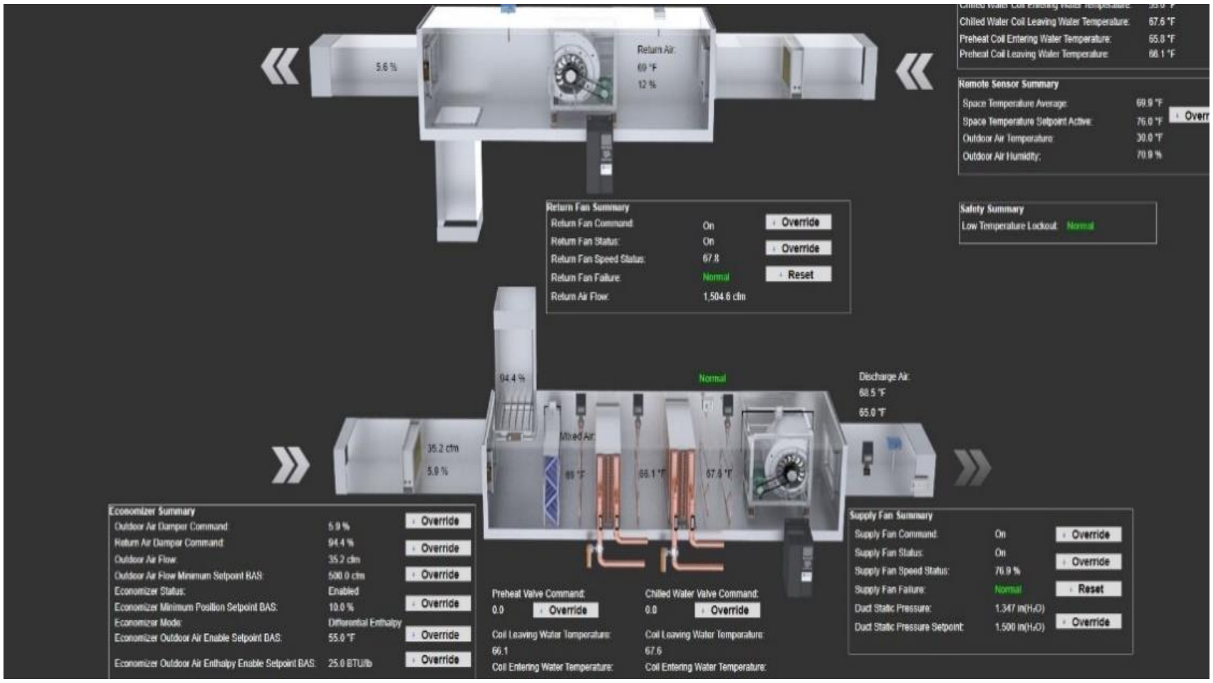

Figure 25. Control display of the chilled water VAV system.

The system is equipped with a supply and return fan responsible for the air circulation. The controlling system also controls the return fan designed to bring the air back from the zones to central chilled water AHU and maintain a positive pressure in the zones. Figure 26 shows the layout of the return fan.

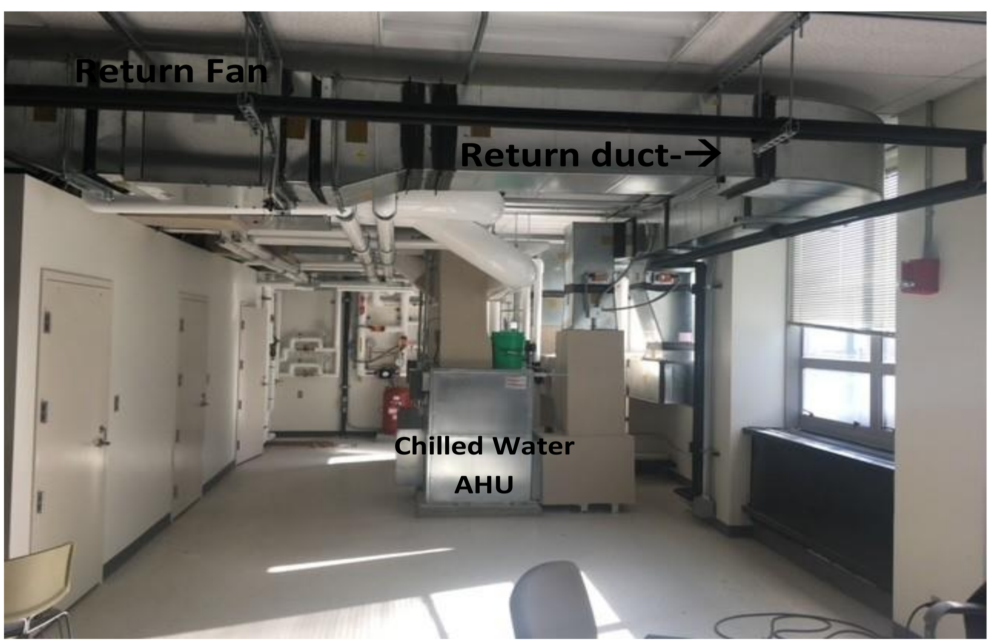

(A)

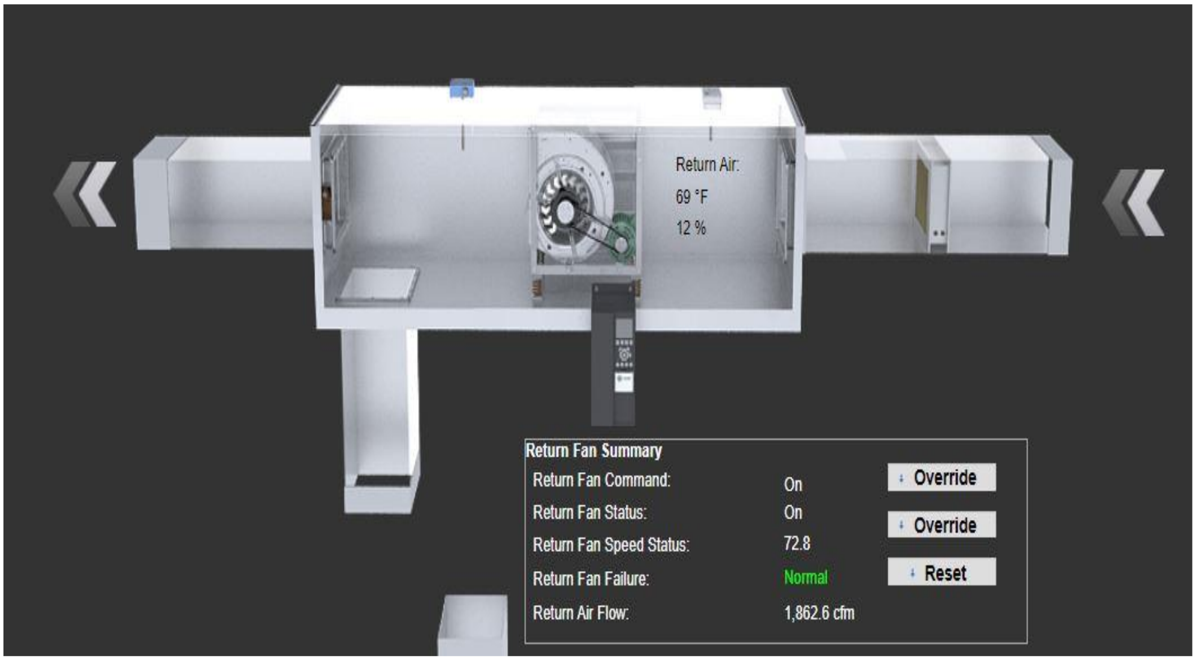

(B)

Figure 26. (A) The chilled water system's return fan layout (B) Control display of the return fan

While the central plant side of the lab is represented by the chilled water central plant (chiller) and the hot water central plant (boiler). The chilled water system consists of one air-cooled chiller with two pumps, as shown in figure 27.

Figure 27. Chilled water central plant pictures.

While the water distribution system consists of a primary-secondary configuration or a primary-only configuration, as shown in figure 28.

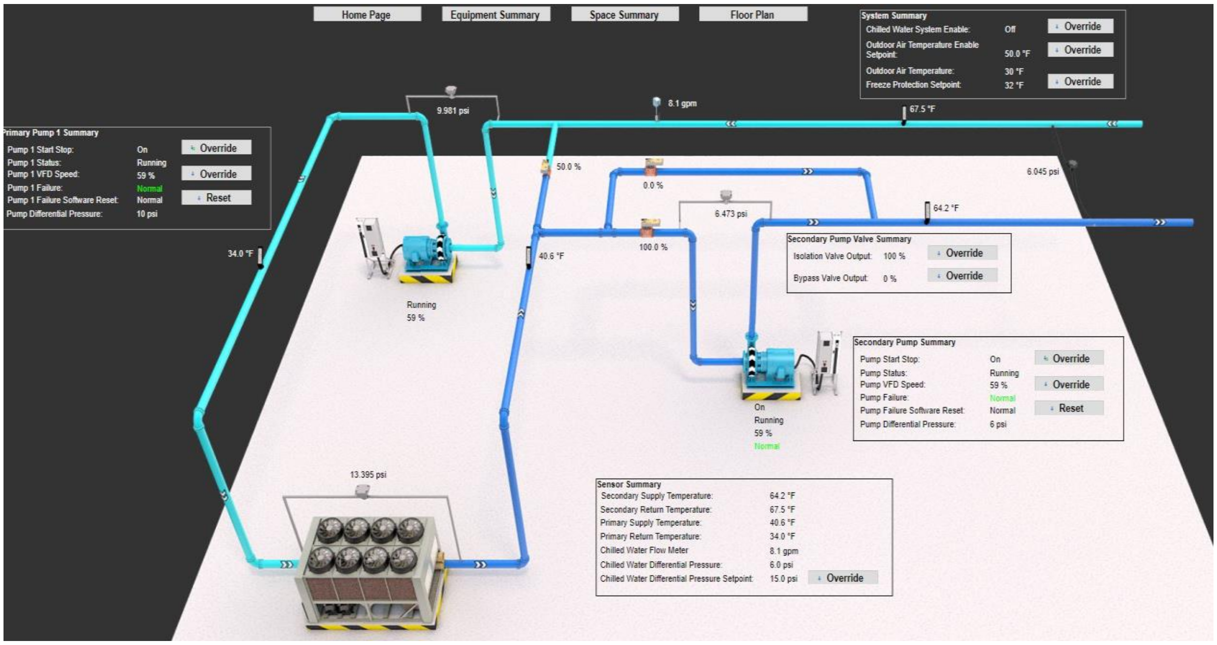

Figure 28. Control display of the chilled water central plant.

On the other hand, the hot water central plant consists of one electric boiler shown in figure 29 and two pumps. Unlike the chilled water that only serves the cooling coil in the AHU, the hot water system serves the AHU heating coil, and the VAV boxes reheat coils required for the reheating process.

Figure 29. Photo of boiler and hot water piping system.

Like the chilled water side, the hot water system has two piping configurations primary-secondary configuration or a primary-only configuration, as shown in figure 30.

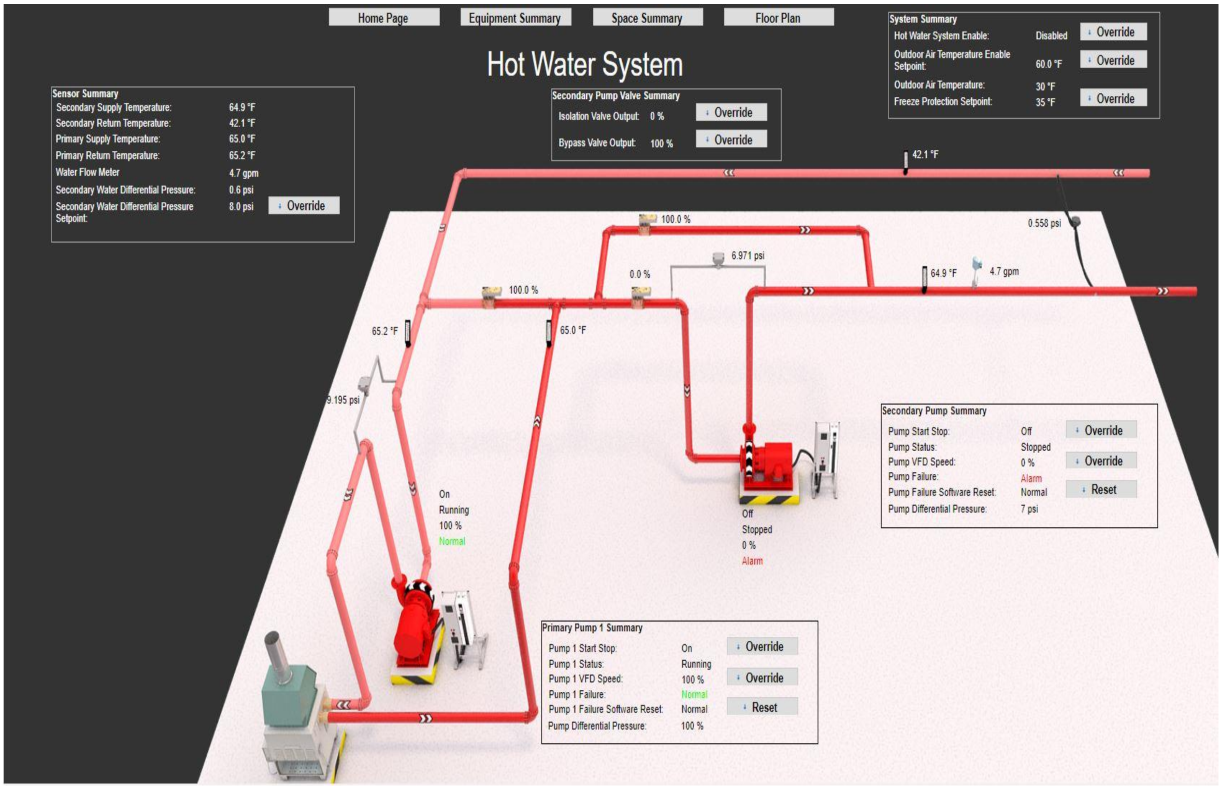

Figure 30. hot water system configuration.

Finally, the DX VAV system shown in figure 31 is an air-sourced heat pump consisting of a cooling and heating coil, fans, filters, dampers, etc. This system will also serve the three insulated zones. The dampers are controlled with the economizer strategy as well.

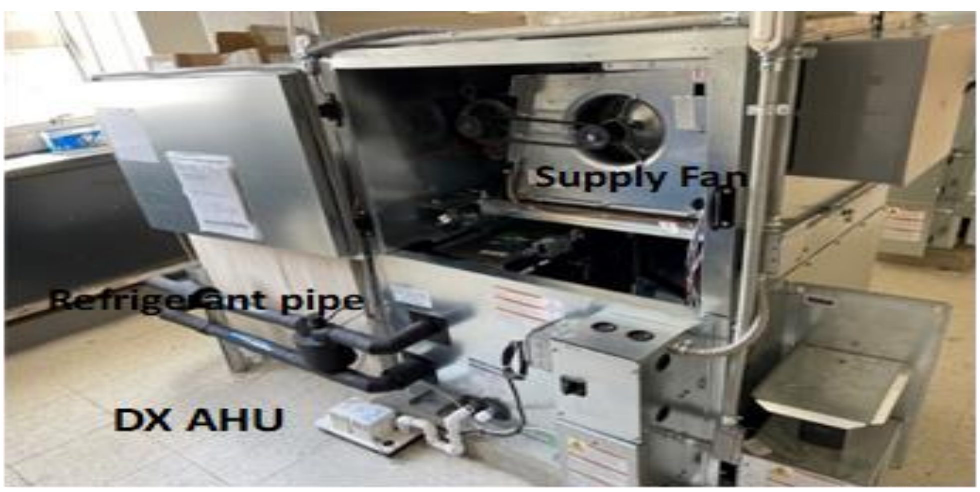

Figure 31. DX VAV system

The DX system serves the three zones through the same VAV boxes. The DX system has the same primary four control loops that the chilled water system has. Space control loops, supply air temperature, SAT control loop, duct static pressure control loop, and ventilation control loop, as shown in figure 32. The DX system is also equipped with a supply and return fan to circulate the air and maintain a positive pressure in the served zones.

Figure 32. Control display of DX VAV system.

The chilled water AHU and DX AHU can operate simultaneously; one supplies cold air, and the other supplies warm air to the three zones (testing chambers) through dual duct VAV boxes. Each zone is served by VAV boxes operating as single or dual inlet VAV boxes. This configuration allows the system to work as single or dual-duct VAV systems, as shown in figure 33.

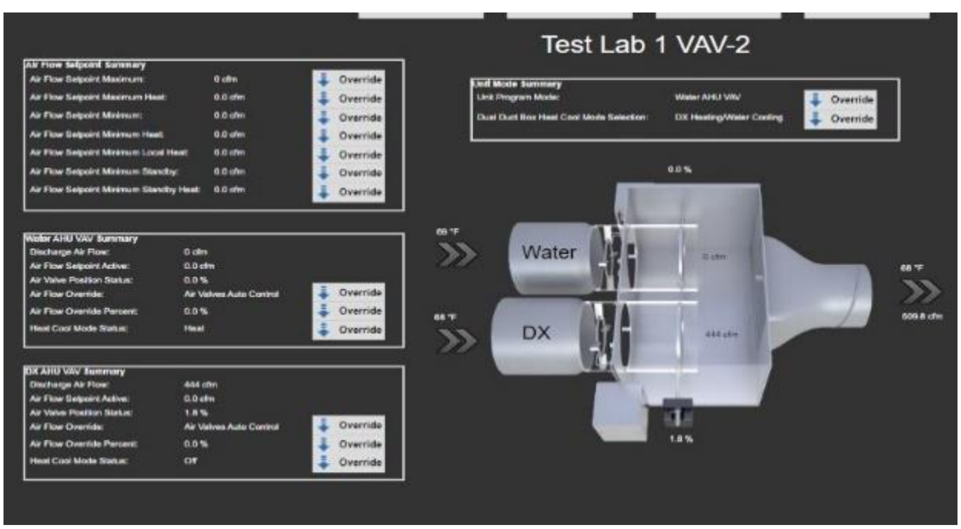

(A)

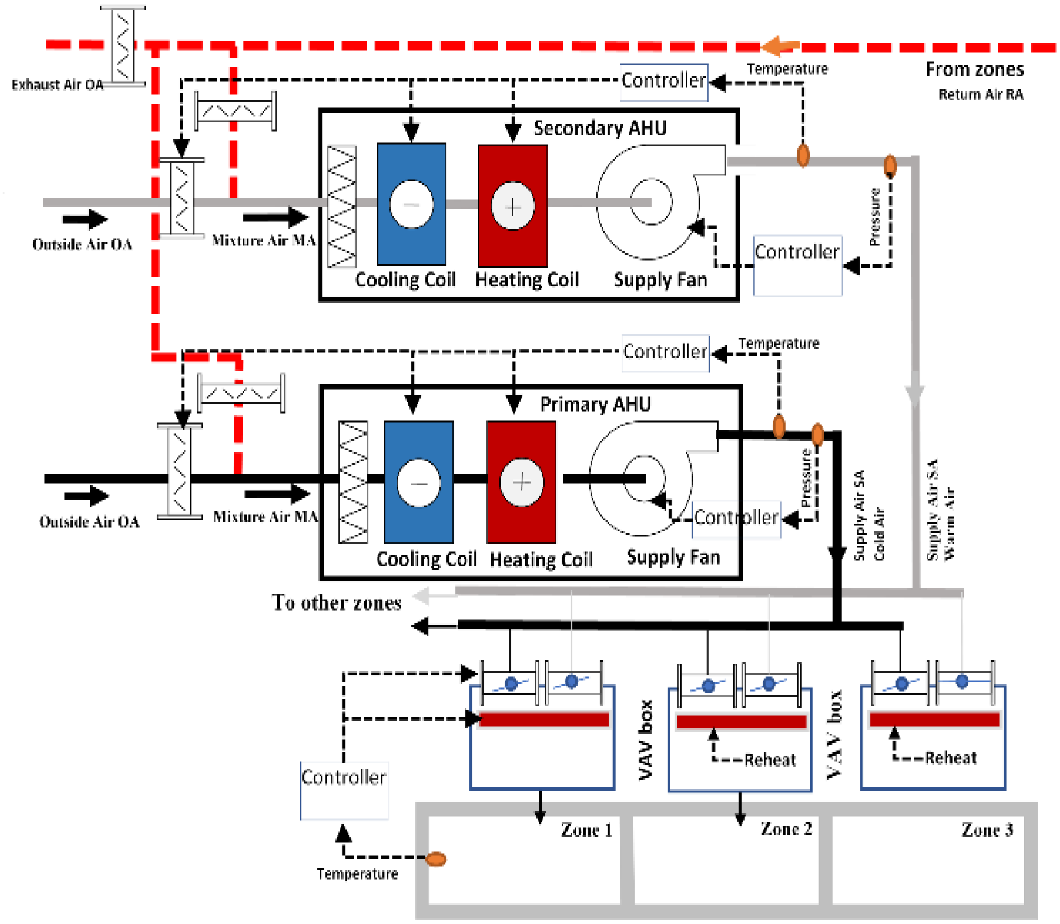

(B)

Figure 33. (A) Control display of dual duct systems Dx system. (B) Dual duct systems schematic.

Performance data were collected over a period of three months. First, the chilled water VAV system and the DX system readings were recorded every 1 minute. Later, data were organized and transferred into Excel sheets to be prepared for experimenting. Figure 34 shows a small sample of the performance data that were collected. The data are from April 26th, showing the supply airflow rate for both the chilled water VAV system and DX system against their power consumption.

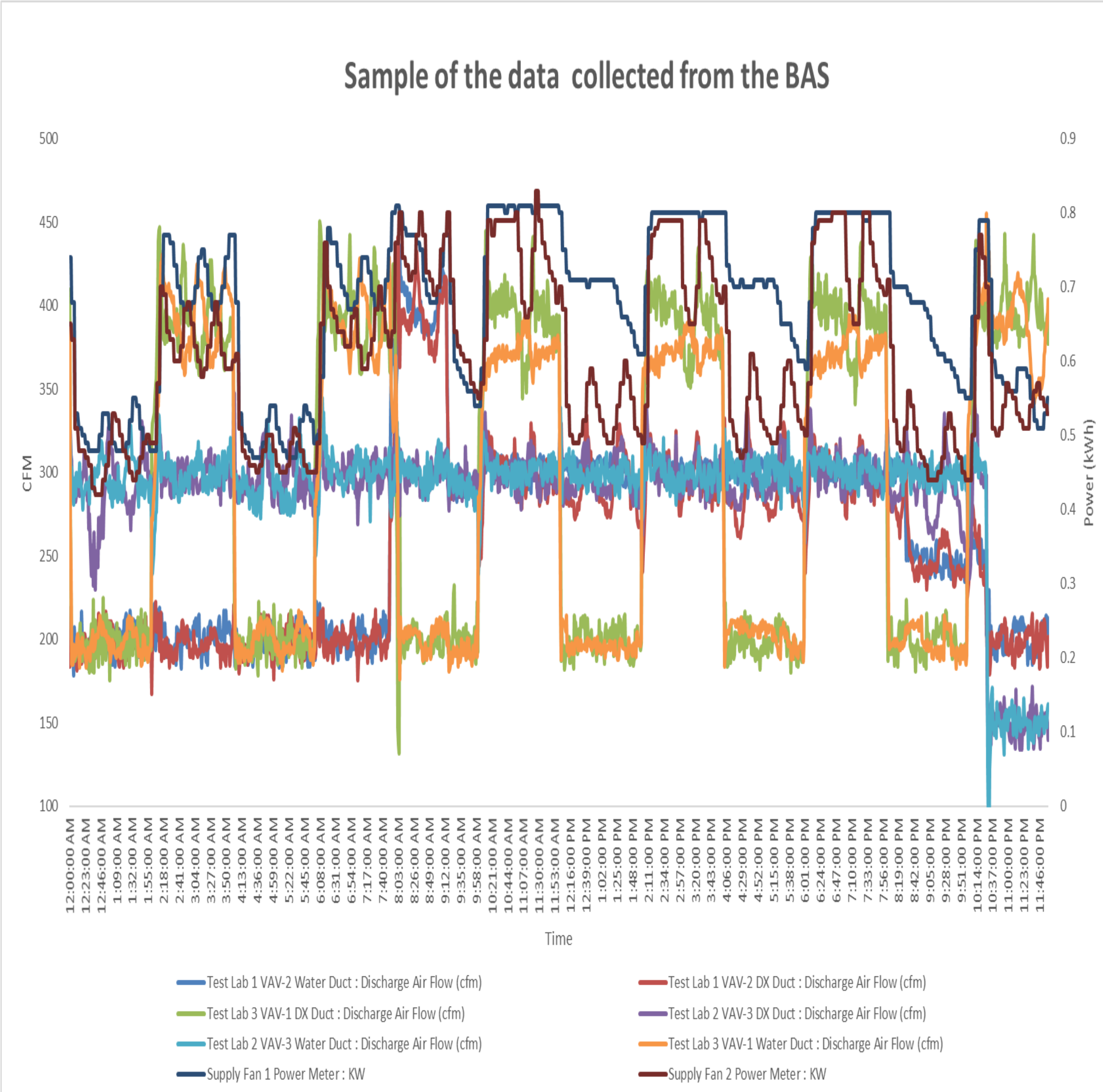

Figure 34. Collected Data from BAS to Microsoft Excel

The performance data gathered for all the components for both systems are summarized in table 3 below.

Table 3. A description of the collected data from the BEAST lab

Abbreviated terms	**Description**
Q_{sys}	Supply airflow (CFM)
Q_o	outside air flow (CFM)
T_{cws}	Chilled water temperature (°F)
T_{cwr}	Return chilled water temperature
CH_{VLV}	Chilled water valve position (%)
T_m	Mixed air temperature (°F)
T_s	Supply air temperature (°F)
T_r	Return air temperature (°F)
T_o	Outside air temperature (°F)
W_s	Supply air humidity ratio
W_r	Return air humidity ratio
P_s	Duct Static Pressure
D_{pw}	Chilled water differential pressure setpoint
P	Power (kWh)
F_s	Fan speed (fpm)
P_s	Pressure (in. w.g)
RH_s	Supply air relative humidity (%)
RH_o	Outside air relative humidity (%)

After organizing the data into the Excel sheets and remove all the anomalies data for when the system is off because those data will affect the accuracy of the models' predictions. The data were then divided into testing and training sets and later imported into the MATLAB software to test and train the created models. Figure 35 shows a sample of the data that were measured and how they were displayed on the BAS before collection.

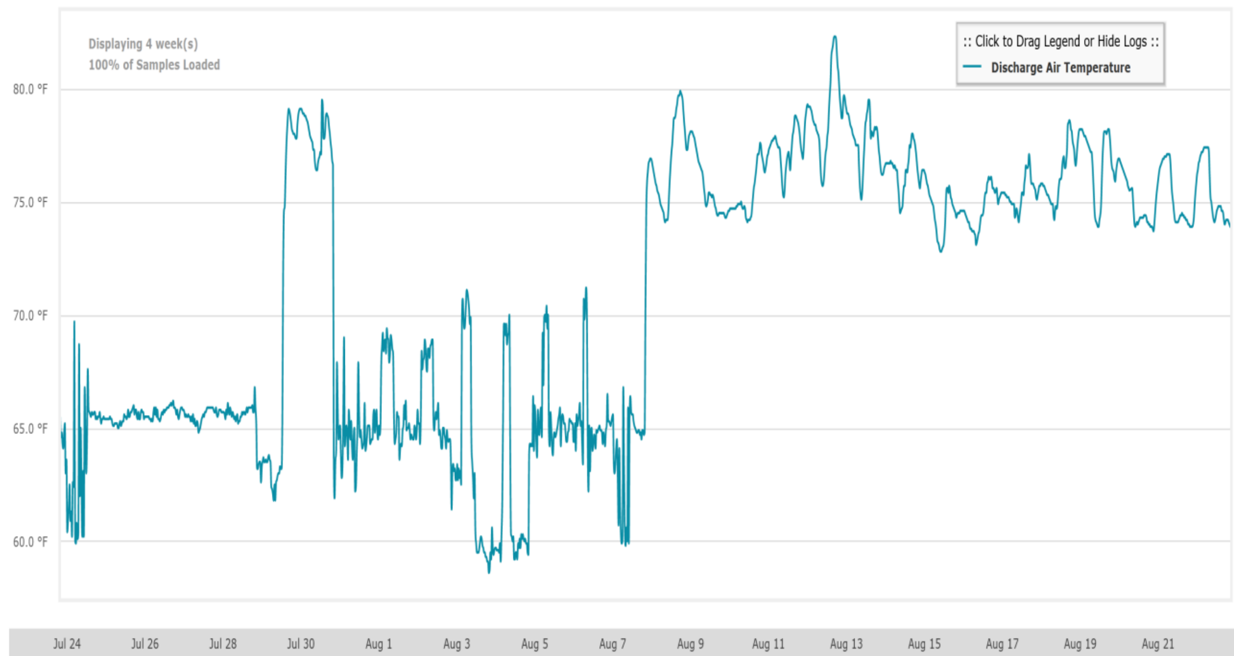

Figure 35. Sample of the collected data displayed on the BAS.

4.2.2 Modeling

Component models that are accurate, reliable, and adjustable are used for applications such as control optimization to minimize the energy consumption of HVAC systems. The prediction component models developed in this research will predict the system's actual performance over a specified period of operation. In addition, the component models are required for the optimization process that will be deployed later on. In this research, MATLAB software was used to develop functional data-driven models for system applications.

The optimal component model structure will be sought in the first optimization level (MLO). Then, all the system optimized, integrated components models together will form the "system model." The output of the system model will be the total system energy consumption that will be optimized in the following optimization level (SLO) that will be discussed in chapter 5. Finally, the HVAC system setpoints required for each component, such as supply air temperature (Ts), airflow rate (CFM), duct static pressures (Ps), chilled and hot water temperature (Tw), and outdoor airflow rate, are determined based on the previous time step reading.

The final objective of this research is to optimize the system's total energy consumption. Therefore, the proposed integrated two-level optimization process will optimize the system operation setpoints every 15 minutes to reduce the total energy consumption for the next timestep. Therefore, if the component models are inaccurate, the total energy consumption prediction will be less accurate. Therefore, the whole process results will be faulty.

Therefore, the sequence of the process can be summarized as follows:

- At the initial time step that is user-defined, the model parameters will be tuned using previous data.
- The tuned parameters will be later used in the next loop to forecast the system performance at the next timestep.
- The models' parameters are the loads and supply air temperatures, etc.
- The parameters are simulated by the load prediction, zones, heating and cooling coil, fan power, reheat, ventilation, pump, chiller, and boiler models.
- The models will be subjected to the constraints and regulations imposed by the energy and mass flow laws and energy codes requirements.
- The created models' final output will be measured in terms of energy consumption to calculate the system's total energy savings.

Figure 36 below shows a basic schematic of the modeling process steps.

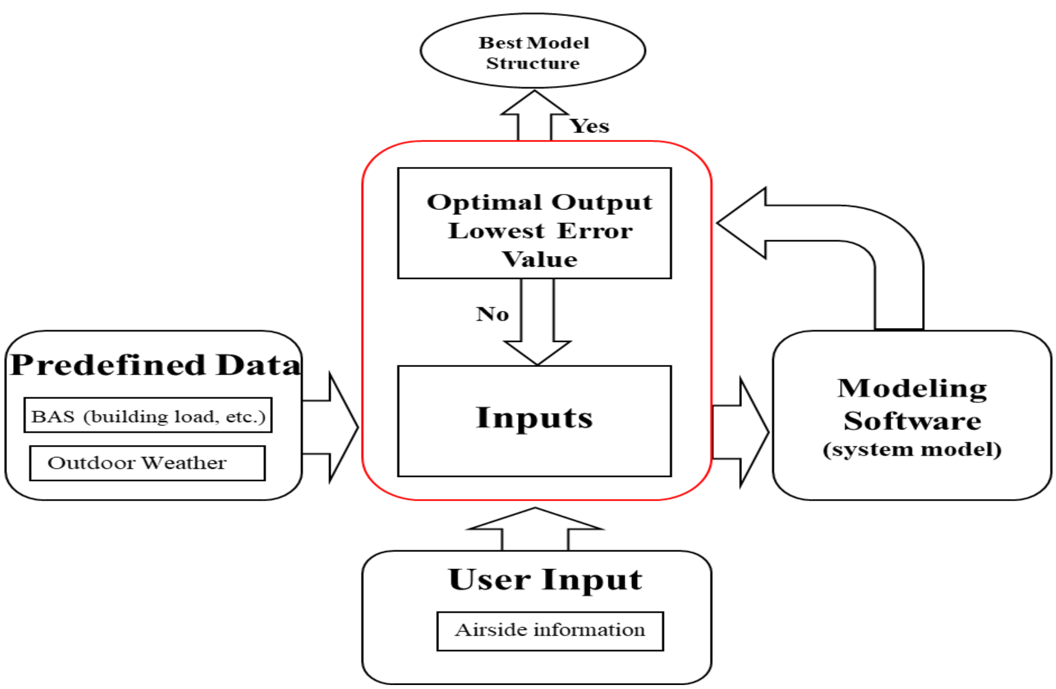

Figure 36. Modeling process concept

4.2.2.1 Chilled water VAV system models

The Airside and waterside of the chilled water VAV system were chosen to be evaluated as part of this research. A variable air volume with a reheat system will control the zone temperature by regulating the system's airflow rate. The supply air temperature is constant throughout the process. Modulating the airflow rate for each zone to maintain the zone temperature setpoint will be through the VAV box of each zone located in each zone's ductwork. The system is equipped with hot water reheat coils that are located in the VAV boxes. If the VAV box has reduced the airflow to the minimum and the zone temperature setpoint was not met, the system will trigger the reheat coils to meet the zone load.

The component of the system will be thoroughly investigated and modeled. Figure 37 shows the system component integrated data-driven models. However, few calculations were needed to link this data-based component model and obtain the whole system model.

The data-driven models were developed to predict the system performance. The created models will be integrated as the output of some models will serve as an input for others. For example, the airside model outputs were fan power, cooling, heating coils, and reheat loads. Those outputs were later linked to the central plant model (water side) as inputs. At the same time, the chiller power, boiler power, and pump were the outputs of the waterside. For this step, choosing the best model structure to replicate the actual physical component is a time-consuming process. Therefore, the MLO process using a genetic algorithm that will be implemented later will help choose the best component model structure.

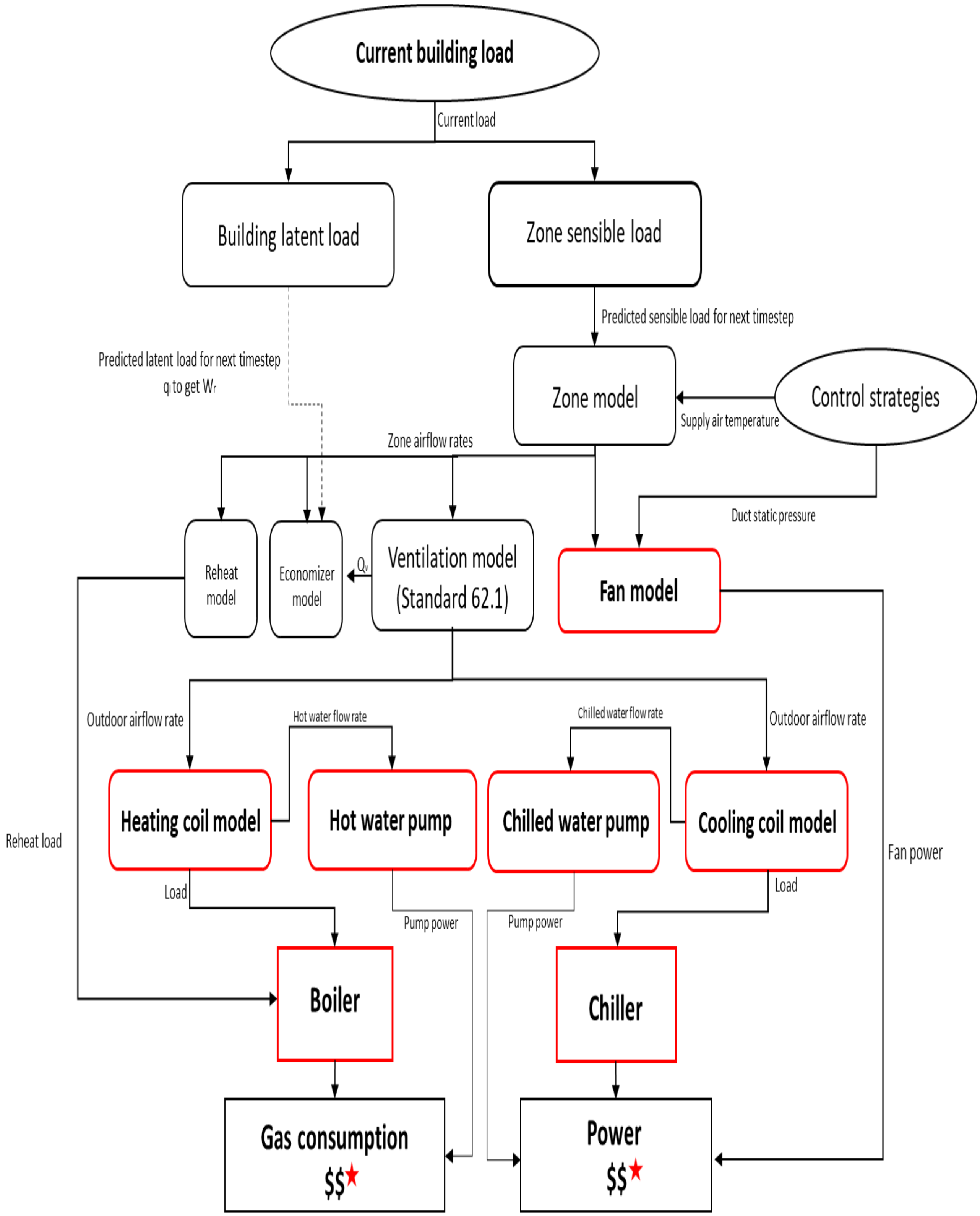

Figure 37. Chilled water VAV system proposed hybrid modeling diagram.

Since the accurate component modeling process is a significant step in predicting the HVAC energy consumption. The component models created for the chilled water VAV system are data-driven models. Table 4 shows the significant data-driven component models. The rest of the components were represented in a series of equations needed to link those data-driven models and obtain the whole system model due to their simplicity and being less dependent on time and the system's current load.

Table 4. The major data-driven models.

Data based models	**Model's output**	**Description**
AHU Model (cooling coil and heating coil)	Supply air temperature, chilled water flow, the total load	This model will capture the performance of the cooling coil and heating coil as the major component of the AHU
AHU Model (fan power model)	Fan power	This model will capture the performance of the fan
Central plant Model (chiller power model)	Compressor power	This model will capture the performance of the chiller
Central plant Model (chilled water and hot water pump)	Pump power	This model will capture the performance of the pumps

4.2.2.1.1 Zone sensible load prediction

The zone sensible load is established to determine the zones sensible load at the next time step. The sensible load is determined based on a series of heat balance equations. The zone sensible load is a function of the zone air flow rate and the difference between the supply and return temperature. In our prediction, we assume that the sensible load is the same for the previous period. Later, the load is calculated for the next timestep based on questions 18-22 using the previous flow and temperature.

$$q_t = ma * \Delta_h \text{ ....}(18)$$

$$q_s = ma * cp * \Delta T \text{ ....}(19)$$

$$ma = \frac{CFM * 60}{V} \dots\dots\dots\dots\dots\dots\dots\dots (20)$$

$$q_t = \frac{CFM * 60}{V} * \Delta_h \dots\dots\dots\dots\dots\dots (21)$$

$$q_s = \frac{CFM * 60}{V} * \Delta_T \dots\dots\dots\dots\dots\dots (22)$$

Where:

q = heat removed (Load) (BTU/h)

q_t = Total load

q_s = Sensible load

CFM = Air flow rate

CP = Specific heat of air= 0.244

V = specific volume = 13.5

Δ_T= temperature difference (F^2)

Δ_T= T_s - T_r

Ts = Supply air temperature

T_r = Return air temperature

Δ_h= h_o - h_s

h_s = Supply air enthalpy

h_r = Return air enthalpy

The initial load essential for the calculations will be estimated. The airflow rate for the current timestep will be assumed to be constant of the next timestep. The model's output will be the predicted load for the next time step (in our case is the next 15 minutes) based on the airflow rate for the current timestep and temperature difference. Assuming that the airflow rate is constant for the next timestep is acceptable since the optimization period is small. This process will be repeated every 15 minutes. The output of this model will be an essential input in the zone model as the predicted sensible zone load is crucial to determine the zone flowrates. Figure 38 shows the zone model proposed inputs and outputs.

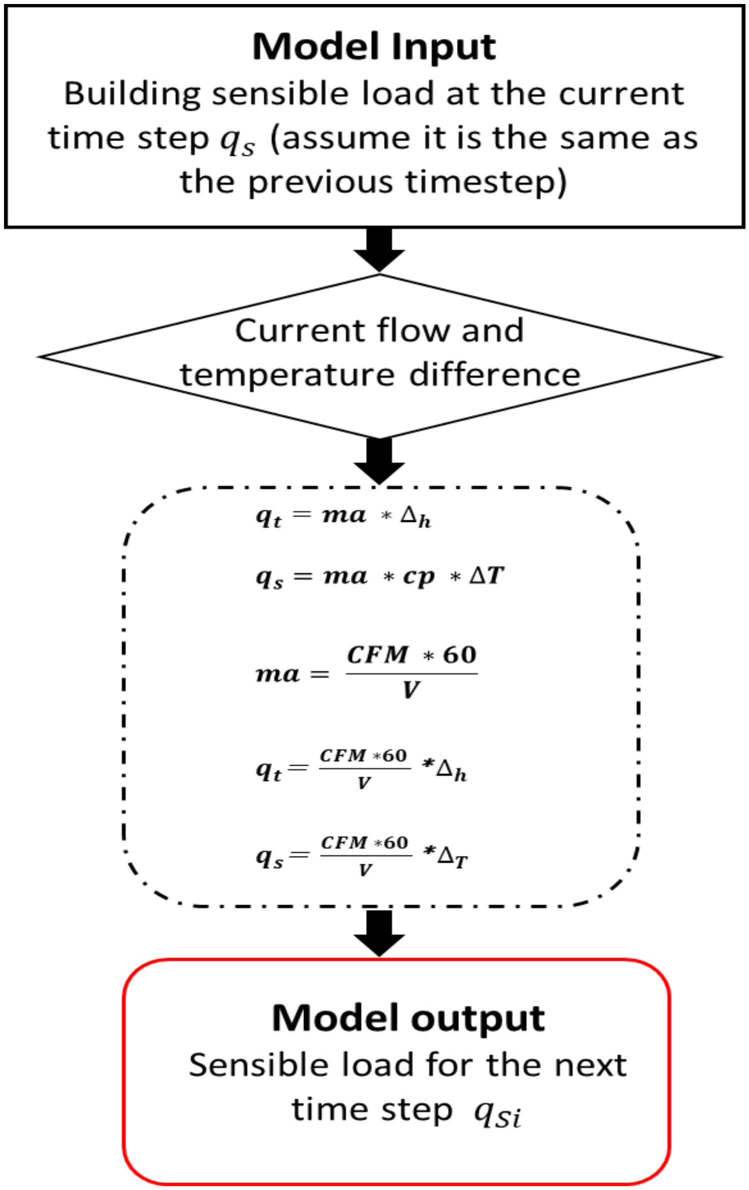

Figure 38. Zone's sensible load model description

4.2.2.1.2 Building latent load prediction

The latent load of the building is the amount of moisture in the air. The latent load prediction process is built based on a series of steady-state heat balance equations, as shown in figure 39. The latent heat is required for the whole system instead of each zone. The latent load will be used to determine the humidity ratio of the building that will be used as an input in other models. The load will be estimated at the first step and later calculated for the next timestep in the same way as the sensible load prediction. The process will be repeated every 15 minutes to assess the latent load for the subsequent timestep optimization.

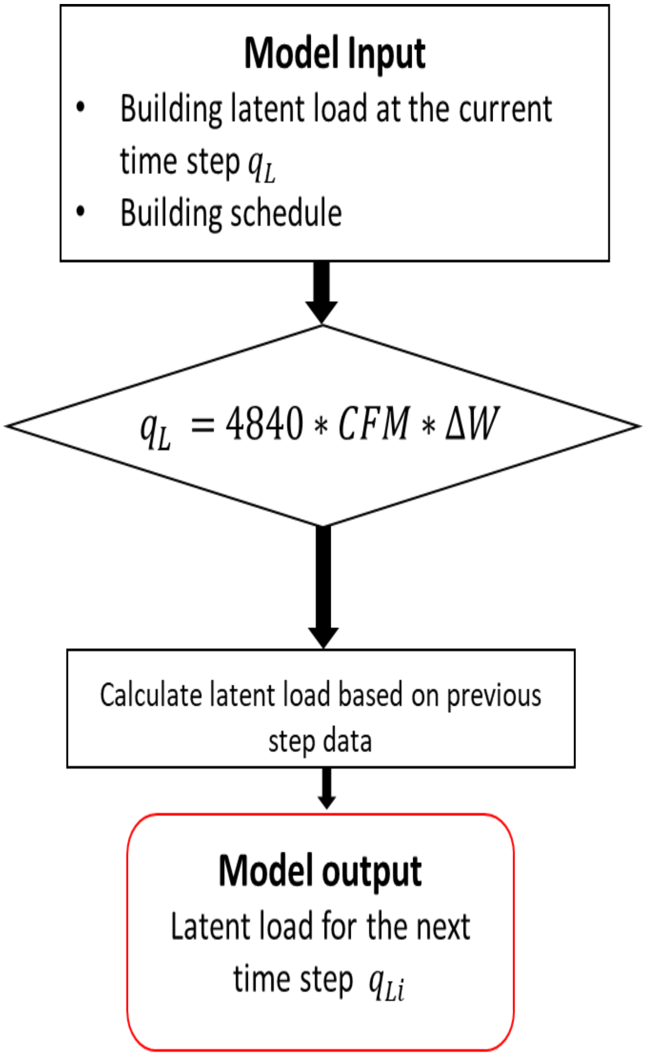

q_l = $Latent\ heat\ (\frac{BTU}{h})$

$q_t = q_s + q_l$

$q_l = P * h_w * CFM * \Delta W$

$p = Density\ of\ air$

$h_w = latent\ heat\ of\ evaporization$

$\Delta_w = Humidity\ ratio\ difference$

$\Delta_w = W_r - W_s$

$W_s = Supply\ air\ humidity\ ratio$

$W_r = Returnair\ humidity\ ratio$

Therefore:

$q_L = 4840 * CFM * \Delta W$

Figure 39. The building latent load model description

4.2.2.1.3 Zones model

The zone model is a series of equations established to determine the zones airflow rate. First, the zone model is constructed based on the heat balance laws, as shown in figure 40, utilizing the total load and the sensible and latent load sum. Next, the zone model will calculate the zone requirements based on the user input specified in the input datasheet. This process will be calculated at each time step.

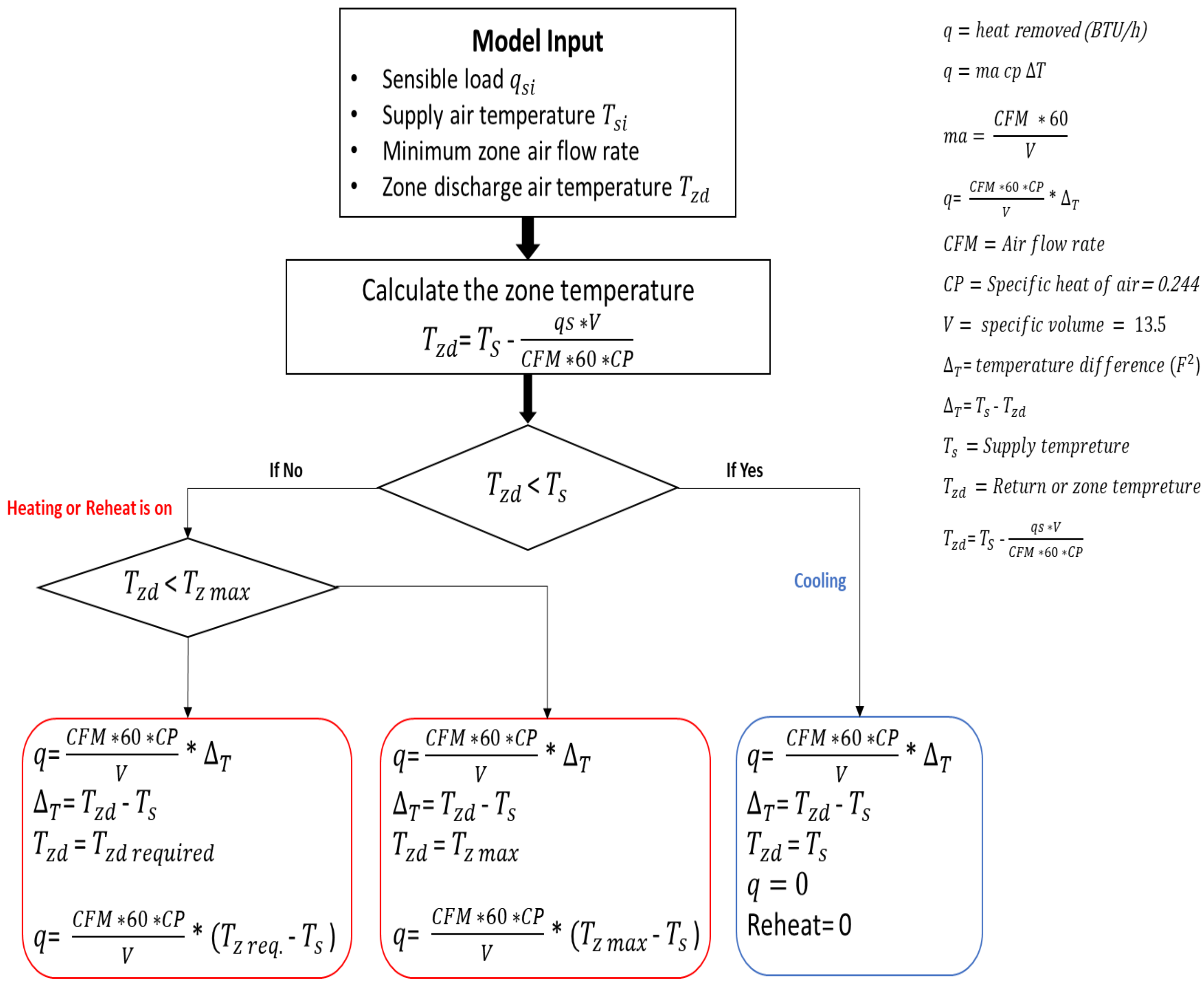

Figure 40. Zone's model description

The zone model has the reheat requirements specified as well. If the zone load is less than 20% of the design load, the reheat coil will be triggered, and the reheating process will begin. The reheating process can be described in equation 23 below.

$$q_{reheat\ zone} = \frac{CFM * 60 * CP}{V} * (T_{z\ required} - T_{supply}) \text{ ....(23)}$$

The function will calculate the zone reheat load and then the sum of the zones reheat load will be used to calculate the total reheat power usage for the system at each time step.

4.2.2.1.4 Fan power model

The fan is one of the significant components of any air handling unit. For the fan model, the fan power was predicted as a function of two inputs, flow rate and fan pressure.

The fan model proposed in this research is a data-driven model that uses the fan flow rate and pressure to indicate the fan power as the model output. Figure 41shows the structure of the ANN model designed to predict the fan power.

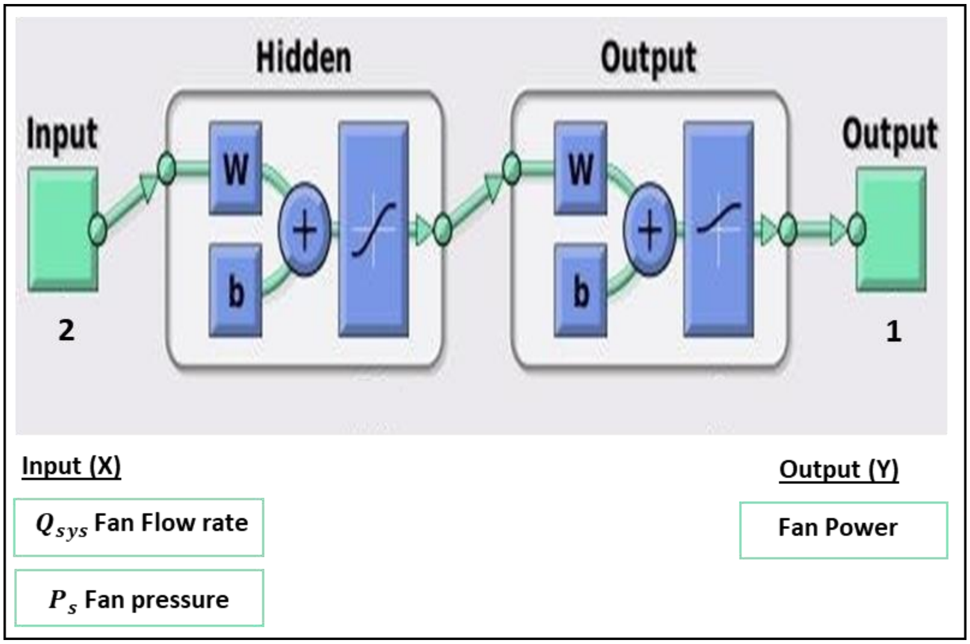

Figure 41. Artificial Neural Network fan model structure

4.2.2.1.5 Minimum zone ventilation model

The outdoor air percentage brought to the building in the process of heating/ cooling and dehumidification is a crucial factor due to its importance in the ventilation and maintaining the inhabitant comfort levels. In some baseline practices, the old rule of thumb methods was used to determine the amount of outdoor air brought to the building. One of these rules of thumb methods is that the amount of outdoor air brought to the building is usually 100 CFM per every 600- 900 ft^2.

However, to comply with ASHRAE standard 62.1 for minimum ventilation rates and air quality, that will be acceptable to human occupants. In addition, many buildings have been following the ASHRAE standard 62.1 for determining the minimum outdoor airflow rates requirements for breathing zones in their design. Therefore, equation 24 is proposed in ASHRAE standard 62.1 to determine the ventilation airflow rates for each zone.

$$V_{bz} = \mathrm{R}_p \times \mathrm{P}_z + \mathrm{R}_a \times \mathrm{A}_z \text{ .... } (24)$$

Where:

V_{bz}: breathing zone outdoor airflow (CFM).

R_p: outdoor airflow rate required per person as determined from Table 6-1 in standard 62.1.

P_z: zone population: the maximum number of people expected in the zone.

R_a: outdoor airflow rate required per unit area (CFM/ft^2) as determined from Table 6-1.

A_Z: zone floor area ft^2.

Now to calculate the zone outdoor air flowrate, which is the amount of outdoor air that must be provided to the ventilated zones by the HVAC system. This will be determined through equation 25 as proposed by ASHRAE standard 62.1.

$$V_{oz} = \frac{V_{bz}}{E_z} \qquad (25)$$

Where:

V_{oz}: outdoor zone airflow (CFM)

V_{bz}: breathing zone outdoor airflow (CFM).

E_z: System efficiency.

In many design cases, the E_z nowadays is considered as 1.0. Therefore, V_{oz} equals $V_{bz,}$ and the systems ventilation air flowrate will equal the sum of zone ventilation airflow rate. This method is acceptable, but it will result in energy waste as not all zones will always require 100% of the maximum ventilation rate. Therefore, in this research, we will be deploying the new ASHRAE 62.1 method to optimize the systems efficiency value E_z so that each zone will get the minimum ventilation flowrate. And this amount will vary throughout the system operation period. The following equations show the process of correcting the efficiency X_{sc} value based on the ASHRAE 62.1 method.

$$Z_{dz} = \frac{V_{oz}}{V_{dz}} \qquad (26)$$

$$V_{ou} = \sum \mathrm{R}_p \times \mathrm{P}_z + \sum \mathrm{R}_a \times \mathrm{A}_z \qquad (27)$$

$$X_s = \frac{V_{ou}}{V_{ps}} \qquad (28)$$

$$E_{vz} = 1 + X_s - Z_{dz} \qquad (29)$$

$$E_v = \min(E_{vz}) \qquad (30)$$

$$V_{ot} = \frac{V_{ou}}{V_{ps}} \qquad (31)$$

$$X_{sc} = \frac{V_{ot}}{V_{ps}} \qquad (32)$$

$$V_{ot} = V_{ps} * X_{sc} \qquad (33)$$

Where:

Z_{dz} = outdoor air fraction in discharge air supplied to each zone, L/s (CFM)

V_{oz} = zone outdoor airflow, L/s (cfm)

V_{dz} = discharge air supplied to the zone, L/s (cfm)

V_{ou} = uncorrected outdoor air intake flow, L/s (cfm)

X_s = uncorrected outdoor fraction in supply air

V_{ps} = system supply air flow, L/s (cfm)

E_{vz} = zone efficiency

E_v = system efficiency

V_{ot} = outdoor air intake flow, L/s (cfm)

X_{sc} = corrected outdoor fraction in supply air

4.2.2.1.6 Economizer model

The system utilized the use of the economizer. Therefore, if the outside air temperature is proper, the control strategies activate the economizer to result in free cooling by introducing the appropriate amount of fresh air.

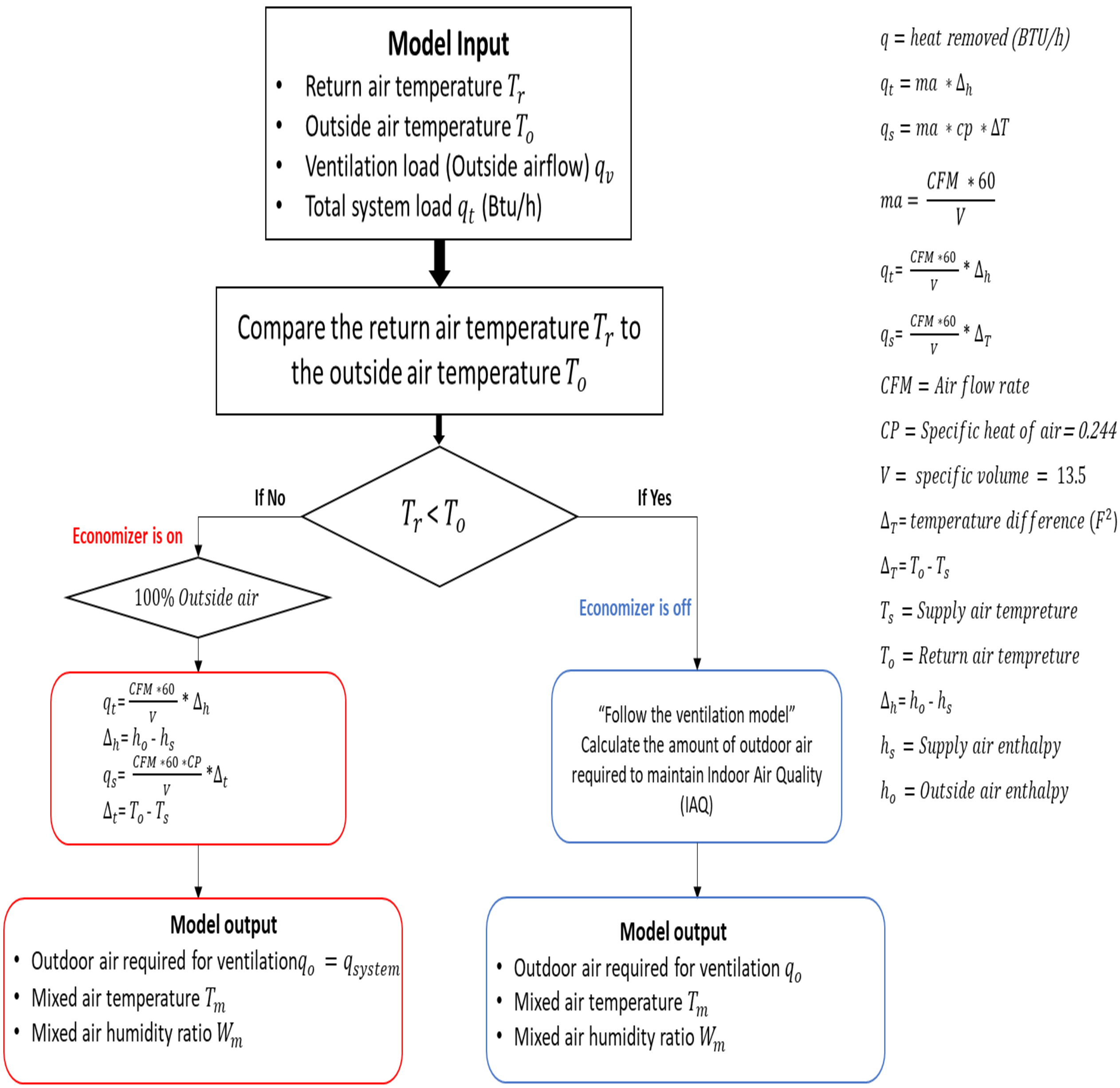

Figure 42. The economizer model description.

4.2.2.1.7 Cooling coil model

As one of the main components of any chilled water VAV system, the cooling coil is responsible for cooling and dehumidifying the air. The cooling load was predicted as a function of chilled water temperature, chilled water flow, mixed air temperature, supply air temperature, and mixed air humidity ratio. At the same time, the chilled water flowrate is calculated as a function of the valve opening. The cooling coil model will be linked to the central plant model to get this value over the specified period. At the same time, the system temperature difference will be determined from the BAS system over time.

Figure 43 shows the structure of the ANN model designed to predict the optimal performance of the cooling coil.

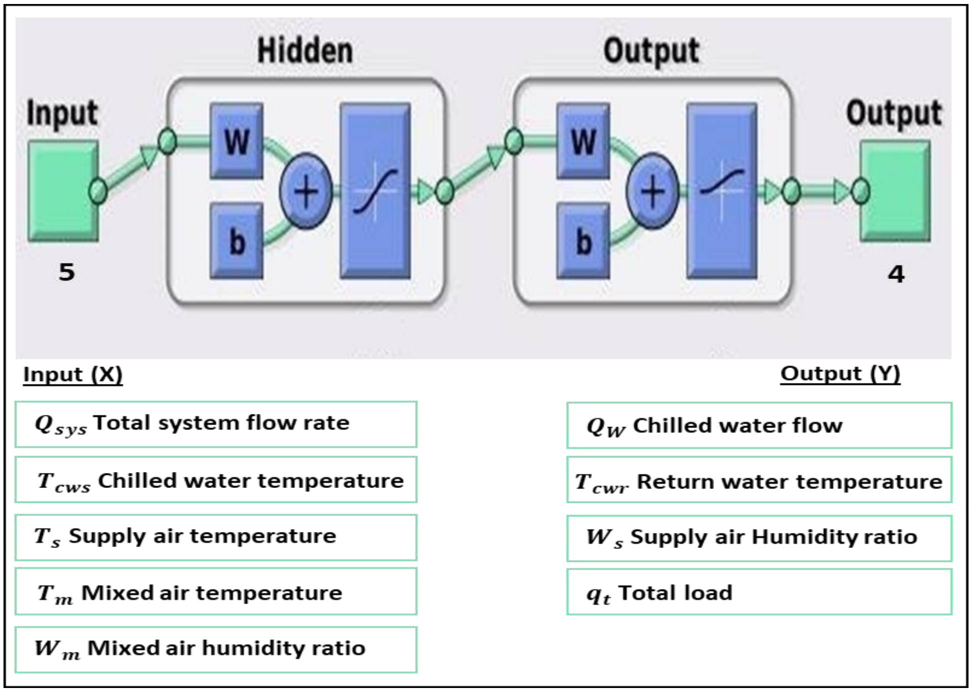

Figure 43. Artificial Neural Network cooling coil model structure

4.2.2.1.8 Heating coil model

As another main component of any chilled water VAV system, the heating coil is responsible for heating and dehumidifying the air in the system heating mode. The heating coil data-driven model is similar to the cooling coil model. The heating load was predicted as a function of supply hot water temperature, hot water flow, mixed air temperature, and supply air temperature. In this model air humidity ratio was not accounted for since it is close to zero in the heating mode. Again, the hot water flowrate is calculated as a function of the valve opening. The heating coil model will be linked to the central plant model to get this value over the specified period. At the same time, the system temperature difference will be determined from the BAS system over time.

Figure 44 shows the structure of the ANN model designed to predict the optimal performance of the heating coil.

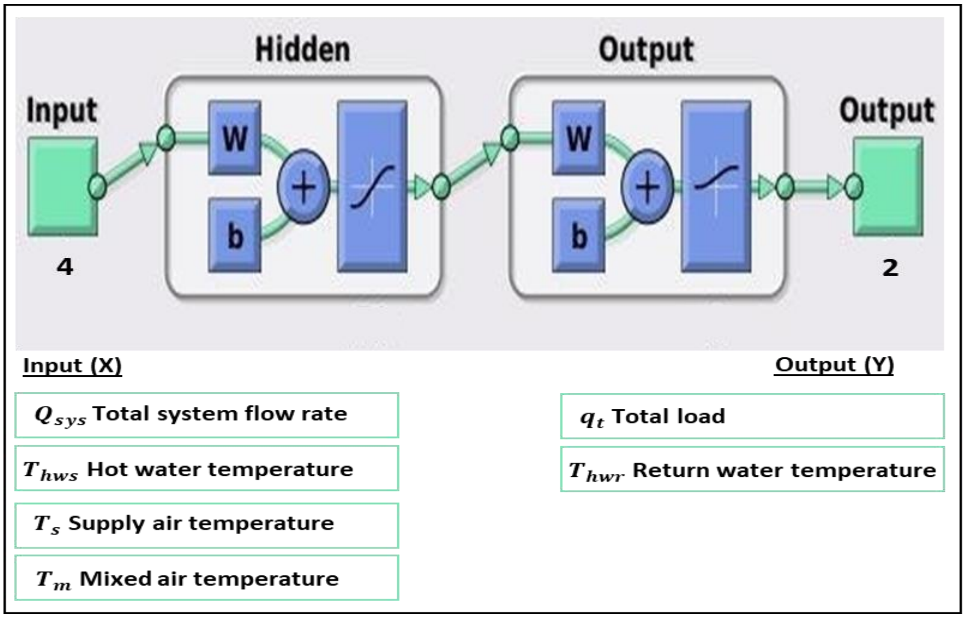

Figure 44. Artificial Neural Network heating coil model structure

4.2.2.1.9 Central plant chiller model

The central plant or the water side of the chilled water VAV systems is responsible for heating, cooling, and both heating and cooling at the same time. The central plants can cool or heat different kinds of coolants, typically water or water/ glycol mix for conditioning or refrigeration. In our research, we are examining a water chiller for air conditioning. The central cooling and heating plants represented by the chiller and boiler are responsible for generating the cold and hot water distributed to multiple locations in the building through the distribution system that includes pipes and pumps, etc. The central plants model discussed in this research consists of the chiller, boiler, and pumps model.

The liquid goes through two primary circuits in the chiller: a refrigeration circuit and a fluid circuit. The refrigeration circuit contains the compressor, the condenser, the expansion valves, and the evaporator. In contrast, the fluid circuit includes the pumps, filters, and heat exchangers. The refrigeration circuit is responsible for removing the heat from the fluid. At the same time, the fluid circuit carries the process fluid back to the building that is being cooled.

The liquid flow rate required to satisfy the building (zones) heat load at a specific temperature drop can be mathematically described in equation 34 below.

$$q_{total} = M_W * C_{PW} * \Delta T \ldots\ldots\ldots\ldots (34)$$

Where:

q_{total} = total heat removed (Btu/h)

M_w = chilled water flow rate (GPM)

C_{pw} = specific heat of liquid (Btu/lb °F)

ΔT = temperature difference (°F)

The chiller model discussed in this research is a data-driven model aiming to predict the chiller compressor power in kWh as an output. While the chilled water flow, supply and return water temperature, and the outside temperature was selected to be the model inputs. Figure 45 shows the structure of the neural network model.

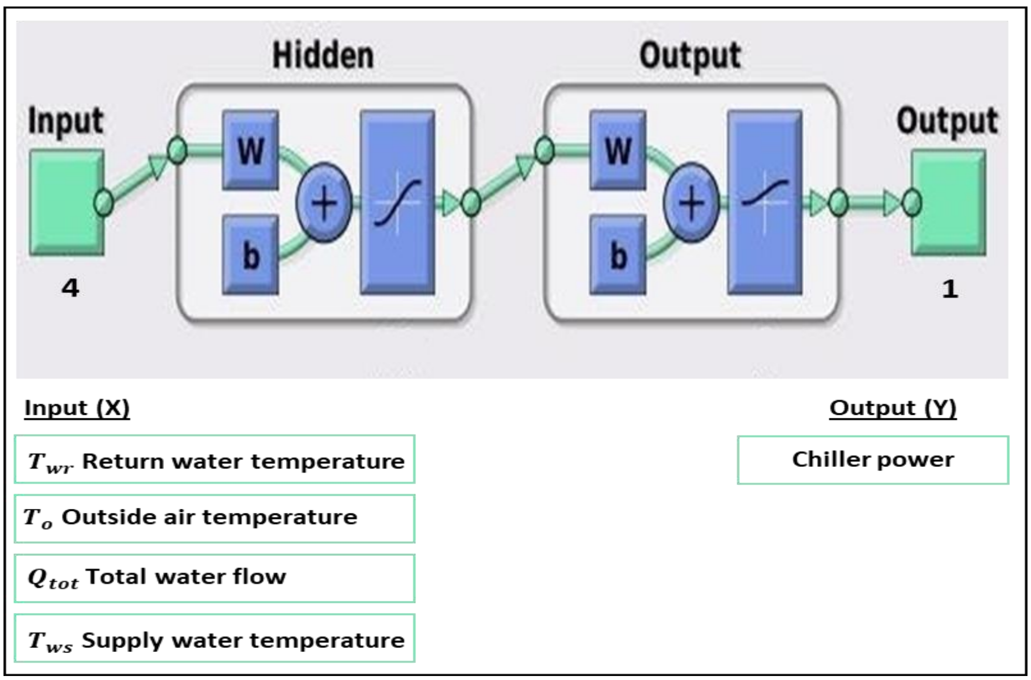

Figure 45. Artificial Neural Network chiller model structure

4.2.2.1.10 Central plant boiler model

The boiler is another component of the central plant. The boiler was examined in this research is a gas furnace boiler. The boiler is responsible for heating the fluid in the heating mode and in the cooling mod where reheating by the reheat coils is required.

Like the chiller, the boiler liquid flow rate required to satisfy the building (zones) heat load at a specific temperature drop can be mathematically described in equation 35 below.

$$q_{total} = M_W * C_{PW} * \Delta T \text{...........} (35)$$

Where:

q_{total} = total heat removed (Btu/h)

M_w = Hot water flow rate (GPM)

C_{pw} = specific heat of liquid (Btu/lb °F)

ΔT = temperature difference (°F)

The boiler discussed in this research is not a data-driven model due to its simplicity, where there is no account for the fluid moisture content. However, as shown in figure 46, a series of equations were used to link the boiler gas consumption to the system model.

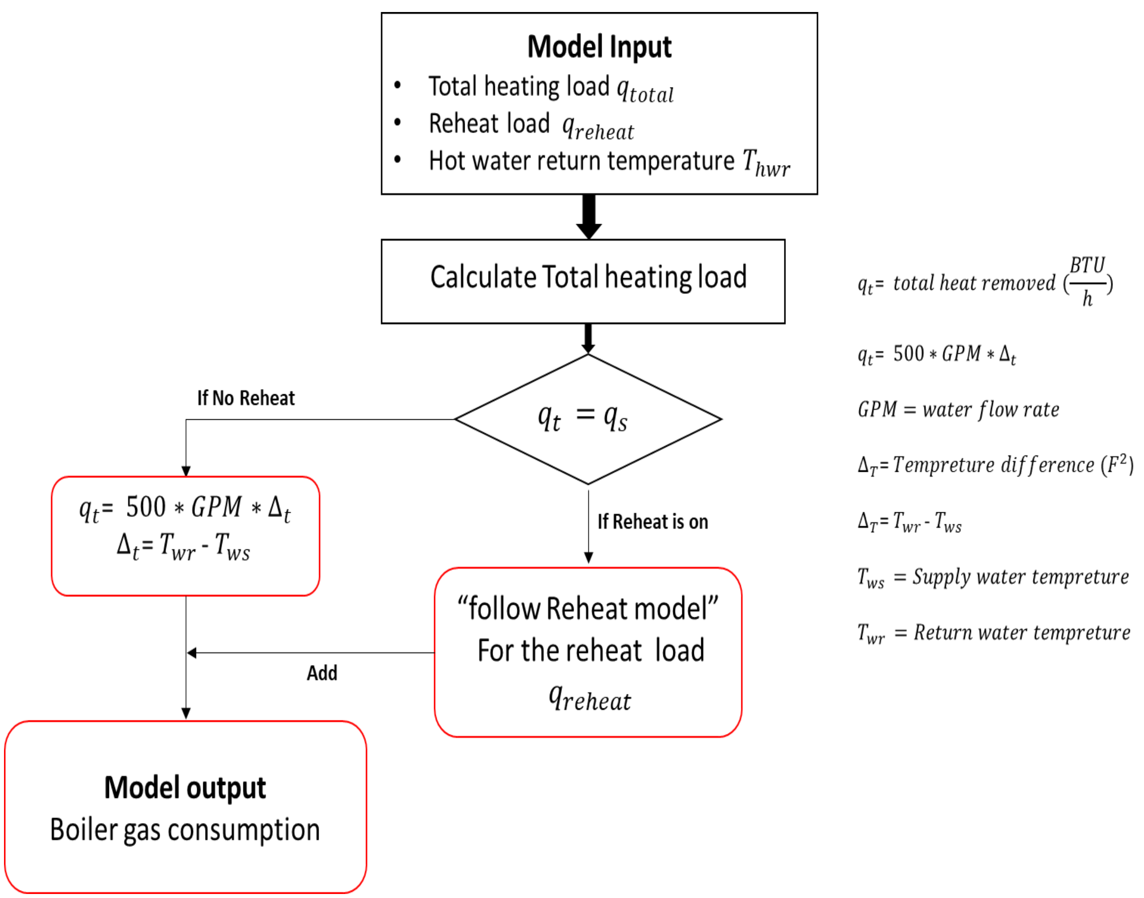

Figure 46. The boiler model structure

4.2.2.1.11 Central plant pump model

The hot water and chilled water pumps are usually represented in other research as a series of equations since the pump model uses a constant fluid density and specific heat values. For reference, the heat balance equations that can link the pump's model to the system model, if the data-driven model is not applicable, are represented in equations 36 and 37 below, showing the pump flow and pressure loss calculations.

$$Pump\ flow = \frac{Q}{\rho * N * d^3} \quad (36)$$

$$Pump\ head\ pressure\ loss = \frac{\Delta P}{\rho * N^2 * d^2} \quad (37)$$

Where:

Q = mass flow rate

d = diameter of pump impeller

P = head pressure

ρ = density of liquid

N = rotation speed

In this research, a data-driven model was constructed to predict the performance of the pumps. The pump power in kWh was indicated as an output of two inputs, the chilled water flow, and pump pressure. Figure 47 and 48 shows the neural network structure selected for the pump model.

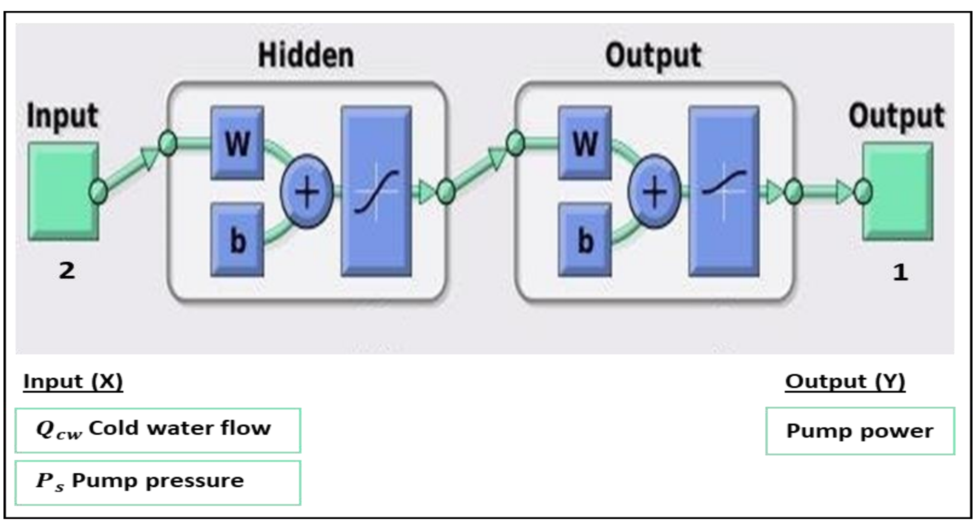

Figure 47. Artificial neural network chilled water pump model structure

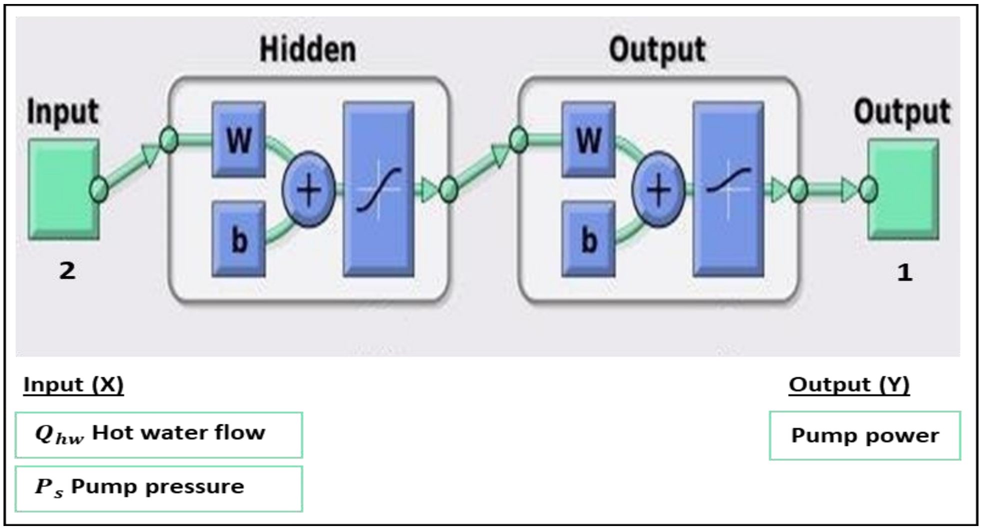

Figure 48. Artificial neural network hot water pump model structure

4.2.2.2 Direct expansion (DX) system models

The second HVAC system investigated in this research is a variable air volume direct expansion (DX) system. The DX system is an air system equipped with electric cooling and heating coils, filters, fans, and dampers. Modulating the airflow rate for each zone to maintain the zone temperature setpoint will be through the VAV box equipped with a reheat coil of each zone located in each zone's ductwork. If the VAV box has reduced the airflow to the minimum and the zone temperature setpoint was not met, the system will trigger the reheat coils to meet the zone load.

The system was thoroughly investigated and analyzed. The unit was run in both the cooling and heating mode and under different weather conditions to model the system accurately.

The DX system components models created in the research are data-driven. However, some calculation models are needed to link the data-driven model and develop the system model. As shown in figure 49 below, as the chilled water VAV system, the DX system models will be integrated with each other's as the output of one model can serve as an input for other models. Finally, the DX system model's intended output is the system compressor power that is the sum of the fan power, cooling coil power, and heating coil power.

Since the DX system is air-only, no central plant models will be linked to the airside models. Finally, the DX system and the air side of the chilled water VAV system are similar in all the components except the heating/cooling coil types. Therefore, the same models created for the rest of the components can be used to model both. Thus, in the next section, we will discuss the fan, the cooling, and the heating coil models, as the rest were previously discussed.

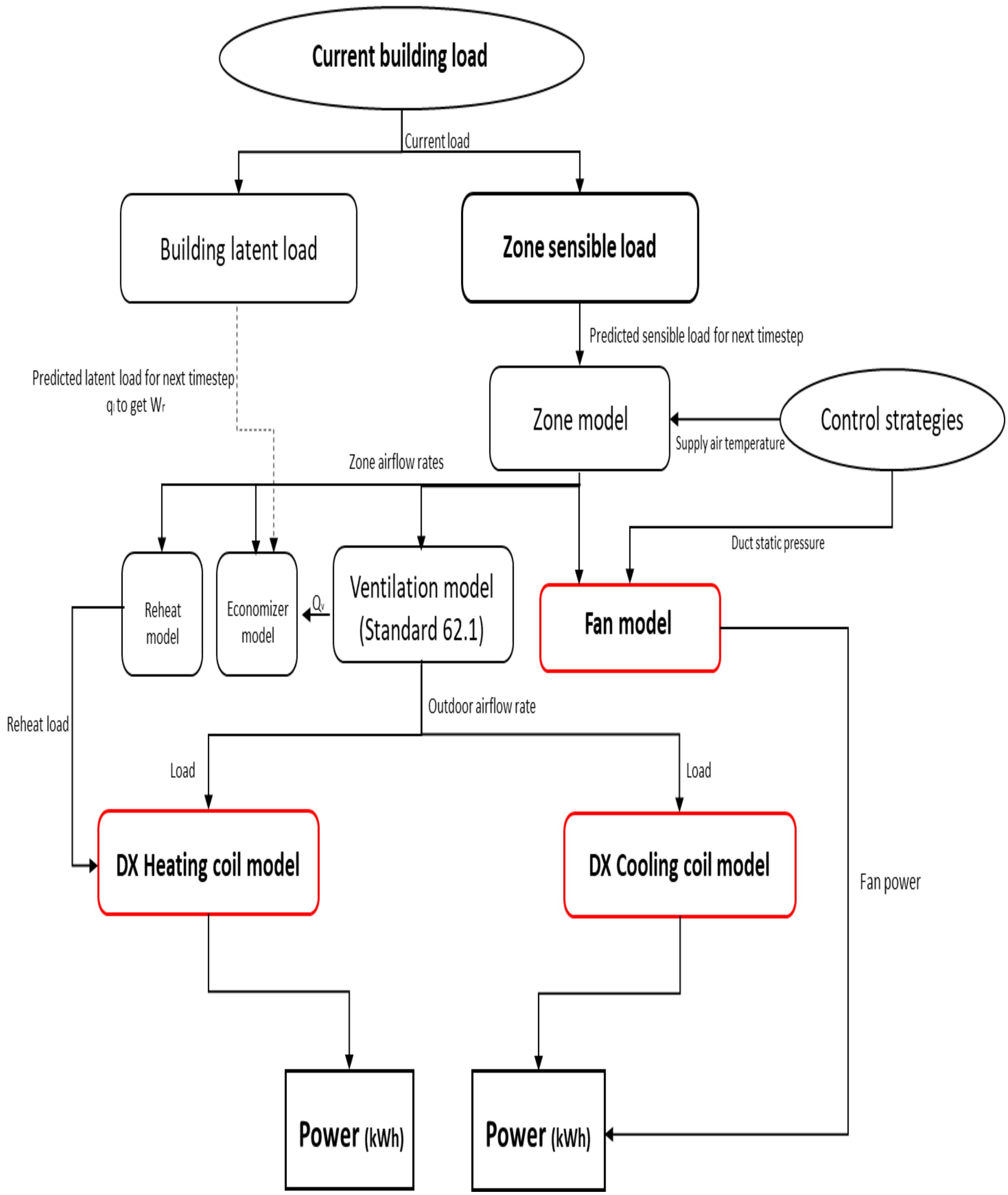

Figure 49. DX variable air volume system proposed hybrid modeling diagram.

Table 5 below shows the major data-driven models created for this part and their predicted output and model description. The rest were linked by calculations due to their simplicity and being less dependent on time and the current system load.

Table 5. The major DX system data-driven models.

Data based models	Model's output	Description
DX Model (cooling coil and heating coil)	Cooling/ heating coil power and humidity ratio	This model will capture the performance of the cooling coil and heating coil as the major component of the DX system.
DX Model (fan power model)	Fan power	This model will capture the performance of the fan.

The DX fan model was the same as the one fr the chilled water system. The two models have the same input and output structure, so this section will not repeat the process. While the cooling and heating coils are different, and their network will be discussed below.

4.2.2.2.1 DX Cooling coil model

The DX cooling coil is an electric coil that is responsible for cooling and dehumidifying the air. The DX power consumption cooling coil was chosen to be the output of the data-driven model. Also, the supply air humidity ratio will be predicted to be optimized and served as an input for other models in other models.

The supply air temperature setpoint dictates the power consumption. Thus, the selected inputs were the outside air temperature, the supply air temperature, the mixed air temperature, and the mixed air humidity ratio. The mixed air temperature and the humidity ratio were calculated by averaging the outdoor and return air conditions. The corrected outdoor air ratio will be determined by the ventilation model as previously described in section 4.2.2.1.5. The corrected value will be linked to the DX cooling coil model.

Figure 50 below shows the DX cooling coil model structure and its inputs and outputs.

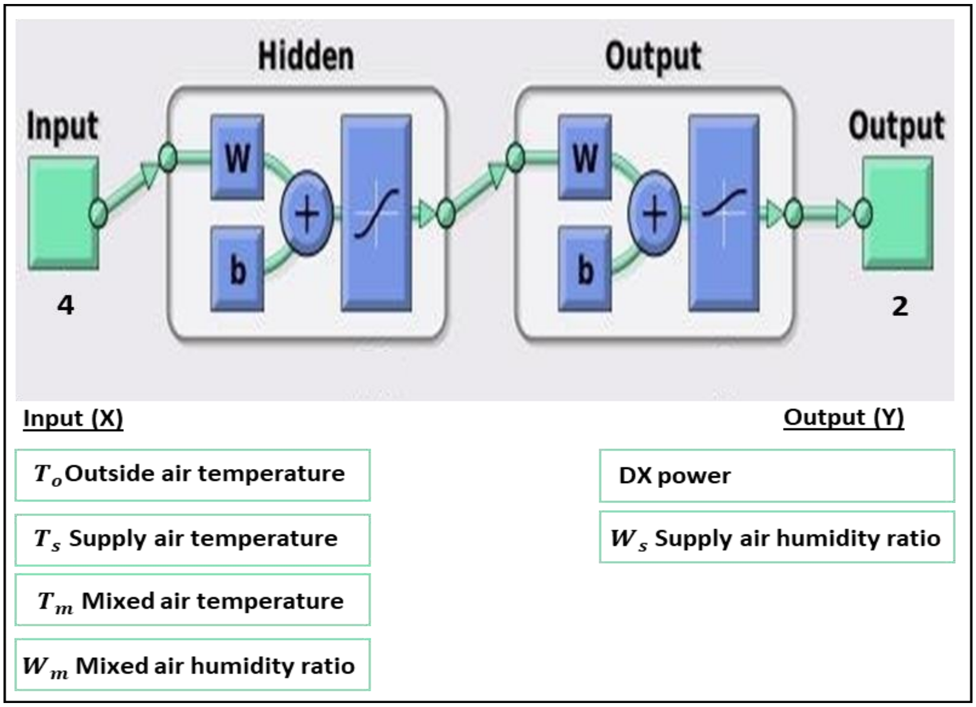

Figure 50. Artificial neural network DX cooling coil model structure.

4.2.2.2.2 DX Heating coil model

The Dx heating coil is similar to the cooling coil. The DX heating coil is an electric coil used to heat the air when the system is in heating mode. The DX heating coil's predicted output is the power consumption. While, the inputs were the outside air temperature, the supply air temperature, mixed air temperature. It is noted that the mixed air humidity ratio will be ignored in modeling the performance of the DX heating coil due to small or close to zero value in the heating mode. Figure 51 below shows the DX heating coil model structure and its inputs and outputs.

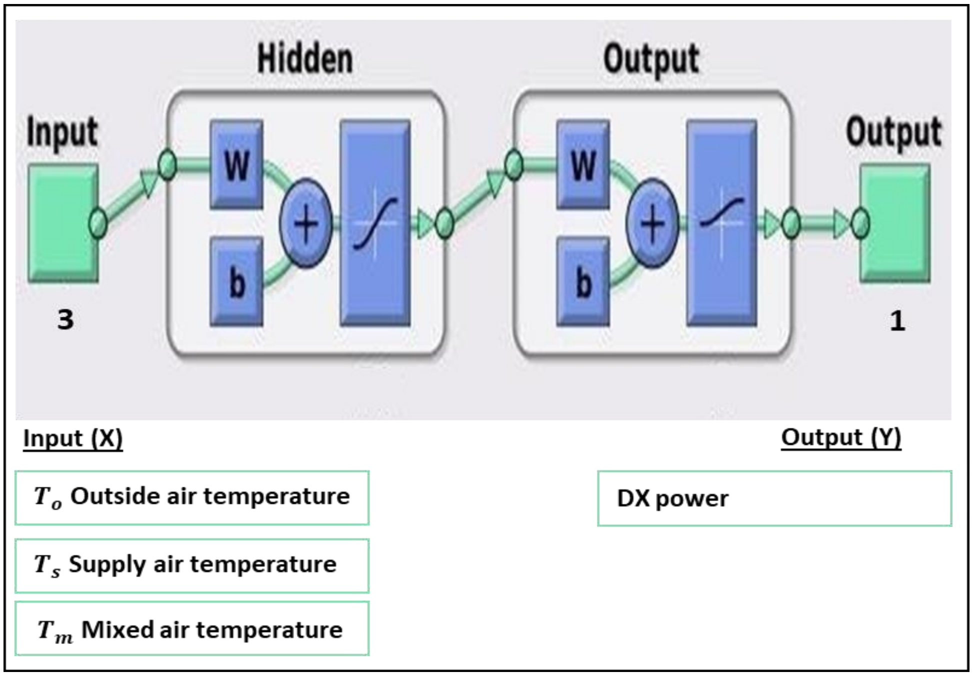

Figure 51. Artificial neural network DX heating coil model structure.

4.2.3 Model-level optimization

As previously stated, this research consists of two levels of optimization. The first level is the component models optimization, while the second level is a whole system performance optimization. The two levels will be later integrated to optimize the system operation, reduce energy consumption, and improve thermal comfort levels. Both levels of optimization will be conducted using GA.

The model level optimization will be implemented to automate the process by determining the best model structure with the minimum error value between the actual performance data and simulated data generated through the parametric study. Thus, the objective of the model level optimization is to find the best model structure with the lowest error value over a predefined (training or testing) period with (n) data sample. The error values were measured in terms of MSE (mean square error) and CV% (coefficient of variation). Figure 52 shows the process of model optimization and objective function using the GA operator.

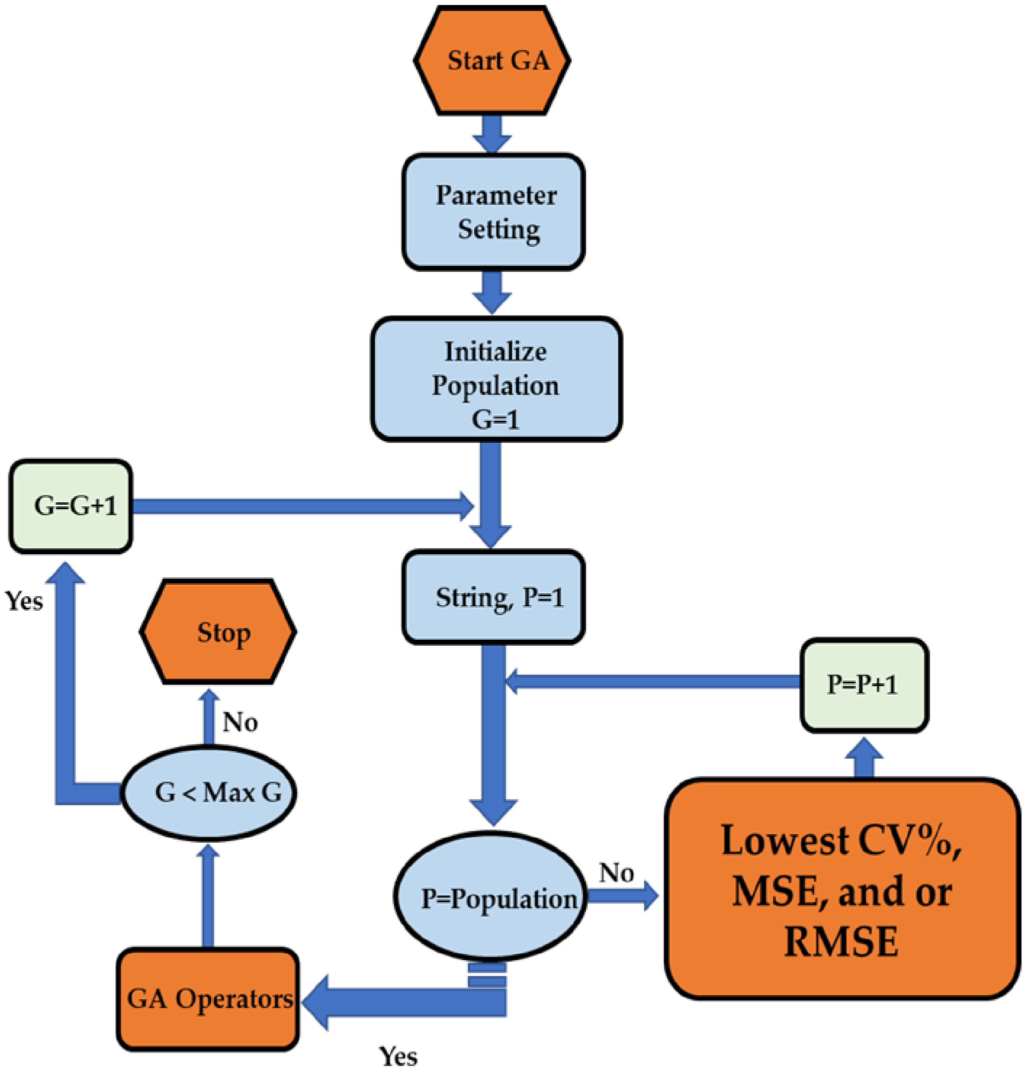

Figure 52. The general layout of the MLO process using GA.

As previously stated, first, a typical learning algorithm was used to tune the model's parameters. For this purpose, artificial neural networks were selected. And the variables that were adjusted in the process are (1) input time delays, (2) feedback time delays, and (3) the number of neurons (hidden layer size). At the same time, the model parameters are such as weights and biases. The tuning of the parameters will be completed on the whole testing data set.

Later the model level optimization is proposed to determine the optimal model structure. Selecting the best model structure manually is a time-consuming process that might take few days for each component model structure. Therefore, a high-level optimization will be performed in this step to select the best model structure that produces the minimum error values in model prediction. This process will not replace the typical learning algorithm. Instead, it will automate the process to deliver more accurate predictions with lower processing time.

4.3 Modeling results

The models were tested and trained using the data collected from the BEAST lab. As previously stated, the data were collected and organized into Excel sheets and then imported into the MATLAB code is designed for each component separately. Finally, the results for each run were collected and stored into an output file named results. The results measured the performance of each model by calculating the error of each model in predicting the specified output. Later all the results were compared together, and the model structure that held the lowest error value was selected as the best model structure. This manual process of choosing the best model structure is called the parametric study.

Therefore, this section shows the parametric study results. And the MLO process results. These results will be later compared against the optimization process results to validate the model-level optimization process results.

4.4.1 Chilled water VAV system component modeling results

The component data-driven models were described previously in the methodology section for the chilled water VAV system. Each model input and output that serve the objective of this research was specified. The tool that was used to test and train the model is artificial neural networks. The script that was used has the ability to predict one output as a function of multiple outputs. Therefore, the models with multiple outputs needed multiple runs, one for each output. This section shows a proposed methodology of modeling.

1. **Cooling coil model results**

After conducting the parametric study and comparing all the results, the following results are for the cooling coil component. It was found that the model structure with 30 number of neurons, three intervals of feedback, and three intervals time delay held the least error values of 1.1059% and 0.0175 in terms of CV% and MSE, respectively. Thus, it was selected to be the best model structure. Figure 53 shows the testing and training period of a model with a number of neurons ranging from (1-100) with a time delay (ID) of three intervals and three intervals time delay. This iteration held the optimal values.

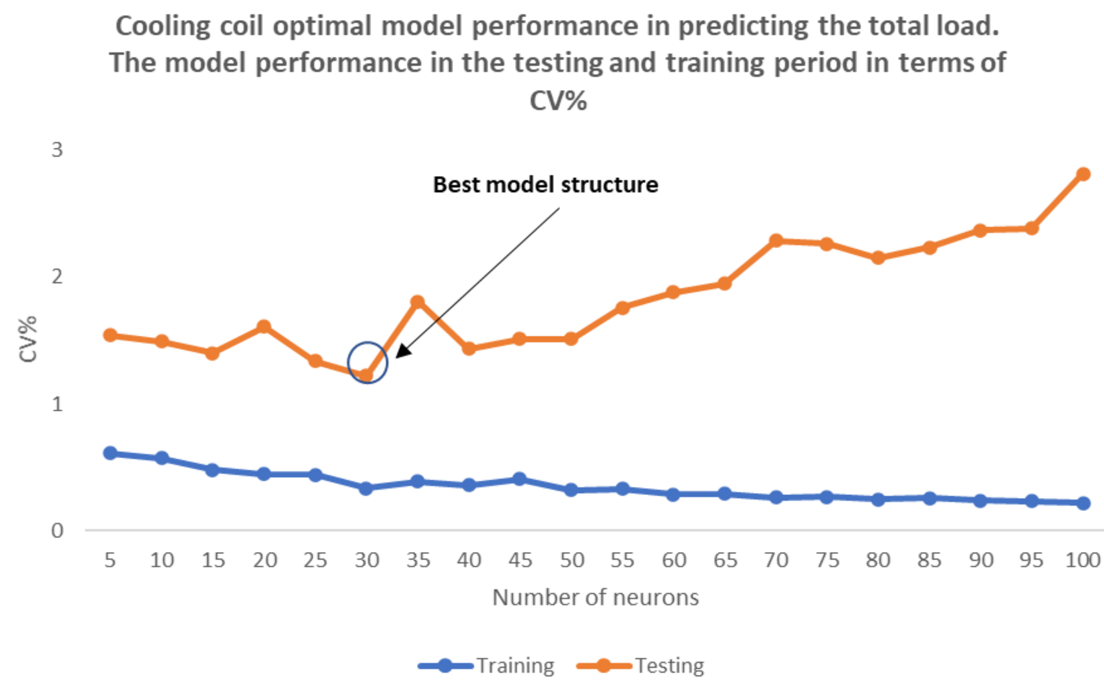

(A)

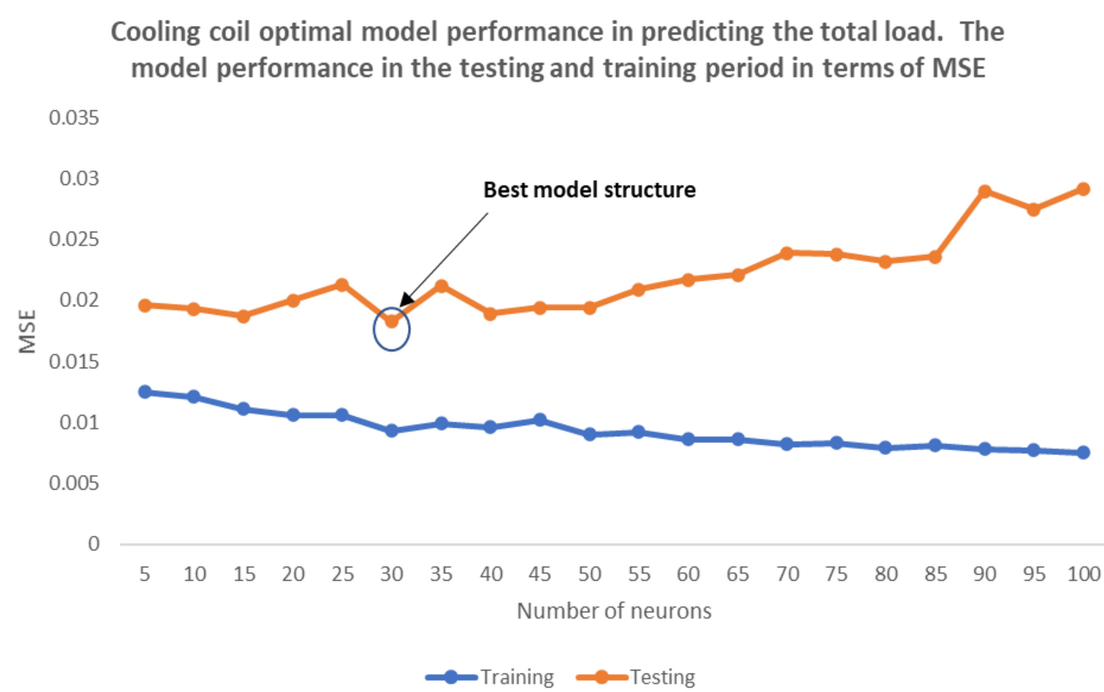

(B)

Figure 53. (A)The Training and testing period of the iteration held the optimal model structure. The error value is measure in terms of CV%. (B) The Training and testing period of the iteration had the optimal model structure. The error value is measure in terms of MSE.

While the results of modeling the cooling coil to predict the chilled water flow have shown that the model structure with one interval of time delay, one interval of feedback delay, and 30 number of neurons held the lowest error values. The CV% and MSE values were recorded as 0.23 and 0.0056, respectively, as shown in figure 54 below.

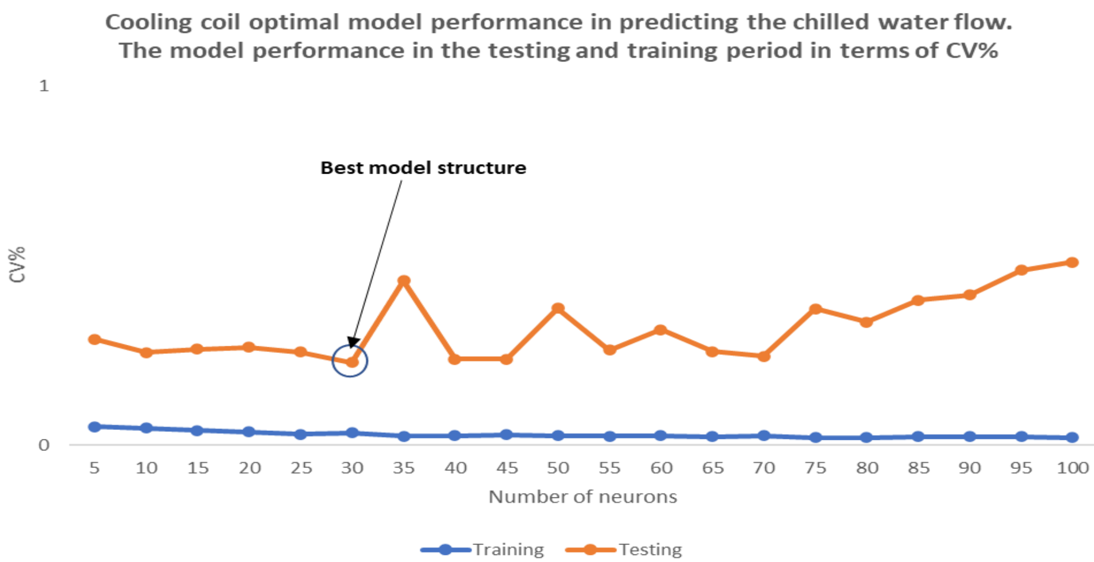

(A)

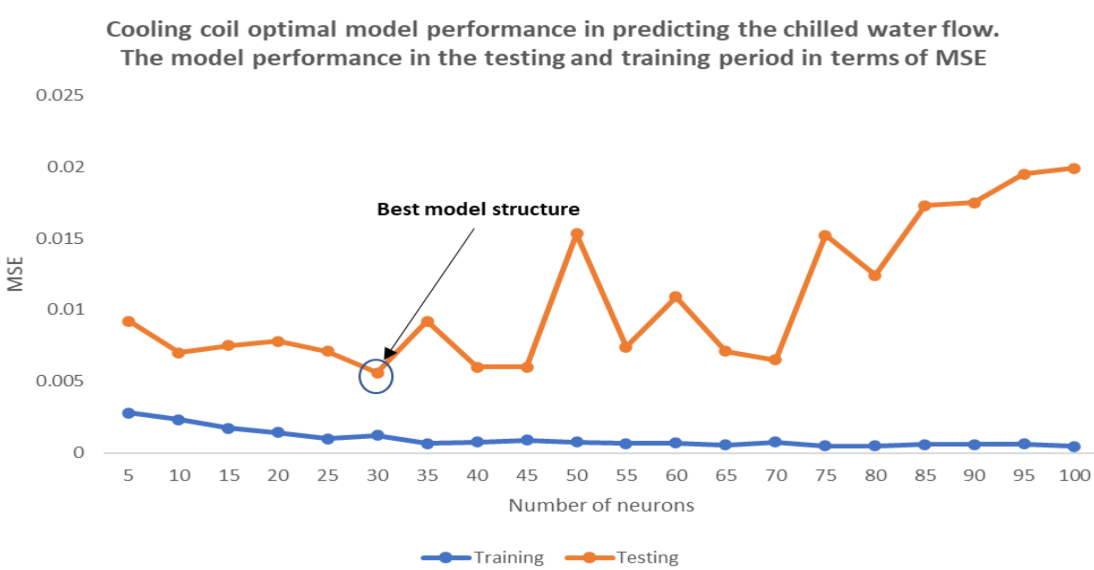

(B)

Figure 54. (A)The Training and testing period of the iteration held the optimal model structure. The error value is measure in terms of CV%. (B) The Training and testing period of the iteration had the optimal model structure. The error value is measure in terms of MSE.

While the results of modeling the cooling coil to predict the chilled water temperature leaving the coil have shown that the model structure with one interval of time delay, three intervals of feedback delay, and 5 number of neurons held the lowest error values. The CV% and MSE values were recorded as 0.230.412 and 0.0535, respectively, as shown in figure 55 below.

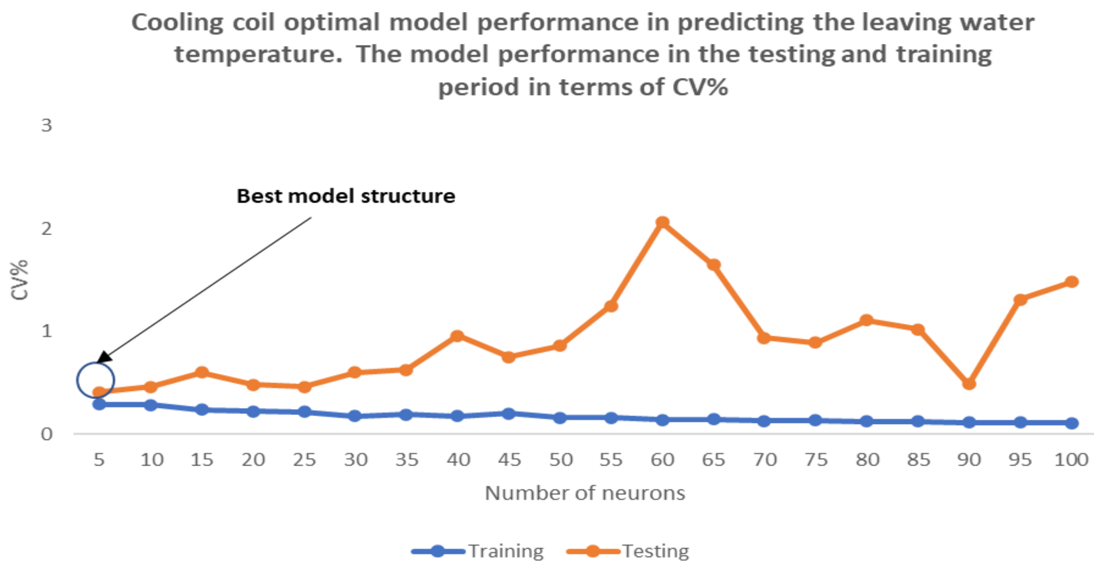

(A)

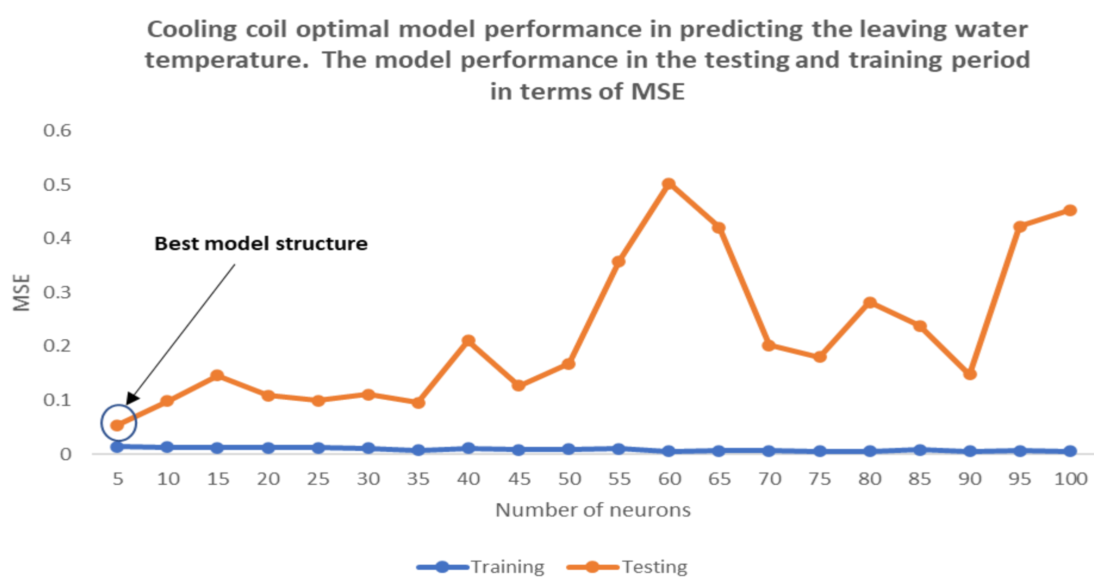

(B)

Figure 55. (A)The Training and testing period of the iteration held the optimal model structure. The error value is measure in terms of CV%. (B) The Training and testing period of the iteration had the optimal model structure. The error value is measure in terms of MSE.

2. **Fan power model results**

While for the fan power model, the same process was applied for the parametric study. The results have shown that the model structure with two intervals of time delay, two intervals of feedback delay, and 20 number of neurons held the lowest error values. The CV% and MSE values were recorded to be 0.4256 and 0.0362, respectively. Figure 56 shows the training and testing results for the iteration that held the optimal value.

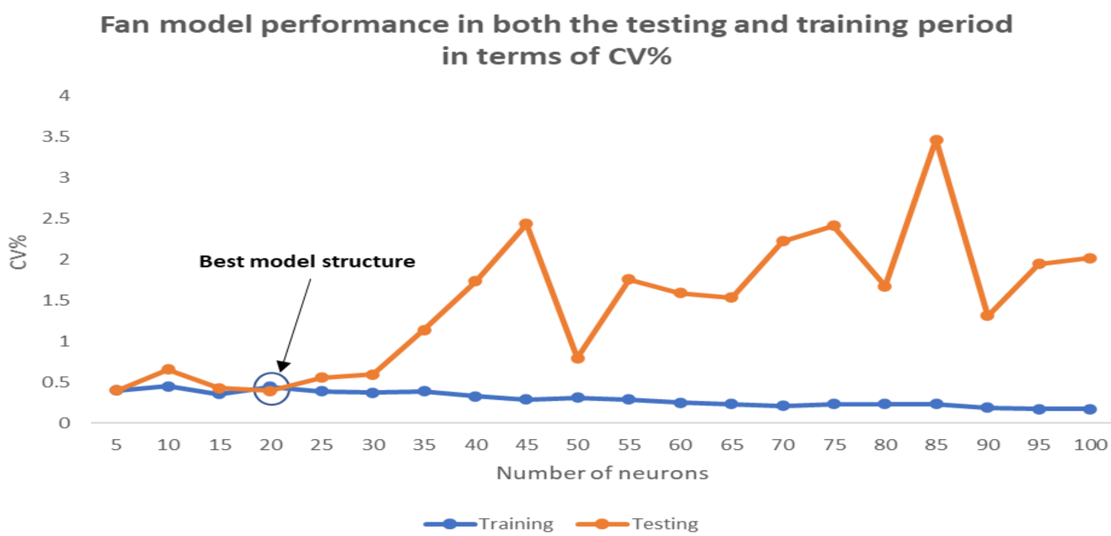

(A)

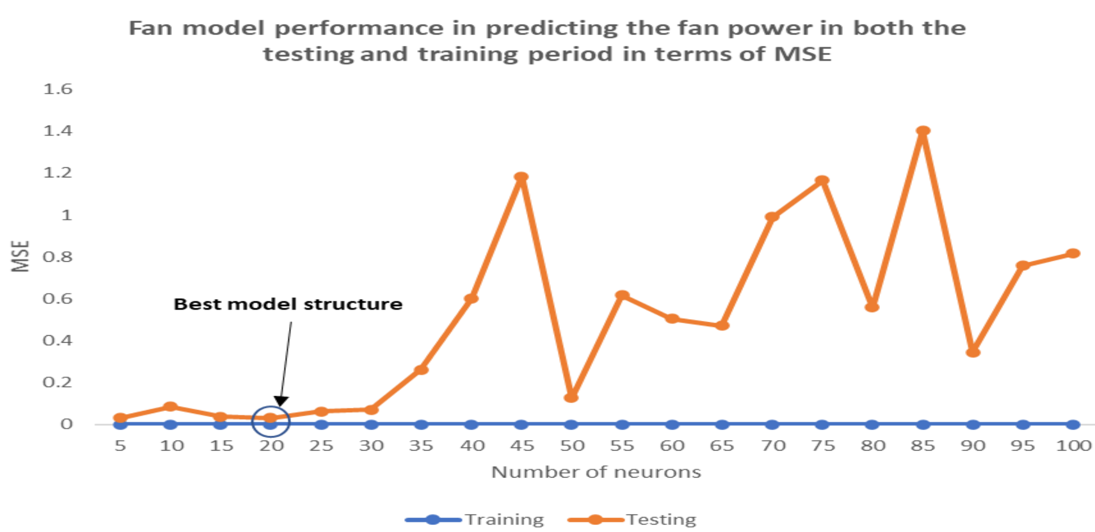

(B)

Figure 56. (A)The Training and testing period of the iteration held the optimal model structure. The error value is measure in terms of CV%. (B) The Training and testing period of the iteration held the optimal model structure. The error value is measure in terms of MSE.

3. Chiller model results

While for the chiller modeling process, the model predicted the chiller power as a function of multiple inputs. The results have shown that the model structure with one interval of time delay, two intervals of feedback delay, and 15 number of neurons held the lowest error values. The CV% and MSE values were recorded to be 2.7135 and 0.0251, respectively. Figure 57 shows the training and testing results for the iteration that held the optimal value.

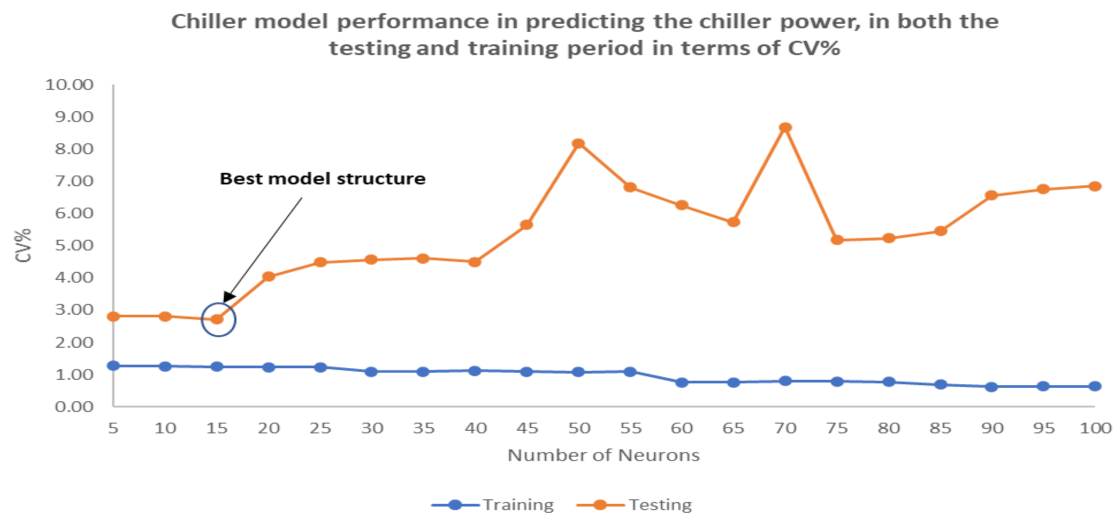

(A)

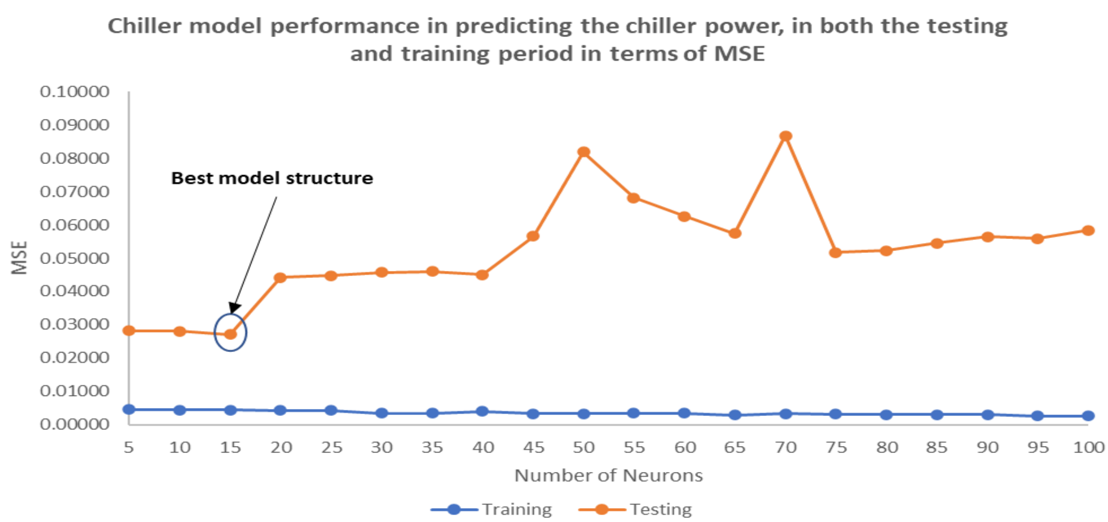

(B)

Figure 57. (A)The Training and testing period of the iteration held the optimal model structure. The error value is measure in terms of CV%. (B) The Training and testing period of the iteration had the optimal model structure. The error value is measure in terms of MSE.

4. Pumps model results

While for the pump's model in predicting the pump power, the same process was applied. For the chilled water pump, the results have shown that the model structure with three intervals of time delay, three intervals of feedback delay, and 5 number of neurons held the lowest error values. The CV% and MSE values were recorded to be 0.5971 and 0.03371, respectively. The model error value results were smaller than other models due to the pump's model simplicity of utilizing two inputs and one output. Figure 58 shows the training and testing results for the iteration that held the optimal value.

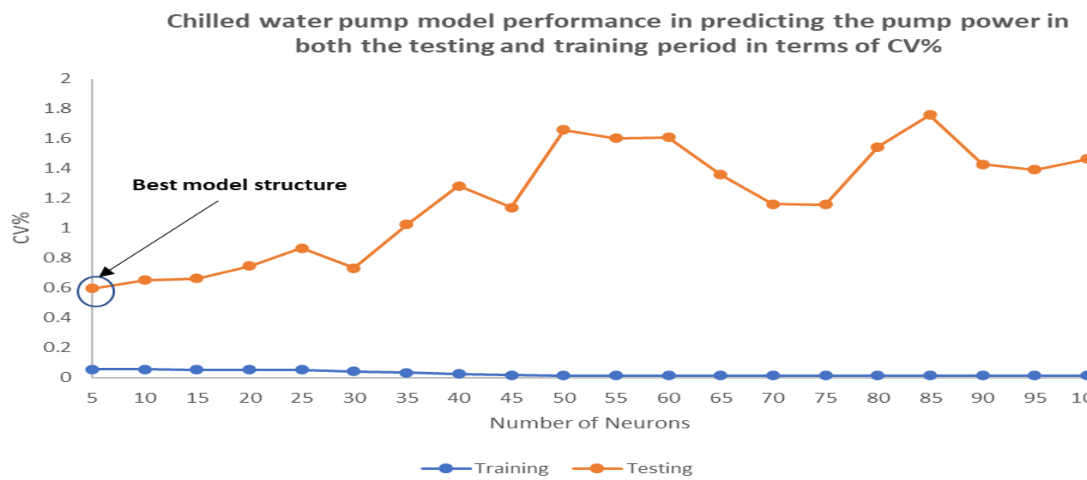

(A)

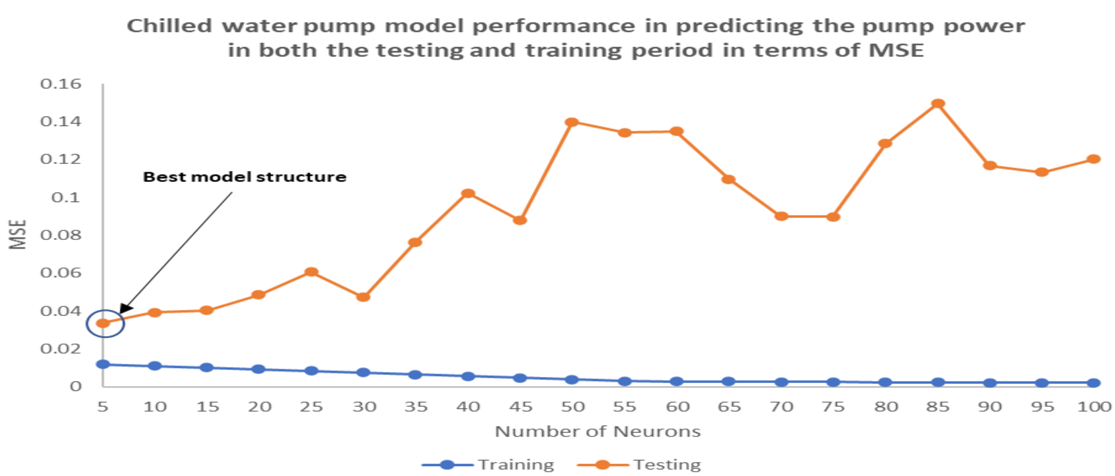

(B)

Figure 58. (A)The Training and testing period of the iteration held the optimal model structure. The error value is measure in terms of CV%. (B) The Training and testing period of the iteration held the optimal model structure. The error value is measure in terms of MSE.

4.4.2 Direct expansion system modeling results.

1. Fan model results

For the DX fan power model, the same process was applied to predict the fan power. The results have shown that the model structure with three intervals of time delay, one interval of feedback delay, and 15 number of neurons held the lowest error values. The CV% and MSE values were recorded to be 0.1211 and 0.0031, respectively. Figure 59 shows the training and testing results for the iteration that held the optimal value.

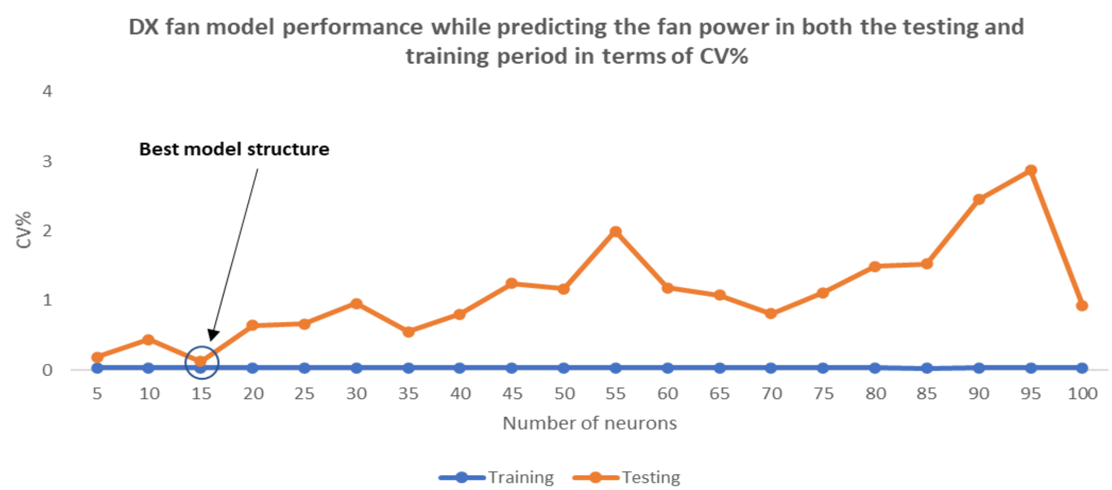

(A)

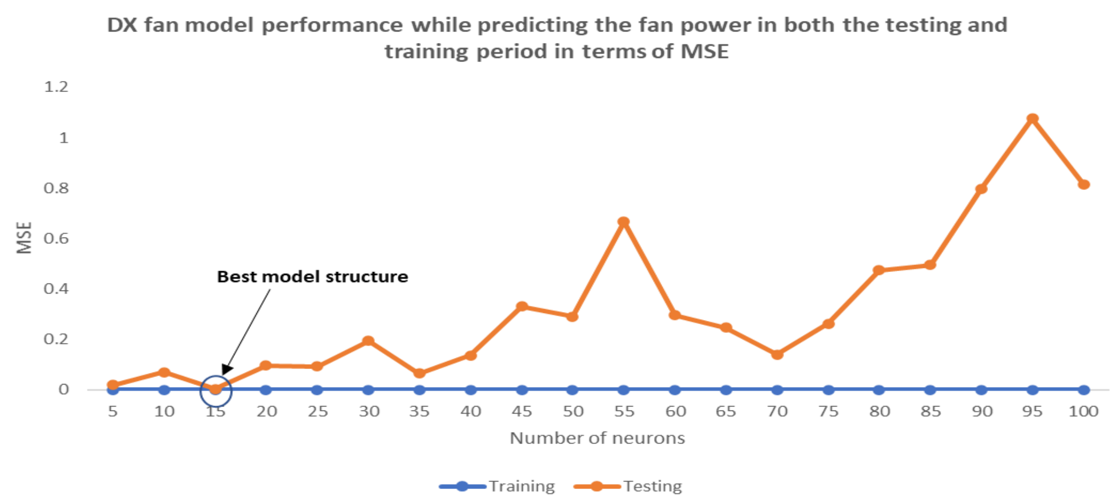

(B)

Figure 59. (A) The Training and testing period of the iteration held the optimal model structure. The error value is measure in terms of CV%. (B) The Training and testing period of the iteration that had the optimal model structure. The error value is measure in terms of MSE.

2. **Cooling coil model results**

For the DX cooling coil that is electric, two outputs were needed to be predicted. The coil power and the humidity ratio of the air leaving the coil. The exact process was applied for the parametric study. In predicting the power, the results have shown that the model structure with one interval of time delay, two intervals of feedback delay, and 20 number of neurons held the lowest error values. The CV% and MSE values were recorded as 0.456 and 0.0102, respectively, shown in figure 60 below.

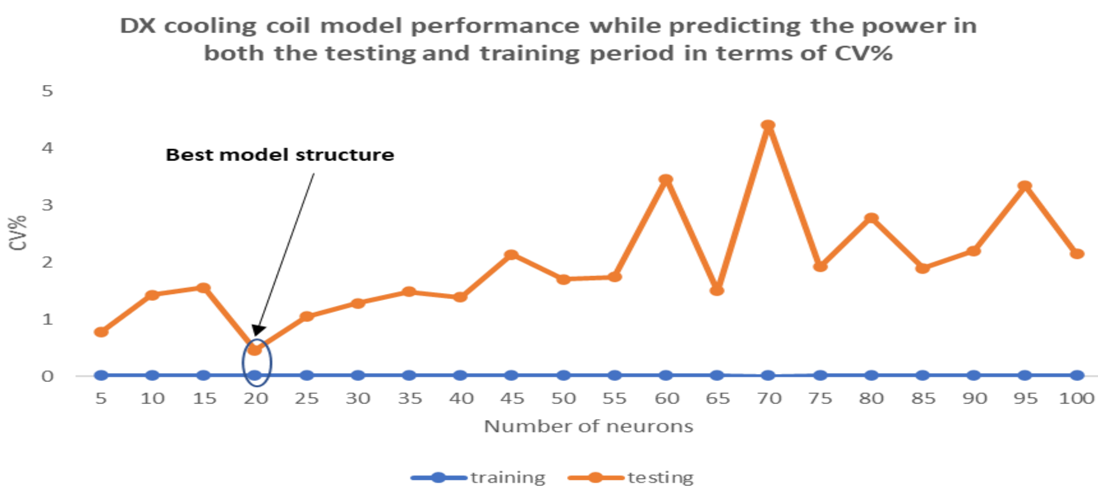

(A)

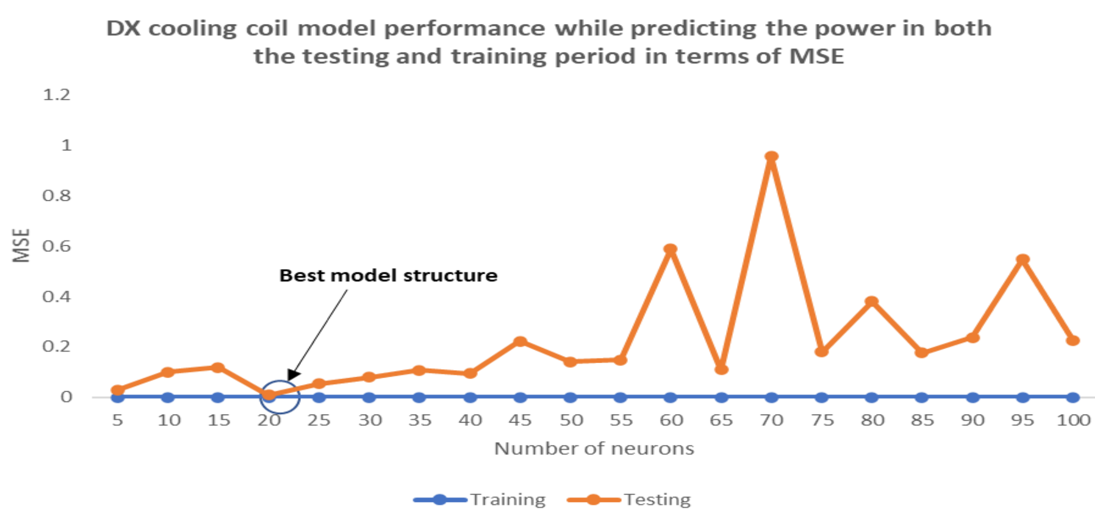

(B)

Figure 60. (A) The Training and testing period of the iteration held the optimal model structure. The error value is measure in terms of CV%. (B) The Training and testing period of the iteration that had the optimal model structure. The error value is measure in terms of MSE.

While the model designed to predict the humidity ratio was slightly more complex and held the highest error values. The results have shown that the model structure with two intervals of time delay, three intervals of feedback delay, and 10 number of neurons held the lowest error values. The CV% and MSE values were recorded to be 5.43 and 0.0563, respectively

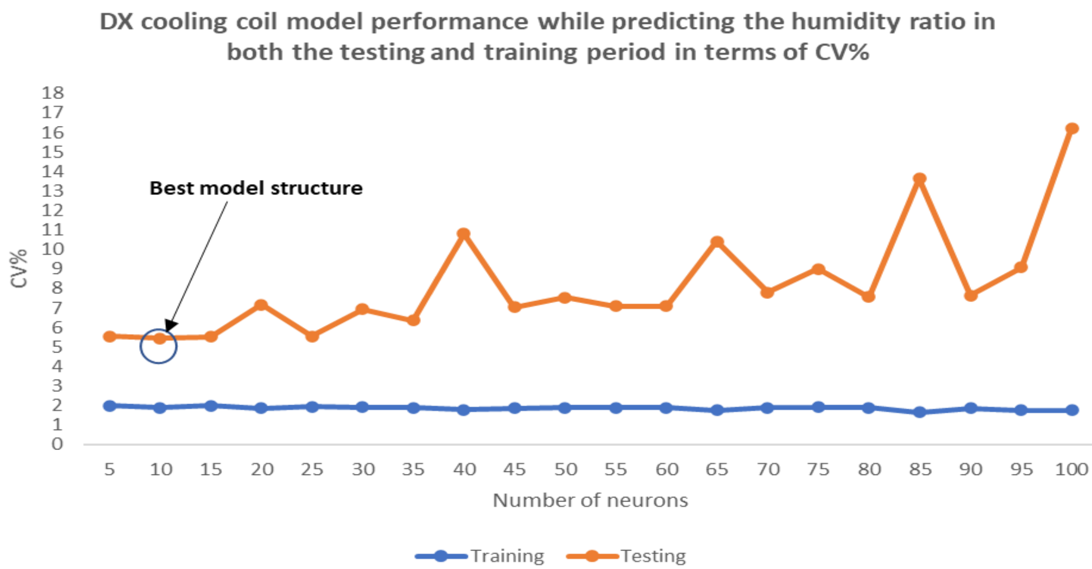

(A)

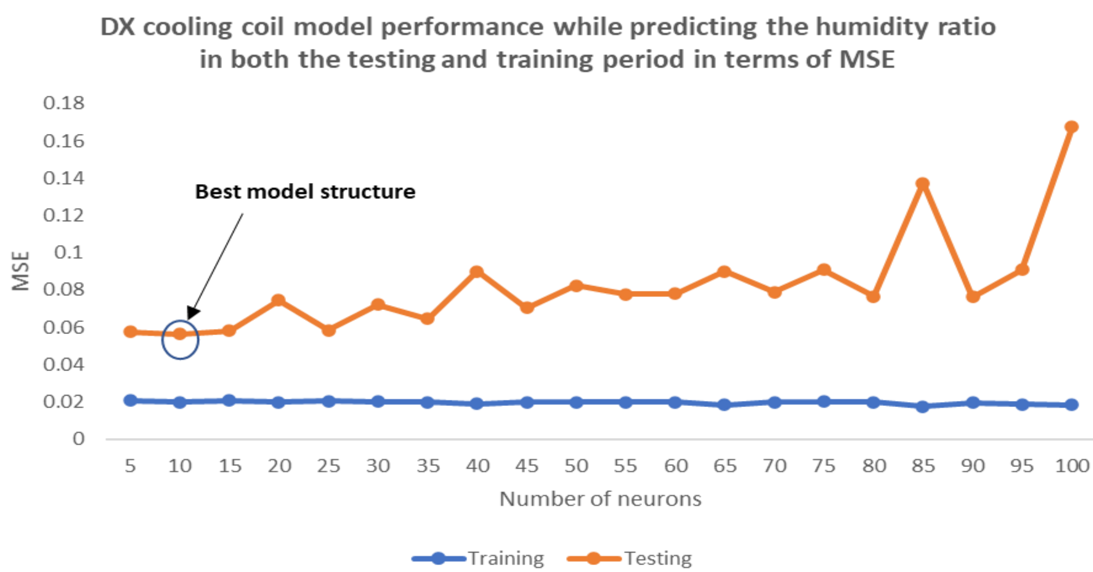

(B)

Figure 61. (A) The Training and testing period of the iteration held the optimal model structure. The error value is measure in terms of CV%. (B) The Training and testing period of the iteration that had the optimal model structure. The error value is measure in terms of MSE.

4.3.3 Model-level optimization process (MLO) results.

The optimization process was deployed after manually conducting the parametric study and selecting the best model structure for each component model. The purpose of the parametric study was to validate the optimization process. As previously stated, the presented modeling process results show a problem-solving methodology, and the results are not fixed for all similar applications. Instead, the results will vary based on the size of the data sets, the collected data's accuracy, and the different inputs tuned to predict the output. But it is crucial to validate the accuracy of the optimization process where similar results are supposed to be found. Also, the modeling process is time-consuming; therefore, implanting an optimization process is crucial to automate the process and help select the best model structure promptly, especially for online applications.

The main objective of this research was to optimize the performance of HVAC systems, which will be done by integrating both the component model optimization level (MLO) and the whole system optimization level (SLO). Therefore, the accuracy of the model-level optimization process is crucial for the system's total energy consumption prediction. It is noted that the results produced by the MLO process are similar in value to those obtained in the parametric study, which gave the green light to continue with the next level of optimization process (SLO).

The GA parameters that were adjusted in the MLO process are the generations and population. The selection of the generation and population size depends on the complexity of the problem that is being assessed. Usually, this is being estimated based on the researcher's experience and previous research work. Researchers typically debate on the generation and population's small size, leading the algorithm to poor solutions. At the same time, the large size will significantly increase the computation time that is required to find the optimal solution. Therefore, close attention should be paid to the population size due to the significant influence on the accuracy of the result.

Therefore, multiple populations and generation sizes were tried in the research, and to each was its pros and cons. A generation size of 150 and a population of 100 were tested at first, and no results were achieved. Due to the higher processer required to execute this size of a population. Later a generation size of 100 and a population of 50 was tried. Each run took almost three days to collect the results. It was concluded that it would be inapplicable to accomplish this research with the available processor at this rate. Lastly, a generation size of 50 and a population size of 50 were chosen to execute the MLO process. It is noted that the lower population size will result in slightly less accurate results, but it was still a valid result. Therefore, for future work, when more advanced equipment with higher processors is available, it is expected to enhance the results further.

Tables 6 show the optimization process, as previously shown in figure 52, results for the chilled water VAV component model. Again, the results produced by the optimization tool are similar in value to those obtained in the parametric study.

Table 6. Optimization Process Results for the chilled water VAV system components

Component	Model's output	Number of neurons	Time Delay	Feedback Delay	Minimum CV%	Minimum MSE
Cooling coil	Total load	30	3	3	1.45	0.019
	Chilled water flow	30	1	1	0.23	0.0056
	Return water temperature	5	1	3	0.401	0.0605
Fan	Fan power	20	2	2	0.4021	0.0322
Chiller	Chiller power	15	1	2	2.702	0.0302
Chilled water pump	Pump power	5	3	3	0.6271	0.0417

Table 7. Optimization Process Results for the DX system components

Component	Model's output	Number of neurons	Time Delay	Feedback Delay	Minimum CV%	Minimu m MSE
Cooling coil	DX coil power	20	1	2	0.365	0.0006
	Supply air humidity ratio	10	2	3	5.225	0.0463
Fan	Fan power	15	3	1	0.1901	0.0042

4.4 Discussion

The HVAC system components are complex nonlinear entities. Therefore, data-driven models were favored against physical models because data-driven models are easier to train, faster, and more suitable for online applications and can be trained to predict the component with less information. In contrast, physical models require detailed information about the component and require more extended periods of time to reach the output, making it less unsuitable for online applications. And due to the significance of each system component, we cannot propose one model to fit all the components in the system. And choosing the best model structure is a time-consuming process. And here comes the optimization process role in automating the process of selecting the optimal model structure for each application.

Each component model trained in this chapter was created based on the previous knowledge and expertise to specify the inputs and outputs. Therefore, the shown models are not fixed for each application. And the model structure will be changed based on the system and application that is being examined.

The best model structure was first selected in the parametric study manually. The variables of each model were changed in each iteration, and the model testing and training error values were recorded. Later the model structure with the lowest error value was selected as the best model structure. Keep in mind that the lower the error values, the better the model is, and an error value of zero refers to a perfect model, and that case is not applicable in real-life applications. Moreover, ASHRAE standards require the data-driven model CV% value to be less than 25% for the models to be acceptable.

The results of each model performance in terms of CV% and MSE shown in the results section are not fixed for each application. Instead, it only reflects the model's performance and how accurate the simulated outputs are against the actual output.

Therefore, due to the significance of each component, the model’s structure and parameters presented in this research reflect the selected systems in this research. Thus cannot be replicated and needs to be adjusted if the application and the system type changes.

The component models are linked later in the two-level optimization process discussed in chapter 5 to predict the total system energy consumption.

Since the parametric study is time-consuming, for example, the cooling coil model took almost three days to complete all the iterations and select the best model structure. For this research, an optimization process to optimize the system setpoints every 15 minutes was proposed, as discussed in chapter 5. Therefore, the best model structure needed to be reached in a period of no more than 10 minutes. Therefore, a model-level optimization process (MLO) was proposed to automate the parametric study and select the best model structure within the specified time frame. As a result, the results were reached in less than 10 minutes.

Instead of only proposing the MLO process using GA, a parametric study was shown to validate the results where the results of the MLO process were compared against the one from the parametric study. Suppose the same results are found for the best model structure that means that the MLO process is accurate. If different results are found, the MLO process is considered faulty, and further examination of each model structure is needed.

Finally, this research has validated the use of the MLO process that achieved similar accuracy values when compared against the one conducted by the parametric study.

Figure 62 below shows the simulated data Vs. the actual performance of the fan power model. Since the data are collected in a 1-minute timestep, the figures are crowded and complex to examine for the entire three months discussed. Therefore, the figure shows ten days of performance only for clarity of the results. The figure shows how accurate the model was in predicting the actual performance.

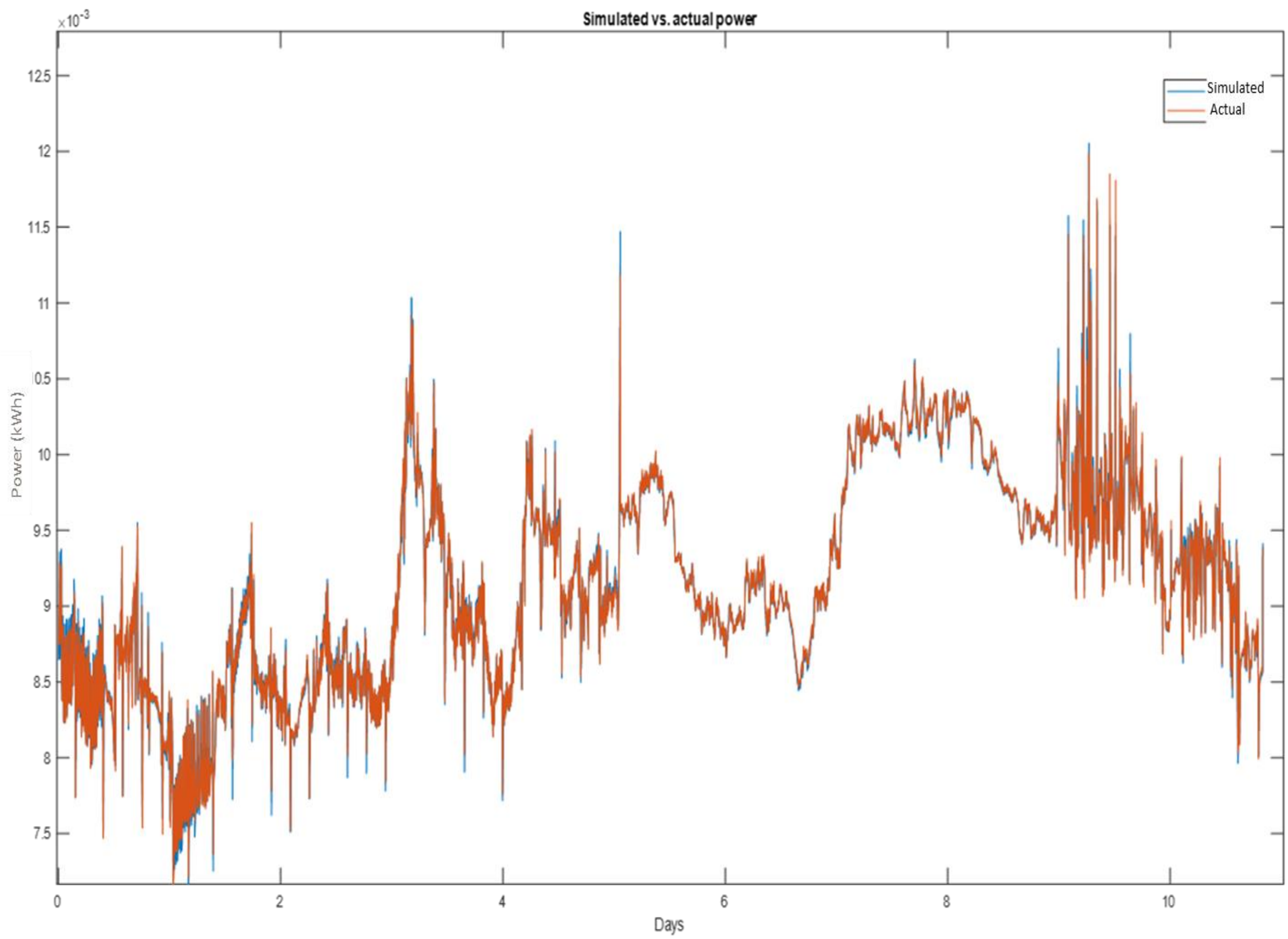

Figure 62. Optimal results with simulated power vs. actual power for the testing period of 10 days.

Chapter 5

Developing and test an integrated two-level performance optimization process

5.1 Introduction

Today, modeling and simulation are established for addressing the problems related to energy consumption in buildings. As a result, energy performance modeling, optimization techniques, and control strategies are gaining ground in research applications. Unfortunately, some of the available tools are not suited to be used for time-dependent applications. However, some artificial intelligence optimization tools are best suited for those applications. Because they have the compatibility to adjust optimal variables setpoints, those tools are fast, adaptive, and capable of promptly solving time-dependent algorithms related to the HVAC performance.

One of the most popular optimization tools broadly used to optimize the performance of HVAC systems is genetic algorithms (GA). As previously discussed in chapter 2, GA will be used as the optimization tool selected for this research due to its capability of handling a wide range of variables at one time, the ability to work with complex simulation programs, proven to be effective in solving complex problems that cannot be easily solved with traditional optimization methods. In addition, it is a publicly available user-friendly tool. The GA was used for the model-level optimization (MLO) and the whole system-level optimization (SLO). The objective function of the GA and the overall objective function of this research is finding the minimum energy use of the selected HVAC system while maximizing the system efficiency.

The data used to evaluate the optimization process are simulated data of a five zones office building using energy plus. While the GA optimization algorithm was developed using MATLAB. The optimization process developed in this research will optimize the system performance for minimal energy use over the period of fifteen minutes. After implementing the proposed optimization process in this chapter, the system that will be evaluated is the chilled water VAV system. Due to its being a popular system in commercial buildings and its complexity, it will allow for more discussion of the results and thoroughly points the main findings. In contrast, the DX system will be evaluated in future work.

The MLO process was previously described in chapter 4. Where the system component modeling and optimization process was explained thoroughly, this chapter will examine the SLO process and how the two optimization levels are integrated.

The proposed integrated two-level optimization process in this research will contribute to the field of modeling and optimization of the HVAC systems performance in many aspects. The main contributions from it are:

1) Reduce the total system energy consumption while improving the zone thermal comfort and therefore reduce the cost of operation and the environmental benefits from lowering the usage of the system that means less greenhouse gas emissions.
2) Introduce the demand control method and implement it in the optimization process after receiving the demand response signal from the utility companies.

Where the demand control is a process that is applied to the demand side to influence and modify the electricity consumption power profile. It is a partnership between the supplier and consumer sides, aiming to maximize mutual benefits.

Demand control is a process of planning, implementing, and monitoring, aiming to modify utility usage by alleviating the peak load demand instead of increasing the power generation and enhancing the transmission and distribution network.

Where electricity companies nowadays are raising the price of electricity kWh in peak hours. Therefore, implementing the demand control to regulate the individual's electricity use through peak hours will have several benefits for the consumer, the provider, and the environment. Through, resulting in financial savings for the consumers without trading the thermal comfort to extent levels. Also, energy and cost savings for the utility supplier by meeting the demand load without increasing the power plant and production process. Lastly, the demand control process significantly impacts the environment by reducing greenhouse gas emissions, especially during peak hours.

Demand control methods include:

- Demand response: The change in the electric usage of the consumers from their normal consumption behavior in response to the change in the electricity prices.

- Traditional energy efficiency methods: Decreasing the demand during the peak load through several ways. Such as replacing the type of lighting with more energy-efficient ones or placing automatic thermostats in the zones.
- Energy conservation methods: Reducing the utility usage during the peak load through the change of the behavioral consumption of the building. Such as lowering the thermostat temperature during the peak load to reduce the use of the HVAC system.

There are multiple ways for the supplier to encourage the consumers to implement the demand control methods, such as Incentive-based programs (IBP) and price-based programs (PBP). In the traditional IBP method, the consumers get paid for their participation in the demand control. This participation payment can occur in terms of a utility bill credit or future discounts as a reward for their participation. In contrast, market-based IBP is where the participants are being rewarded money for their performance. In addition, in the PBP programs, the electricity price is not flat, and it fluctuates, reflecting the real-time cost of electricity.

For our research, we will be implementing the demand response method and energy conservation methods with the proposed optimization process. A methodology was proposed that responds to the demand signal from the electricity companies for the peak hour usage when the electricity prices increase. The system will respond to this signal with an energy conservation method that reduces the zone flow rate to less than the minimum. Under normal conditions, each zone's minimum zone flow rate is 20%, while through the peak load where the demand signal is received, the zone flow rate will drop to 10%. This approach will lower the energy consumption for that period, as shown in the results section. This demand response method will happen for only a few hours through the peak load and not for extensive periods. Therefore, the building will not be starving for air for an extended period, and it will not affect the thermal comfort. The thermal comfort can be met for each zone by increasing the outside airflow rate ratio to maintain healthy breathing zone levels. Also, decreasing or increasing the supply air temperature depending on the heating or cooling load to try and maintain the zone setpoints.

3. The proposed optimization process had an occupancy scheduling method implemented in it. Where most of the base case systems nowadays do not count for real-time occupancy, that will eventually affect the ventilation flow rate of the system. Thus, the constant occupant count in the base case designs will require more ventilation flow rate, increasing

the total system flow rate and requiring more energy. On the other hand, implementing the accurate, current occupancy schedules method will reduce the ventilation rate to the required flow rate. This approach will enhance the sustainability goals of ASHRAE 62.1 by optimizing the zone level ventilation ratio and fulfilling the gap in this related code. While at the same time reduce energy usage. The occupancy schedule can be updated based on real-time knowledge of the occupant's count, zones type of use, and schedule. For example, in conference rooms and meetings times or lecture rooms and when there are lectures in the schedule against when it is empty. And the occupant behaviors such as lunchtimes and breaks, etc. Another method to get an accurate occupant count is CO2 sensors if the building is equipped with ones.

4. Occupancy sensors implementation. The other approach implemented in the optimization process is the occupancy sensor readings against the baseline cases that do not count for occupancy sensors in adjusting the system performance, such as flow rates and ventilation ratio. This approach will crucially affect the zones' ventilation flowrates and zones minimum flowrates. For example, some zones might not be occupied at specific times during the day. Updating that information in real-time applications will lower ventilation flow rates and reduce total energy consumption.
5. Zone Minimum airflow rate setpoint. Optimizing the minimum zone air flowrate setpoint will be crucial to reduce the reheat energy. The codes and regulations suggested using 20% of the total design flow rate as a minimum flow rate for each zone. In this research, the zone minimum flowrate range that was examined is from 20-30%. Savings in the reheat energy will be reviewed and discussed later.

Therefore, to better examine the benefit of those contributions, this research will analyze the optimization process's results under normal conditions and under demand response.

Lastly, to test the proposed integrated two-level optimization process methodology and its contributions since it is designed to be implemented in commercial buildings. Also, because there was a lack of access to an actual building with accurate performance data available, five zones simulated office building was selected to be the baseline case of this study to evaluate the process. Therefore, a simulation building using Energyplus was used. As a result, the accuracy of the whole system optimization process can be tested, and actual energy savings can be calculated.

5.2 Methodology

The innovative integrated whole system optimization process developed in this research will optimize the system setpoints over a short period of optimization (15 minutes). First, the genetic algorithm is used to find the energy used by each system component in the model level (MLO). Later, the integrated components model together will form the system model. And the total system energy use will be calculated as the output of the system model at each time step in response to the controller setpoints and operating modes. Later, the system-level optimization process (SLO) using GA will optimize the total energy consumption by optimizing the setpoints at each time step to reduce the energy consumption at the next time step (15 minutes).

The SLO process developed in this research using genetic algorithm will optimize the system operation set points at each timestep. The setpoints (problem variables) that are selected to be optimized in this research are:

- The optimal supply air temperature setpoint,
- duct static pressure setpoint,
- minimum zone airflow setting,
- minimum outdoor air ventilation rate,

Optimizing those set points at the current operation time step will reduce the energy consumption for the next timestep. The SLO process will use the current system load to calculate the total power and energy consumption. Later an output file with the optimal operation setpoints values will be generated by the GA. This output file also includes the system energy consumption and thermal comfort at that time step. The energy consumption consists of the total power, chiller power, fan power, pumps power, heating energy, reheat, and constraints. The optimization process controls and initiates the "HVAC simulation model," where the output file is generated.

Those outputs will be sent back to the "system model" to serve as the new setpoints for the next time step instead of the constant design setpoints. Next, the energy use and thermal comfort are calculated at the system model and sent back to the optimization process. This process will be repeated throughout the whole operation period. Optimizing those setpoints over operation time will help reduce the energy consumption at every time step, resulting in more energy and a cost-efficient building system.

GA controls the optimization process. Were the size and population of the GA were predefined. Those GA variables are usually specified based on previous knowledge and the complexity of the topic that is being examined. For our research purpose, the GA population of 1000 and 2500 generations was selected. Figure 63 shows a schematic of the whole system-level optimization process using GA.

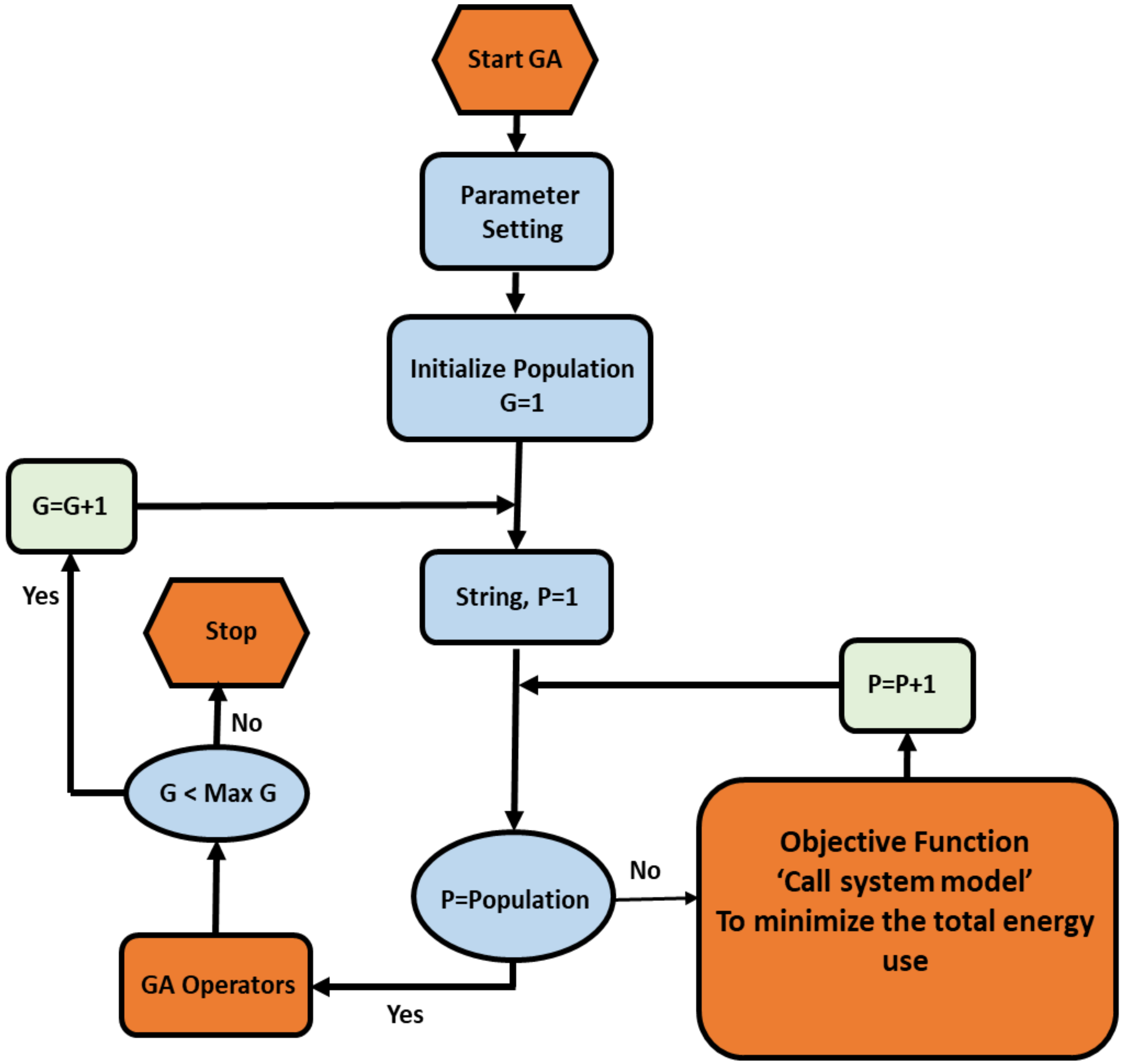

Figure 63. A schematic of the SLO process.

This SLO process is fast and efficient. The time needed to complete the process depends on the number of variables specified, number of generations and GA populations, and number of data points. This process was tested using a regular desktop when each iteration took less than 10 minutes to complete. This time can be reduced using faster and more suitable processors. This short computation time allows the proposed optimization process to be implemented for online applications.

5.2.1 Process setup

In developing the whole system integrated optimization process proposed in this research, accurate modeling and optimization of the system components (MLO) was crucial. Since those components' models impact the accuracy of the objective function of the optimization process, this component modeling and optimization process was thoroughly discussed in chapter 4. Those component models integrated will be the central part of the system model. The system-level optimization process, besides the component models, will include a few other models and calculations as follow:

- The system basic calculations model calculates the zones' humidity ratios, supply, return, mixed air temperatures, and economizer condition (on/off).
- Constraint model that specifies the design constraints and assigns a power penalty.
- An HVAC simulation model to calculate the total power. This model will read the user inputs like the system loads, outside air conditions, design system parameters like efficiencies and pressure drop, schedule, and electricity demand signal.
- Total pressure model that specifies all the design static pressure values and limits.
- A ventilation model, that specifies the zone minimum air flowrate requirements based on ASHRAE 62.1 standard. This model will call for the occupancy sensor signal, schedule number of people, and demand signal.
- The zone model specifies all the zones' design conditions and requirements in terms of supply air temperature, sensible load, minimum airflow rate, and reheat loop.
- System model to simulate total energy use as a function of optimal variables. This model will specify the variables optimized in this research. At the same time, call for all the component models previously described and all the models and calculations above.

Figure 64 shows a schematic of the whole system-level optimization process.

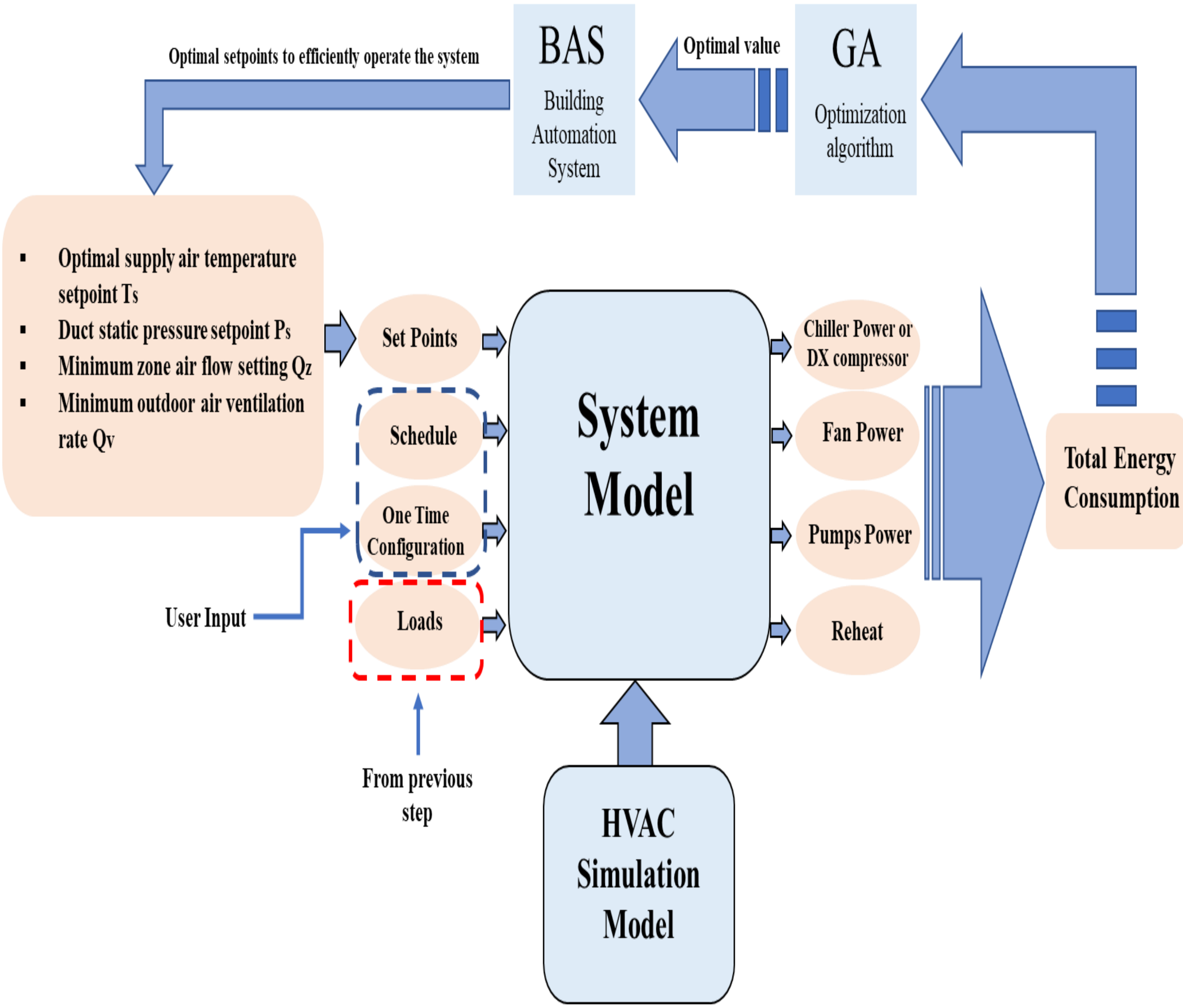

Figure 64. optimization process schematic diagram.

The proposed integrated two-level optimization process is designed to be implemented in commercial buildings. However, this research tested the method using a simulation building due to the difficulty of accessing an existing building equipped with a BAS system. Therefore, the technique can slightly change when implemented in actual buildings against when implemented in simulation buildings, as shown in figure 64 below.

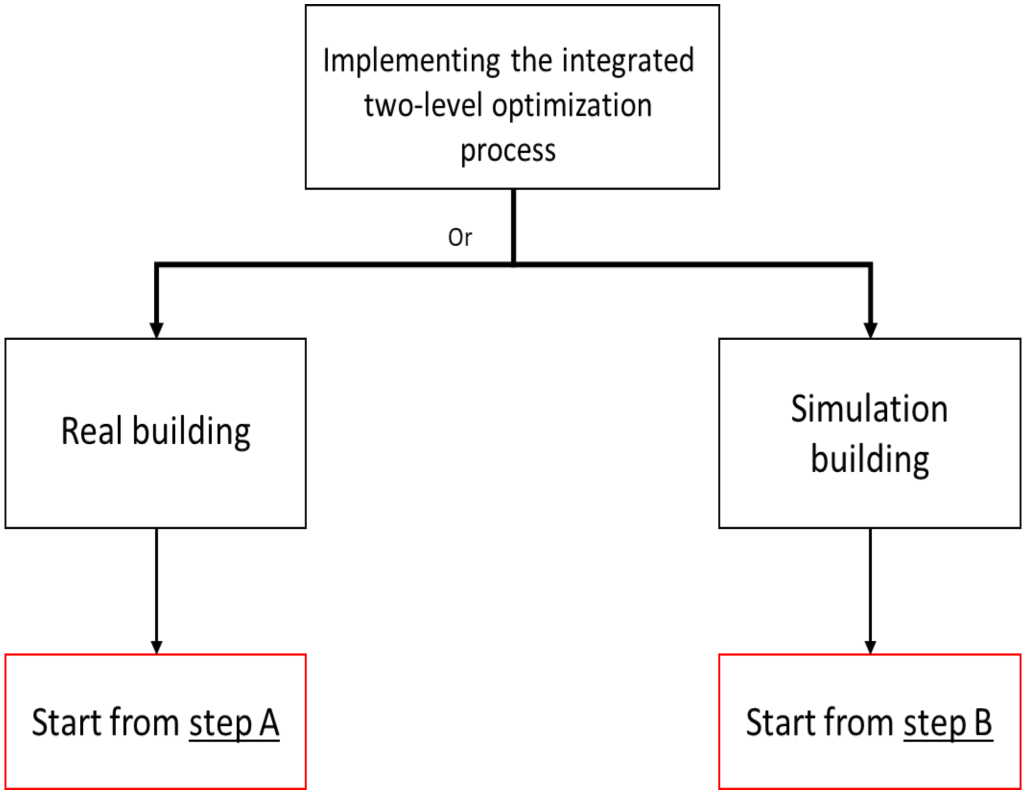

Figure 65. The integrated two-level optimization process testing approach.

The component models that are proposed in chapter 4 are integrated to form the system model. The system model output is the total system energy consumption. The proposed integrated two-level optimization process is designed to optimize the system setpoints every 15 minutes to reduce the total system energy consumption as the output of the system model. To test the proposed optimization process and examine the saving results, the process can be implemented in a simulated or actual building and the process will be as follow:

In actual building implementing the integrated optimization process will start from step A in figure 66 below as follow.

- The loads of the building will be estimated at the first timestep required to start the process. Later, the system airflow will be calculated to be used as an input for the remaining models.
- For the next timestep, the loads will be predicted at the sensible and latent load model after getting all the system performance inputs from the first timestep.

- The loads will be assumed constant for the next timestep. As well as the system model output, the total system energy consumption, will be calculated for the current timestep and assumed to be constant for the next timestep.
- The integrated optimization process will optimize the system setpoints for the next timestep to reduce that energy consumption. The process will be repeated every 15 minutes for the selected period of operation. Assuming that the loads are constant for the next timestep will be acceptable due to the small optimization period. The sensible load depends on the system airflow and temperature difference. In contrast, the latent load depends on the people count where not many changes in the weather conditions and the system airflow rate can happen in 15 minutes period.

In simulation buildings, as discussed later in this chapter, implementing the integrated optimization process will start from step B in figure 66 below as follow.

- In the simulation buildings the building loads are provided by the simulation software. Therefore, there is no need to predict the loads for this case.
- First, the loads will be collected as part of the data collection process every 15 minutes.
- Later, the loads will be fed manually to the code for every timestep, replacing step A.
- Finally, the rest of the process will perform in the same way where the zone model will calculate the system flow required as an input for all the component models. And the total system energy consumption for the next timestep will be calculated.

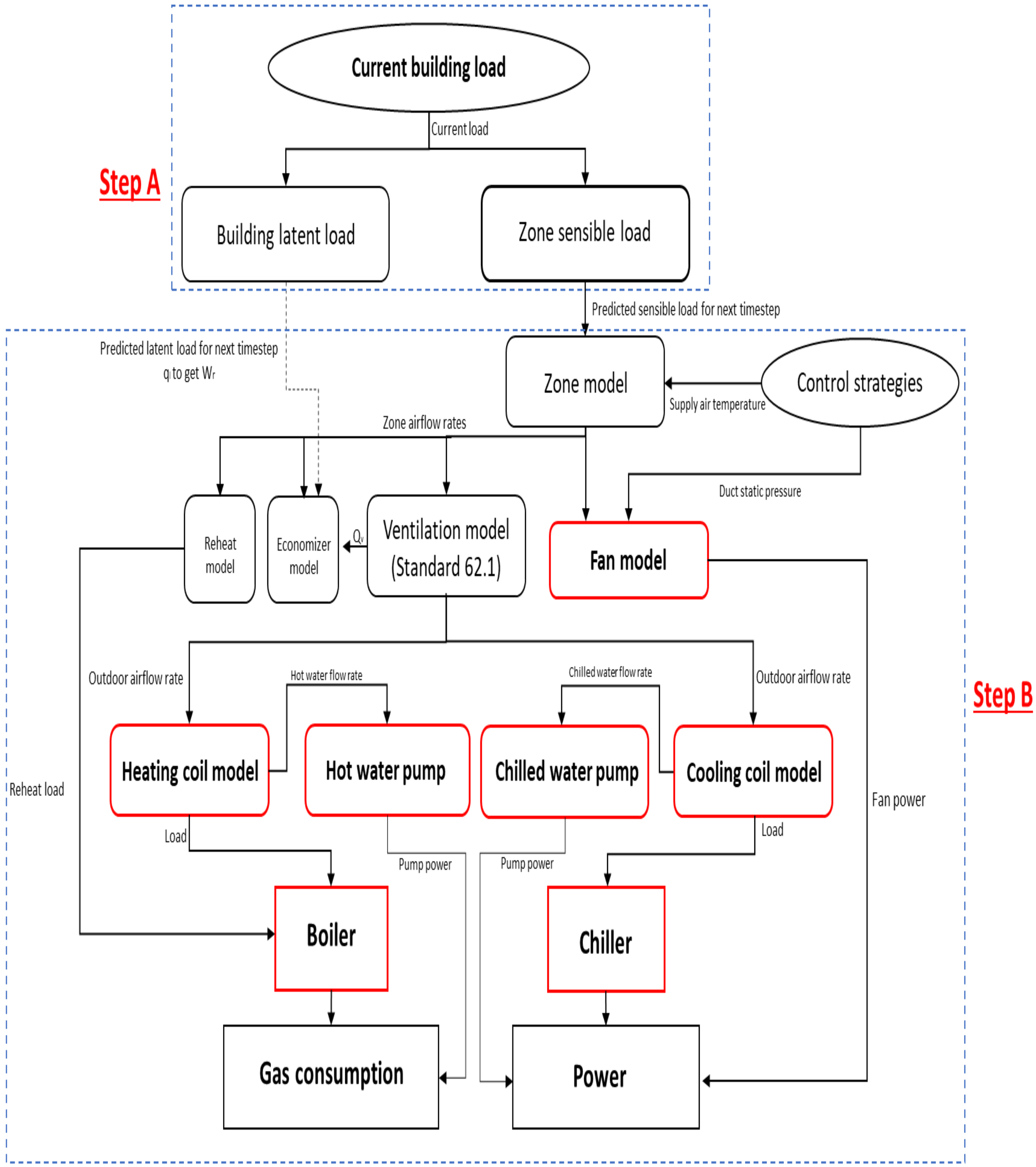

Figure 66. The integrated two-level optimization process testing approach for both actual building and simulation buildings.

The SLO process, using GA, will call the HVAC simulation model to calculate the total power consumption using equation 38 below.

$$Total = Total\ power + chiller\ power + fan\ power + heating\ enrgy + reheat \ldots\ldots\ldots\ldots\ldots \quad (38)$$

In our case study, which will be described in the next section, the building is equipped with an air-cooled electric chiller and a gas furnace. It was noted that the chiller power and fan power are electric output measured in kWh. At the same time, the heating energy and reheat are measured in BTU. Therefore, to examine the total power correctly, the units need to be uniformed first.

According to (EIA, 2021), the price of kWh of electricity in Ohio is 9.78 cents/ kWh. In contrast, the average Ohio price of natural gas is $0.85 per therm. The energy use was converted to the total cost as in equations 39 and 40 below. Later in equation 41, the total cost was divided by the kWh price to get the equivalent energy use in one form (kWh). As discussed in the results section, this approach was implemented in the optimization process to calculate energy use accurately.

$$Therm = 100{,}000\ BTU \ldots\ldots\ldots\ldots \quad (39)$$

$$Total\ cost = (ChillerPower + FanPower) * 0.10 + ((abs(Reheat) + abs(qht))/100000) * 0.85 + PowerPenalty \quad \ldots\ldots\ldots (40)$$

$$Total = Total\ cost/0.10 \ldots\ldots\ldots\ldots \quad (41)$$

After specifying all the inputs in the user input file, as shown in the data collection section, and import into the integrated whole system optimization process as a one-time configuration. This will happen at the HVAC simulation model; the code is shown in appendix H. Also collecting all the building loads provided by the simulation software (EnergyPlus). Those loads will be imported manually to the HVAC simulation model, as shown in the first part of the code (lines 3-7). Those loads will be changed every 15 minutes based on the loads collected. Keep in mind in an actual building the process will predict the building loads as previously described. When the process is linked to the BAS system that collects the system airflow, the process will call for the system flow (lines 12-16 in the code) and allow for the process to predict the sensible and latent load accordingly.

The SLO process will calculate the total energy consumption and the optimal variables (setpoints) at each time step. At the same time, it considered all the design constraints imposed by the codes and regulations for the system design. For example, the range of temperature examined in this research is 55- 65 F^o for the supply air temperature. While the fan duct static pressure range was 0.2-2.5 in. w.g. Any zone with less than 0.2 ducts static pressure will be starving for air, and that will cause for termination of that iterations.

5.2.2 Data collection and building description

For this research, a medium office building of 53660 ft^2 located in Cincinnati, OH, will be simulated using Energyplus software. The main goal of this simulation process is to test and validate the proposed integrated optimization process. In addition, building performance data was required as the user input for the optimization process was collected. Those data are total, sensible, and latent load, system flow rates, occupancy schedule, simulation weather conditions, ventilation flow rates, supply, return, and mixed air temperatures and humidity ratios.

The building is a three-story 53,660 ft^2 (163.8 ft x 109.2 ft) medium office building. The floor-to-floor height is 13 ft. The floor-to-ceiling height is 9 ft (4 ft above the ceiling plenum) with a window to wall ratio of 33%. The glazing still height is 3.35 ft. The windows are evenly distributed along four building sides. And there is no shading provided.

The thermal zoning of the building is a core and perimeter zoning. The percentage of the floor area is 40% perimeter and 60% core. Figure 67 is a footprint of the building's thermal zoning. Openstudio software was used to generate the building’s thermal zoning layout and geometry for better graphical visualization that was not an option in Energyplus.

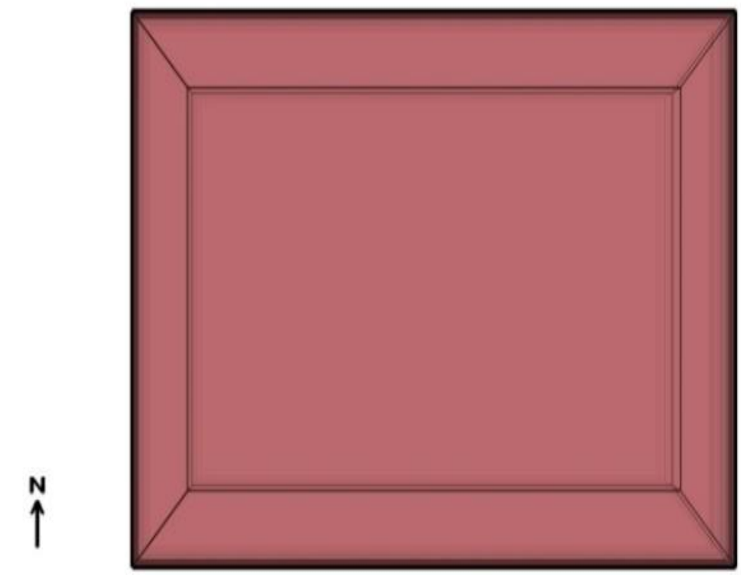

Figure 67. Thermal zoning footprint.

The HVAC system types used are a gas furnace used for heating and a packaged air conditioning unit for cooling. At the same time, the distribution and terminal units that are used are VAV terminal boxes with dampers.

The HVAC design condition is a thermostat setpoint of 75 F^o for cooling and 70 F^o for heating. At the same time, the thermostat setback is 80 F^o for cooling and 60 F^o for heating. The supply air temperature is a maximum of 104 F^o and a minimum of 55 F^o. Figure 68 shows a schematic of the packaged chilled water VAV unit that serves the five zones and how they are connected. Each floor is equipped with a separate and identical VAV packaged unit.

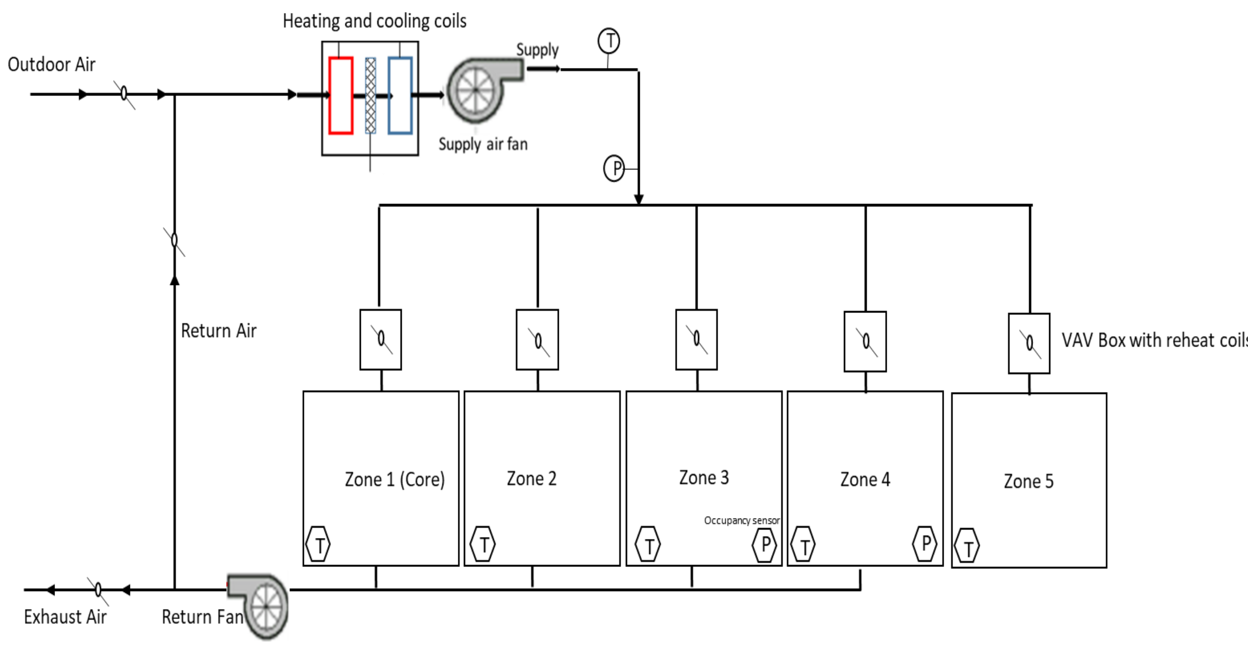

Figure 68. The layout of the packaged VAV unit that serves each five zones.

Since the building is large and contains 15 zones, the time and processor capabilities required to optimize the performance of such a building are extensive. In comparison, each floor includes five zones and is equipped with a separate VAV packaged unit that gives it the ability to serve as a separate floor. Therefore, only one floor was selected examined for this floor, and the building is treated as five zones with one packaged unit, a chiller, and a gas furnaced boiler. Figure 69 shows the building geometry and how the other floors were excluded in the simulation process.

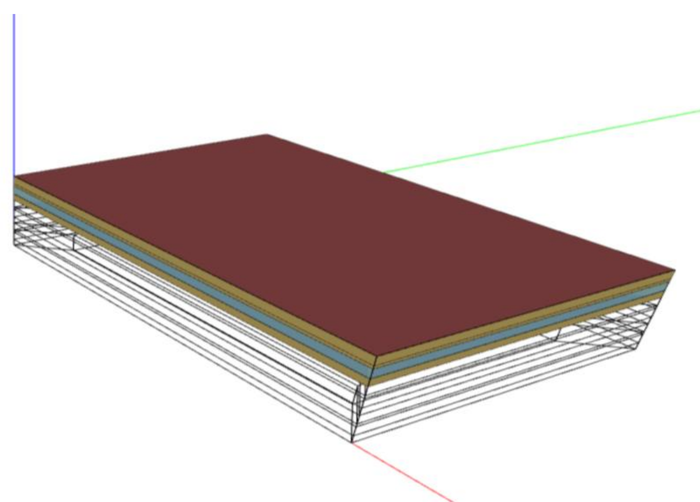

Figure 69. The building geometry. "Source: OpenStudio software"

The zones patterns and conditioned spaces are shown in the following table:

Table 8. Conditioned/ non-conditioned zones

Zone	Area [ft²]	Conditioned [Y/N]	Space type	Total occupants
Zone 1 "Core"	10,588	Yes	Office space	53
Zone 2	2,232	Yes	Office space	11
Zone 3	1,413	Yes	Office space	7
Zone 4	2,232	Yes	Office space	11
Zone 5	1,413	Yes	Office space	7
PLENUM	17,878	No		

The building was simulated to be located in Cincinnati, OH. The weather file used in the simulation process was (Weather File>>Cincinnati Municipal Ap Lunki OH USA TMY3 WMO#=724297). Table 9 below shows the location information.

Table 9. Location weather information.

Data	Value
Latitude	39.10
Longitude	-84.4
Elevation	489 (ft)
Time Zone	-5.0
North Axis Angle	0.00
ASHRAE Climate Zone	4A

Table 10 shows the minimum, maximum, and average dry bulb temperature as extracted from the weather file for analysis. Note the values in the file were in C^0 units and were converted into imperial units.

Table 10. Monthly statistics for dry bulb temperatures in F°.

Month	Jan	Feb	Mar	Apr	May	Jun	July	Aug	Sep	Oct	Nov	Dec
Max	55.94	66.92	71.96	80.06	86.9	87.98	97.88	93.2	89.96	84.02	71.96	64.94
Min	3.02	1.94	10.94	33.98	39.92	42.98	53.96	57.2	41	33.98	24.98	6.08
Daily Avg	31.64	32	42.8	56.48	63.32	68	77.36	73.94	65.12	53.6	48.02	36.32

Table 11 shows the dew point minimum, maximum, and average dry bulb temperature in C^0

Table 11. Monthly statistics of dew point temperature in F°.

Month	Jan	Feb	Mar	Apr	May	Jun	July	Aug	Sep	Oct	Nov	Dec
Max	48.92	51.98	60.08	64.04	70.88	71.96	81.86	78.8	77	71.96	62.06	55.94
Min	-0.94	-10.1	-2.02	26.06	27.86	37.94	45.86	53.6	37.04	28.94	24.08	1.94
Daily Avg	24.62	22.64	31.46	45.14	52.34	59.54	66.38	65.3	57.56	47.48	40.28	27.5

Also, by examining the heating and cooling degree days for a 50 and 65 F° balance temperature in the weather file and the "ASHRAE 2005 ASHRAE Handbook - Fundamentals (SI)" weather file in appendix E. And the minimum, maximum, and average precipitation. Precipitation is the probability for water vapors to condense and form rain, and when it is too cold, it can form snow.

It is noted that the cooling degree days around June, July, August, and September are the most, indicating that those are the hottest months in Cincinnati. Conversely, the heating degree days show that the coldest months in Cincinnati are January, February, November, and December.

Therefore, Cincinnati weather tends to be hot and humid in the summer and cold and snowy in the winter.

To look at the system performance and calculating the expected system savings after implementing the proposed optimization process. We can't examine the performance all year round since it is a time-consuming and redundant process. Instead, a day was selected from each season, reflecting the heating and cooling performance of the system. Therefore, the days analyzed are a day from January reflecting the winter system performance and a day from July reflecting the maximum system performance in the summer. Also, a day from October or May will be examined, reflecting the fall or spring performance.

After simulating the specified building using EnergyPlus software to generate the building loads, supply airflow rates, supply, mixed and outdoor air conditions, and occupancy schedule at each time step of 15 minutes. Those variables are crucial for the proposed whole system optimization process to calculate the optimal system setpoints. After simulation, all the loads, building simulated data, and program reads were exported and organized into an Excel file. That system information was generated for a period of one year of system performance with a time step of 15 minutes. Later, the three days selected earlier reflecting the system's performance in each season were highlighted and stored. The days were July 12th representing the summer performance when the system is in the cooling mode. January 9th representing the winter season and when the system is in the heating mode, and October 10th representing the fall season when the system will have simultaneous heating and cooling depending on the zone location and outside temperature. Figure 70 shows a small example of the organized data in preparing for the optimization process execution.

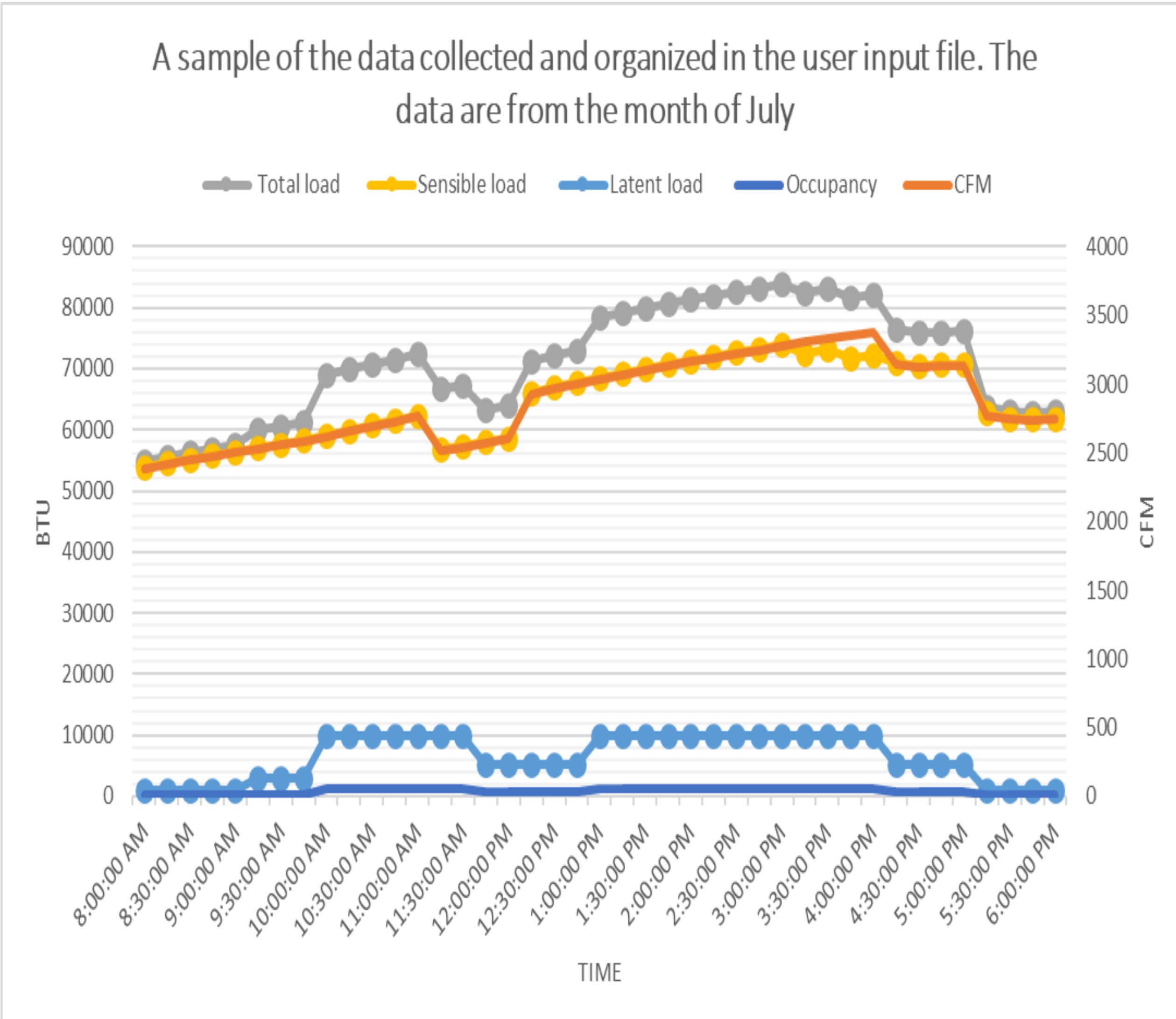

Figure 70. A sample of the data collected and organized in the user input file. The data are from the month of July.

The user input file that is a one-time configuration contains the weather condition for each month as extracted from the simulation weather file and the ASHRAE 2005 ASHRAE Handbook - Fundamentals (SI) weather file. In addition, the dry bulb and dew point temperatures were extracted from the file, while for the wet-bulb temperature, a psychometric chart was used to find the equivalent value. Table 12 shows the one-time configuration used for each month analyzed in this process.

Table 12. The one-time configuration for each month that is used in the design process.

Month	Condition	Max	Min	Daily Avg.
July	Dry bulb	97.88	53.96	77.36
	Wet bulb	85.28	49.64	69.71
	Dew point	81.86	45.86	66.38
January	Dry bulb	55.94	3.02	31.64
	Wet bulb	51.98	2.3	28.94
	Dew point	48.92	-0.94	24.62
October	Dry bulb	84.02	33.98	53.6
	Wet bulb	75.2	31.87	50.24
	Dew point	71.96	28.94	47.48

The integrated process will optimize the previously described setpoints in the methodology section. The setpoints will be optimized based on the loads and the weather conditions imported by the user input file. After running the optimization process for each timestep, an output file will be generated with all the process results in energy consumption and system performance measures. Those outputs will be fully described in the results section.

5.3 Results

After running the simulation process for the specified building using EnergyPlus software, the data were collected over a span of one year and recorded every fifteen minutes (timestep). The information that is now organized and sorted was then implanted into the proposed whole systems integrated two-level optimization process created using MATLAB software. The optimization process will be run every 15 minutes using the user input information for that timestep.

For clarity of discussion, only one day from each season will be analyzed, reflecting the system performance in the cooling mode, heating mode, and simultaneous heating and cooling. The savings were calculated for each day in terms of kWh, Btu and the cost of operation in US dollars.

The results of the optimized performance of the system will be compared against the standard practice used in most systems nowadays to calculate the proposed method savings. The setpoints vary based on the outside temperature in standard practice, as shown in figure 71 below. The supply air temperature is fixed to 55 F^{o} when the temperature outside is more than 65F^{o}, which is the case in the summer season. And the supply air temperature is set to 65 F^o in the winter when the temperature outside is less than 55 F^o. However, in the fall and spring seasons, the temperature outside varies. Therefore, some practices set the supply air temperature to 60 F^o, while the best practices reset the supply air temperature based on the outside temperature.

The relationship between the supply air temperature and the outside air temperature is linear, as shown in figure 71 below.

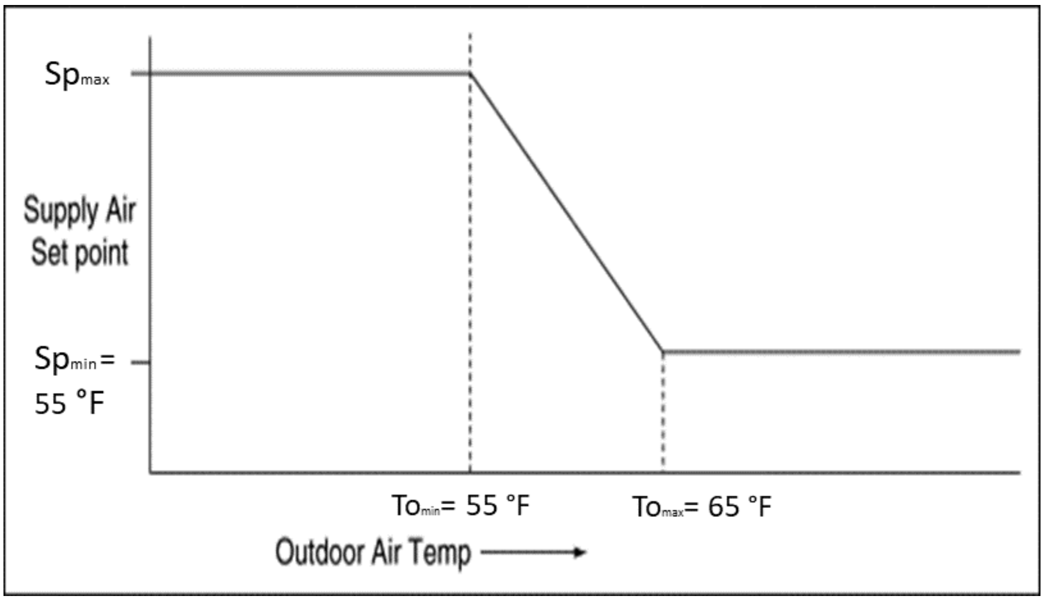

Figure 71. Supply air temperature as a function of outside air temperature.

The equation used to describe that linear relation and find the supply air temperature based on the outside air temperature is shown in equation 42 below.

$$SP = \frac{(SP_{max} - SP_{min})}{(To_{max} - To_{min})} \times (To - To_{min}) + SP_{max} \;\ldots\ldots\ldots\ldots (42)$$

Where:

SP_{max}: Maximum design supply air temperature (70 F^0)

SP_{min}: Minimum design supply air temperature

To: Actual outside temperature at the specified time step.

To_{max}: Maximum outside air temperature.

To_{min}: Minimum outside air temperature.

Therefore, the baseline case selected for this research will follow the best practice supply air temperature reset process instead of a fixed supply air temperature of 55 F^o throughout the year. The supply air temperature will be 55 F^o for the summer season and 65 F^o for winter. And for the spring and fall season, equation 42 will be used to reset the supply air temperature when the outside air temperature is less than 65 F^o and more than 55 F^o.

While the duct static pressure of the fan is set to 2.5 in. w.g, all year round, the zone minimum airflow rate is set to be 20% of the design flow. At the same time, the occupancy of the standard practice is fixed throughout the operation period. And it equals the design maximum number of people for each zone. For the baseline case, as shown in the building description section, the occupancy for zone 1, 2, 3, 4, and 5 was 53 people, 11people, 7 people, 11people, and 7 people, respectively.

The baseline case was run for the previously mentioned set points, and the system performance at each timestep was saved as the baseline case output file. The output file contains the total energy consumption and the system performance. The total energy includes the total energy, chiller power, fan power, heating energy, and reheat. In comparison, the system performance consists of the Q_{sys} (system flowrate), Q_z (minimum flowrate for each zone), Q_o (outdoor airflow), Q_v (ventilation flow), and T_m (mixed air temperature). The standard practice results are the base case scenario.

Later the system was run at each timestep with implementing the proposed integrated two-level optimization process. The optimization process proposed to optimize the system setpoints had a range of supply air temperature from 55-65 F^o. While the fan duct static pressure ranged from 0.2-2.5 in. w.g. Also, the outdoor air ranged from 20- 30% of the design flow. Also, the optimization process had the demand control methodology applied to it. The demand control was selected to be from 1:00- 3:00 PM based on electricity peak hour prices. Finally, the output file of the optimization process was saved as the near-optimal performance scenario.

While the occupancy schedule, unlike the fixed type for the standard practice, was implemented as a user input that varies throughout the operation period. The occupancy schedule proposed for this research is represented in table 13 below. For zones 3 and 4, the occupancy was zero for the period of 10:00-11:30 AM, assuming that this reflects the occupancy sensors' readings.

Table 13. Proposed occupancy schedule.

Time of day	Zone 1	Zone 2	Zone 3	Zone 4	Zone 5	Zone 6	Assumptions
8:00-9:00 AM	10%	10%	10%	10%	10%	10%	Beginning of the workday, gradually
9:00-10:00 AM	30%	30%	30%	30%	30%	30%	Beginning of the workday, gradually
10:00-11:30 AM	95%	95%	0%	0%	95%	95%	close to full working staff
11:30 AM-1:00 PM	50%	50%	50%	50%	50%	50%	Lunch break period
1:00-4:00 PM	100%	100%	95%	95%	95%	95%	close to full working staff
4:00-5:00 PM	50%	50%	50%	50%	50%	50%	End of workday, gradually
5:00-6:00 PM	10%	10%	10%	10%	10%	10%	End of workday, gradually

Later the two results were compared together, and the savings were calculated. The results of each specified day will be thoroughly investigated. This research results have proven that implementing the proposed integrated two-level optimization process can significantly save system energy consumption while improving indoor thermal conditions.

5.3.1 Energy Savings results

1. **July 12th results**

Figure 72 shows the sensible load for the five zones. It is noted that the zones are occupied and require cooling from around 7:00 AM until around 6:00 PM, where the load starts decreasing gradually until 8:00 PM, where it is almost zero after that. Therefore, the system will be analyzed from 8:00 AM until 6:00 PM when the system is fully operating. And this period is usually the standard commercial building operation schedule.

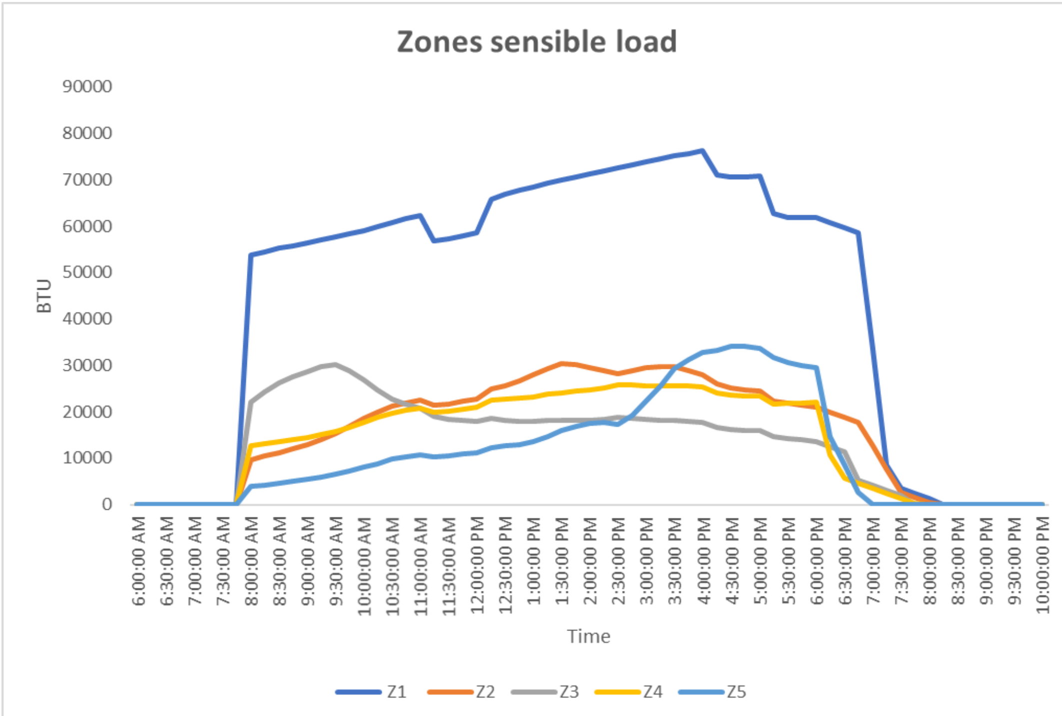

Figure 72. The five zones sensible load in BTU.

Like previously mentioned, the baseline case will have a fixed setpoint. In comparison, the near-optimal case will have optimized setpoints that vary for each timestep. Figure 73 shows near-optimal supply air temperature and fan duct static pressure for July 12th.

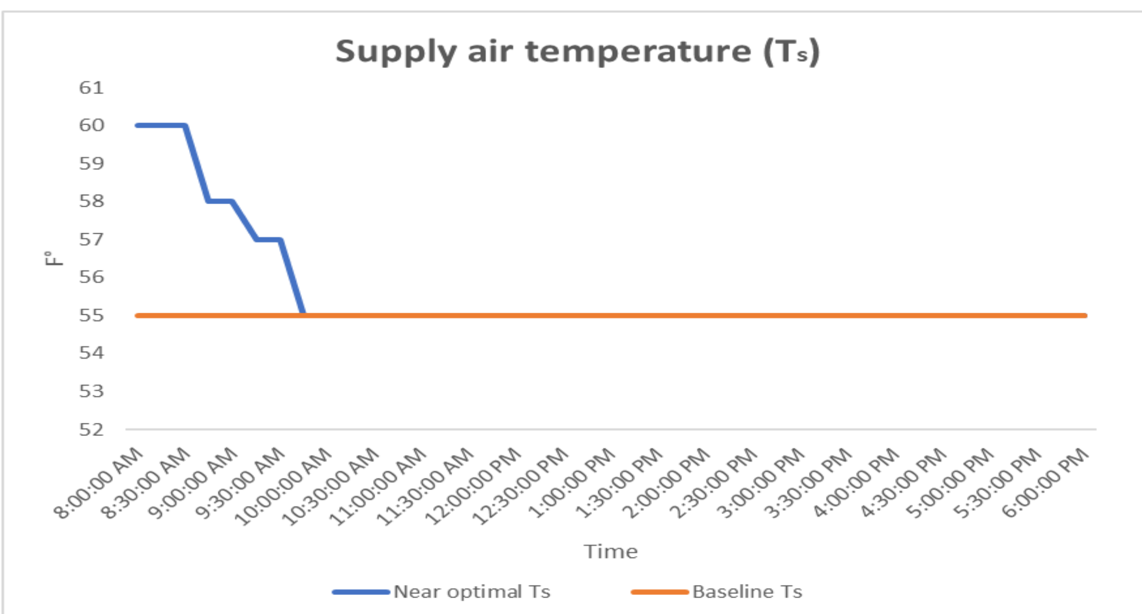

(A)

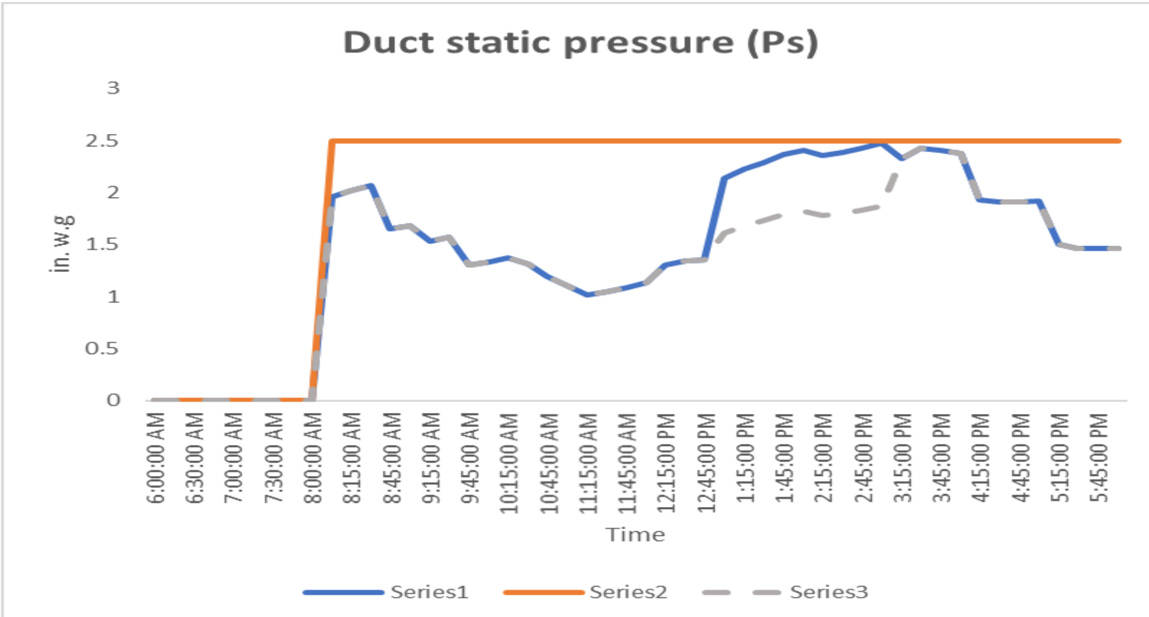

(B)

Figure 73. (A) near-optimal supply air temperature against the baseline case. (B) near-optimal duct static pressure against the baseline case.

It is noted from figure 73 (A) that the near-optimal supply air temperature is primarily close to the baseline case 55 F^{o,} which is expected in July, where mainly cooling is required. Except before 10:00 AM, where the temperature is around 60 F^{o} and then starts dropping until it is fixed to 55 F^{o}. This temperature rise is justified to save on the reheat. The zones are minimally occupied, and the cooling loads are low at that period, so the zone temperature starts dropping, which will trigger the reheat to be turned on. Raising the supply air temperature will require less chiller power and help maintain the zone setpoints as the boilers are typically turned off in the summer season, so reheat is not an option.

While part (B) of the figure shows the near-optimal duct static pressure against the baseline case of a constant 2.5 in. w.g. It is noted that the near-optimal duct static pressure is always less than the baseline case, which means resulting in fan power savings.

However, it is noted that the Ps have increased significantly from 1:00-4:00 PM, where values got close to the baseline case. Due to the building having a higher cooling load and 100% occupancy schedule during that period meaning more airflow rate is required. Later, the building cooling load has dropped, and the occupancy dropped to 50% from 4:00-5:00 PM, meaning the cooling load drops and less airflow rate was required; therefore, P_S started dropping again. It is noted that implementing the optimization process with demand control from 1:00-3:00 PM has helped in lowering the duct static pressure more. That is attributed to the demand control methodology of dropping the zone flow rate to less than the minimum for the selected period. Therefore, resulting in more fan power savings compared to the optimization process under normal conditions. Figure 74 shows the system flow rate for the analyzed period.

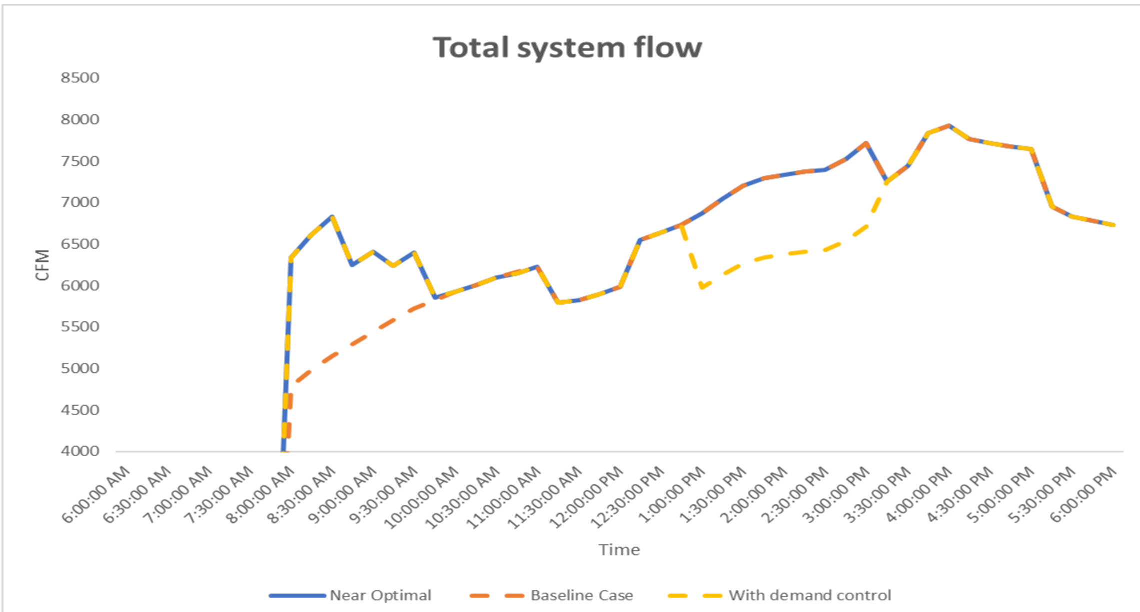

Figure 74. The system airflow rate for the day of July 12th.

The trend in the total system airflow rate is expected and reflecting the zone cooling loads. Most of the system flow is from 1:00-4:00 PM when the building cooling load is higher and decreases afterward. Thus, we can see that the near-optimal performance and the baseline case are the same except for the early morning for the purpose discussed above and also when the demand control method is implemented.

After examining the duct static pressure trends, the total fan power savings were analyzed. It was found that the total fan power savings after implementing the integrated two-level optimization technique were 16.7%, as shown in figure 75 below.

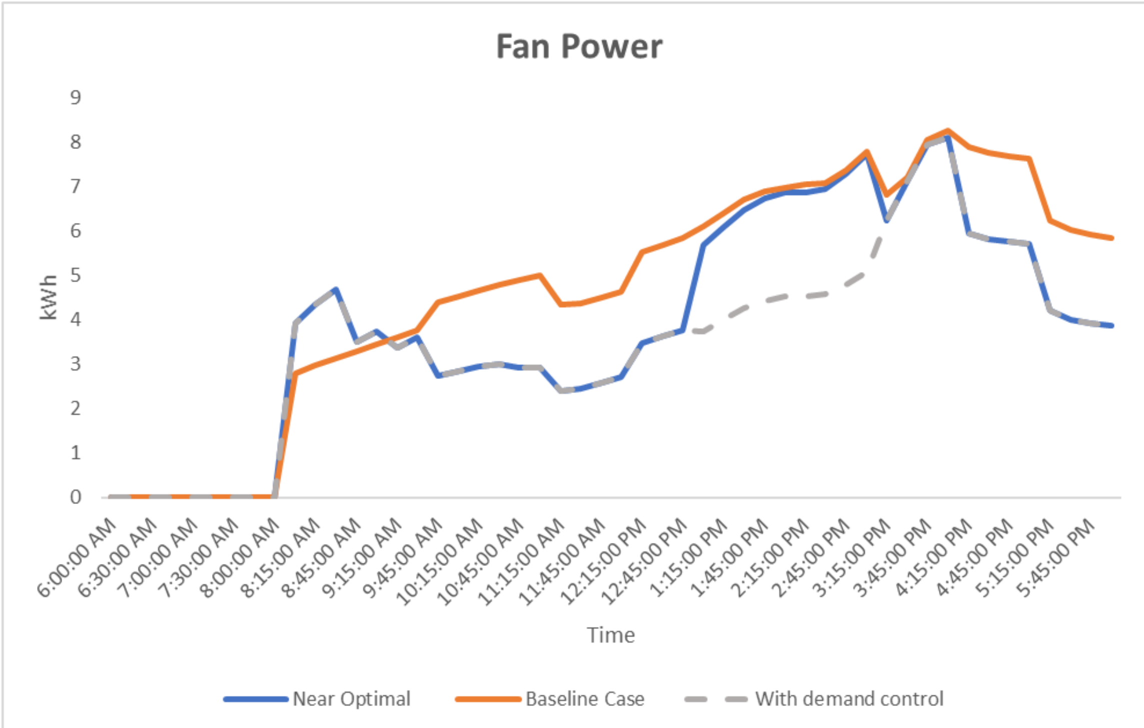

Figure 75. Fan power savings results when comparing the baseline case against the optimal performance.

It is noted that the trend of the fan performance follows the optimization in the duct static pressure setpoint. The fan power of the optimized case was less than the baseline case through the day except from around 8:00-10:00 AM when the system airflow rate of the optimized case was more at this timestep. The higher flow rate in the early morning, as previously described, was due to the higher supply temperature that will help reduce the chiller power, but more airflow rate is required to maintain the zone setpoints. Also, implementing the demand control process affected the fan power savings significantly. Due to the minimum zone airflow rate reduction, the savings were 16.7% and increased to 25.5% afterward.

However, the ventilation flow rate required for each zone followed the occupancy schedule, as shown in figure 76 below. Therefore, most of the ventilation was required from 1:00-4:00 PM when the building is at 100% occupancy and starts to decrease afterward. That explains the peak fan power consumption around that period.

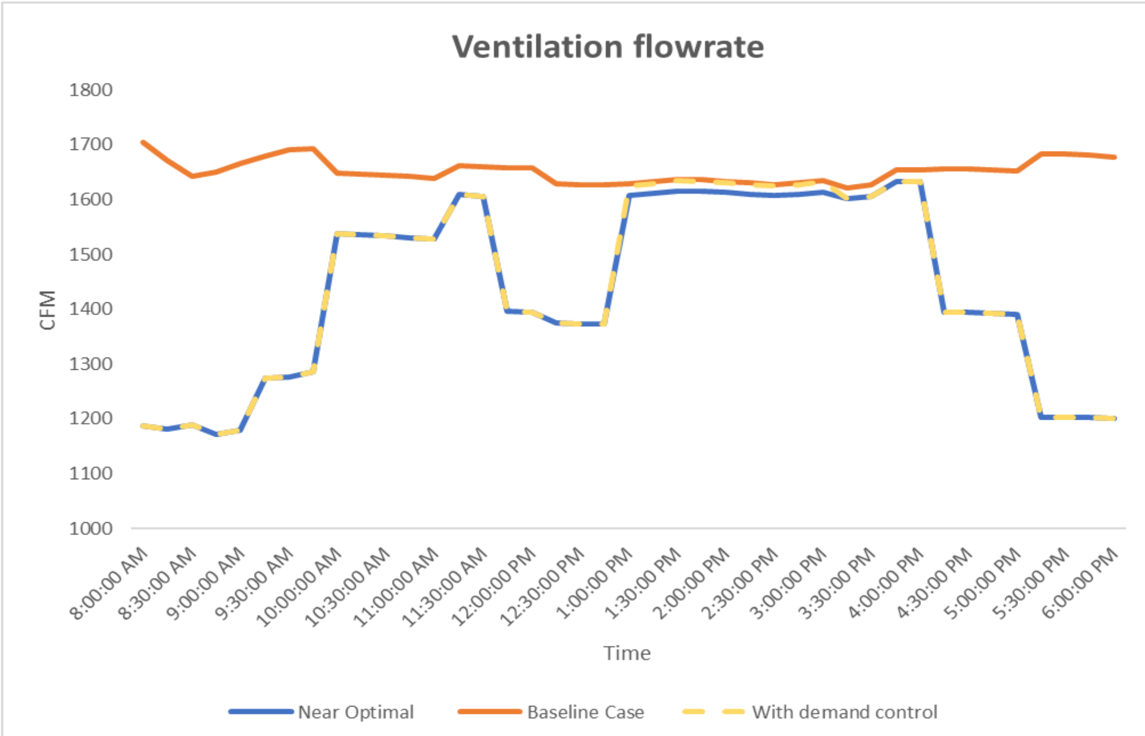

Figure 76. The system ventilation airflow rate for the day of July 12th.

While the ventilation airflow rate for the baseline case was close to constant since the occupancy schedule was fixed for that scenario. Implementing the demand control process has increased the ventilation airflow rate due to minimizing the zone airflow rate. Therefore the percentage of fresh air required to maintain the codes and regulations requirements of healthy breathing zones has increased.

Lastly, the chiller power was also calculated and compared to the baseline case. The savings in the chiller power was found to be 9.74%. Figure 77 shows the chiller power performance after implementing the optimization process against the baseline case.

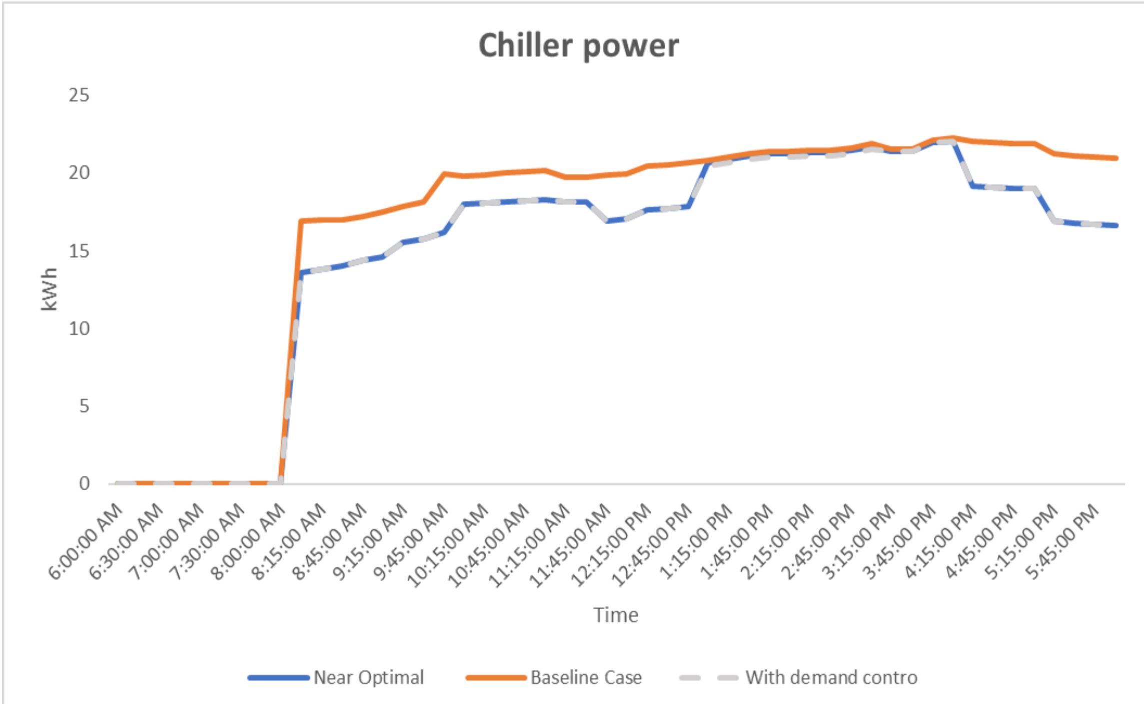

Figure 77. The chiller power savings trend.

The chiller savings were trending with the supply air temperature, the building load, and the occupancy schedule. The trend is almost identical in both cases since the load is the same and the occupancy schedule dominated the power savings where less fresh air was introduced that needed to be treated.

The higher supply air temperature at 8:00-10:00 has helped in decreasing the chiller power. Later the chilled power increased from 10:00-11:00 AM when the building cooling load increased. Finally, at 1:00-4:00 PM, when the building cooling load is at its max, it is the peak of the chiller power consumption.

Also, implementing the demand control process has minimally affected the chiller power savings by increasing it to 10%.

Therefore, the total energy savings of the system after implementing the two-level optimization process was calculated to be 11.3% when compared against the baseline case.

Also, implementing the demand control method into the optimization process has increased the total energy savings to 13.4%. Figure 78 shows the system's total energy savings for July 12th.

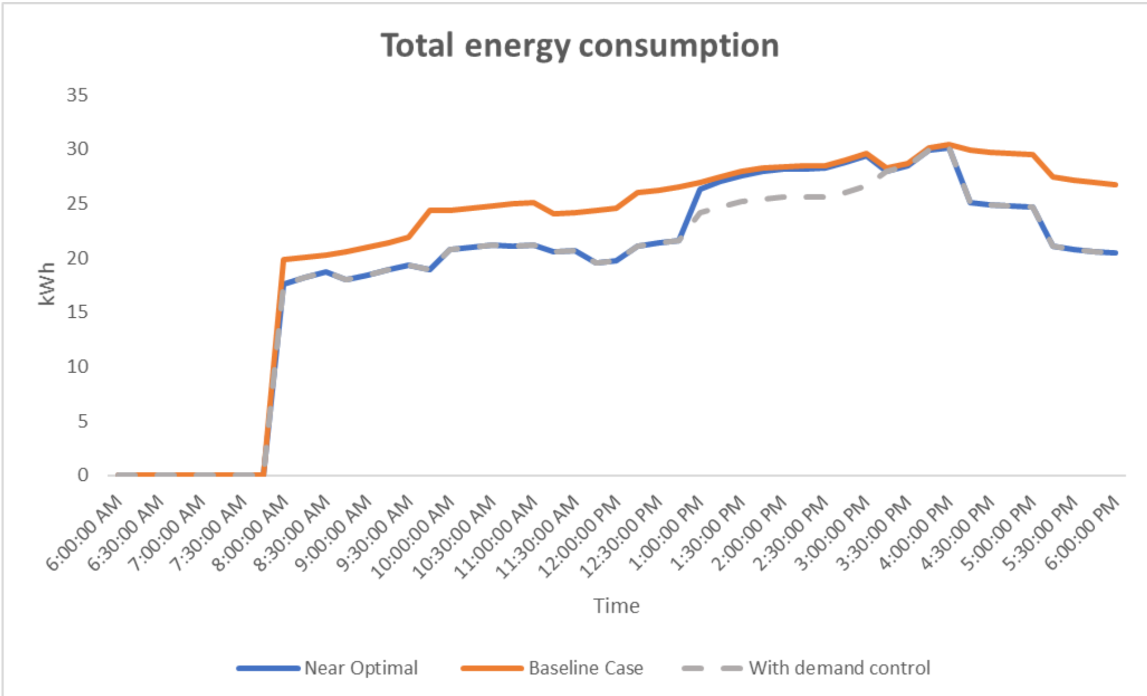

Figure 78. Total energy savings for July 12th.

The previously analyzed results are shown in Table 14 below for better visualization of the results.

Table 14. The energy savings for July 12th.

Component	Savings % under normal conditions optimization	Savings % under optimization with demand control
Total	11.3 %	13.4%
Fan	16.7%	25.5%
Chiller	9.74%	10%

2. January 9th results

January 9th was chosen in this research as the day representing the winter season when the system will be entirely in heating mode. Figure 79 shows the sensible load for the five zones for January 9th. The period of operation of the system that will be analyzed is from 8:00 AM to 6:00 PM. It is noted that all five zones require heating for that period. The heating load of the building is higher in the early morning due to the lower outside temperatures. It starts dropping at around 10:00 PM due to the increase in the temperature outside in the afternoon.

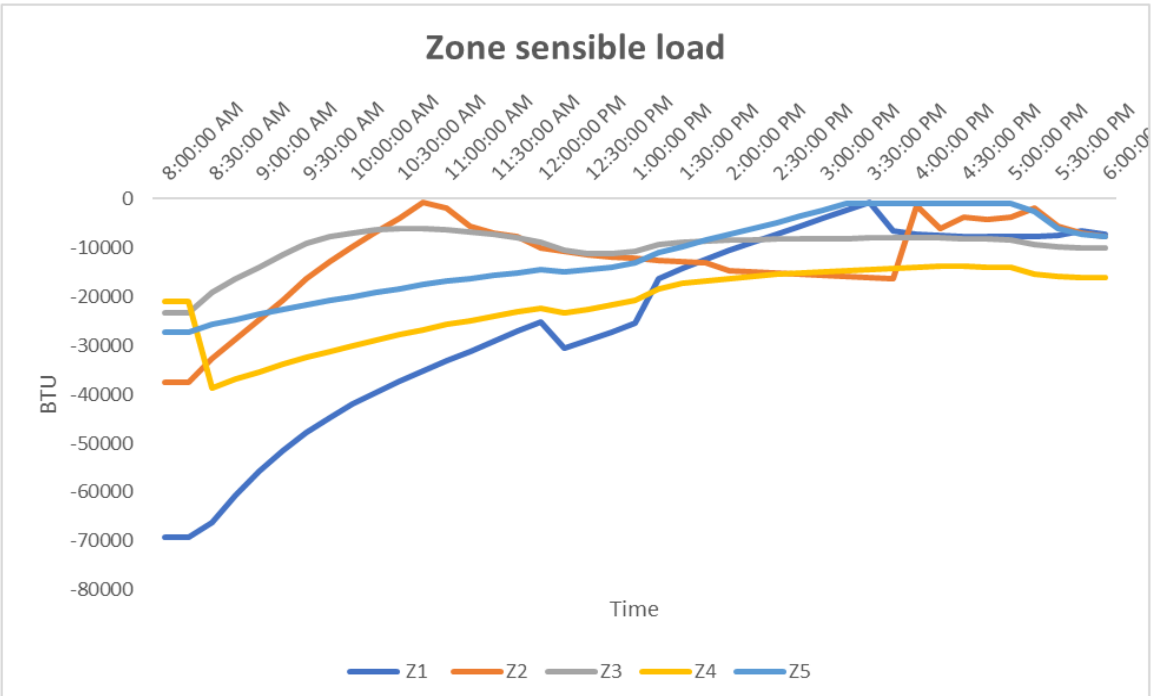

Figure 79. The sensible load for the five zones in BTU.

As previously discussed, as in the best practice, the baseline case will have fixed setpoints of 65 F° and 2.5 in.w.g duct static pressure. In other cases, buildings use a fixed setpoint of 55 F° throughout the year, resulting in more energy consumption. Therefore, case analysis for this type of operation was examined. The results are shown in appendix G. In contrast, the near-optimal case will have the optimized setpoints, which will lower the total energy consumption calculated later. Figure 80 (A) shows the supply air temperature over time in (F°) while (B) shows the duct static pressure in (in. w.g).

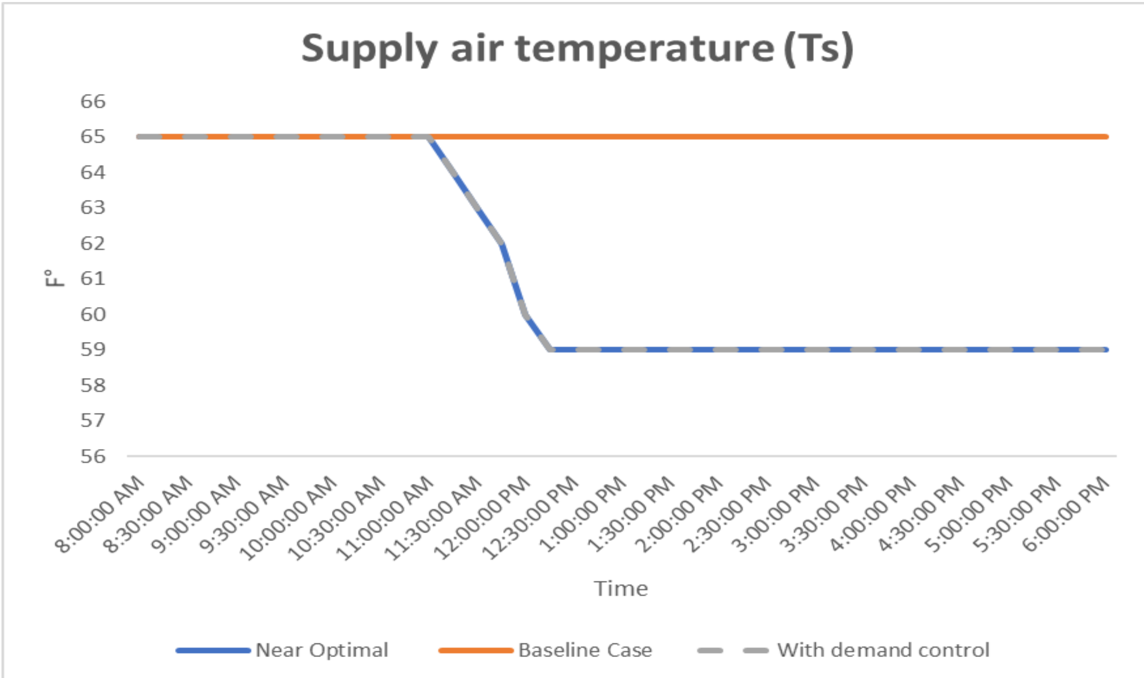

(A)

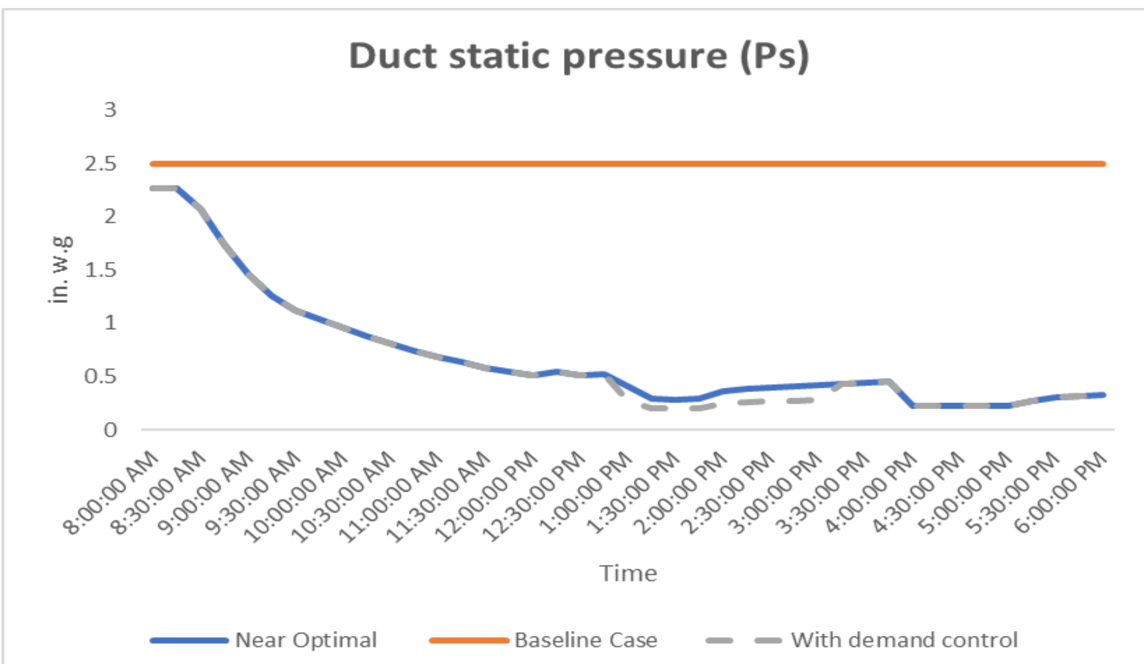

(B)

Figure 80. (A) near-optimal supply air temperature against the baseline case. (B) near-optimal duct static pressure against the baseline case.

Figure 80 (A) shows that the near-optimal supply air temperature is 65 F^0 in the early morning due to the higher building heating load. Therefore, the maximum supply air temperature is necessary to meet the building load. However, the supply air temperature starts dropping slowly at around 11:30 AM due to the decrease in the building heating load until it reaches the minimum of 59 F^0 at 12:15 PM. The drop in the supply air temperature is expected to save on the heating power at that period. Still, it is also anticipated to raise the reheat power necessary to maintain the zone setpoints. However, the savings in the heating power have exceeded the rise in reheat energy, as will be explained later.

Part (B) shows the optimal duct static pressure (P_s) compared to the baseline case. The near-optimal P_s is at its highest in the early morning from 8:00-11:30 AM, where the building heating load is at its highest, and the system flow rate is the maximum. Figure 81 below shows the total building load for January 9th in Btu/hr, explaining the duct static pressure performance trend.

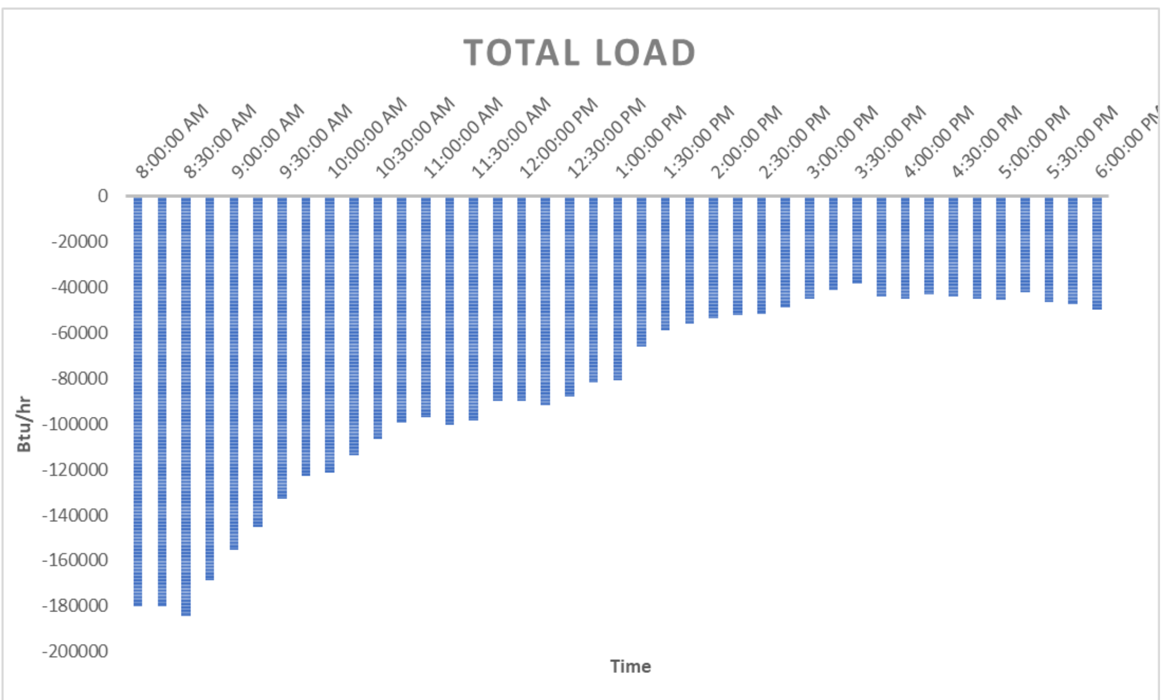

Figure 81. Total building load in Btu/hr.

The P_s dropping does mimic the building load. In addition, implementing the demand control process has reduced the duct static pressure more due to decreasing the amount of minimum zone flowrate.

Unlike the near-optimal case, the baseline case has constant T_s and P_s. Therefore, maintaining the zone setpoint will become an issue when the building load drops to a specific value. Thus, the system will allow for more outside air to drop down the mixed air temperature. Unfortunately, that will result in excessive fan power and heating power usage in the baseline case scenario. Figure 82 shows the amount of fresh air introduced by the system in the baseline and near-optimal cases. Therefore, the airflow rate trend is explained by the supply air temperature.

Also, implementing the demand control methodology has increased the outdoor airflow rate due to reducing the zone minimum flow rate, which requires increasing the percentage of ventilation airflow rate to maintain the code requirements and regulations.

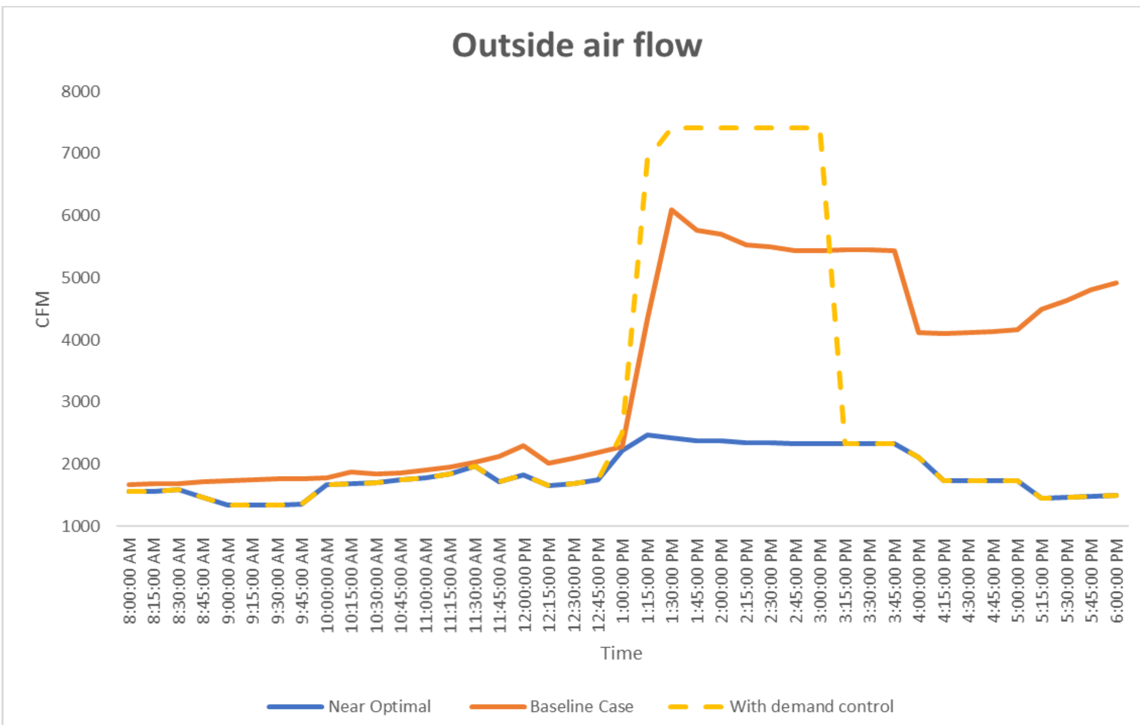

Figure 82. Outside air flow rate for January 9th.

Therefore, the near-optimal case has resulted in a 38.6% savings in the fan power compared to the baseline scenario. Figure 83 below shows the fan power savings for January 9th.

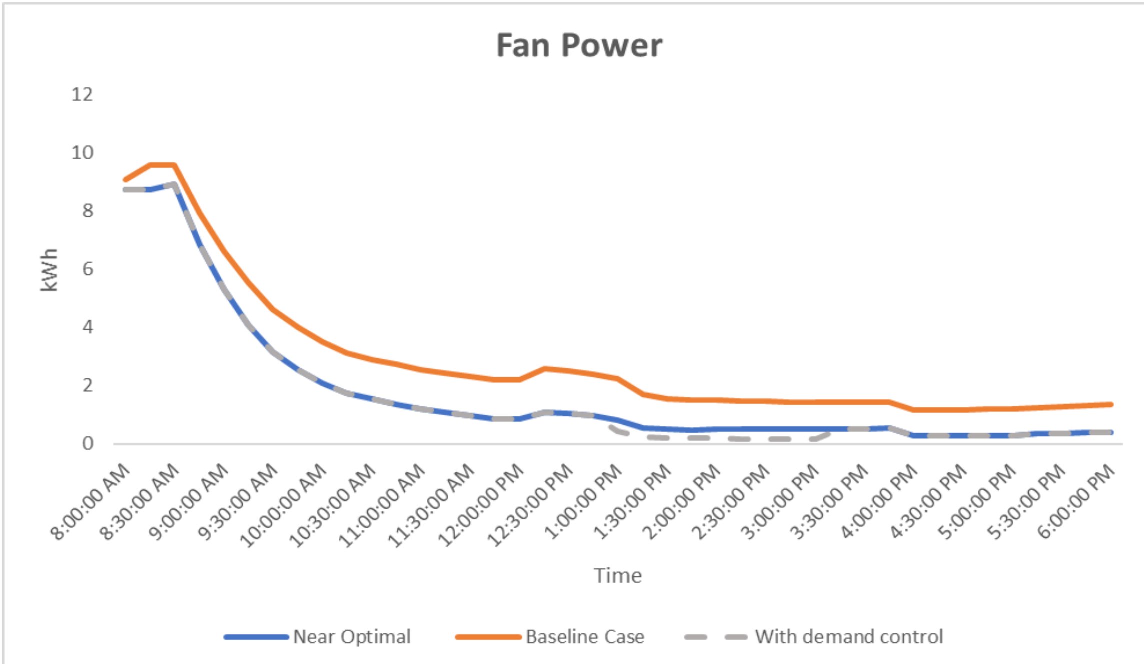

Figure 83. Fan power savings for January 9th.

While implementing the demand control process has increased the fan power savings to 41% by reducing the minimum zone airflow rate from 20% to 10%. Figure 84 shows the system airflow rate value over the period of analysis.

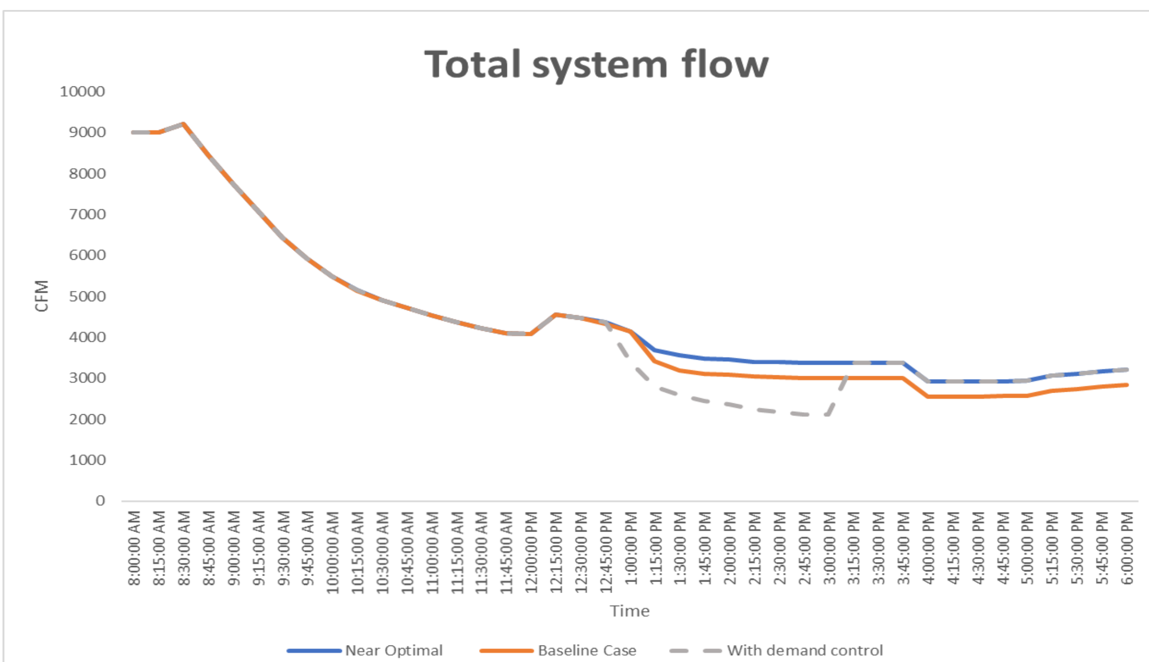

Figure 84. The total system flow for January 9th.

The system airflow rate for January 9th is the same for all cases until 1:00 PM, when the supply air temperature is the same. Afterward, the system flow for the baseline case is lower due to a higher supply air temperature than the near-optimal case.

A constant supply air temperature of 65 F° requires more heating energy, unlike the optimized case with a lower supply air temperature resulting in lower heating energy consumed by the boiler. Still, it will result in increasing the reheat energy needed to maintain the zone setpoint. Therefore, implementing the two-level optimization process has resulted in 50% savings in the reheat energy. While implementing the demand control method has resulted in lowering that percentage of savings by almost 10.5%. The amount of heating energy savings was 44.7% after implementing the demand control method due to introducing more outdoor airflow rates required for ventilation that needed to be heated. Figure 85 shows the heating energy savings for the proposed optimized case against the baseline case.

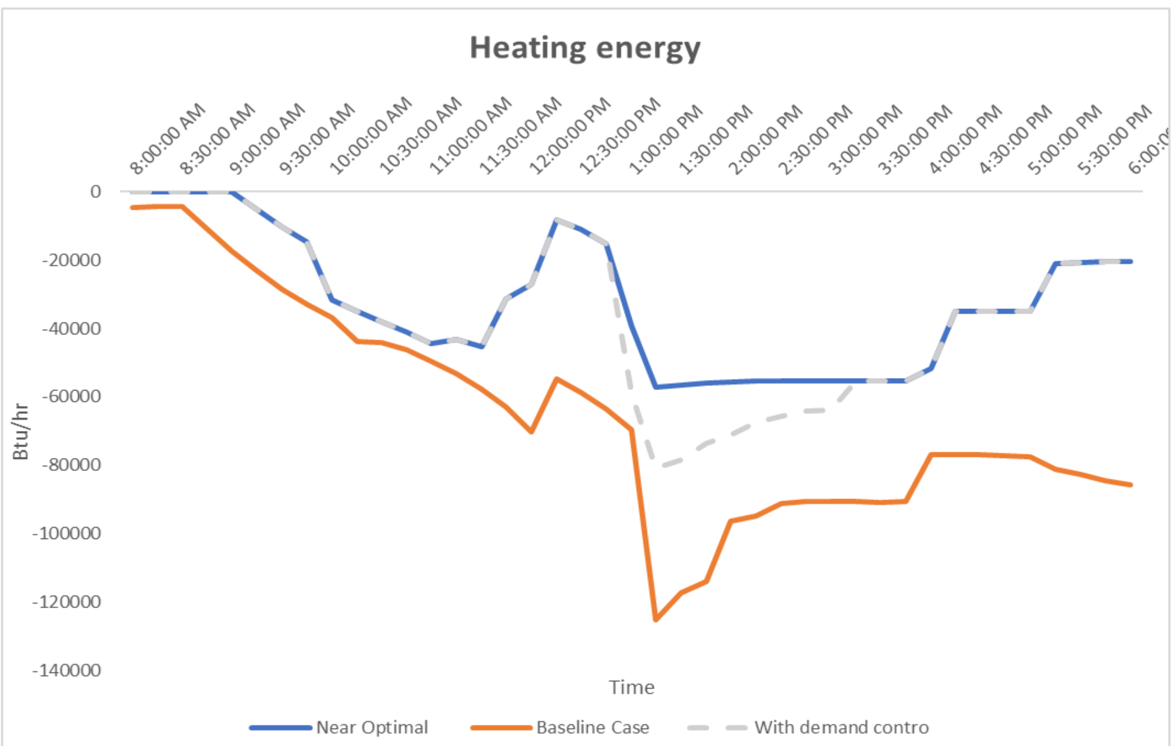

Figure 85. The heating energy for January 9th.

The heating energy for the near-optimal case was the highest from 10:00-11:30 AM due to the higher heating load. And at 1:00-4:00 PM, when the occupancy schedule is almost 100%, more fresh air is introduced to the system. While for the baseline case, it is after 1:00 PM when more fresh air was introduced to maintain the zone setpoint as previously explained.

As mentioned, the reheat energy was anticipated to increase in the near-optimal case in favor of saving on the heating energy. Thus, the reheat energy increased by 5.4% for the near-optimal case when compared against the baseline case due to the lower supply air temperature starting at 11:30 AM, as shown in figure 86.

On the other hand, implementing the demand control method has lowered this percentage to 0.5% due to reducing the zone airflow rate and, therefore, less reheat energy required to treat that amount of air and raise its temperature to meet the zone setpoints.

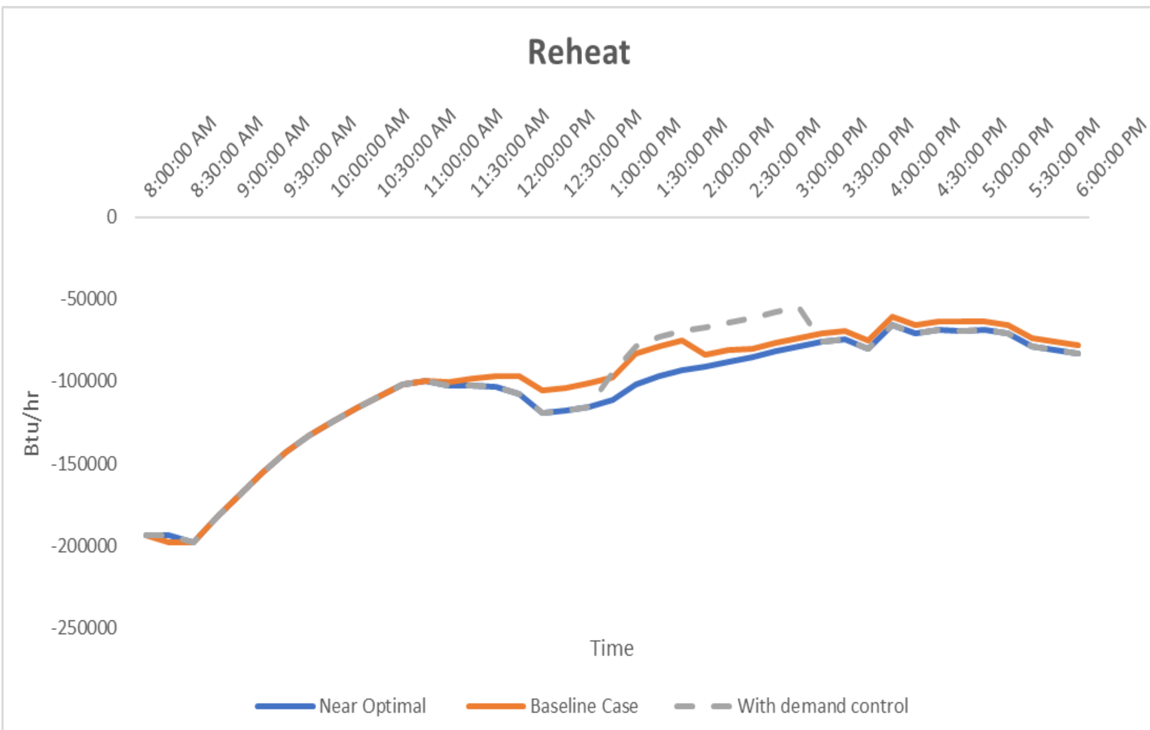

Figure 86. Reheat energy for the near-optimal case and the demand control method compared against the baseline case.

Resetting the supply air temperature and duct static pressure have increased the reheat energy but significantly reduced the heating energy. Therefore, savings were still achieved. And the total energy savings for the system after implementing the two-level optimization process was calculated to be 19.9% when compared against the baseline case of constant setpoints.

Also, implementing the demand control method into the optimization process has increased the total energy savings of the system to 21.2%. Figure 87 shows the system's total energy savings for January 9th.

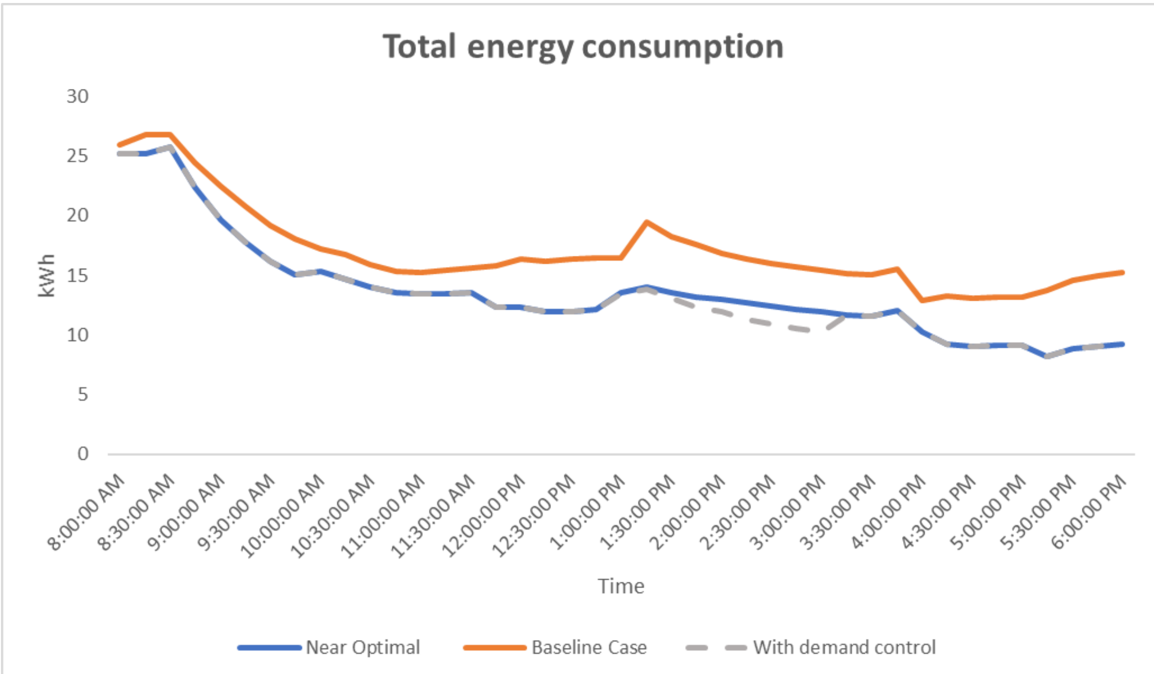

Figure 87. Total energy savings for January 9th.

Table 15 below shows the previously discussed savings in table form for clarity of the discussion.

Table 15. The energy savings for January 9th.

Component	Savings % under normal conditions optimization	Savings % under optimization with demand control
Total	19.9 %	21.2%
Fan	38.6%	41%
Boiler	50%	44.7%
Reheat	-5.4%	-0.5%

3. October 10th results

Figure 88 shows the sensible load for the five zones on October 10th for the specified analyzing period from 8:00 AM to 6:00 PM. The building, as shown, requires heating in the morning until around 10:00 AM then cooling afterward when the outside temperature increases. The cooling load starts dropping again at around 6:00 PM to go back to the heating load when the temperature outside decreases. This is the case in most fall and spring seasons when the system simultaneously operates in the cooling and heating mode.

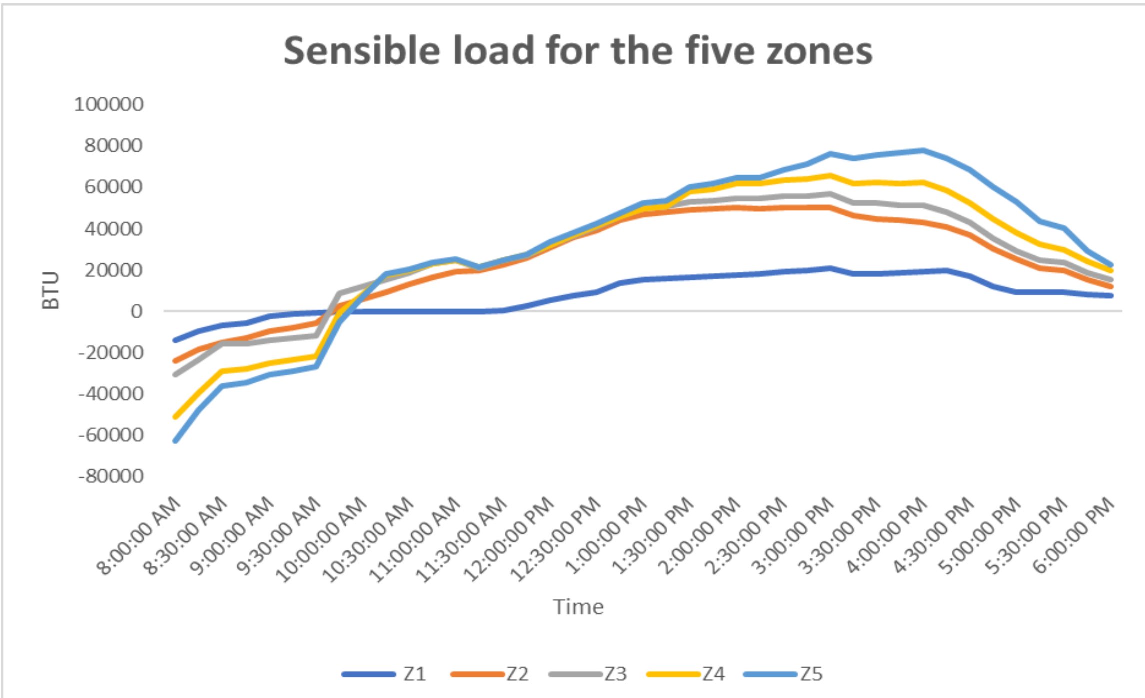

Figure 88. The sensible load for the five zones in BTU.

As previously mentioned, the baseline case should have fixed setpoints. However, when the temperature outside is less than 55 F^{o,} the T_s is set to 65 F^o. And in the summer season, when the temperature outside is more than 65 F^{o,} the T_s is set to 55 F^o. While in the fall and spring seasons, when the temperature outside is between those two values, the best practices use the temperature reset method previously described to set the T_s value. In contrast, other practices set it to be 55 F^o all season. Therefore, our research will follow the best practice supply air temperature reset method to decide the baseline case T_s value. Another case with the Ts set to 55 F^o will be shown in Appendix H. Figure 89 below shows the supply air temperatures used for the baseline case at each timestep. The outside temperature that driven this reset method is shown in appendix G. Simultaneously, the duct static pressure for the baseline case was set to be 2.5 in. w.g.

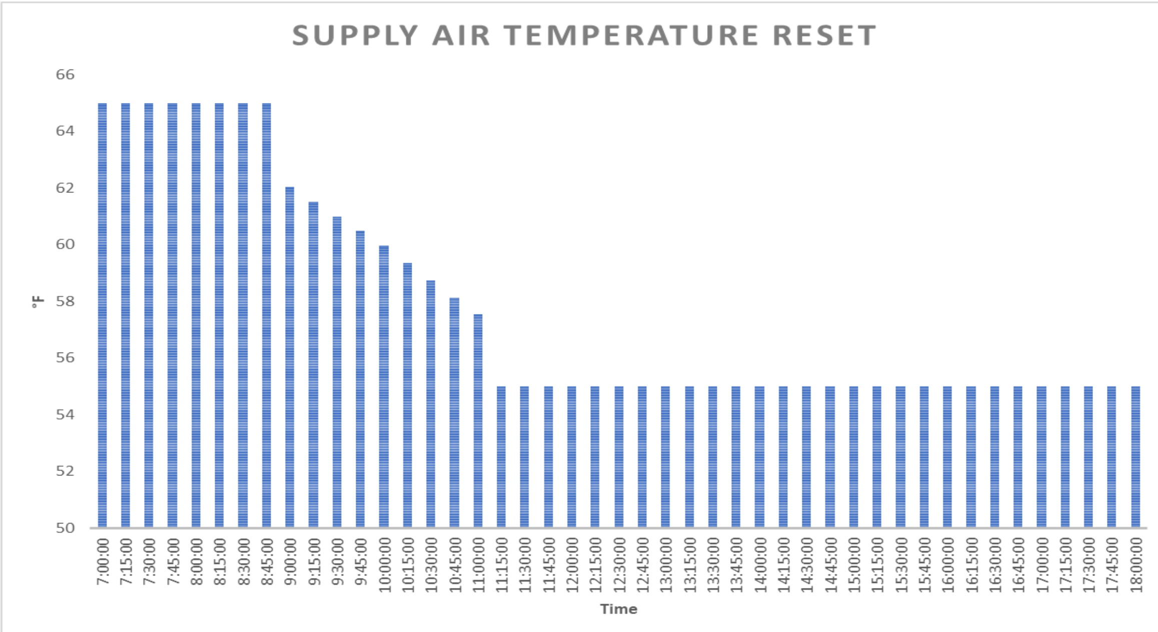

Figure 89. Supply air temperatures used for the baseline case on October 10th.

Figure 90 shows the near-optimal supply air temperature after implementing the integrated two-level optimization against the baseline case with the previously specified T_s.

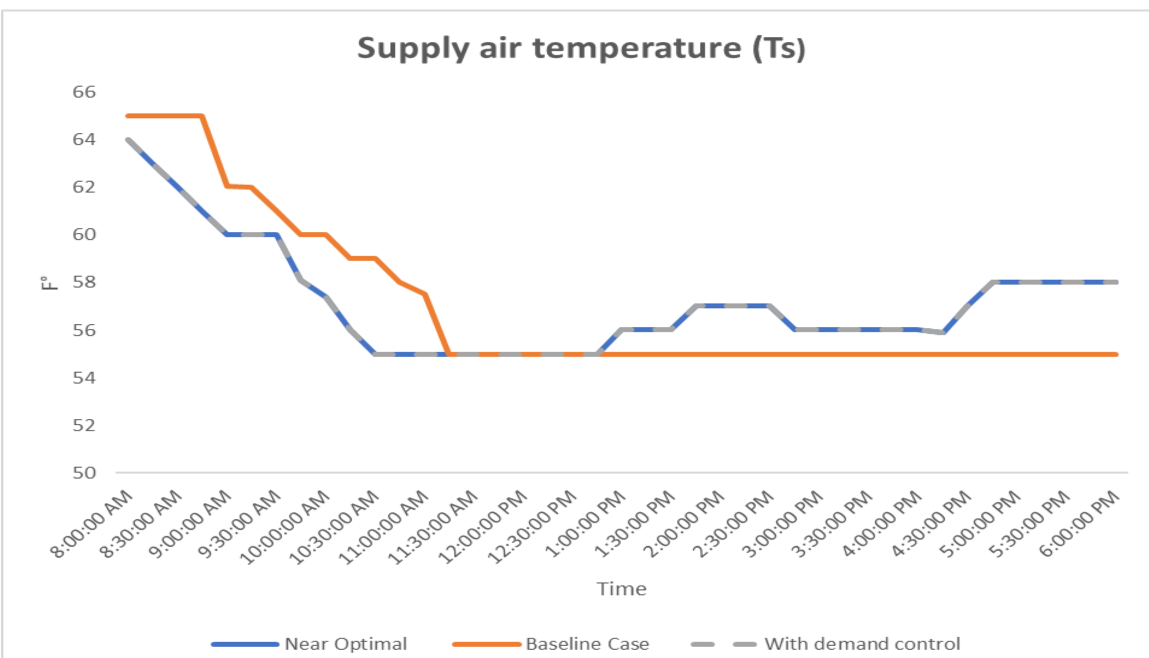

Figure 90. Near-optimal supply air temperature against the baseline case.

The system's performance in the spring and fall seasons is a little tricky, where it is hard to find the appropriate supply air temperature to meet the different heating and cooling loads throughout the day. Therefore, implementing the optimization process was anticipated to have significant savings compared to the summer and winter seasons due to its ability to accommodate the weather change outside and optimize the supply air temperature accordingly.

As shown in figure 90, in the early morning, the building load was a heating load, and the baseline case T_s was at 65 F^o until 9:00 AM and started dropping until it reached the minimum of 55 F^o 11:30 AM. Thus, this approach will require excessive heating energy consumed by the boiler but, at the same time, less reheat energy. Keeping in mind that this means less system airflow rate is required to maintain the zone setpoint.

On the other hand, the near-optimal case introduced a lower supply air temperature for the same period until 11:30 AM. Meaning savings on heating energy will be achieved. In contrast, more reheat energy will be required to maintain the zone setpoint. And, more system flowrate will be introduced.

After 10:30 AM, when the temperature outside is more than 65 F^o where the building requires cooling, the supply air temperature for the baseline case will be set to 55 F^o. This implies more power consumed by the chiller to maintain that low setpoint and lower system airflow rate.

While for the near-optimal case, the supply air temperature after 11:30 AM, reached the minimum of 55 F^o to meet the building cooling load and started to increase again gradually until 6:00 PM. This slight increase in the supply air temperature will result in lower chiller power consumption. However, this will also happen at a higher system flow rate than the baseline case since we need to push more air into the zones at a slightly higher temperature to maintain the zone setpoint than the lowest air temperature, meaning more fan power.

Figure 91 below shows the total system airflow rate that justifies our explanation above.

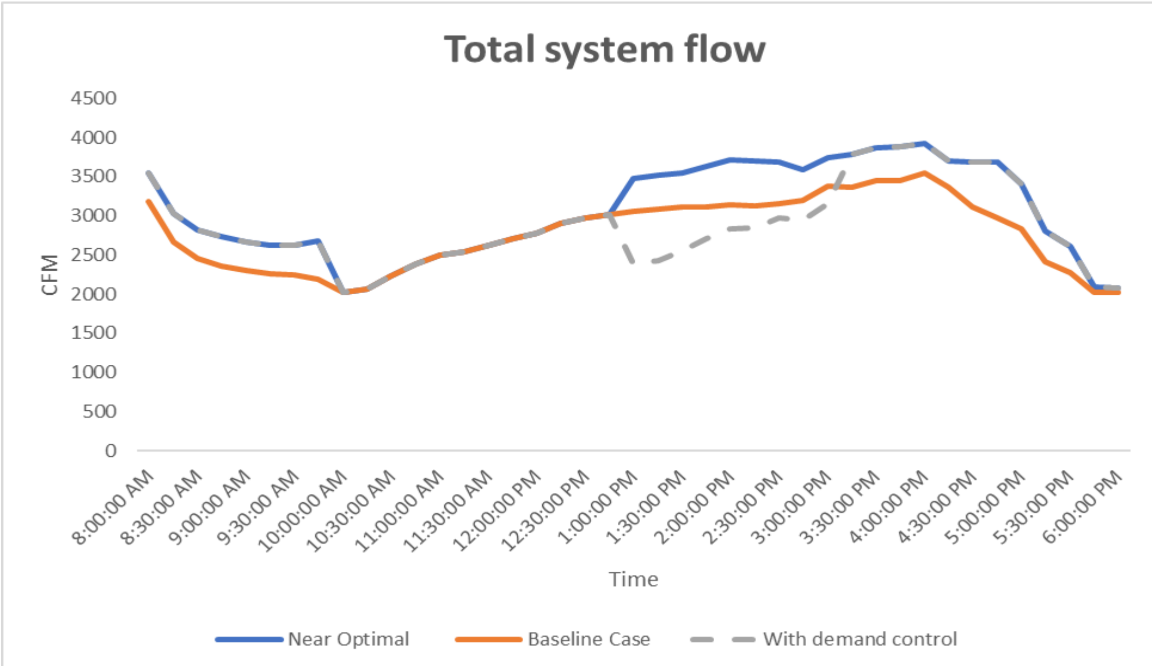

Figure 91. The total system flow rate for October 10th.

Figure 92 shows the ventilation flow rate for the same operation period. Again, the ventilation airflow rate trend follows the occupancy schedule like in the summer and winter seasons. While implementing the demand control method has increased the percentage of ventilation required due to dropping the zone minimum airflow rate.

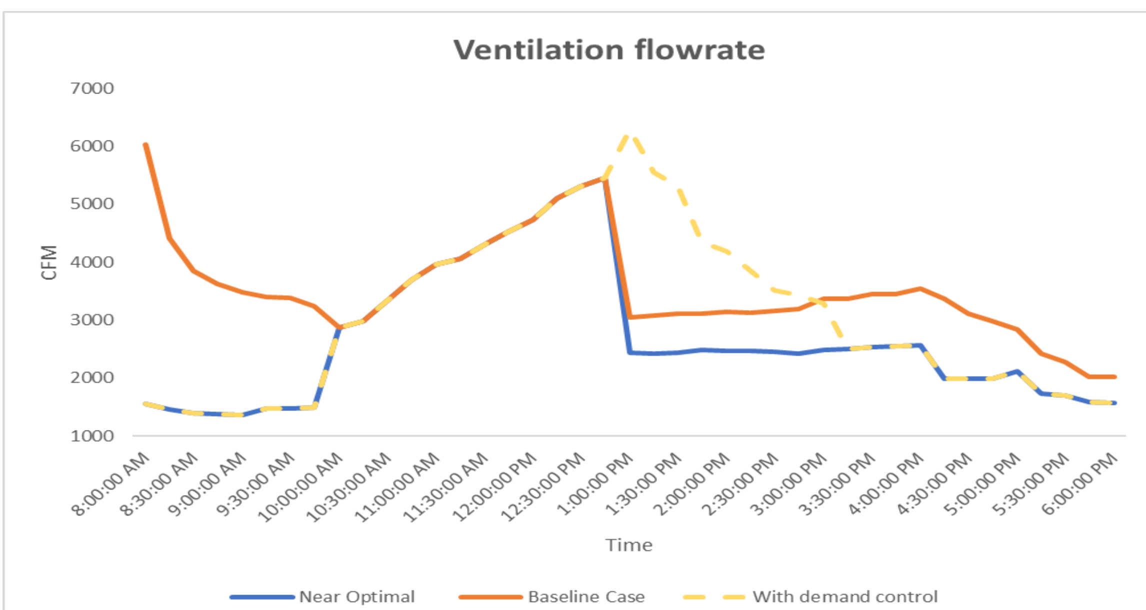

Figure 92. The ventilation flow rate for the analyzed operation period of October 10th.

Figure 93 shows the duct static pressure for the analyzed period. The duct static pressure of the near-optimal case has a steady trend close to the minimum value of 0.2 in. w.g. in the early morning until 1:00 PM. That is due to the system supplying a lower T_s when the system is in heating mode. Therefore, less airflow rate is needed, which implies lower duct static pressure.

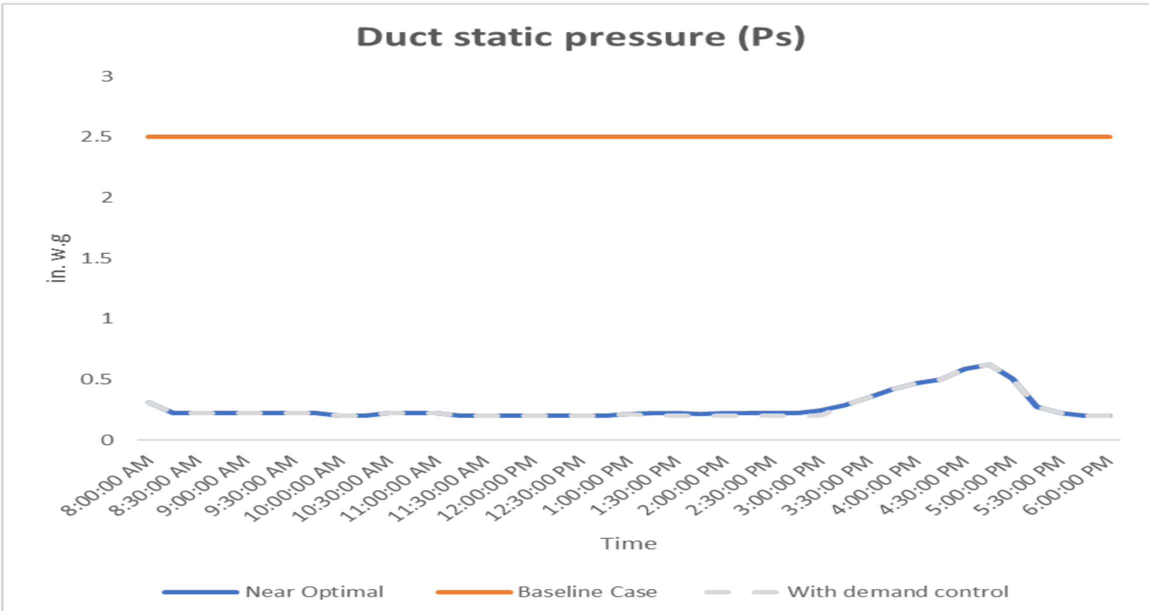

Figure 93. Near-optimal duct static pressure against the baseline case.

The duct static pressure increases after 1:00 PM with the slight increase in the supply air temperature while the system is in the cooling mode. Therefore, more airflow rate is required to maintain the zone setpoint, which implies more fan power.

However, the near-optimal duct static pressure is significantly less than the fixed baseline case duct static pressure. Therefore, significant fan savings were recorded. The total fan savings recorded after implementing the integrated two-level optimization process was 70% compared to the baseline case.

While implementing the demand control process has increased the fan power savings from 70% to 74% due to reducing the system airflow rate. Figure 94 shows the fan power savings for the analyzed period. The fan power savings follows the duct static pressure trend.

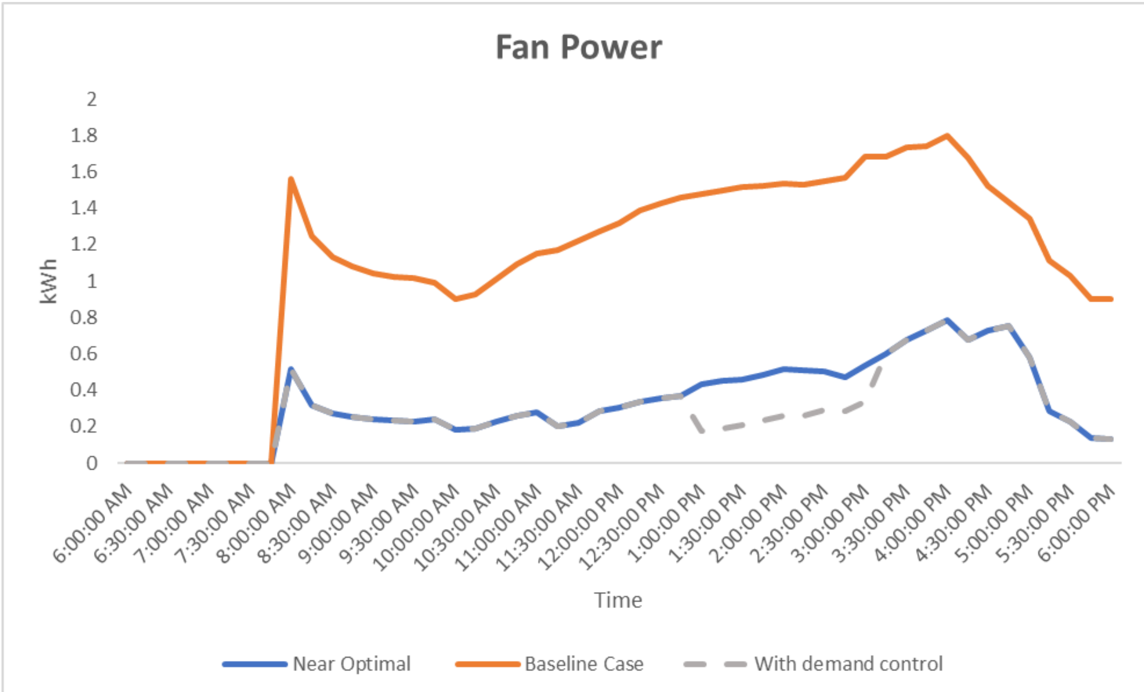

Figure 94. the fan power savings for October 10th.

Increasing the supply air temperature after 1:00 for the near-optimal case when the system was in the cooling mode resulted in chiller power savings compared to the baseline case with a minimum supply air temp of 55 F^{o}. Therefore, the chiller power savings after implementing the optimization process was calculated to be 30.4%.

Also, implementing the demand control process has increased from 30.4% to 32.4% due to reducing the system airflow rate. Figure 95 below shows the chiller power savings for the analyzed period.

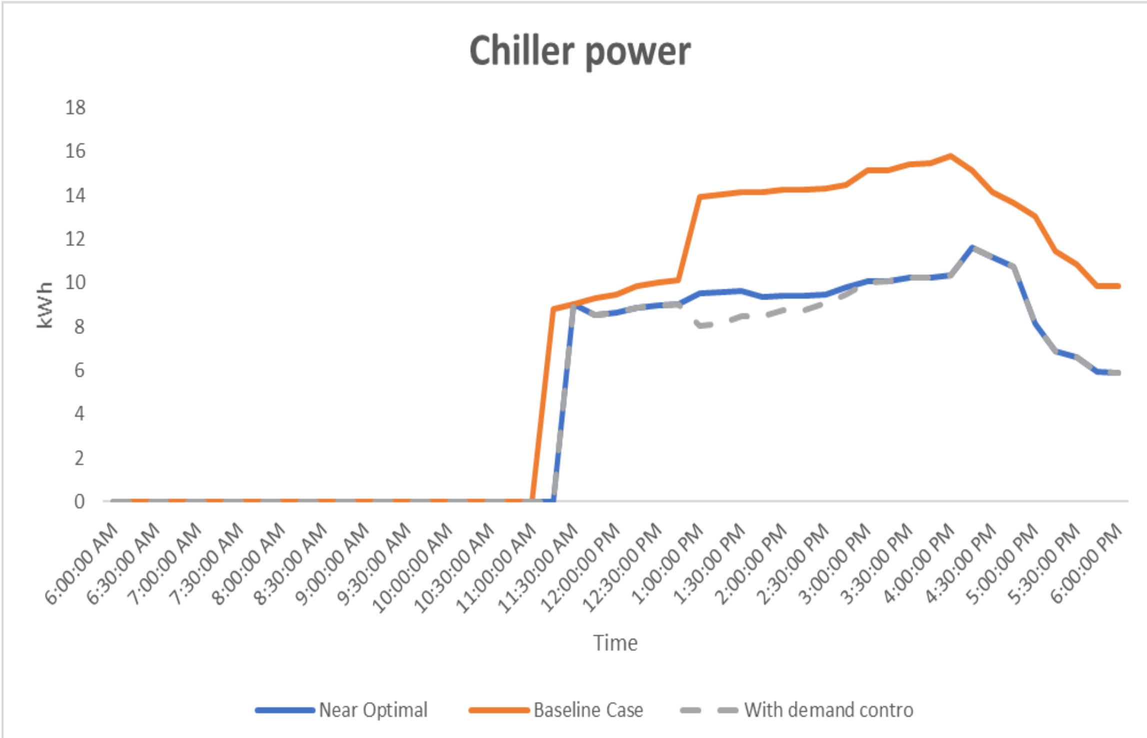

Figure 95. The chiller power savings for October 10th.

While slightly reducing the supply air temperature when the system was in the heating mode reduced the boiler's heating power when compared against the baseline case. The heating power savings were calculated to be 47%. While no changes were recorded after implementing the demand control process. Because no heating was required for the proposed implementation period. Figure 96 shows the heating power savings for the analyzed period.

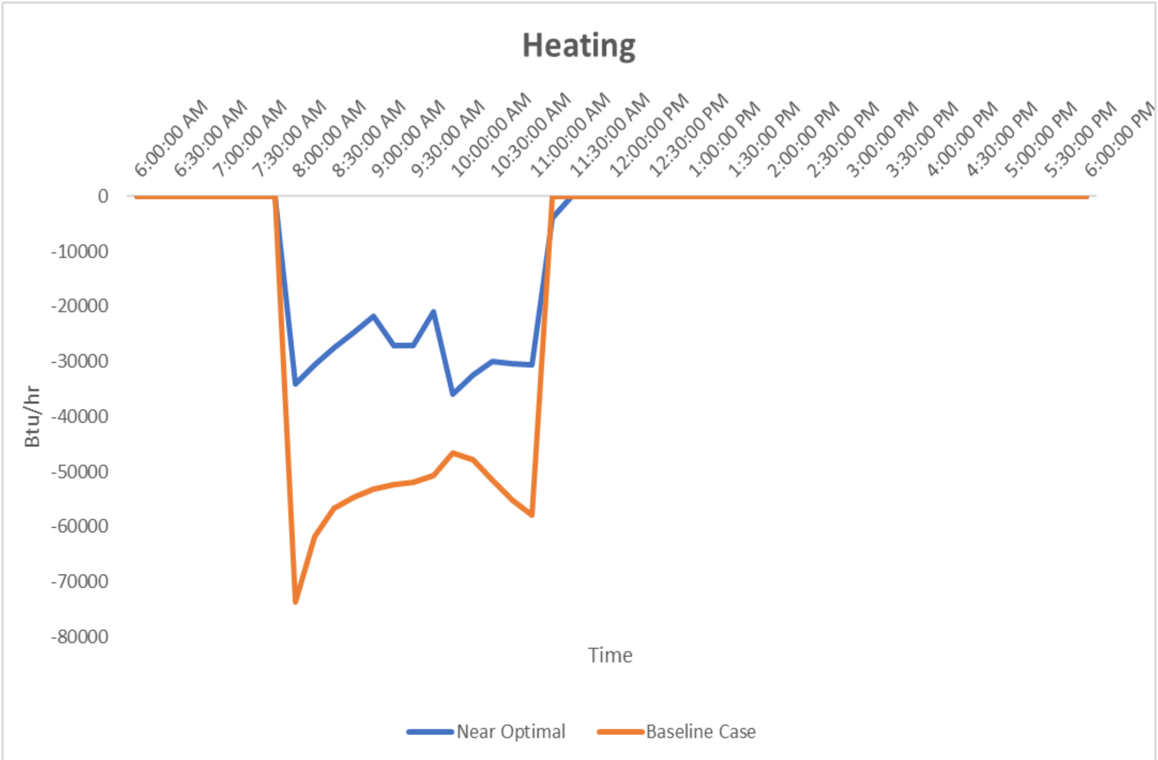

Figure 96. Heating power savings for October 10th.

As previously stated, dropping the supply air temperature for the near-optimal case until 1:00 has decreased the heating energy, but it also means requiring more reheat energy. At the same time, the higher supply air temperature of the baseline case does not necessarily imply requiring zero reheat energy. This is because the baseline case had lower system flow. As a result, the higher supply air temperature was not enough to meet the zone load. Therefore, more reheat energy was consumed to raise the supply air temperature and meet the zone setpoint. Thus reheat energy savings was still recorded after dropping the supply air temperature for the near-optimal case.

The total reheat energy saving after implementing the optimization method was calculated to be 2.3%. While implementing the demand control process has increased the percentage of savings to 6.7%.

Figure 97 shows the reheat energy saving for the analyzed period.

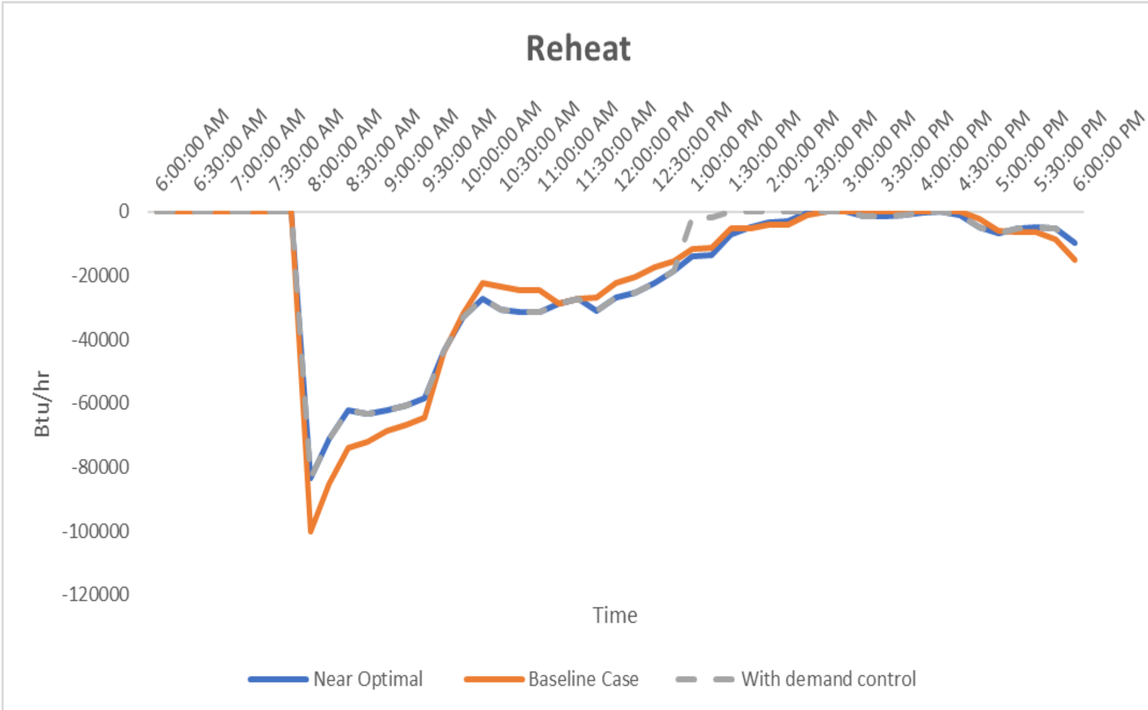

Figure 97. The reheat energy savings for October 10th.

Lastly, the total system savings were calculated after uniforming all the units using the equations 39-41 described in the methodology section. Thus, the total system savings for October 10th that was chosen to represent the fall season was recorded to be 32%.

Also, implementing the demand control methodology in the integrated two-level optimization process has increased the total system savings from 32% to 34.4%. Figure 98 shows the total energy savings that were recorded for October 10th.

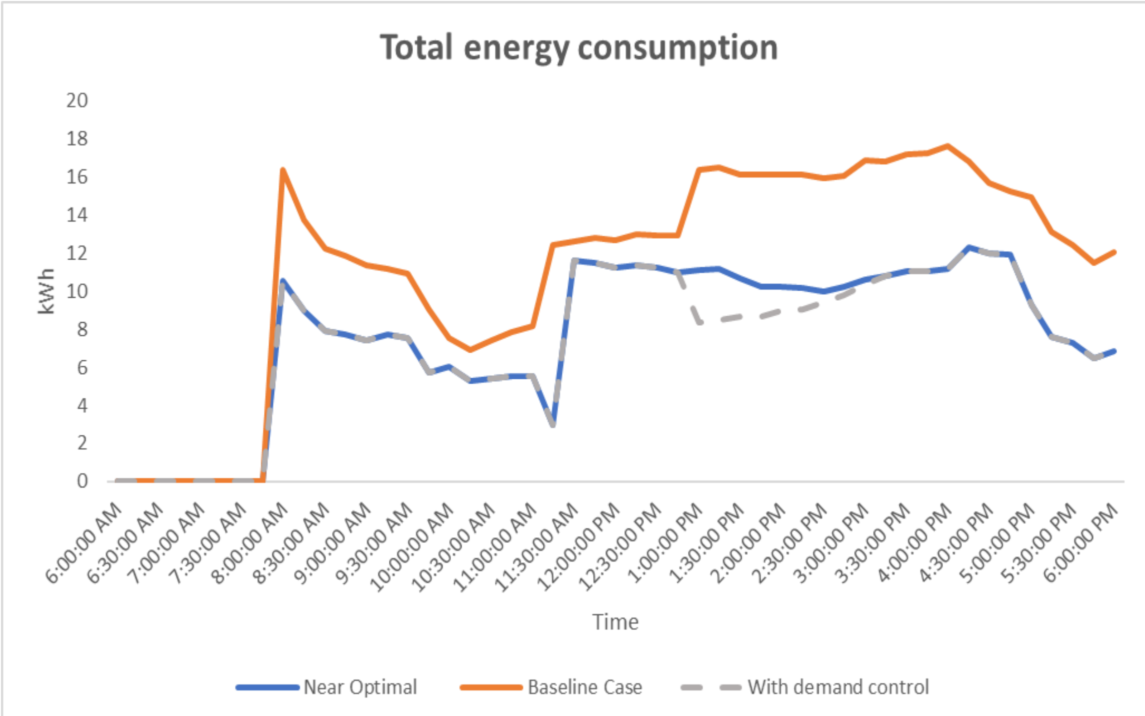

Figure 98. Total energy savings of October 10th.

Table 16 shows the savings results below to clarify the discussion as previously presented for July and January analysis.

Table 16. The savings for October 10th.

Component	Savings % under normal conditions optimization	Savings % under optimization with demand control
Total	32 %	34.4%
Fan	70%	74%
Chiller	30.4%	32.4%
Boiler	47%	47%
Reheat	2.3%	6.7%

5.3.2 Cost savings results

From the energy analysis, we calculated the total energy savings for the chilled water VAV system component. The total energy savings was calculated as the sum of chiller power, fan power, heating energy, and reheat.

The chiller power and fan power are measured in kWh per hour of electricity. The average kWh of electricity price in Cincinnati, Ohio, is 9.78 Cents. While the heating energy consumed by the boiler and the hot water reheat coils are measured in BTU, the heating price is 0.85 Cents per therm of natural gas.

Therms are not SI unit, that is used to measure the consumption of natural gas. It is equivalent to burning roughly 100 cubic feet of natural gas. Therefore each therm is equal to 100000 BTU.

The total energy consumption that is calculated by the optimization process, as described above, is the sum of two different components, kWh and BTU. Thus, an approach described in the methodology section to uniform the units before adding them together was introduced to sum the two.

Therefore, this section will show the cost savings resulting from the energy savings achieved after implementing the integrated two-levels optimization approach without the demand control and the optimization process with the demand control. Furthermore, the savings will be discussed per each component and the total savings to better understand the discussion. To break down the cost savings, we will be looking at the portion of savings from each element to give a better idea of the most savings methods. This will help in realizing what factors most in the HVAC cost of operation savings, and therefore more research focus on that factor is recommended to improve the savings even more.

1. **July 12th cost savings**

As previously discussed, July 12th will be analyzed as the day representing the summer season and the system heating mode. The two levels optimization process was optimizing the setpoint every 15 minutes. So, the energy and cost savings were calculated cumulatively. Again, the operation period that was analyzed for savings is from 8:00 AM- 6:00 PM.

For July 12th, implementing the integrated two-level optimization technique has dropped the chilled water VAV system's total energy consumption for the optimized period from 1068.98 kWh to 948.986 kWh. So that resulted in lowering the cost of operating the VAV from $106.898 to $94.8986. So, if we assume that this saving trend will be consistent for the whole month of July, then the total savings in operating the HVAC system only will be around $375.

While implementing the optimization process with the demand control method has reduced the chilled water VAV system total energy consumption for the optimized period from 1068.98 kWh to 926.276 kWh, therefore reducing the cost of operation from $106.898 to $92.63. Again, if we assume that this saving trend will be consistent throughout the month of July, the savings in the cost of operation is anticipated to be around $450 for the month of July only.

Figure 99 shows the total savings for the analyzed day. The graph shows the near-optimal case total operation cost and the near-optimal case with the demand control method total operation cost against baseline case total operation cost.

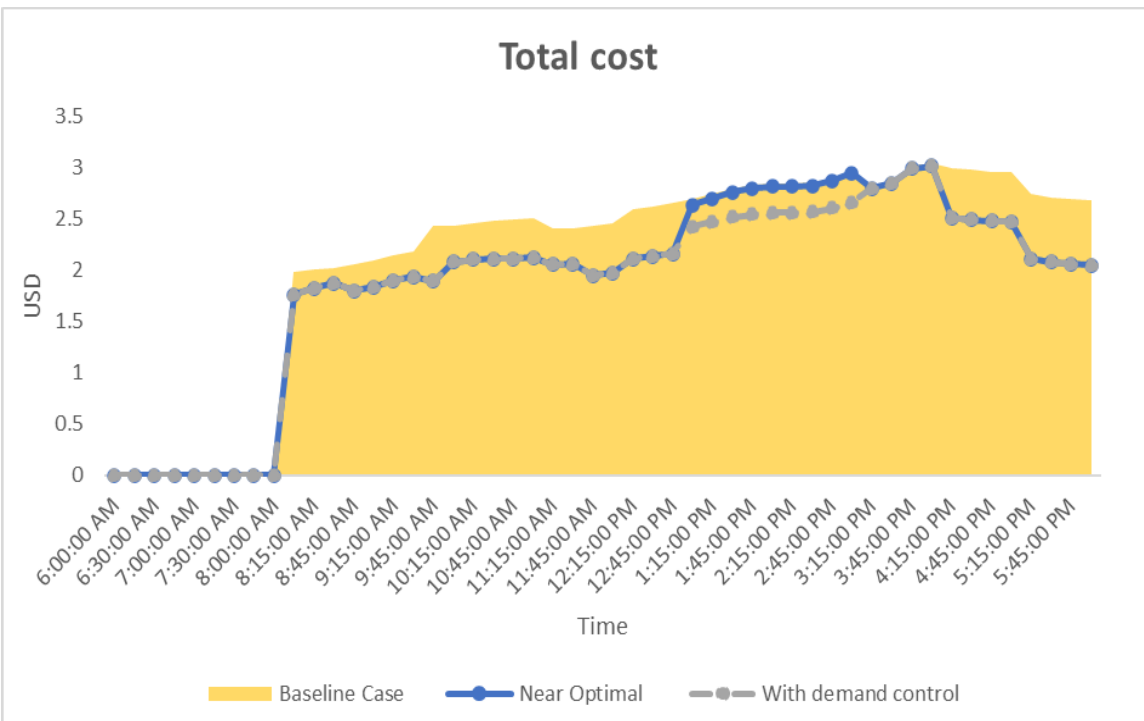

Figure 99. Total operation cost savings for July 12th.

To break down the cost savings, we will be looking at the portion of savings from each component to give a better idea of the most savings methods.

Figure 100 shows the cost savings associated with the fan power. Implementing the optimization process has dropped the fan power consumption from 234.2279 kWh to 195.2566 kWh and, therefore, lowered the fan power electricity cost from $23.42 to $19.53.

While implementing the demand control has increased the savings by dropping the fan power consumption from 234.2279 kWh to 174.4439 kWh and, therefore, decreased the fan power cost from $23.42 to $17.44.

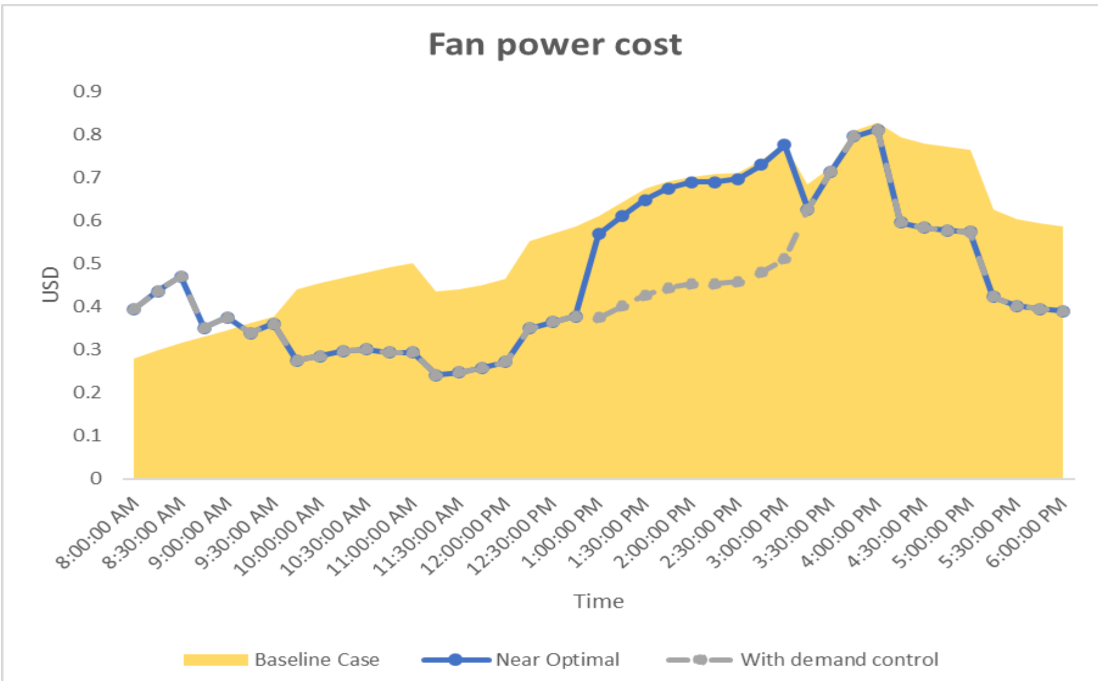

Figure 100. The fan power cost of operation for July 12th

While implementing the optimization process have dropped the chiller power consumption from 834.152 kWh to 752.972 kWh and, therefore, lowered the chiller power electricity cost from $83.42 to $75.30.

While implementing the demand control has increased the savings by dropping the chiller power consumption from 834.152 kWh to 751.076 kWh and, therefore, lowering the cost of operation from $83.42 to $75.11, as shown in figure 101 below for cost savings.

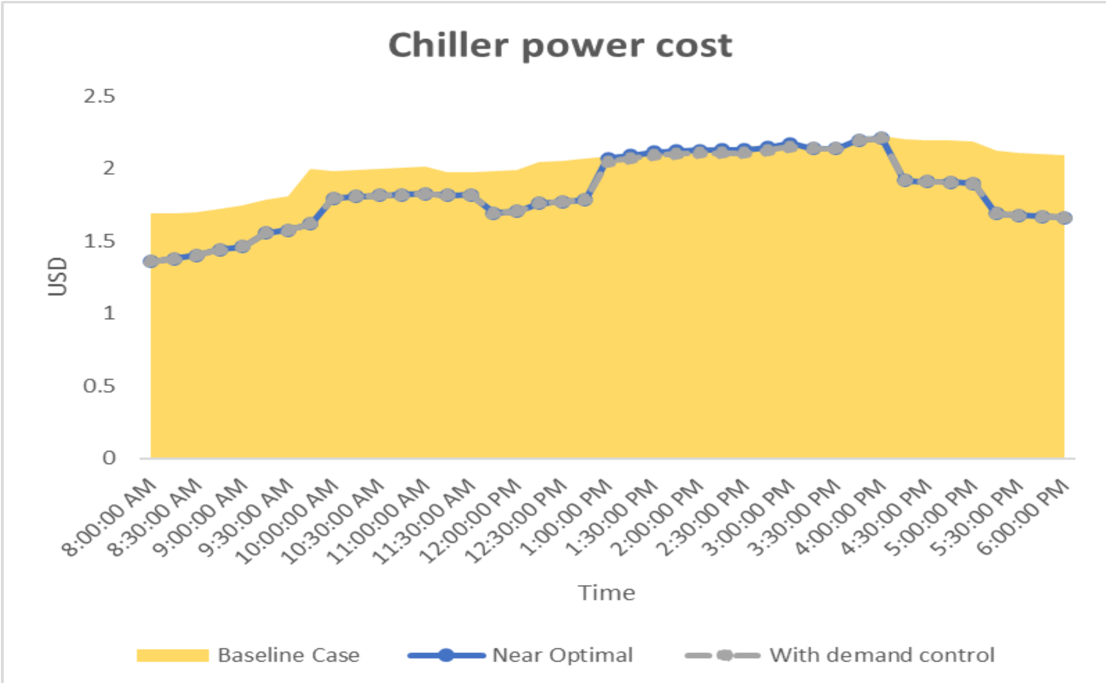

Figure 101. Chiller cost of operation for July 12th

2. January 9th cost savings

For January 9th, implementing the integrated two-level optimization technique has dropped the chilled water VAV system's total energy consumption for the optimized period from 698.94 kWh to 559.861 kWh. So that resulted in lowering the cost of operating the VAV from $69.89 to $55.99. But, again, if we assume that this saving trend will be consistent for the whole month of January, then the total savings in operating the HVAC system only will be around $450.

While implementing the optimization process with the demand control method has reduced the chilled water VAV system total energy consumption for the optimized period from 698.94 kWh to 550.958 kWh and, therefore, lowering the cost of operation from $69.89 to $55.10. Again, assuming that this saving trend will be consistent throughout the month of January. In that case, the savings in the cost of operation is anticipated to be around $500 for the month of January only.

Figure 102 shows the total operation cost for the analyzed day. The graph shows the near-optimal case total operation cost and the near-optimal case with the demand control method total operation cost against baseline case total operation cost.

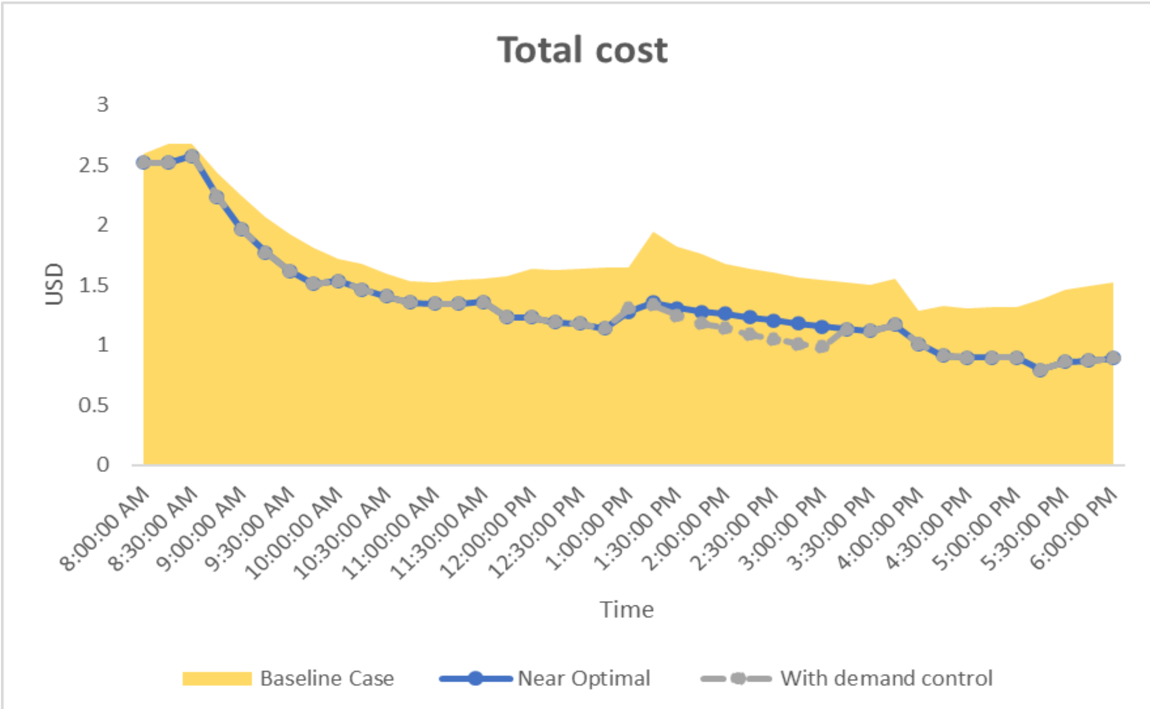

Figure 102. Total operation cost for January 9th.

By looking at the major aspects that contributed to this savings, we notice that operating the boiler responsible for heating the zone and the reheating process was the most significant portion compared to the fan power cost savings.

Implementing the proposed optimization technique has dropped the heating energy consumption for the optimized period from -2649307.7 BTU to -1327378 BTU. So that resulted in decreasing the cost of operating the boiler from $22.52 to $11.28.

While implementing the optimization process with the demand control method has reduced the boiler energy consumption for the optimized period from -2649307.7 BTU to --1465378 BTU, reducing the cost of operation from $22.52 to $12.46. Figure 103 shows the cost of operating the boiler under normal conditions against the optimization process.

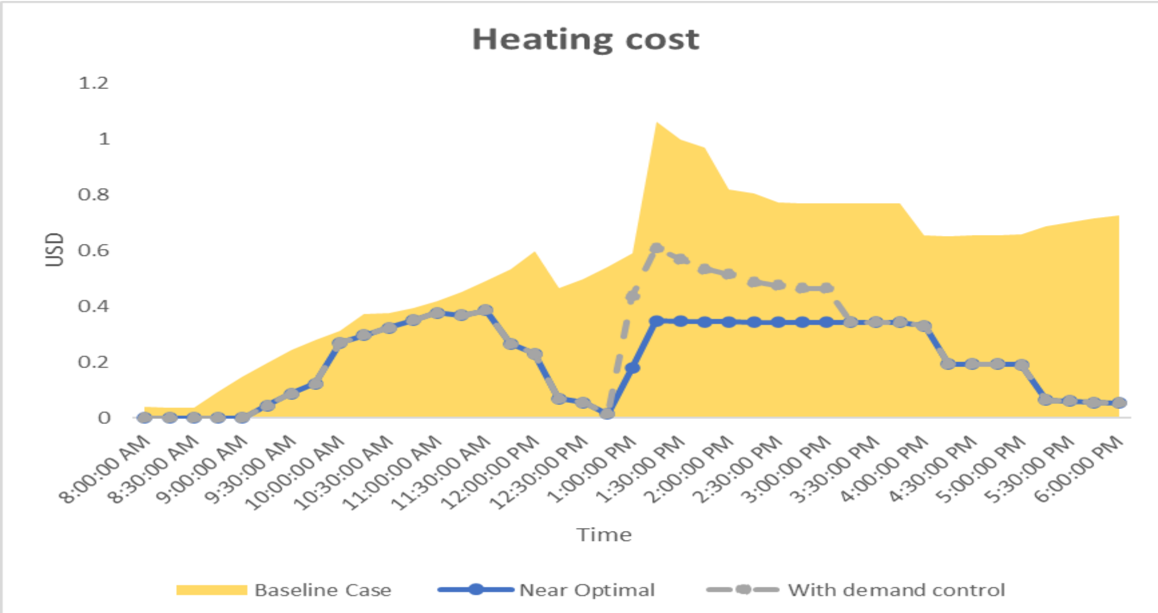

Figure 103. The boiler operation cost for January 9th.

While the fan power savings came next, the optimization process helped drop the fan power from 118.512 kWh to 72.779 kWh. So that resulted in lowering the cost of operating the fan from \$11.85 to \$7.28. While implementing the optimization process with the demand control method has reduced the fan power from 118.512 kWh to 69.86 kWh, reducing the cost of operation from \$11.85 to \$6.99, as shown in figure 104.

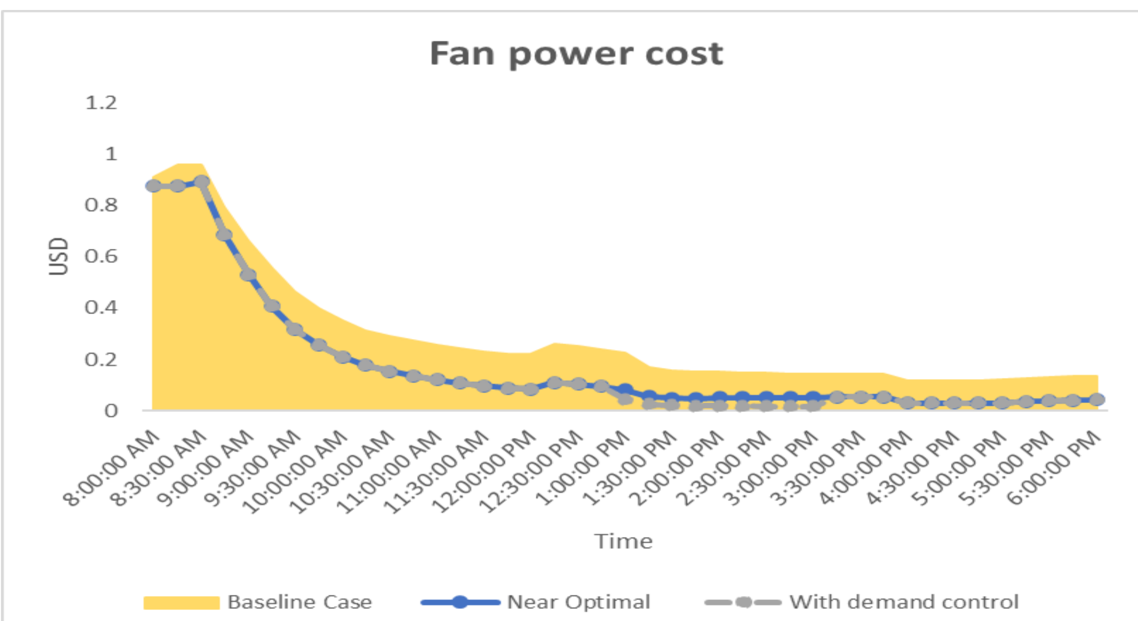

Figure 104. The fan cost of operation for January 9th.

3. October 10th cost savings

October 10th was chosen as the day representing the fall season. In the fall and spring season, most of the baseline system operating under normal conditions tends to consume a lot of energy due to the difficulty of finding the appropriate setpoint when the outside weather conditions fluctuate throughout the day. Therefore, implementing the optimization process significantly saves those seasons since it considers the outdoor weather conditions when resetting the system setpoints.

Implementing the proposed integrated two-level optimization process has reduced the system's total energy consumption on October 10th from 550.304 kWh to 374.042 kWh and, therefore, reduced the cost of operating the system from $55.03 to $37.40. If this trend stays consistent throughout October, the anticipated monthly savings are about $550.

And implementing the demand control method with the optimization process has improved the savings even more. In October, the system's total energy consumption has dropped from 550.304 kWh to 361.300 kWh, resulting in reducing the cost of operation from $55.03 to $36.13. Again, if this trend stays consistent throughout October, the anticipated monthly savings are about $600. The cost of operating the system on October 10th is shown in figure 105.

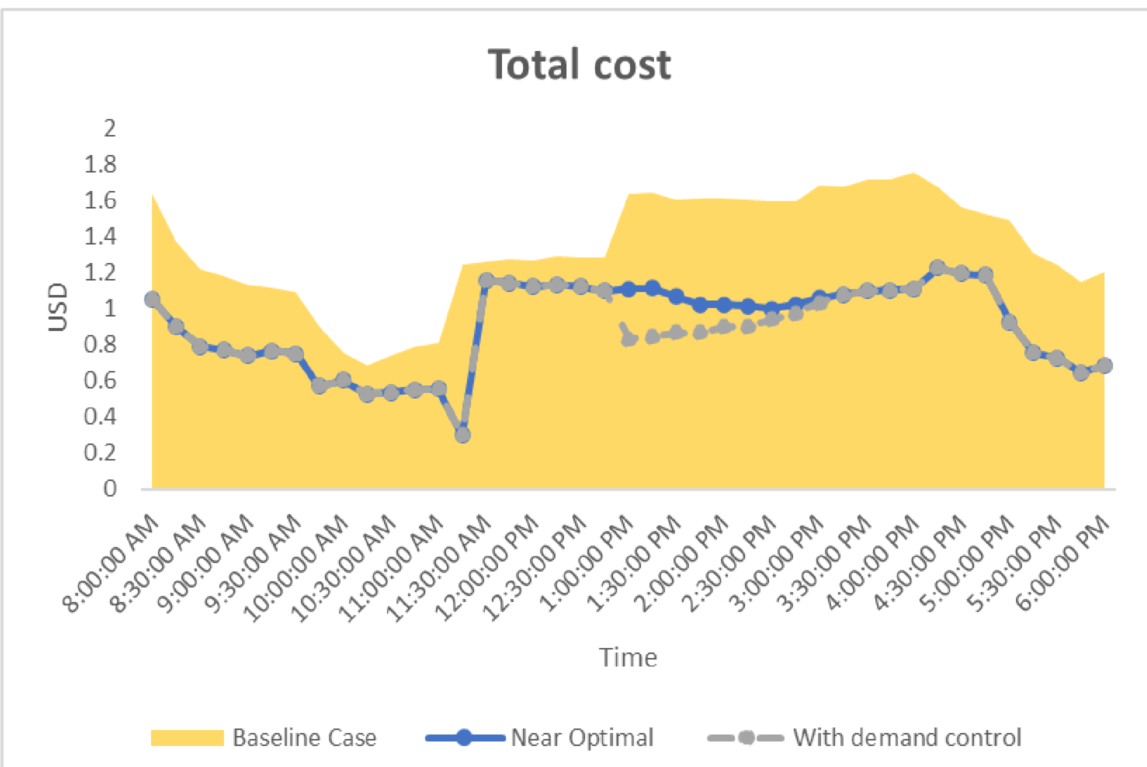

Figure 105. The total operation cost of October 10th.

The most significant contribution to the cost-saving came from the chiller power savings. The chiller power consumption has dropped from 354.852 kWh to 246.993 kWh after implementing the proposed optimization process. Thus, the cost of operating the chiller has dropped from $35.49 to $24.70.

And implementing the demand control in the optimization process has helped increase the savings in the energy consumption to 114.912 kWh. Therefore, the cost of operating the chiller has dropped from $35.49 to $23.99. Figure 106 shows the chiller power cost of operation for the baseline case against the optimization process without the demand control and the one with the demand control.

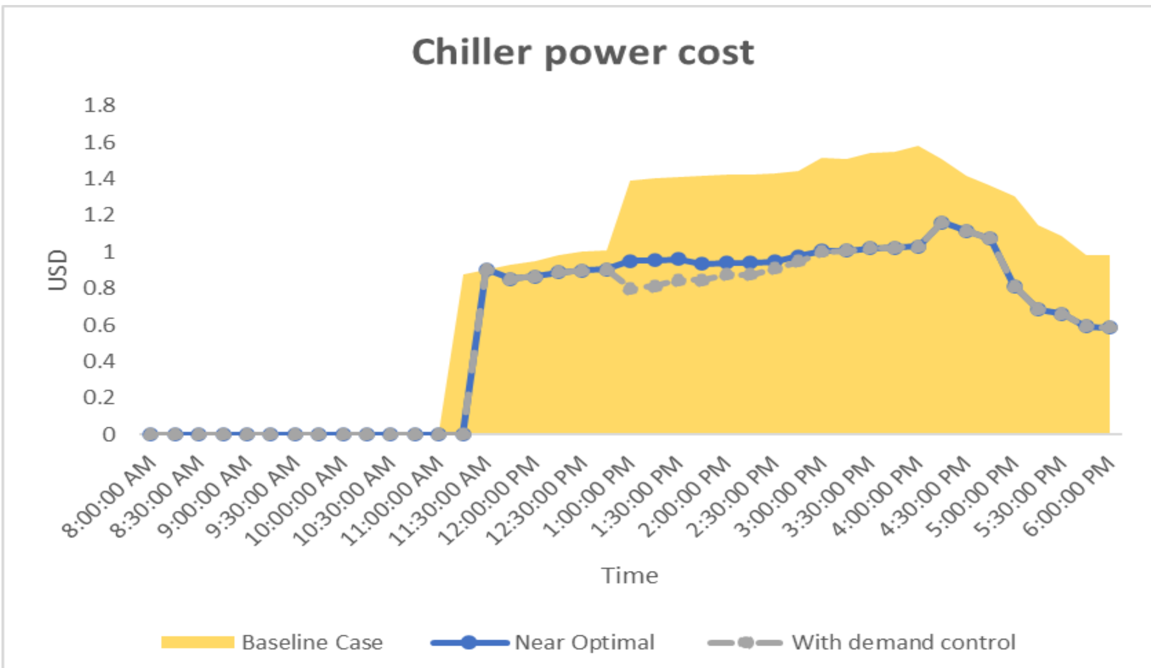

Figure 106. The chiller cost of operation for October 10th.

The second significant contribution to the total cost savings came from the fan power, where the optimization process dropped the fan power from 54.19306 kWh to 16.21591 kWh. Resulting in lowering the cost of operating the fan from $5.42 to $1.62. While implementing the optimization process with the demand control method has resulted in reducing the fan power from 54.19306 kWh to 14.09818 kWh. Therefore, reducing the cost of operation from $5.42 to $1.41, as shown in figure 107.

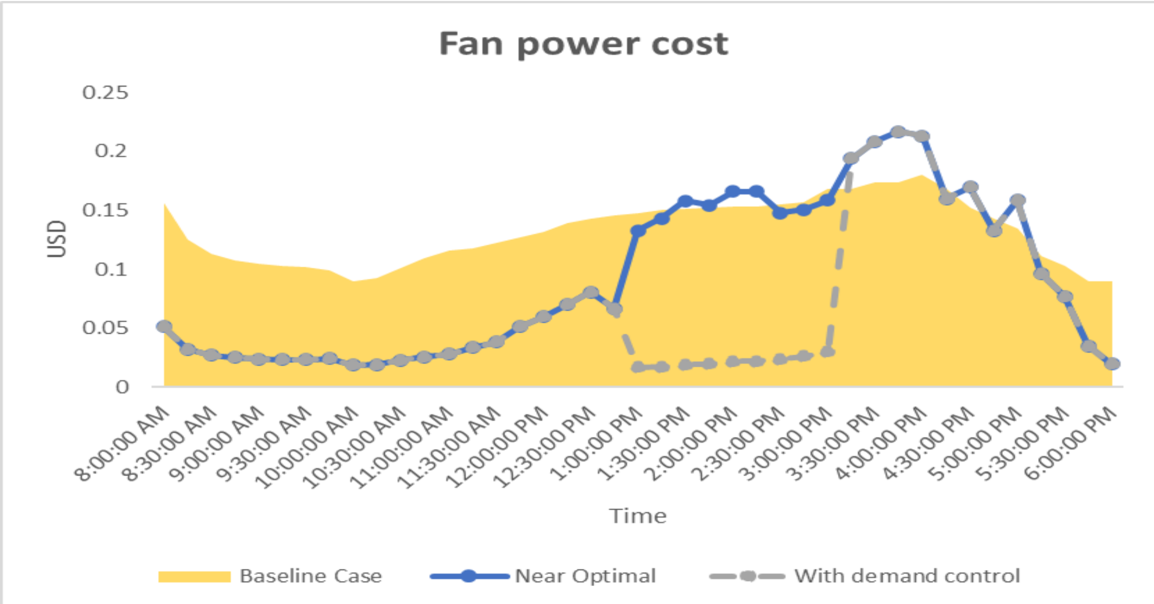

Figure 107. The coast of fan operation for October 10th.

Third came the boiler energy consumption that is used for heating the spaces. The heating energy has dropped from -713917 BTU to -377544.7 BTU after implementing the proposed optimization process. Thus, the cost associated with operating the chiller has dropped from \$6.07 to \$3.21.

Notice that implementing the demand control process has not changed the heating energy described previously in the energy analysis. Figure 108 below shows the cost of operating the boiler on October 10th.

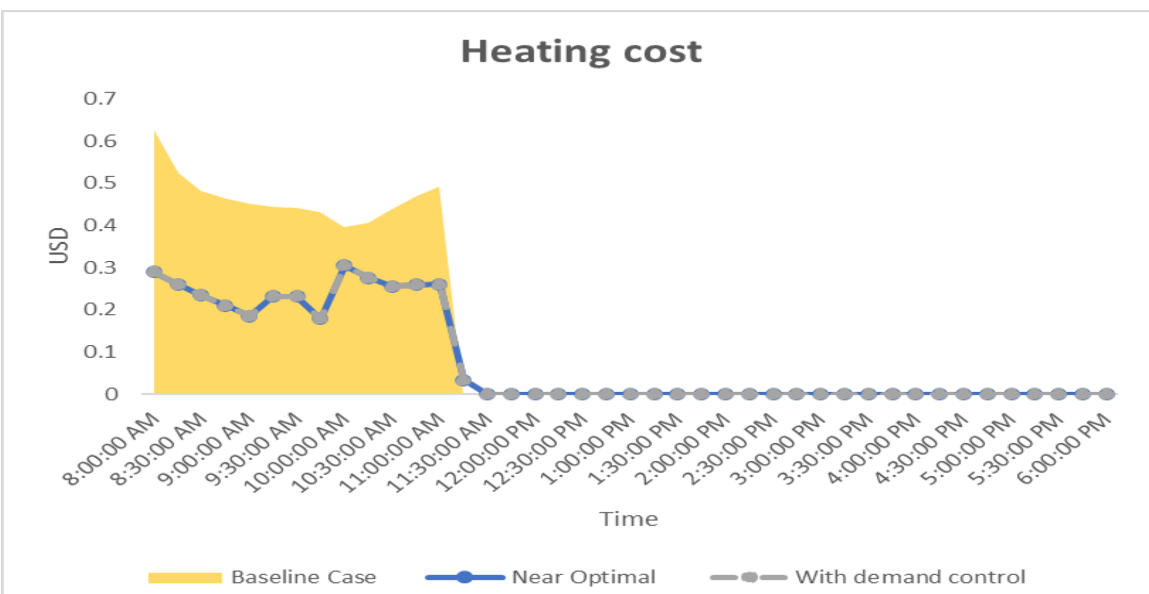

Figure 108. The boiler cost of operation for October 10th.

5.4 Discussion

This chapter has discussed the proposed method of implementing the integrated two-level optimization technique that has two levels MLO and SLO. The MLO process was described in chapter 4 that shows a data-driven modeling and optimization technique for the HVAC system component. The chilled water VAV and DX system were modeled in chapter 4 but only the chilled water VAV system was tested in chapter 5.

The building that was used to test the proposed integrated two-level optimization process is a simulation building. The building was simulated using EnergyPlus software. The building performance loads, and weather conditions were collected and imported in the optimization process created using MATLAB. The loads were imported manually because there was no platform connecting the two software for this type of application. However, we propose creating a platform that will ease the transition between the two in future work.

On the other hand, in actual building implementation, no building loads will be available. Instead, the system airflow rate information will be available, and the total building load will be calculated at the sensible and latent load models.

From the result section, we can clearly see that implementing the integrated two-level optimization process has resulted in significant savings in the energy consumption of the chilled water VAV system. At the same time, implementing the demand control methodology with the optimization process to shift the peak load when the demand response signal is received has improved the results even more.

The proposed method has achieved savings in the system's total energy consumption ranging from 13.4% to 34.4%. The most significant saving happened in the fall season when it was hard for systems operating under normal conditions to adapt to the change in the outside temperature resulting in excessive energy usage.

The cost savings of implementing the integrated two-level optimization technique ranged between $400-600 a month. However, keep in mind that there is no capital cost for implementing this method. Furthermore, the proposed method can be easily implemented in the existing BAS system and reduce the total energy consumption while improving indoor thermal comfort.

The proposed optimization process was proved to be a time and cost-efficient method that can be implemented in several building types and systems to improve the system efficiency and thermal comfort levels.

Chapter 6

Conclusion and future work

This research was conducted to develop a computational data-enabled two-level optimization technique to reduce the building HVAC energy use in large commercial buildings, improve the whole system efficiency and maintain the occupant's comfort level. The research has examined two systems commonly used in commercial buildings, chilled water VAV systems and direct expansion systems (DX).

The research proposed an innovative optimization method. The method integrated two levels of optimization. The first level of the process was a component modeling optimization (MLO) designed to optimize the model's structure. The models were tested and trained and using actual performance data collected from an exciting system located in the BEAST lab at the University of Cincinnati, Cincinnati, Ohio. The model that held the lowest error value was selected as the best modeling structure. The error values were measured in terms of MSE and CV%.

Accurate component modeling and optimization techniques are crucial for the accuracy of the whole system optimization process results. Therefore, all the component models will be integrated to form the system model that mimics the performance of the existing physical system.

Several machine learning tools were compared to choose the best modeling tool to model the selected HVAC systems components. Therefore, the Support Vector Machine (AVM), Artificial Neural Network (ANN), and Aggregated Bootstrapping (BSA) were examined. First, the three modeling tools were tested and trained using the same data set to predict the same output. Then, the modeling techniques were compared in terms of their accuracy (R^2) in predicting the output. For the SVM, ANN, BSA, the accuracy value in the testing period was 98.2%, 98.5%, and 99.3%, respectively. Also, the training time was the cutting edge in the model selection. The training time in seconds was 1349.3, 341.3, and 2335.1, respectively, thus, all the models held a high accuracy value, but the ANN training time was three times less than the rest. Therefore, we can conclude that all the described algorithms are good predictors and can be utilized in modeling the HVAC systems components. But the artificial neural network was chosen to be the tool used in this research since it was the fastest and less complex tool.

While the genetic algorithm was used as the optimization algorithm for the proposed two levels of optimization, due to its capability of handling a wide range of variables at one time, the ability to work with complex simulation programs, proven to be effective in solving complex problems that cannot be easily solved with traditional optimization methods, and it is a publicly available user-friendly tool.

After modeling all the components of the selected HVAC systems, a parametric study was conducted to choose the best model structure manually. Later the MLO was implemented to automate the process and validate the results. The MLO results were compared against the one conducted through the parametric study. The optimization process has supported the parametric results where similar results were found.

It was found that for the chilled water VAV system, the best cooling coil model structure with 30 neurons held an error value of 1.1059 and 0.017 in terms of CV% and MSE, respectively, in predicting the load. At the same time, the best fan power model structure of 20 number of neurons held an error value of 0.4256 and 0.0362 in terms of CV% and MSE, respectively. Also, the chiller was examined. The chiller power best model was at 15 number of neurons and held an error value of 3.0635 and 0.0101 in terms of CV% and MSE, respectively.

For the DX system, all the system components were modeled as well. It was found that for the DX coils, the best model was at 20 number of neurons and held an error value of 0.456 and0.0102 in terms of CV% and MSE, respectively. While the DX fan model, the best model was at 15 number of neurons and held an error value of 0.1211 and 0.0031in terms of CV% and MSE, respectively.

The previous values are not standard values for any type of application, but the findings of this research are based on its inputs and outputs and the selected datasets. The models can be adjusted to different applications and data sets and will hold different structure and error values. It was only showing a proposed methodology and used to test the accuracy of the MLO process. Also, these results have proved that artificial neural networks can be a valuable tool in modeling the performance of HVAC systems.

The second level of optimization was the whole system-level optimization (SLO). Where all the optimized components models were integrated and optimized to form the "system model." The output of the system model is the total energy consumption of the system at each time step. Later, the two optimization levels are integrated to optimize the system setpoints that will reduce the total energy consumption.

That is why the accurate component modeling and optimization technique is crucial for the system’s performance optimization. If the component models were not accurate, then the system's total energy consumption prediction would be faulty, resulting in less precise SLO performance when optimizing the system setpoints.

The proposed integrated two-level optimization technique designed to be implemented in large commercial buildings was tested using a simulation building due to the lack of accessibility to an existing large system. The facility that is equipped with a chilled water VAV system was simulated using the Cincinnati weather conditions. A day from each season was chosen to be analyzed to show the result of the proposed method in optimizing the system performance in the cooling, heating, and both simultaneous heating and cooling mode.

The proposed optimization process was applied to optimize the system performance by optimizing the operation setpoints every 15 minutes. The system setpoints that were selected to be optimized are the supply air temperature (T_s), duct static pressure (P_s), minimum zone air flowrates (Q_z), and minimum outdoor air ventilation rate (Q_v).

The system setpoints were optimized while maintaining or improving the zone thermal comfort levels and ventilation requirements to comply with the codes and regulations. This research has implemented few approaches to enhance system performance and reduce total system energy consumption. (1) Implementing the demand response methodology with the optimization process to modify the electricity consumption power profile by alleviating the peak load demand when the demand signal is received from the utility-providing companies. (2) Implement the occupancy schedule inputs into the optimization process to account for the number of occupants at each time step and reduce the ventilation airflow rates to the required amounts. This approach will enhance the sustainability goals of ASHRAE 62.1 by optimizing the zone level ventilation ratio and fulfilling the gap in this related code, as well as reducing the total system energy consumption. (3) Implement the real-time zones occupancy sensor readings. This approach will crucially affect the zones' ventilation flowrates and zones minimum flowrates. (4) lastly, this research has implemented the method of zone minimum air flowrates setpoint rests. This approach will allow this setpoint to be adjusted over the operation time instead of using the constant design minimum values. This method is crucial to reduce reheat energy consumption.

Implementing demand control ways is getting more attention nowadays. It can help the consumer reduce operation costs without trading thermal comfort and energy and cost savings for the utility supplier by meeting the demand load without increasing the power plant and production process. Therefore, the results have shown the savings after implementing the optimization process under normal conditions Vs. With demand control proposed method.

Implementing the proposed two-levels optimization technique has resulted in 11.3% savings in the total energy consumption that increased to 13.4% after implementing the demand control method for the day analyzed in the month of July. And for the month of January, when the system is in heating mode, the total energy savings was 19.9%. Therefore, the savings have increased to 21.2% savings after implementing the demand control method. While for the month of October, when the system is operating in both the heating and cooling mode simultaneously, the regular systems consume more significant amounts of energy due to the complexity of the typical operating methods in meeting the fluctuating loads throughout the day. Thus, the optimization process has resulted in 32% savings in the system's total energy consumption, and this percentage of savings increased to 34.4% after implementing the demand control method.

This research has validated the use of the proposed optimization technique in improving the energy efficiency of exciting systems. As well as the capability of this method to be successfully implemented in online HVAC system applications. At the same time, developing several aspects of the industry.

6.1 Future work

The results achieved through introducing the integrated two-level optimization approach enhanced the HVAC system performance. However, multiple enhancements can be implemented to further extend and improve this research work for anticipated postdoctoral work. For example, introducing more advanced models and exploring other learning algorithms for modeling and optimization can possibly achieve different results. Also, exploring the possibility of optimizing other system setpoints, system equipment, and components other than the ones introduced in this research is another way to advance this work further. The future work can include but is not limited to:

- Implementing the proposed optimization process in the DX system that was modeled in chapter 4. Examining the savings results and ways of improvement will be the first focus.
- Investigating the ability to optimize the waterside setpoints like the condenser water temperature, the pressure drops of the waterside piping, the mixing air temperature setpoints that will trigger the heat recovery operation, and others.
- If applicable, modeling and optimization of more complex equipment not introduced in this research, such as the cooling tower and a thermal storage unit.
- Explore the other time of occupancy other than the period of operation examined in this work (from 8:00 AM to 6:00 Pm). Such as weekend and nighttime operations where the occupancy is almost zero, fresh air will drop considerably. Thus, optimizing the system setpoints during those periods will result in more significant savings than the ones achieved in this research for average working days.
- The work introduced in this research is aimed to improve the performance of the existing systems. However, implementing the modeling and optimization method has a significant impact on a building's energy performance. And the selection of efficient HVAC systems is vital at any design stage. Therefore, exploring the ability to introduce the simulated system performance, component modeling, and optimization that can accurately predict the interactions between the occupants and the equipment performance is vital. Therefore, exploring the proposed optimization process and its effect in the new building design stage and its impact on the energy consumption and the building footprint can be studied.
- Explore the possibility of simplifying the proposed integrated optimization method and make it more user-friendly.
- Simplifying the modeling and optimization strategy and smooth the transition between the proposed process and the building automation system (BAS).
- Exploring a way to create a platform where the process can be linked to the simulation tools such as eQuest and EnergyPlus. And automatically read the user input without having to export the inputs and then introduce it manually to the process.
- Discuss the method of implementing the process in the existing BAS systems. Therefore, the optimization algorithm will automatically read the system current load and setpoints and optimize the system setpoints for the next timestep in real online applications.

- Explore the ability to develop this optimization algorithm into an online user-interface software that will allow the public to access it online. Where the variables can be specified, and the system performance outputs will be calculated. This can be used for research purposes or by other engineering practices.
- Use a higher processers speed to increase the GA populations and generations, which will more likely result in a more precise result.
- Use other optimization tools such as Bee Colony Optimization, Ant Colony Optimiser, etc. And compare the results to the one achieved with GA.

References

Arabali, A., Ghofrani, M., Etezadi-Amoli, M., Fadali, M. S., & Baghzouz, Y. (2013). Genetic-algorithm-based optimization approach for energy management. IEEE Transactions on Power Delivery, 28(1), 162-170. https://doi.org/10.1109/TPWRD.2012.2219598

Afram, A., & Janabi-Sharifi, F. (2014). Review of modeling methods for HVAC systems. OXFORD: Elsevier Ltd. doi:10.1016/j.applthermaleng.2014.03.055

Afram, A., & Janabi-Sharifi, F. (2014). Theory and applications of HVAC control systems – A review of model predictive control (MPC). Building and Environment, 72, 343-355. doi:10.1016/j.buildenv.2013.11.016

Afram, A., & Janabi-Sharifi, F. (2015). Black-box modeling of residential HVAC system and comparison of gray-box and black-box modeling methods. LAUSANNE: Elsevier B.V. doi:10.1016/j.enbuild.2015.02.045

Afram, A., & Janabi-Sharifi, F. (2015). Black-box modeling of residential HVAC system and comparison of gray-box and black-box modeling methods. Energy and Buildings, 94, 121-149. https://doi.org/10.1016/j.enbuild.2015.02.045

Afram, A., & Janabi-Sharifi, F. (2015). Gray-box modeling and validation of residential HVAC system for control system design. Applied Energy, 137, 134-150. https://doi.org/10.1016/j.apenergy.2014.10.026

Afroz Chakure. (2019). Random Forest Regression. Web. https://medium.com/swlh/random-forest-and-its-implementation-71824ced454f

Afroz, Z., Shafiullah, G., Urmee, T., & Higgins, G. (2018). Modeling techniques used in building HVAC control systems: A review. Renewable and Sustainable Energy Reviews, 83, 64-84. doi:10.1016/j.rser.2017.10.044

Agbi, C., Song, Z., & Krogh, B. (2012). Parameter identifiability for multi-zone building models. Paper presented at the 6951-6956. doi:10.1109/CDC.2012.6425995

Ahmad, M. W., Mourshed, M., & Rezgui, Y. (2017). Trees vs. neurons: Comparison between random forest and ANN for high-resolution prediction of building energy consumption. Energy and Buildings, 147, 77-89. https://doi.org/10.1016/j.enbuild.2017.04.038

Ahmad, M. W., Mourshed, M., Yuce, B., & Rezgui, Y. (2016). Computational intelligence techniques for HVAC systems: A review. Building Simulation, 9(4), 359-398. doi:10.1007/s12273-016-0285-4

Allen, D. M. (1971). Mean square error of prediction as a criterion for selecting variables. Technometrics, 13 (3), 469-475.

Allen, D. M. (1971). Mean square error of prediction as a criterion for selecting variables. Technometrics, 13(3), 469-475. https://doi.org/10.1080/00401706.1971.10488811

Arida, M., Nassif, N., Talib, R., & Abu-Lebdeh, T. (2017). Building Energy Modeling using Artificial Neural Networks. Energy Research Journal, 7(2), 24-34.

Arsov, N., Pavlovski, M., Basnarkov, L., & Kocarev, L. (2017). Generating highly accurate prediction hypotheses through collaborative ensemble learning. Scientific Reports, 7(1), 44649-44649. https://doi.org/10.1038/srep44649

ASHRAE 62.1. (2016). Ventilation for Acceptable Indoor Air Quality. American Society of Heating, Refrigerating, and Air-Conditioning Engineers, Inc.

ASHRAE 36. (2018). High-Performance Sequences of Operation for HVAC Systems. American Society of Heating, Refrigerating, and Air-Conditioning Engineers, Inc.

ASHRAE. (2011). ASHRAE Handbook Applications. Chapter 41. Atlanta: American Society of Heating Refrigeration and Air Conditioning Engineers, Inc. Print. 2011.

BEAST lab. (2020). https://nassifnl.wixsite.com/beast1/lab-mission.

Bell, A. A., & Angel, W. L. (2016). HVAC equations, data, and rules of thumb (Third ed.). New York: McGraw-Hill Education.

Bishop, C.M. (1995). Neural Networks for Pattern Recognition. Oxford University Press, New York.

Brian Hafendorfer. (2017). Condensation in Air-Handling Systems. Trane, engineering newsletter. Volume 46-4.

Breiman, L. (1994). Bagging predictors (Technical Report 421). University of California, Berkeley.

Buford, J. M. (2016). The dynamic modeling of a chilled water air handling unit using system identification methods

Caldas, L. G., & Norford, L. K. (2003). Genetic algorithms for optimization of building envelopes and the design and control of HVAC systems. Journal of Solar Energy Engineering, Transactions of the ASME, 125(3), 343-351. doi:10.1115/1.1591803

Chai, T., & Draxler, R. R. (2014). Root mean square error (RMSE) or mean absolute error (MAE)? -arguments against avoiding RMSE in the literature. Geoscientific Model Development, 7(3), 1247-1250. https://doi.org/10.5194/gmd-7-1247-2014

Chakraborty, D., & Elzarka, H. (2018). Performance testing of energy models: Are we using the right statistical metrics? Journal of Building Performance Simulation, 11(4), 433-448. doi:10.1080/19401493.2017.1387607

Wang, W., Chau, K., Cheng, C., & Qiu, L. (2009). A comparison of performance of several artificial intelligence methods for forecasting monthly discharge time series. Journal of Hydrology (Amsterdam), 374(3), 294-306. https://doi.org/10.1016/j.jhydrol.2009.06.019

Mitrovic, J. (Ed.). (2012). Heat Exchangers: Basics Design Applications. BoD–Books on Demand.

Cunningham, P., Cord, M. and Delany, S. (2008). Machine Learning Techniques for Multimedia. Springer-Berlin Heidelberg, Berlin, Germany.

Curto, J. D., & Pinto, J. C. (2009). The coefficient of variation asymptotic distribution in the case of non-iid random variables. Journal of Applied Statistics, 36(1), 21-32. https://doi.org/10.1080/02664760802382491

Dave Guckelberger. (1989). Chiller plant system performance. Trane, engineering newsletter. Vol. 18- 2.

Del Carmen Ruiz-Abell n, María, Gabaldón, A., & Guillamón, A. (2018). Load forecasting for a campus university using ensemble methods based on regression trees. Energies (Basel), 11(8), 2038. https://doi.org/10.3390/en11082038

Dey, D., & Dong, B. (2016). A probabilistic approach to diagnose faults of air handling units in buildings. Energy and Buildings, 130, 177-187. https://doi.org/10.1016/j.enbuild.2016.08.017.

Draper, N. R., & Smith, H. (1981). Applied regression analysis (2d ed.). Wiley

EIA. (2019). "How Much Energy Is Consumed in Residential and Commercial Buildings in the United States?". US Energy Information Administration –Independent Statistics and Analysis. Web.

EIA. (2021). "Ohio State Energy Profile". US Energy Information Administration –Independent Statistics and Analysis. Web. 2021.

EIA. (2016). commercial building energy consumption survey. Web. https://www.eia.gov/energyexplained/use-of-energy/commercial-buildings.php.

ENERGY STAR. Portfolio Manager. Technical reference. ENERGY STAR Score. 2018. https://portfoliomanager.energystar.gov/pdf/reference/ENERGY%20STAR%20Score.pdf

EPA. (2018). "Introduction to Indoor Air Quality." The United States Environmental Protection Agency. Web.

Eppelheimer, D. (2002). Keystone of system performance cooling- coil heat transfer. Trane, engineering newsletter. Volume 31, 1.

Eric Strum. (2016). Multiple Zone VAV System- Finding the Right Balance for VAV Energy Saving. Trane, Engineering Newsletter. Volume 45-3.

Frausto, H. U., Pieters, J. G., & Deltour, J. M. (2003). Modeling greenhouse temperature by means of auto regressive models. Biosystems Engineering, 84(2), 147-157. doi:10.1016/S1537-5110(02)00239-8

Garnier, A., Eynard, J., Caussanel, M., & Grieu, S. (2014). Low computational cost technique for predictive management of thermal comfort in non-residential buildings. Journal of Process Control, 24(6), 750-762. doi:10.1016/j.jprocont.2013.10.005

Garnier, A., Eynard, J., Caussanel, M., & Grieu, S. (2015). Predictive control of multizone heating, ventilation and air-conditioning systems in non-residential buildings. Applied Soft Computing, 37, 847-862. https://doi.org/10.1016/j.asoc.2015.09.022

Garrett, A., & New, J. (2016). Suitability of ASHRAE guideline 14 metrics for calibration. ASHRAE Transactions, 122(1), 469.

Ghiaus, C., & Hazyuk, I. (2010). Calculation of optimal thermal load of intermittently heated buildings. Energy and Buildings, 42(8), 1248-1258. https://doi.org/10.1016/j.enbuild.2010.02.017

Guideline 14-2014: Measurement of Energy, Demand, and Water Savings. ASHRAE. Atlanta, GA 2014

Han, H., Gu, B., Kang, J., & Li, Z. R. (2011). Study on a hybrid SVM model for chiller FDD applications. Applied Thermal Engineering, 31(4), 582-592. https://doi.org/10.1016/j.applthermaleng.2010.10.021

He, X., Zhang, Z., & Kusiak, A. (2014). Performance optimization of HVAC systems with computational intelligence algorithms. Energy & Buildings, 81, 371-380. doi:10.1016/j.enbuild.2014.06.021

Ho, Y., Zhao, Q., & Jia, Q. (2007). Ordinal optimization: Soft optimization for hard problems. Springer. https://doi.org/10.1007/978-0-387-68692-9

Homod, R. Z. (2013). Review on the HVAC system modeling types and the shortcomings of their application. Journal of Energy (Hindawi), 2013, 1-10. https://doi.org/10.1155/2013/768632

Huang, H., Chen, L., & Hu, E. (2015). A neural network-based multi-zone modeling approach for predictive control system design in commercial buildings. Energy & Buildings, 97, 86-97. doi:10.1016/j.enbuild.2015.03.045

Huang, S., Nianguang, C. A. I., Penzuti Pacheco, P., Narandes, S., Wang, Y., & Wayne, X. U. (2018). Applications of support vector machine (SVM) learning in cancer genomics. Cancer Genomics & Proteomics, 15(1), 41-51. https://doi.org/10.21873/cgp.20063

Hyvikinen, J. (1996). Real-Time Simulation of HVAC Systems for Building Optimization, Fault Detection and Diagnosis Technical Papers of IEA Annex 25. International Energy Agency.

Janis, R. R., & Tao, W. K. Y. (2014). Mechanical and electrical systems in buildings. Boston: Pearson.

Jee-Heon, K., Nam-Chul Seong, & Choi, W. (2020). Forecasting the energy consumption of an actual air handling unit and absorption chiller using ANN models. Energies, 13(17), 4361. doi:http://dx.doi.org.proxy.libraries.uc.edu/10.3390/en1317436

Khan, G., Siddiqi, A., Ghani Khan, M. U., Qayyum Wahla, S., & Samyan, S. (2019). Geometric positions and optical flow based emotion detection using MLP and reduced dimensions. IET Image Processing, 13(4), 634-643. https://doi.org/10.1049/iet-ipr.2018.5728

Khazaii, J., & Ohio Library and Information Network. (2014). Energy-efficient HVAC design: An essential guide for sustainable building (2014th ed.). Cham: Springer. doi:10.1007/978-3-319-11047-9

Kim, J., Seong, N., & Choi, W. (2019). Modeling and optimizing a chiller system using a machine learning algorithm. Energies (Basel), 12(15), 2860. https://doi.org/10.3390/en12152860

Kulkarni, M. R., & Hong, F. (2004). Energy optimal control of a residential space-conditioning system based on sensible heat transfer modeling. Building and Environment, 39(1), 31-38. doi:10.1016/j.buildenv.2003.07.003

Kusiak, A., Li, M., & Tang, F. (2010). Modeling and optimization of HVAC energy consumption. Applied Energy, 87(10), 3092-3102. doi:10.1016/j.apenergy.2010.04.008

Lee, C. W., Liao, W. T., Chen, C. W., & Chang, Y. C. (2014). Application of genetic programming method combined with neural network in HVAC optimal operation. Applied Mechanics and Materials, 548-549(Achievements in Engineering Sciences), 1030-1034. https://doi.org/10.4028/www.scientific.net/AMM.548-549.1030

Lee, J. M., Kang, W. H., & Lee, K. H. (2019). ANN based optimized AHU discharge air temperature control of conventional VAV system for minimized cooling energy in an office building. E3S Web of Conferences, 111, 5014. https://doi.org/10.1051/e3sconf/201911105014

Leephakpreeda, T. (2008). Grey prediction on indoor comfort temperature for HVAC systems. Expert Systems with Applications, 34(4), 2284-2289. https://doi.org/10.1016/j.eswa.2007.03.003

Li, J., Guo, Y., Wall, J., & West, S. (2019). Support vector machine based fault detection and diagnosis for HVAC systems. International Journal of Intelligent Systems Technologies and Applications, 18(1-2), 204-222. https://doi.org/10.1504/IJISTA.2019.097752

Li, X., & Wen, J. (2014). Review of building energy modeling for control and operation. Renewable and Sustainable Energy Reviews, 37, 517-537. doi:10.1016/j.rser.2014.05.056

Li, Y., Liu, M., Lau, J., & Zhang, B. (2014). Experimental study on electrical signatures of common faults for packaged DX rooftop units. Energy and Buildings, 77, 401-415. https://doi.org/10.1016/j.enbuild.2014.04.008

Li, Z., Xu, X., Deng, S., & Pan, D. (2015). A novel neural network aided fuzzy logic controller for a variable speed (VS) direct expansion (DX) air conditioning (A/C) system. Applied Thermal Engineering, 78, 9-23. https://doi.org/10.1016/j.applthermaleng.2014.12.030

Liang, J., & Du, R. (2007). Model-based fault detection and diagnosis of HVAC systems using support vector machine method. International Journal of refrigeration, 30(6), 1104-1114.

LIN, Z. (2019). Power load prediction algorithm based on genetic algorithm and support vector machine

Livshin, I. (2019). Artificial neural networks with java: Tools for building neural network applications. Apress. https://doi.org/10.1007/978-1-4842-4421-0

Madison Schott. (2019). Random Forest Algorithm for Machine Learning. Web. https://medium.com/capital-one-tech/random-forest-algorithm-for-machine-learning-c4b2c8cc9feb

Manimaran, S., AlBastaki, I., & Mangai, J. A. (2015). An ensemble model for predicting energy performance in residential buildings using data mining techniques. ASHRAE Transactions, 121(2), 402-402.

Mansour, M. Khamis and M. Hassab. (2012). Thermal Design of Cooling and Dehumidifying

Mathew, P. A., Dunn, L. N., Sohn, M. D., Mercado, A., Custudio, C., & Walter, T. (2015). Big-data for building energy performance: Lessons from assembling a very large national database of building energy use. Applied Energy, 140(C), 85-93.

Mathew, P. A., Dunn, L. N., Sohn, M. D., Mercado, A., Custudio, C., & Walter, T. (2015). Big-data for building energy performance: Lessons from assembling a very large national database of building energy use. Applied Energy, 140(C), 85-93. doi:10.1016/j.apenergy.2014.11.042

McCulloch Mitchell, Melanie. (1998). "Chapter 1: Genetic Algorithms: An Overview." An Introduction to Genetic Algorithms. Cambridge, (MA): MIT Press. Print.

McHugh, M. K., Isakson, T., & Nagy, Z. (2019). Data-driven leakage detection in air-handling units on a university campus. ASHRAE Transactions, 125(2), 391-398.

Meredith MacLeod. (2014). SAVING ENERGY, SAVING MONEY: Businesses are cashing in on grants that will help them conserve power. The Spectator, 11(1), HB. 11.

Mick Schwedler. (2007). Waterside heat recovery Everything old is new again. Trane, engineering newsletter. Volume 36-1.

Mills, E. (2011). Building commissioning: A golden opportunity for reducing energy costs and greenhouse gas emissions in the united states. Energy Efficiency, 4(2), 145-173. doi:10.1007/s12053-011-9116-8

Mirnaghi, M. S., & Haghighat, F. (2020). Fault detection and diagnosis of large-scale HVAC systems in buildings using data-driven methods: A comprehensive review. Energy and Buildings, 229, 1. https://doi.org/10.1016/j.enbuild.2020.110492

Mohanraj, M., Jayaraj, S., & Muraleedharan, C. (2012). Applications of artificial neural networks for refrigeration, air-conditioning and heat pump systems - A review. Renewable and Sustainable Energy Reviews, 16(2), 1340-1358. doi:10.1016/j.rser.2011.10.015

Mohebbi, A., Taheri, M., & Soltani, A. (2008). A neural network for predicting saturated liquid density using genetic algorithm for pure and mixed refrigerants. International Journal of Refrigeration, 31(8), 1317-1327.

Mtibaa, F., Nguyen, K., Dermardiros, V., & Cheriet, M. (2021). Context-aware model predictive control framework for multi-zone buildings. Journal of Building Engineering, 42, 102340. https://doi.org/10.1016/j.jobe.2021.102340

Murphy, J. (2006). Energy saving control strategies for Rooftop VAV System. Trane, engineering newsletter. Volume 35-4.

Murphy, J. and Bakkum, B. (2013). Understanding Single Zone VAV Systems. Tane, Engineering Newsletter. Volume 42-2.

Mustafaraj, G., Chen, J., & Lowry, G. (2010). Development of room temperature and relative humidity linear parametric models for an open office using BMS data. Energy & Buildings, 42(3), 348-356. doi:10.1016/j.enbuild.2009.10.001

Nasruddin, Sholahudin, Satrio, P., Mahlia, T. M. I., Giannetti, N., & Saito, K. (2019). Optimization of HVAC system energy consumption in a building using artificial neural network and multi-objective genetic algorithm. Sustainable Energy Technologies and Assessments, 35, 48-57. https://doi.org/10.1016/j.seta.2019.06.002

Nassif, N. (2014). Modeling and Optimization of HVAC Systems sing Artificial Neural Network and Genetic Algorithm. International Journal of Building Simulation, 7 (3), 237.245.

Nassif, N., Arida, M., & Talib, R. (2016). Development and testing of building energy model using non-linear auto regression neural networks. In ASHRAE Annual Conference, St Louis, MO, June (Vol. 2329).

Nayak, P.C., Sudheer, K.P., Rangan, D.M., Ramasastri, K.S. (2004). A neuro-fuzzy computing technique for modeling hydrological time series. Journal of Hydrology 291 (1–2), 52–66.

Olama, A. (2017). District Cooling. Boca Raton: CRC Press, https://doi-org.proxy.libraries.uc.edu/10.4324/9781315371634

Khan, G., Siddiqi, A., Ghani Khan, M. U., Qayyum Wahla, S., & Samyan, S. (2019). Geometric positions and optical flow based emotion detection using MLP and reduced dimensions. IET Image Processing, 13(4), 634-643. https://doi.org/10.1049/iet-ipr.2018.5728

Page, J., Robinson, D., Morel, N., & Scartezzini, J. -. (2008). A generalised stochastic model for the simulation of occupant presence. Energy & Buildings, 40(2), 83-98. doi:10.1016/j.enbuild.2007.01.018

Pang, X., Piette, M. A., & Zhou, N. (2017). Characterizing variations in variable air volume system controls. Energy and Buildings, 135, 166

Parzinger, M., Hanfstaengl, L., Sigg, F., Spindler, U., Wellisch, U., & Wirnsberger, M. (2020). Residual analysis of predictive modelling data for automated fault detection in building's heating, ventilation and air conditioning systems. Sustainability (Basel, Switzerland), 12(17), 6758. https://doi.org/10.3390/su12176758

Patil, S. L., Tantau, H. J., & Salokhe, V. M. (2007). Modelling of tropical greenhouse temperature by auto regressive and neural network models. Biosystems Engineering, 99(3), 423-431. doi:10.1016/j.biosystemseng.2007.11.009

Pérez-Lombard, L., Ortiz, J., & Pout, C. (2008). A Review on Buildings Energy Consumption Information. Energy and buildings, 40 (3), 394-398.

Piepho, H. (2019). A coefficient of determination (R2) for generalized linear mixed models. Biometrical Journal, 61(4), 860-872. https://doi.org/10.1002/bimj.201800270

R. Caffrey. (1998). The intelligent building: an ASHRAE opportunity intelligent buildings. ASHRAE Technical Data Bulletin, vol. 4, no. 1, pp. 1–9, 1998.

Reddy, T.A., and Claridge, D.E. (2000). Uncertainty of “Measured” Energy Savings from Statistical Baseline Models. HVAC&R RESEARCH. VOL. 6, NO. 1

Reynolds, J., Rezgui, Y., Kwan, A., & Piriou, S. (2018). A zone-level building energy optimisation combining an artificial neural network, a genetic algorithm, and model predictive control. Energy, 151, 729-739. doi:10.1016/j.energy.2018.03.113

Reynolds, J., Rezgui, Y., Kwan, A., & Piriou, S. (2018). A zone-level, building energy optimisation combining an artificial neural network, a genetic algorithm, and model predictive control. Energy (Oxford), 151, 729-739. https://doi.org/10.1016/j.energy.2018.03.113

Ríos-Moreno, G. J., Trejo-Perea, M., Castañeda-Miranda, R., Hernández-Guzmán, V. M., & Herrera-Ruiz, G. (2007). Modelling temperature in intelligent buildings by means of autoregressive models. Automation in Construction, 16(5), 713-722. doi:10.1016/j.autcon.2006.11.003

Rohith Gandhi. (2018). Support Vector Machine — Introduction to Machine Learning Algorithms. Web. https://towardsdatascience.com/support-vector-machine-introduction-to-machine-learning-algorithms-934a444fca47.

Ruiz, G. R., & Bandera, C. F. (2017). Validation of calibrated energy models: Common errors. Energies (Basel), 10(10), 1587. https://doi.org/10.3390/en10101587

Sakthivel, N. R., Sugumaran, V., & Nair, B. B. (2010;2009;). Application of support vector machine (SVM) and proximal support vector machine (PSVM) for fault classification of monoblock centrifugal pump. International Journal of Data Analysis Techniques and Strategies, 2(1), 38-61. https://doi.org/10.1504/IJDATS.2010.030010

Schölkopf, B., & Smola, A. J. (2002). Learning with kernels: Support vector machines, regularization, optimization, and beyond. MIT Press.

Sector-Specific needs and improvements. (2016). In I. M. Shapiro (Ed.), (pp. 271-280). John Wiley & Sons, Inc. https://doi.org/10.1002/9781119174851.ch19

Seyam, S. (2018). Types of HVAC systems. HVAC System, 49-66.

Sivanandam, S. N., and S. N. Deepa. (2006). "Introduction to Neural Networks Using Matlab 6.0." Google Books. Tata McGraw-Hill Education. Web.

Sivanandam, S. N., Deepa, S. N., & Books24x7, I. (2007;2008;). Introduction to genetic algorithms (1. Aufl. ed.). Springer. https://doi.org/10.1007/978-3-540-73190-0

Smola, A. J., & Schölkopf, B. (2004). A tutorial on support vector regression. Statistics and Computing, 14(3), 199-222. https://doi.org/10.1023/B:STCO.0000035301.49549.88

Solazzo, E., & Galmarini, S. (2016). Error apportionment for atmospheric chemistry-transport models - A new approach to model evaluation. Atmospheric Chemistry and Physics, 16(10), 6263-6283. https://doi.org/10.5194/acp-16-6263-2016

Stanford, H. W. (2012;2011;). HVAC water chillers and cooling towers: Fundamentals, application, and operation (2nd ed.). Boca Raton, FL: CRC Press

Stanke, D. (1991). VAV System Optimization Critical Zone Reset. Trane, engineering newsletter. Volume 20, No. 2.

Stanke, D. (2011). Minimum Outdoor Airflow Using the IAQ Procedure. Trane, engineering newsletter. Volume 40-3.

National Renewable Energy Laboratory (U.S.), International Performance Measurement & Verification Protocol Committee, & United States. Department of Energy.Office of Energy Efficiency and Renewable Energy. (2001). Statistics and Uncertainty for IPMVP.

Sturm, E. (2015). Airside Economizers and ASHRAE standard 90.1-2013. Trane, engineering newsletter. Volume 44-2.

Sun, K., Yan, D., Hong, T., & Guo, S. (2014). Stochastic modeling of overtime occupancy and its application in building energy simulation and calibration. Building and Environment, 79, 1-12. doi:10.1016/j.buildenv.2014.04.030

Svetnik, V., Liaw, A., Tong, C., Culberson, J. C., Sheridan, R. P., & Feuston, B. P. (2003). Random forest: A classification and regression tool for compound classification and QSAR modeling. Journal of Chemical Information and Computer Sciences, 43(6), 1947-1958. https://doi.org/10.1021/ci034160g

Tahmasebi, M., Eaton, K., Nassif, N., & Talib, R. (2019). Integrated Machine Learning Modeling and Fault Detection Approach for Chilled Water Systems. International Conference on Artificial Intelligence. Las Vegas, NV, October (67-71).

Talib, R., & Nassif, N. (2021). Heating ventilation and air conditioning systems performance optimization using a two-level optimization approach. ASHRAE Transactions, 127(1), 505

Talib, R., Nassif, N., Arida, M., & Abu-Lebdeh, T. (2018). Chilled Water VAV System Optimization and Modeling Using Artificial Neural Networks. American Journal of Engineering and Applied Sciences, 11 (4), 1188-1198.

Talib, R., Rai, P., Nassif, N., & Tahmasebi, M. (2019). Modeling of Chilled Water VAV Systems Using a Machine Learning Approach. International Conference on Artificial Intelligence. Las Vegas, NV, October (72-78).

Talib, R., Nabil, N., & Choi, W. (2020). Optimization-based data-enabled modeling technique for HVAC systems components. Buildings (Basel), 10(9), 163. https://doi.org/10.3390/BUILDINGS10090163

Teoh, W. L., Khoo, M. B. C., Castagliola, P., Yeong, W. C., & Teh, S. Y. (2017;2016;). Run-sum control charts for monitoring the coefficient of variation. European Journal of Operational Research, 257(1), 144-158. https://doi.org/10.1016/j.ejor.2016.08.067

Tian, W., Lei, C., & Tian, M. (2018). Dynamic prediction of building HVAC energy consumption by ensemble learning approach. Paper presented at the 254-257. https://doi.org/10.1109/CSCI46756.2018.00055

Tjur, T. (2009). Coefficients of determination in logistic regression models-A new proposal: The coefficient of discrimination. The American Statistician, 63(4), 366-372. https://doi.org/10.1198/tast.2009.08210

Tse, W. L., & Chan, W. L. (2005). An automatic data acquisition system for on-line training of artificial neural network-based air handling unit modeling. Measurement, 37(1), 39-46.

Turner, C., & Frankel, M. (2008). Energy performance of LEED for new construction buildings. New Buildings Institute, 4, 1-42

Vakiloroaya, V., Ha, Q. P., & Samali, B. (2013). Energy-efficient HVAC systems: Simulation–empirical modelling and gradient optimization. Automation in Construction, 31, 176-185. https://doi.org/10.1016/j.autcon.2012.12.006

Van Every, P. M., Rodriguez, M., Jones, C. B., Mammoli, A. A., & Martínez-Ramón, M. (2017). Advanced detection of HVAC faults using unsupervised SVM novelty detection and gaussian process models. Energy and Buildings, 149(C), 216-224. https://doi.org/10.1016/j.enbuild.2017.05.053

Van Liew, M.W., Arnold, J.G., Garbrecht, J.D. (2003). Hydrologic simulation: choosing between two models. Transactions of the ASAE 46 (6), 1539–1551.

Vapnik, V. (2013). The nature of statistical learning theory. Springer science & business media.

Wang, J., Zhang, C., & Jing, Y. (2008). Analytical design of decoupling control for variable-air-volume air-conditioning system. Paper presented at the 630-635. https://doi.org/10.1109/ICCIS.2008.4670836

Wang, Y., Cai, W., Soh, Y., Li, S., Lu, L., & Xie, L. (2004). A simplified modeling of cooling coils for control and optimization of HVAC systems. Energy Conversion and Management, 45(18), 2915-2930. https://doi.org/10.1016/j.enconman.2003.12.024

Werbos PJ. (1974). Beyond Regression: New Tools for Prediction and Analysis in the Behavioral Sciences." [Ph.D. Thesis]. Cambridge, (MA): Harvard Univ., 19 (1).

William Landman. (1991). Two Good Old Ideas Combine to Form One New Great Idea. Trane, engineering newsletter. Volume 20-1

Willmott, C. J., & Matsuura, K. (2005). Advantages of the mean absolute error (MAE) over the root mean square error (RMSE) in assessing average model performance. Climate Research, 30(1), 79-82. https://doi.org/10.3354/cr030079

Xia, Y., Jiangzhou, S., Zhang, X., & Zhang, Z. (2020). Steady-state performance prediction for a variable speed direct expansion air conditioning system using a white-box based modeling approach. Energies (Basel), 13(18), 4757. https://doi.org/10.3390/en13184757

Xiao, F., & Fan, C. (2014). Data mining in building automation system for improving building operational performance. Energy & Buildings, 75, 109-118. doi:10.1016/j.enbuild.2014.02.005

Xuemei, L., Ming, S., Lixing, D., Gang, X., & Jibin, L. (2009). Novel HVAC fan machinery fault diagnosis method based on KPCA and SVM. Paper presented at the 492-496. https://doi.org/10.1109/ICIMA.2009.5156671

Yan, K., Diduch, C., & Kaye, M. E. (2019). An improved temperature prediction technique for HVAC units using intelligent algorithms. Paper presented at the 490-494. doi:10.1109/ECCE.2019.8912944

Zhang, C., & Ma, Y. (2012;2015;). Ensemble machine learning: Methods and applications (1. Aufl. ed.). Springer. https://doi.org/10.1007/9781441993267

Zhao, J., Duan, Y., & Liu, X. (2018). Uncertainty analysis of weather forecast data for cooling load forecasting based on the monte carlo method. Energies (Basel), 11(7), 1900. https://doi.org/10.3390/en11071900

Tesiero, R. C., III. (2014). Intelligent approaches for modeling and optimizing HVAC systems

APPENDIX A

Data collection

The following is a small sample of some of the performance data collected from the BAS and then transferred to Microsoft Excel to prepare for the modeling process. The data were used to create figure 34.

Date	Time	Time Zone	AHU-VAV : Duct Static Pressur	AHU-VAV : Duct Static Pressu	Test Lab 1 VAV-2 Water Duct : Discharge Air Flo	Test Lab 1 VAV-2 DX Duct : Discharg	Test Lab 3 VAV-1 DX Duct : Discha	Test Lab 2 VAV-3 DX Duct : Disch	AHU-01 VAV : Supply Fan Speed Status
25-Apr-21	7:45:00 PM	America/Detroit	0.517	0.404	160.9	226.6	300.7	241	33.1
25-Apr-21	7:46:00 PM	America/Detroit	0.447	0.215	172.4	196.4	352.5	245.2	33.4
25-Apr-21	7:47:00 PM	America/Detroit	0.345	0.195	183.6	196.1	357	274.4	33.4
25-Apr-21	7:48:00 PM	America/Detroit	0.323	0.188	186.5	187.3	364	274.2	35.2
25-Apr-21	7:49:00 PM	America/Detroit	0.313	0.193	189.7	186.3	364.8	282.4	36.4
25-Apr-21	7:50:00 PM	America/Detroit	0.288	0.2	190.3	188.9	355.8	284.6	37.7
25-Apr-21	7:51:00 PM	America/Detroit	0.313	0.209	194.1	185.7	355.4	284.3	38.5
25-Apr-21	7:52:00 PM	America/Detroit	0.288	0.212	197.8	179.4	374.8	269.1	39.6
25-Apr-21	7:53:00 PM	America/Detroit	0.285	0.208	202.6	187	347.9	270.7	43.5
25-Apr-21	7:54:00 PM	America/Detroit	0.292	0.237	204.4	184	359.3	263.2	45.8
25-Apr-21	7:55:00 PM	America/Detroit	0.245	0.199	395.7	180.4	334.1	258.1	100
25-Apr-21	7:56:00 PM	America/Detroit	0.336	0.324	455.4	309.4	495.4	362.4	100
25-Apr-21	7:57:00 PM	America/Detroit	0.357	0.293	439.1	324.6	463.1	380.9	100
25-Apr-21	7:58:00 PM	America/Detroit	0.388	0.289	448	313.2	500.1	364.7	100
25-Apr-21	7:59:00 PM	America/Detroit	0.391	0.307	443.6	313.2	489.9	370.6	100
25-Apr-21	8:00:00 PM	America/Detroit	0.395	0.316	448.2	330.6	469.8	385	100
25-Apr-21	8:01:00 PM	America/Detroit	0.423	0.285	448	323.5	488.3	382.6	100
25-Apr-21	8:02:00 PM	America/Detroit	0.464	0.293	445.1	334.4	484.6	384.5	100
25-Apr-21	8:03:00 PM	America/Detroit	0.449	0.281	450.9	329.7	481	380.6	100
25-Apr-21	8:04:00 PM	America/Detroit	0.448	0.271	448.2	335.7	473.4	390.1	100
25-Apr-21	8:05:00 PM	America/Detroit	0.384	0.272	445.1	337	465.2	390.9	100
25-Apr-21	8:06:00 PM	America/Detroit	0.432	0.295	449.6	321.4	498.2	374.5	100
25-Apr-21	8:07:00 PM	America/Detroit	0.407	0.267	449.2	329.9	483.8	384.5	100
25-Apr-21	8:08:00 PM	America/Detroit	0.413	0.277	448.2	327	478.7	385.1	100
25-Apr-21	8:09:00 PM	America/Detroit	0.404	0.279	450.2	327.9	479.1	379.5	100
25-Apr-21	8:10:00 PM	America/Detroit	0.452	0.279	452	331.9	487.8	381.8	100
25-Apr-21	8:11:00 PM	America/Detroit	0.464	0.277	405.6	334.6	474.7	386.9	50
25-Apr-21	8:12:00 PM	America/Detroit	0.251	0.185	311.7	299.5	404.3	341.9	50
25-Apr-21	8:13:00 PM	America/Detroit	0.265	0.167	320.2	290.1	401	334	50
25-Apr-21	8:14:00 PM	America/Detroit	0.296	0.177	318.2	291.7	405.5	332	50
25-Apr-21	8:15:00 PM	America/Detroit	0.237	0.161	321.6	289.6	400.1	330.8	50
25-Apr-21	8:16:00 PM	America/Detroit	0.261	0.173	318.2	285.9	400	327.5	50
25-Apr-21	8:17:00 PM	America/Detroit	0.292	0.161	321.2	287.6	407.3	332.6	50
25-Apr-21	8:18:00 PM	America/Detroit	0.272	0.169	322.1	286.9	406.8	328.4	50
25-Apr-21	8:19:00 PM	America/Detroit	0.3	0.176	314.9	288.8	394.6	330.6	50
25-Apr-21	8:20:00 PM	America/Detroit	0.236	0.179	311.5	289.2	395	333.1	50
25-Apr-21	8:21:00 PM	America/Detroit	0.287	0.147	318.7	291.3	403.3	335.1	50
25-Apr-21	8:22:00 PM	America/Detroit	0.257	0.172	318.9	291.7	403	333.7	50

APPENDIX B

MATLAB

The following is a section of one of the scripts developed using MATLAB for the components data-driven models.

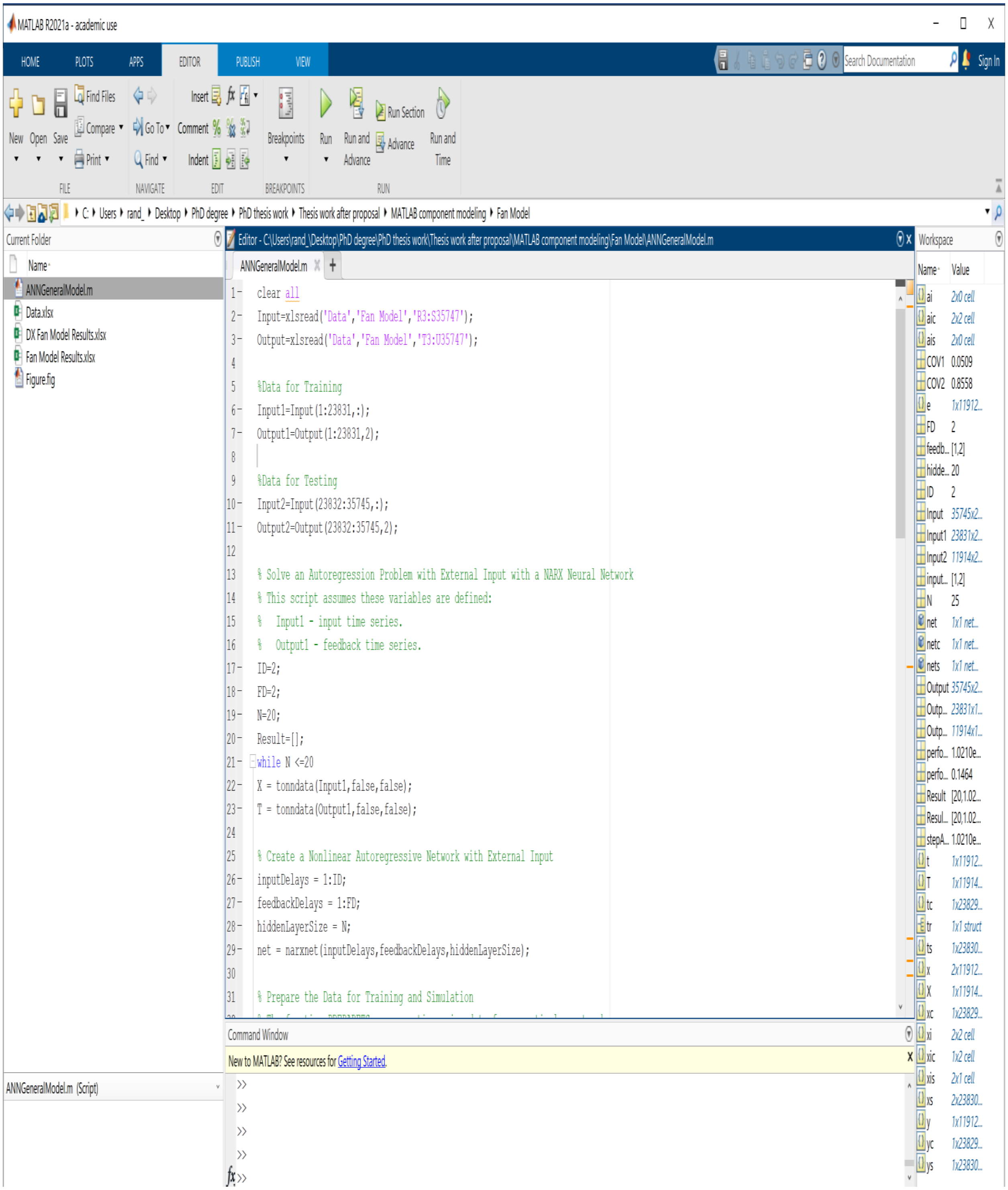

APPENDIX C

Parametric study

The following is a section of one set produced in the parametric study to manually select the best model structure. The data are for the DX fan models in predicting the fan power.

ID1-FD1	Training		Testing	
N	MSE1	COV1	MSE2	COV2
5	0.0151	0.0336	0.0722	0.05902
10	0.0139	0.0328	0.0719	0.5807
15	0.0138	0.0326	0.1992	0.9665
20	0.0135	0.0327	1.6318	2.7659
25	0.0134	0.0326	0.2442	1.07
30	0.0133	0.0319	1.6564	2.7866
35	0.013	0.0321	7.853	6.0677
40	0.0128	0.0318	1.2259	2.3974
45	0.0126	0.0318	0.2847	6.9438
50	0.0125	0.0318	0.8789	2.0299
55	0.0126	0.0317	3.1947	3.8701
60	0.0123	0.0317	1.3325	2.4994
65	0.0123	0.0317	0.7576	1.8846
70	0.0122	0.0316	3.568	4.0899
75	0.0121	0.0317	2.529	3.4433
80	0.0119	0.0317	3.6888	4.1586
85	0.0118	0.0317	1.8486	6.795
90	0.0117	0.0316	4.7694	4.7286
95	0.0118	0.0316	1.2871	2.4565
100	0.0116	0.0316	2.9026	3.6889
			0.0719	**0.5807**

ID2-FD1	Training		Testing	
N	MSE1	COV1	MSE2	COV2
5	0.0148	0.0323	0.0591	0.5543
10	0.0139	0.0318	0.0562	0.5135
15	0.0133	0.0314	2.4802	3.4099
20	0.0132	0.0314	0.0804	0.6139
25	0.0127	0.0312	0.6469	1.7415
30	0.0124	0.0312	0.1782	0.9141
35	0.0124	0.0312	0.1396	0.8089
40	0.0122	0.0312	0.2058	0.9823
45	0.0121	0.0311	0.2274	1.0325
50	0.0117	0.0311	0.3674	1.3124
55	0.0115	0.0311	1.3337	2.5005
60	0.0117	0.0311	0.4291	1.4184
65	0.0113	0.0311	0.4537	1.4584
70	0.0114	0.0311	0.9256	2.0831
75	0.0114	0.031	1.9236	3.0031
80	0.0111	0.031	0.8108	1.9497
85	0.0108	0.031	1.4336	2.5925
90	0.0107	0.031	0.4939	1.5217
95	0.0106	0.031	0.3041	1.194
100	0.0106	0.031	0.4639	1.4748
			0.0562	**0.5135**

ID3-FD1	Training		Testing	
N	MSE1	COV1	MSE2	COV2
5	0.0128	0.0333	0.0192	0.1862
10	0.0121	0.0316	0.0706	0.4364
15	0.0115	0.0316	0.0031	0.1211
20	0.0108	0.0311	0.0974	0.6404
25	0.0106	0.0311	0.0932	0.6609
30	0.0104	0.031	0.1952	0.9567
35	0.0101	0.0311	0.0644	0.5495
40	0.0099	0.0309	0.1373	0.8022
45	0.0095	0.0309	0.3302	1.2441
50	0.0094	0.0308	0.291	1.1679
55	0.0094	0.0308	0.6662	1.9949
60	0.0092	0.0308	0.2967	1.1793
65	0.0089	0.0307	0.2463	1.0746
70	0.0088	0.0307	0.1406	0.8118
75	0.0087	0.0308	0.2628	1.11
80	0.0085	0.0307	0.4745	1.4916
85	0.0083	0.0306	0.4954	1.5241
90	0.0082	0.0307	0.796	2.4493
95	0.0081	0.0307	1.0759	2.8723
100	0.0079	0.0307	0.8161	0.9256
			0.0031	**0.1211**

ID1-FD2	Training		Testing	
N	MSE1	COV1	MSE2	COV2
5	0.0134	0.0342	0.0192	0.299
10	0.0129	0.0328	0.2444	1.0704
15	0.0127	0.0329	0.2015	0.972
20	0.0122	0.0324	0.0181	0.291
25	0.0121	0.0319	5.2672	4.9693
30	0.012	0.0319	0.2019	0.9728
35	0.0118	0.0318	1.0944	9.4614
40	0.0114	0.0318	2.8783	3.6734
45	0.0115	0.0317	3.5607	4.0858
50	0.0112	0.0317	0.2831	1.1521
55	0.0111	0.0317	3.2589	3.9088
60	0.0109	0.0316	1.5218	2.6711
65	0.0108	0.0316	2.9403	3.7128
70	0.0105	0.0317	7.152	5.7905
75	0.0104	0.0317	0.785	1.9183
80	0.0106	0.0316	2.6442	3.5209
85	0.0102	0.0316	7.2615	5.8347
90	0.0104	0.0316	1.8625	2.9549
95	0.0101	0.0316	2.6116	3.4991
100	0.0102	0.0316	1.9032	8.3588
			0.0181	**0.291**

ID2-FD2	Training		Testing	
N	MSE1	COV1	MSE2	COV2
5	0.0133	0.033	0.0444	0.4616
10	0.0126	0.0317	0.0605	0.5326
15	0.0121	0.0315	0.3639	1.3061
20	0.0118	0.0313	0.0725	0.5829
25	0.0115	0.0312	0.8575	2.005
30	0.0114	0.0312	0.1232	0.76
35	0.0113	0.0312	0.2187	1.0126
40	0.0109	0.0312	0.0436	0.4522
45	0.0107	0.0311	0.2396	1.0599
50	0.0105	0.0311	0.2263	1.03
55	0.0105	0.0311	0.3885	1.3496
60	0.0105	0.0311	1.43	2.5893
65	0.0101	0.0311	0.0817	0.6189
70	0.0099	0.031	0.5583	1.6179
75	0.0097	0.031	1.1741	2.3462
80	0.0097	0.031	0.5644	1.6267
85	0.0097	0.031	0.3057	1.1972
90	0.0097	0.031	0.9185	2.0752
95	0.0093	0.031	1.2658	2.4361
100	0.0093	0.031	0.3617	1.3022
			0.0436	**0.4522**

ID3-FD2	Training		Testing	
N	MSE1	COV1	MSE2	COV2
5	0.1531	0.0325	0.0023	0.1044
10	0.1256	0.0316	0.0178	0.2889
15	0.1156	0.0314	0.0276	0.3595
20	0.1159	0.0311	0.4524	4.0231
25	0.106	0.0311	0.3769	1.3292
30	0.1031	0.031	0.1254	0.7668
35	0.0955	0.0309	0.6689	1.7709
40	0.0998	0.0309	0.6537	1.7506
45	0.098	0.0308	0.1011	0.6885
50	0.0991	0.0308	0.2001	0.9687
55	0.0961	0.0309	0.283	1.1518
60	0.0958	0.0307	0.1776	0.9124
65	0.1126	0.0307	0.1218	0.7557
70	0.0948	0.0307	0.6712	1.7739
75	0.09	0.0307	0.6437	1.7371
80	0.0892	0.0307	1.2617	2.4321
85	0.0879	0.0307	0.636	1.7268
90	0.0824	0.0307	0.0834	0.6255
95	0.0863	0.0306	0.4995	1.5302
100	0.0857	0.0306	0.2085	0.9887
			0.0178	**0.2889**

ID1-FD3	Training		Testing	
N	MSE1	COV1	MSE2	COV2
5	0.0129	0.0334	0.6314	1.7205
10	0.0119	0.0331	0.0306	0.3788
15	0.0119	0.0324	0.1697	0.892
20	0.0111	0.0323	0.4064	1.3804
25	0.011	0.032	0.6954	1.8056
30	0.0109	0.0321	0.4282	1.4169
35	0.0106	0.0319	0.2017	0.9723
40	0.0101	0.0319	0.2736	1.1326
45	0.0102	0.0317	1.1056	2.2766
50	0.0099	0.0317	0.552	1.6087
55	0.0096	0.0317	0.3035	1.1928
60	0.0098	0.0316	1.265	2.4352
65	0.0096	0.0316	1.7512	2.8653
70	0.0094	0.0316	0.5563	1.615
75	0.0092	0.0316	2.5988	3.4905
80	0.0091	0.0316	0.7044	1.8173
85	0.009	0.0316	0.9339	2.0924
90	0.0089	0.0316	2.7395	3.5838
95	0.0087	0.0316	16.6463	8.8341
100	0.0088	0.0316	1.0576	2.2267
			0.0306	**0.3788**

ID2-FD3	Training		Testing	
N	MSE1	COV1	MSE2	COV2
5	0.0131	0.0326	0.0109	0.227
10	0.0119	0.0317	0.0252	0.3435
15	0.0114	0.0314	0.0246	0.3395
20	0.0109	0.0314	0.0109	0.226
25	0.0106	0.0312	0.362	1.3028
30	0.0104	0.0312	0.0919	0.6565
35	0.01	0.0311	2.165	3.1859
40	0.0098	0.0311	1.0836	2.2539
45	0.0098	0.031	0.4027	1.374
50	0.0094	0.031	0.7663	1.8954
55	0.0093	0.031	0.1096	0.7167
60	0.0091	0.031	0.3743	1.3248
65	0.009	0.031	0.2513	1.0855
70	0.0086	0.031	0.1273	0.7727
75	0.0086	0.031	0.4677	1.4807
80	0.0084	0.031	0.2872	1.1603
85	0.0084	0.0309	0.2884	1.1628
90	0.0082	0.0309	0.7381	1.8602
95	0.0081	0.0309	0.2934	1.1728
100	0.008	0.0309	0.2161	1.0065
			0.0109	0.226

ID3-FD3	Training		Testing	
N	MSE1	COV1	MSE2	COV2
5	0.0125	0.0319	0.0026	0.1108
10	0.0121	0.0315	0.5424	**1.5946**
15	0.0111	0.0312	0.05	0.484
20	0.0106	0.0311	0.3897	1.3517
25	0.0106	0.031	0.3029	1.1916
30	0.0093	0.0309	0.1581	0.8609
35	0.0099	0.0309	0.6267	1.7142
40	0.0096	0.0308	0.5001	1.5312
45	0.0102	0.0308	0.3545	1.2891
50	0.009	0.0308	0.0936	0.6623
55	0.0092	0.0307	0.3243	1.233
60	0.0086	0.0307	1.2966	2.4655
65	0.0086	0.0307	0.2914	1.1689
70	0.0082	0.0307	0.4845	1.5072
75	0.0083	0.0306	0.3873	1.3475
80	0.0079	0.0306	0.265	1.1147
85	0.0081	0.0306	0.2484	1.0792
90	0.0078	0.0306	0.2442	1.07
95	0.0077	0.0306	1.0102	2.1763
100	0.0075	0.0306	0.6915	1.8005
			0.05	**0.484**

APPENDIX D

MATLAB

The following is a section of one of the scripts developed for the MLO process using MATLAB.

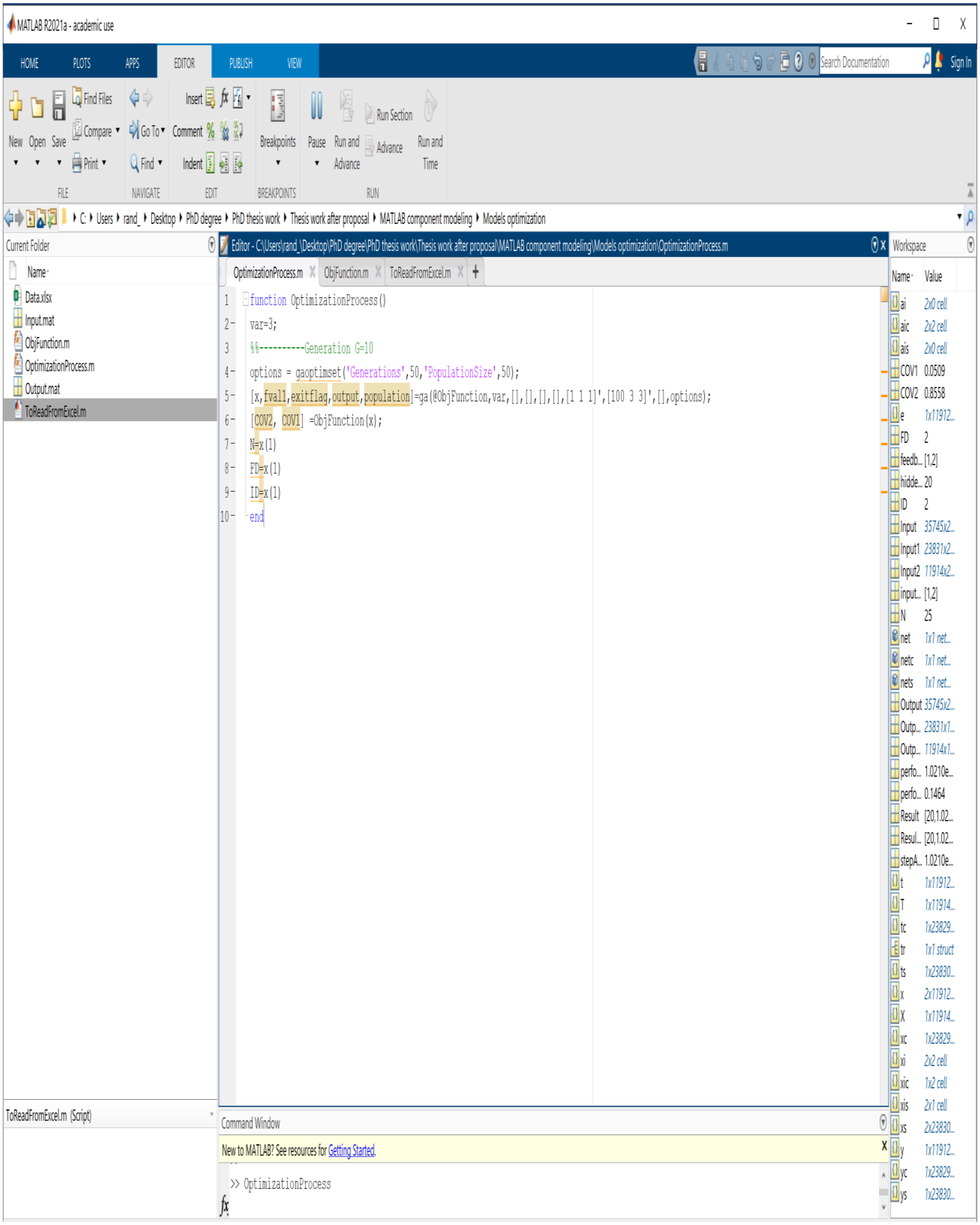

APPENDIX E

Weather conditions

The following are Cincinnati weather conditions from the 2005 ASHRAE Handbook - Fundamentals (SI).

2005 ASHRAE Handbook - Fundamentals (SI)

Design conditions for CINCINNATI MUNICIPAL AP L, OH, USA

Station Information

Station name	WMO#	Lat	Long	Elev	StdP	Hours +/- UTC	Time zone code	Period
1a	*1b*	*1c*	*1d*	*1e*	*1f*	*1g*	*1h*	*1i*
CINCINNATI MUNICIPAL AP L	**724297**	**39.10N**	**84.42W**	**149**	**99.55**	**-5.00**	**NAE**	**8201**

Annual Heating and Humidification Design Conditions

Coldest month	Heating DB		Humidification DP/MCDB and HR						Coldest month WS/MCDB				MCWS/PCWD to 99.6% DB	
			99.6%			99%			0.4%		1%			
	99.6%	99%	DP	HR	MCDB	DP	HR	MCDB	WS	MCDB	WS	MCDB	MCWS	PCWD
2	*3a*	*3b*	*4a*	*4b*	*4c*	*4d*	*4e*	*4f*	*5a*	*5b*	*5c*	*5d*	*6a*	*6b*
1	**-14.9**	**-11.3**	**-20.3**	**0.6**	**-14.1**	**-16.8**	**0.9**	**-10.3**	**10.9**	**2.9**	**9.6**	**0.9**	**4.0**	**240**

Annual Cooling, Dehumidification, and Enthalpy Design Conditions

Hottest month	Hottest month DB range	Cooling DB/MCWB						Evaporation WB/MCDB						MCWS/PCWD to 0.4% DB	
		0.4%		1%		2%		0.4%		1%		2%			
		DB	MCWB	DB	MCWB	DB	MCWB	WB	MCDB	WB	MCDB	WB	MCDB	MCWS	PCWD
7	*8*	*9a*	*9b*	*9c*	*9d*	*9e*	*9f*	*10a*	*10b*	*10c*	*10d*	*10e*	*10f*	*11a*	*11b*
7	**11.1**	**33.8**	**23.8**	**32.4**	**23.5**	**31.1**	**22.8**	**25.5**	**31.3**	**24.8**	**30.2**	**24.1**	**29.0**	**4.4**	**240**

Dehumidification DP/MCDB and HR									Enthalpy/MCDB					
0.4%			1%			2%			0.4%		1%		2%	
DP	HR	MCDB	DP	HR	MCDB	DP	HR	MCDB	Enth	MCDB	Enth	MCDB	Enth	MCDB
12a	*12b*	*12c*	*12d*	*12e*	*12f*	*12g*	*12h*	*12i*	*13a*	*13b*	*13c*	*13d*	*13e*	*13f*
23.9	**19.1**	**28.2**	**23.2**	**18.3**	**27.4**	**22.6**	**17.6**	**26.8**	**78.8**	**31.5**	**75.8**	**30.2**	**73.0**	**29.1**

Extreme Annual Design Conditions

Extreme Annual WS			Extreme Max WB	Extreme Annual DB				n-Year Return Period Values of Extreme DB							
				Mean		Standard deviation		n=5 years		n=10 years		n=20 years		n=50 years	
1%	2.5%	5%		Max	Min	Max	Min	Max	Min	Max	Min	Max	Min	Max	Min
14a	*14b*	*14c*	*15*	*16a*	*16b*	*16c*	*16d*	*17a*	*17b*	*17c*	*17d*	*17e*	*17f*	*17g*	*17h*
9.1	**8.2**	**7.5**	**29.0**	**35.8**	**-19.4**	**1.9**	**5.1**	**37.2**	**-23.1**	**38.3**	**-26.1**	**39.3**	**-28.9**	**40.7**	**-32.6**

Monthly Design Dry Bulb and Mean Coincident Wet Bulb Temperatures

%	Jan		Feb		Mar		Apr		May		Jun	
	DB	MCWB	DB	MCWB	DB	MCWB	DB	MCWB	DB	MCWB	DB	MCWB
	18a	*18b*	*18c*	*18d*	*18e*	*18f*	*18g*	*18h*	*18i*	*18j*	*18k*	*18l*
0.4%	**17.8**	**14.3**	**20.8**	**13.9**	**26.0**	**16.0**	**29.3**	**18.3**	**31.3**	**21.1**	**34.1**	**22.7**
1%	**16.3**	**13.5**	**19.1**	**12.7**	**24.5**	**15.7**	**28.0**	**18.2**	**30.4**	**20.8**	**33.0**	**23.6**
2%	**14.8**	**11.7**	**17.3**	**11.7**	**22.7**	**14.6**	**26.6**	**17.6**	**29.5**	**20.2**	**32.3**	**23.3**

%	Jul		Aug		Sep		Oct		Nov		Dec	
	DB	MCWB	DB	MCWB	DB	MCWB	DB	MCWB	DB	MCWB	DB	MCWB
	18m	*18n*	*18o*	*18p*	*18q*	*18r*	*18s*	*18t*	*18u*	*18v*	*18w*	*18x*
0.4%	**36.3**	**24.8**	**35.2**	**24.4**	**33.4**	**22.6**	**28.3**	**19.5**	**23.7**	**16.4**	**19.8**	**15.4**
1%	**35.2**	**24.2**	**34.2**	**24.0**	**32.2**	**22.2**	**27.2**	**19.2**	**21.9**	**15.4**	**18.3**	**15.2**
2%	**34.2**	**24.3**	**33.2**	**24.0**	**31.1**	**22.0**	**26.0**	**18.5**	**20.8**	**15.0**	**17.0**	**14.2**

Monthly Design Wet Bulb and Mean Coincident Dry Bulb Temperatures

%	Jan		Feb		Mar		Apr		May		Jun	
	WB	MCDB	WB	MCDB	WB	MCDB	WB	MCDB	WB	MCDB	WB	MCDB
	19a	*19b*	*19c*	*19d*	*19e*	*19f*	*19g*	*19h*	*19i*	*19j*	*19k*	*19l*
0.4%	**15.1**	**17.4**	**15.2**	**18.7**	**18.0**	**23.4**	**20.2**	**26.1**	**23.7**	**28.6**	**25.8**	**31.4**
1%	**14.0**	**16.3**	**14.3**	**17.5**	**16.9**	**21.8**	**19.5**	**25.3**	**23.0**	**28.0**	**25.2**	**30.5**
2%	**12.6**	**14.6**	**13.2**	**16.0**	**15.9**	**20.7**	**18.6**	**24.2**	**22.3**	**27.1**	**24.6**	**29.9**

%	Jul		Aug		Sep		Oct		Nov		Dec	
	WB	MCDB	WB	MCDB	WB	MCDB	WB	MCDB	WB	MCDB	WB	MCDB
	19m	*19n*	*19o*	*19p*	*19q*	*19r*	*19s*	*19t*	*19u*	*19v*	*19w*	*19x*
0.4%	**26.6**	**33.2**	**26.3**	**31.8**	**24.5**	**29.7**	**21.5**	**24.7**	**18.0**	**21.0**	**16.5**	**19.0**
1%	**26.1**	**32.3**	**25.8**	**31.3**	**24.1**	**29.2**	**20.8**	**24.2**	**17.3**	**19.8**	**15.6**	**17.9**
2%	**25.7**	**31.7**	**25.4**	**31.0**	**23.7**	**28.6**	**20.1**	**23.8**	**16.5**	**19.2**	**14.6**	**16.5**

Monthly Mean Daily Temperature Range

Jan	Feb	Mar	Apr	May	Jun	Jul	Aug	Sep	Oct	Nov	Dec
20a	*20b*	*20c*	*20d*	*20e*	*20f*	*20g*	*20h*	*20i*	*20j*	*20k*	*20l*
8.8	**10.0**	**11.1**	**12.2**	**11.8**	**11.2**	**11.1**	**11.3**	**12.0**	**12.6**	**10.4**	**8.6**

WMO# World Meteorological Organization number
Lat Latitude, °
Long Longitude, °
Elev Elevation, m
StdP Standard pressure at station elevation, kPa
DB Dry bulb temperature, °C
DP Dew point temperature, °C
WB Wet bulb temperature, °C
WS Wind speed, m/s
Enth Enthalpy, kJ/kg
HR Humidity ratio, grams of moisture per kilogram of dry air
MCDB Mean coincident dry bulb temperature, °C
MCWB Mean coincident wet bulb temperature, °C
MCWS Mean coincident wind speed, m/s
PCWD Prevailing coincident wind direction, °, 0 = North, 90 = East

APPENDIX F

Data collection

A sample of the building simulation performance data. Those were collected and organized in preparation to test the optimization process. The data are for one zone from the month of July and were used to create figure 68.

Zone 1

Time	Zone occupancy	CFM	Total load BTU	Sensible load BTU	Latent load BTU
8:00:00 AM	50.28846842	2381.6521	63786.51589	53728.82221	10057.69368
8:15:00 AM	50.28846842	2416.630362	64580.14048	54522.4468	10057.69368
8:30:00 AM	50.28846842	2446.941662	65265.71727	55208.02358	10057.69368
8:45:00 AM	50.28846842	2474.051448	65878.51995	55820.82627	10057.69368
9:00:00 AM	50.28846842	2500.227172	66473.26964	56415.57596	10057.69368
9:15:00 AM	50.28846842	2527.001548	67077.59734	57019.90366	10057.69368
9:30:00 AM	50.28846842	2555.590989	67724.18243	57666.48874	10057.69368
9:45:00 AM	50.28846842	2586.188684	68412.41332	58354.71964	10057.69368
10:00:00 AM	50.28846842	2618.830317	69152.65628	59094.9626	10057.69368
10:15:00 AM	50.28846842	2653.226069	69932.7615	59875.06782	10057.69368
10:30:00 AM	50.28846842	2691.408611	70792.43426	60734.74057	10057.69368
10:45:00 AM	50.28846842	2728.460508	71627.41435	61569.72067	10057.69368
11:00:00 AM	50.28846842	2765.750858	72469.50815	62411.81446	10057.69368
11:15:00 AM	26.46761496	2509.165519	62032.15055	56738.62756	5293.522991
11:30:00 AM	26.46761496	2537.376307	62555.04474	57261.52174	5293.522991
11:45:00 AM	26.46761496	2568.525628	63248.14366	57954.62067	5293.522991
12:00:00 PM	26.46761496	2600.607697	63968.1377	58674.6147	5293.522991
12:15:00 PM	50.28846842	2927.849209	75969.20476	65911.51108	10057.69368
12:30:00 PM	50.28846842	2967.815638	77013.11227	66955.41859	10057.69368
12:45:00 PM	50.28846842	3003.399205	77810.46894	67752.77526	10057.69368
1:00:00 PM	50.28846842	3037.748805	78572.62938	68514.9357	10057.69368
1:15:00 PM	50.28846842	3071.479012	79322.25506	69264.56137	10057.69368
1:30:00 PM	50.28846842	3099.357551	79955.43313	69897.73945	10057.69368
1:45:00 PM	50.28846842	3131.262053	80686.93066	70629.23697	10057.69368
2:00:00 PM	50.28846842	3161.687785	81381.25236	71323.55868	10057.69368
2:15:00 PM	50.28846842	3190.608866	82035.50156	71977.80788	10057.69368
2:30:00 PM	50.28846842	3217.550226	82651.05283	72593.35915	10057.69368
2:45:00 PM	50.28846842	3246.811248	83270.12245	73212.42876	10057.69368
3:00:00 PM	50.28846842	3275.869837	83898.90762	73841.21393	10057.69368
3:15:00 PM	50.28846842	3303.590665	84528.38712	74470.69344	10057.69368
3:30:00 PM	50.28846842	3334.38202	85207.0779	75149.38422	10057.69368
3:45:00 PM	50.28846842	3356.34118	85772.4574	75714.76372	10057.69368
4:00:00 PM	50.28846842	3377.483126	86269.73455	76212.04086	10057.69368
4:15:00 PM	37.05466094	3139.75218	78481.20436	71070.27217	7410.932188
4:30:00 PM	37.05466094	3126.625087	77984.61911	70573.68692	7410.932188
4:45:00 PM	37.05466094	3129.490402	78052.03844	70641.10625	7410.932188
5:00:00 PM	37.05466094	3136.070958	78195.00452	70784.07233	7410.932188
5:15:00 PM	21.17409197	2766.871034	66932.064	62697.24561	4234.818393
5:30:00 PM	21.17409197	2741.835288	66128.4667	61893.6483	4234.818393
5:45:00 PM	21.17409197	2737.767866	66021.78027	61786.96188	4234.818393
6:00:00 PM	21.17409197	2741.012314	66090.84598	61856.02759	4234.818393

APPENDIX G

Optimization process results

January 21st different case analysis

The following is a case analysis for January 21st, when the baseline case scenario has a supply air temperature setpoint of 55F°. This case happens in some buildings, unlike the best practice that resets the supply air temperature to 65 F° in the winter season as the case that was discussed in chapter 5.

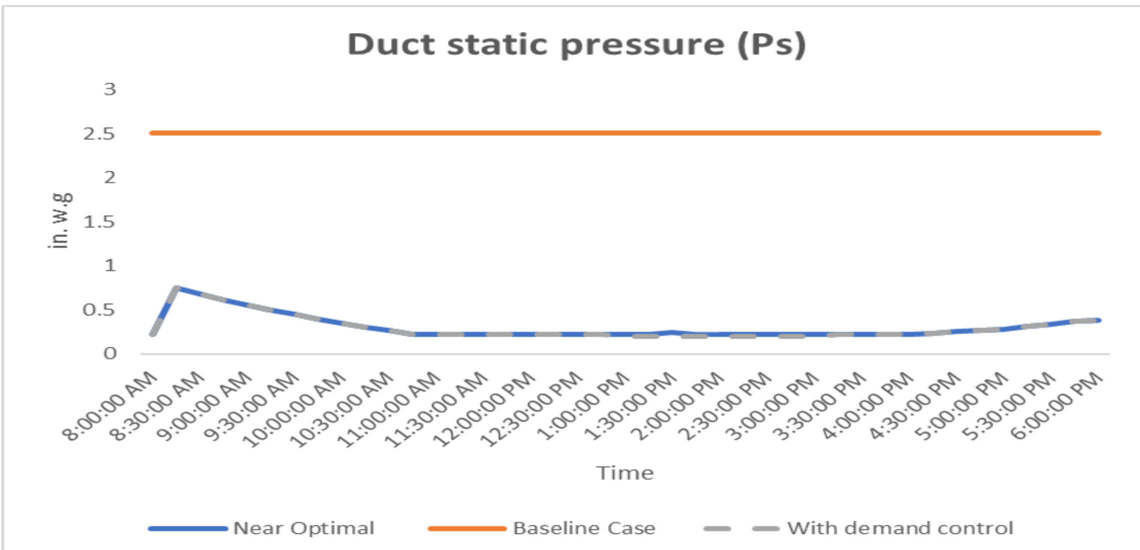

(A)

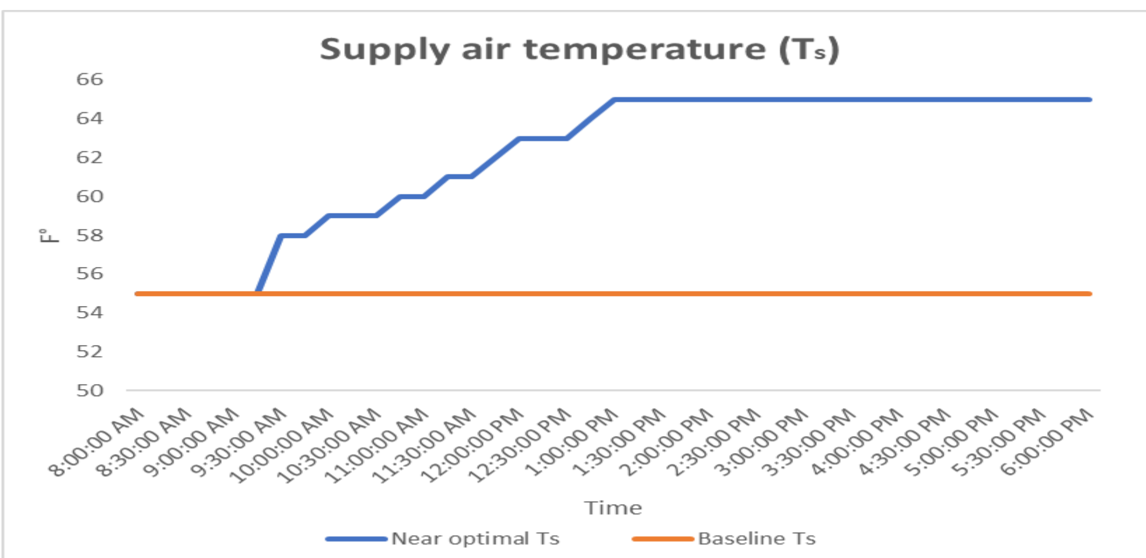

(B)

Figure 109. (A) near-optimal supply air temperature against the baseline case. (B) near-optimal duct static pressure against the baseline case.

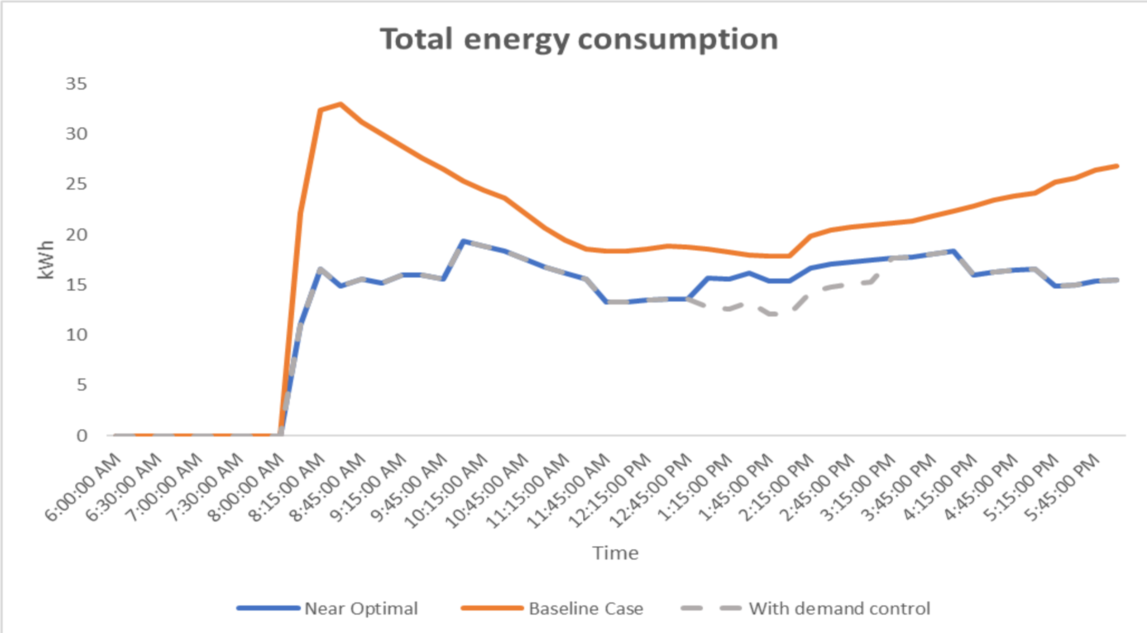

Figure 110. Total energy savings for January 21st. The total savings for the typical optimization case was 30%. While the total savings after implementing the demand control method increased to 32.6%.

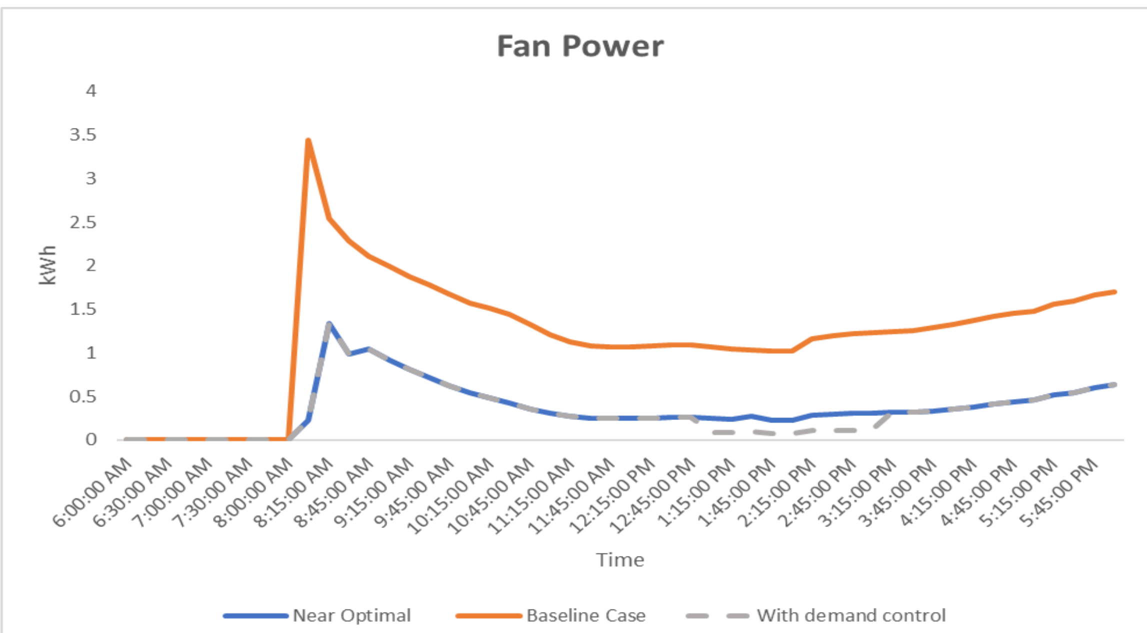

Figure 111. Fan power savings for January 21st. The total savings for the typical optimization case was 69%. While the total savings after implementing the demand control method increased to 71%.

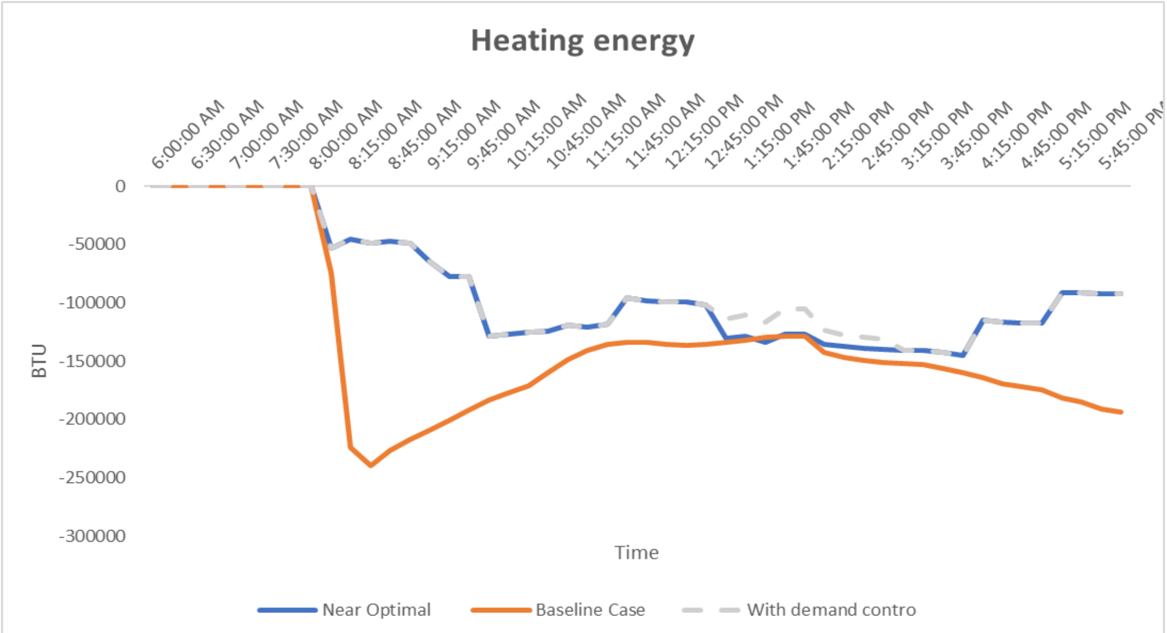

Figure 112. Heating energy savings for January 21st. The total savings for the typical optimization case was 33.7%. While the total savings after implementing the demand control method increased to 35.7%.

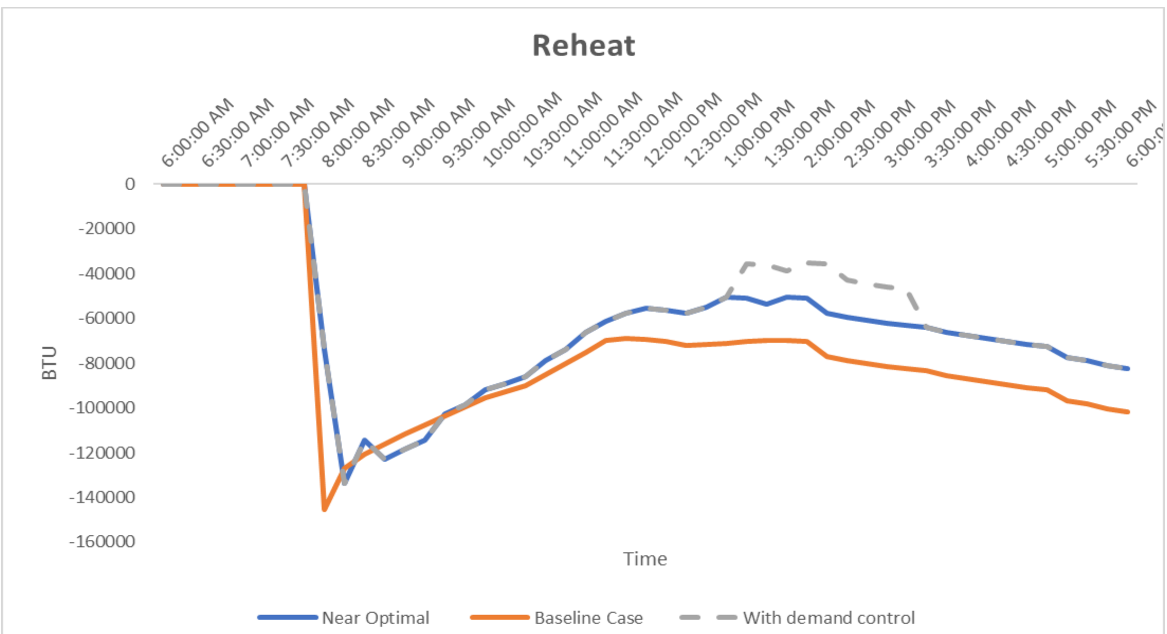

Figure 113. Reheat energy savings for January 21st. The total savings for a typical optimization case was 15.6%. While the total savings after implementing the demand control method increased to 19.6%.

APPENDIX H

Optimization process results

October 10th different case analysis

The following is a case analysis for October 10th, when the baseline case scenario has a supply air temperature setpoint of 55F^{o}. This case happens in some buildings, unlike the best practice that resets the supply air temperature in the spring and fall season, as the case that was discussed in chapter 5.

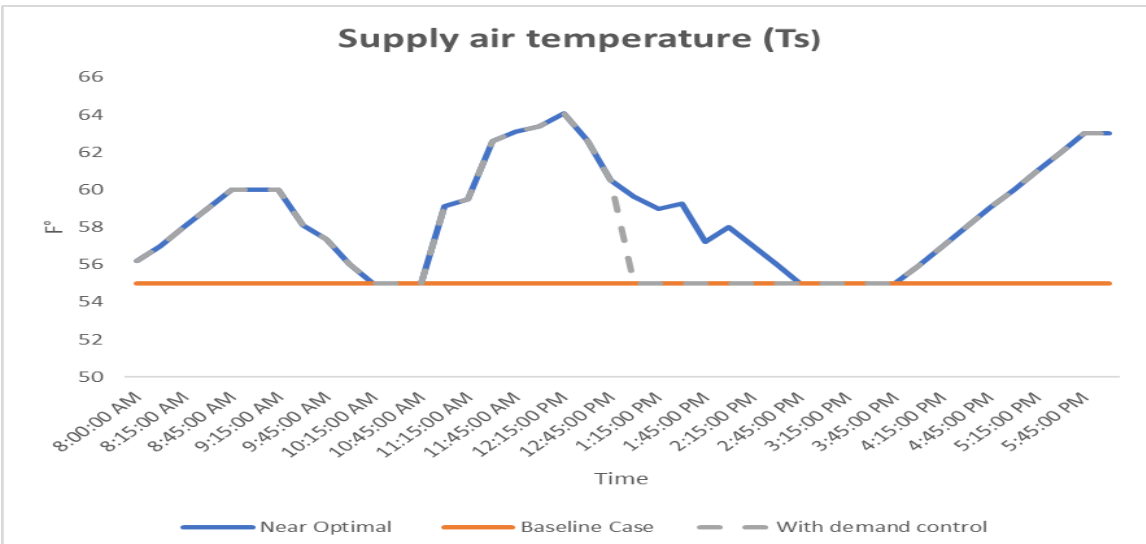

(A)

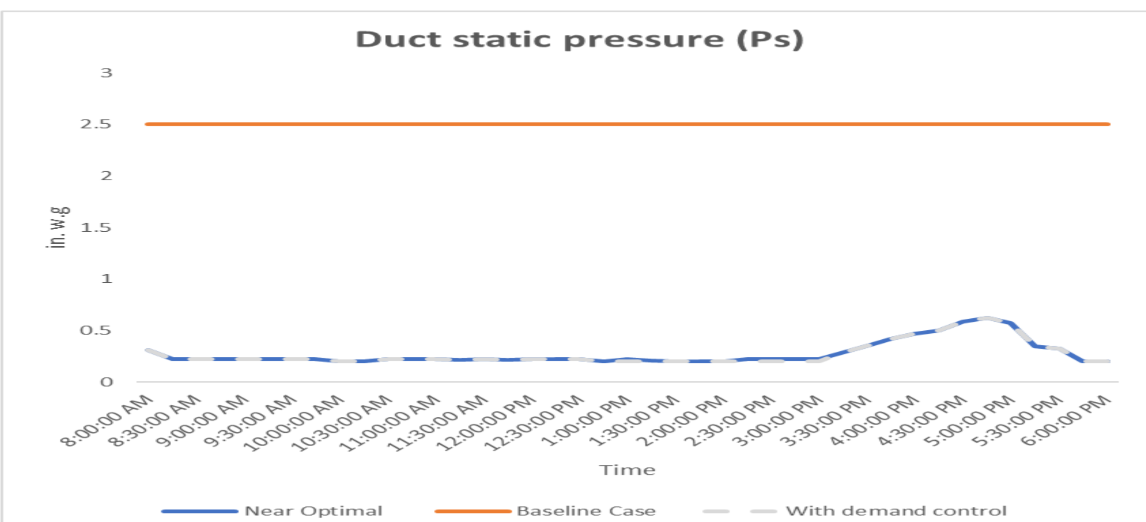

(B)

Figure 114. (A) near-optimal supply air temperature against the baseline case. (B) near-optimal duct static pressure against the baseline case.

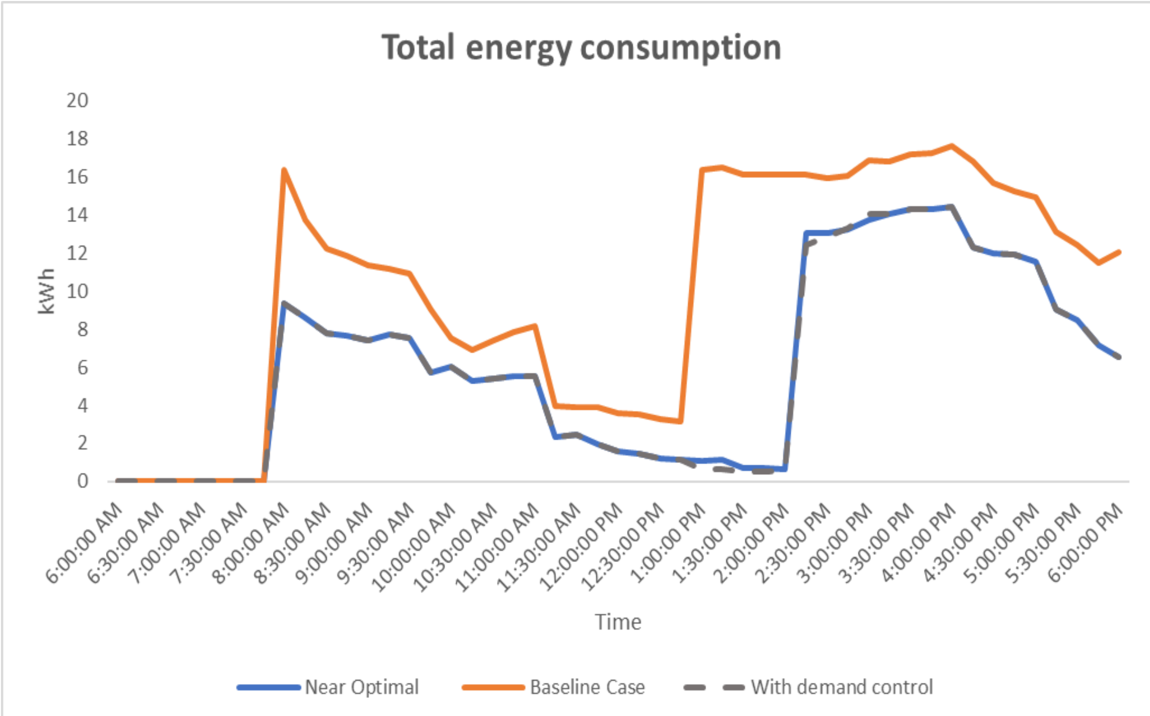

Figure 115. Total energy savings for October 10th. The total savings for the usual optimization case was 39%. While the total savings after implementing the demand control method increased to 40%.

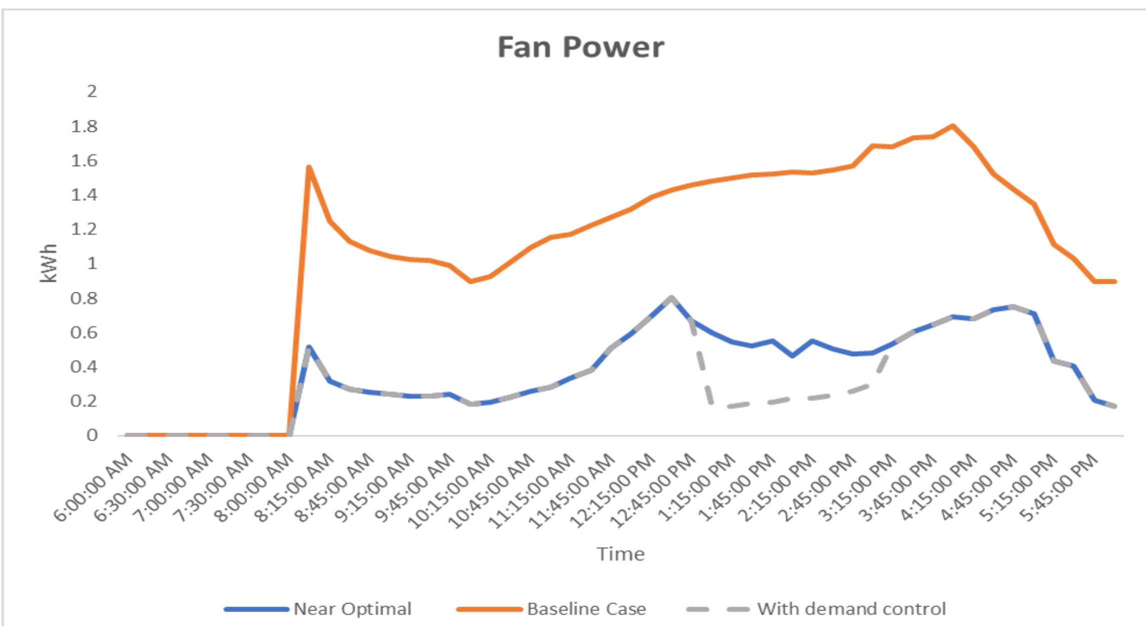

Figure 116. Fan power savings for October 10th. The total savings for the usual optimization case was 65%. While the total savings after implementing the demand control method increased to 75.5%.

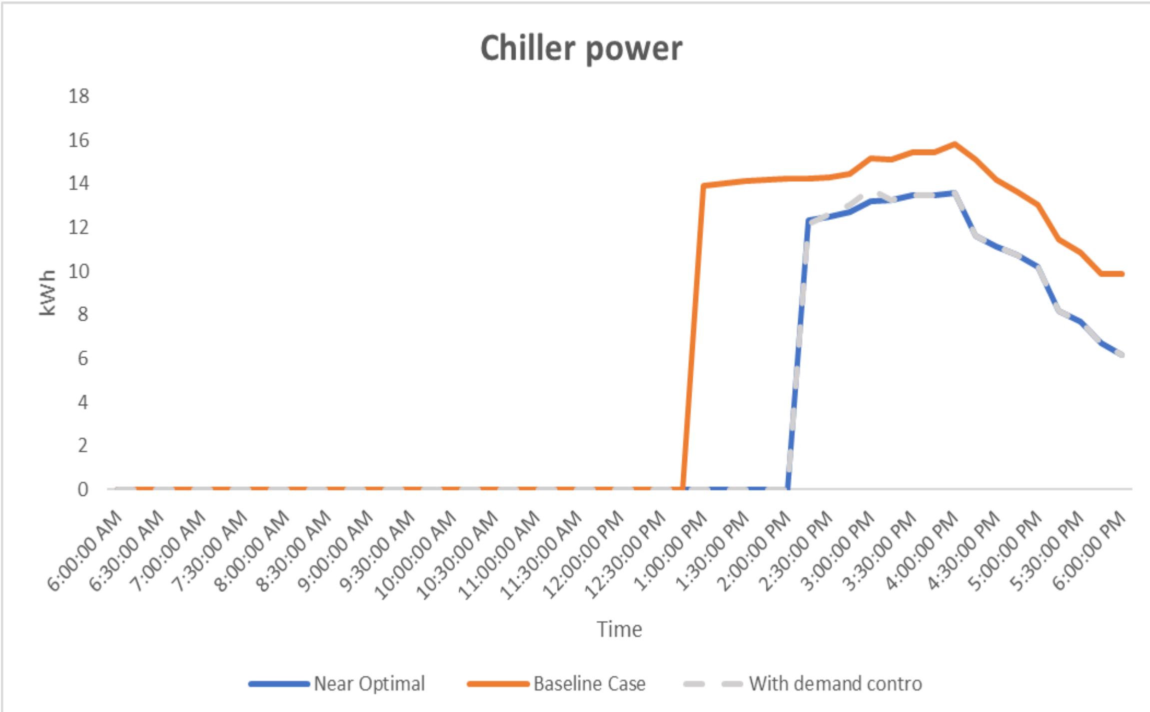

Figure 117. Chiller power savings for October 10th. The total savings for the usual optimization case was 38.6%. While the total savings after implementing the demand control method decreased to 38%.

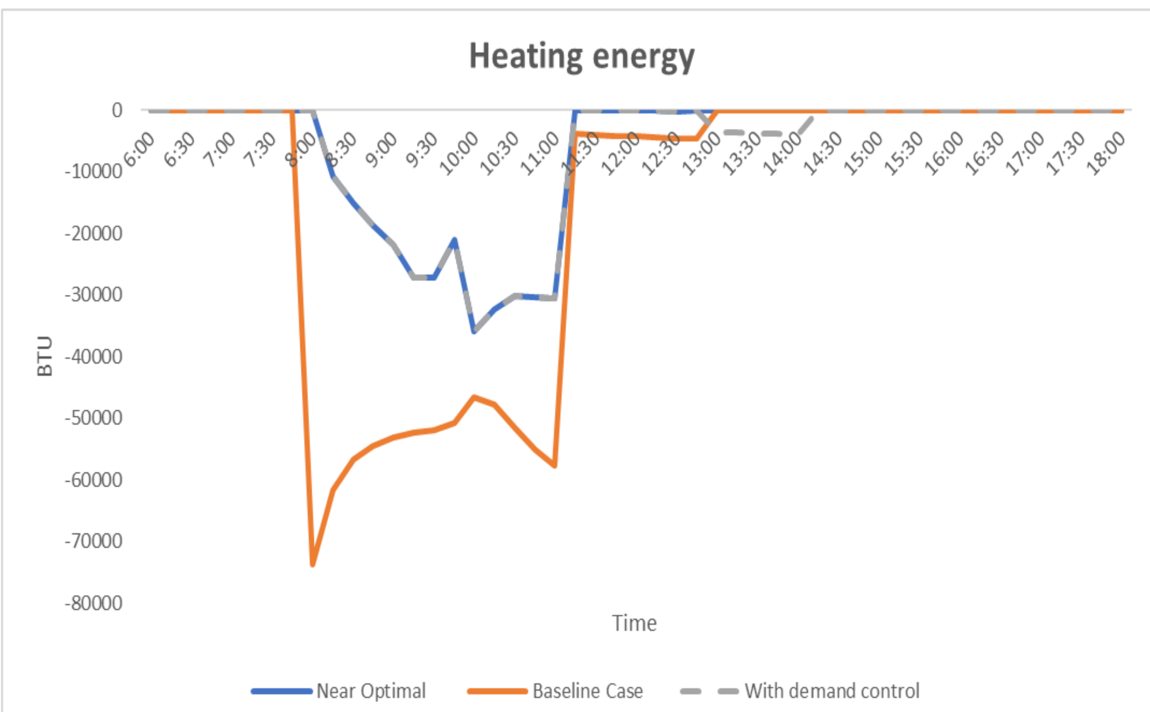

Figure 118. Heating energy savings for October 10th. The total savings for the usual optimization case was 59.4%. While the total savings after implementing the demand control method decreased to 57%.

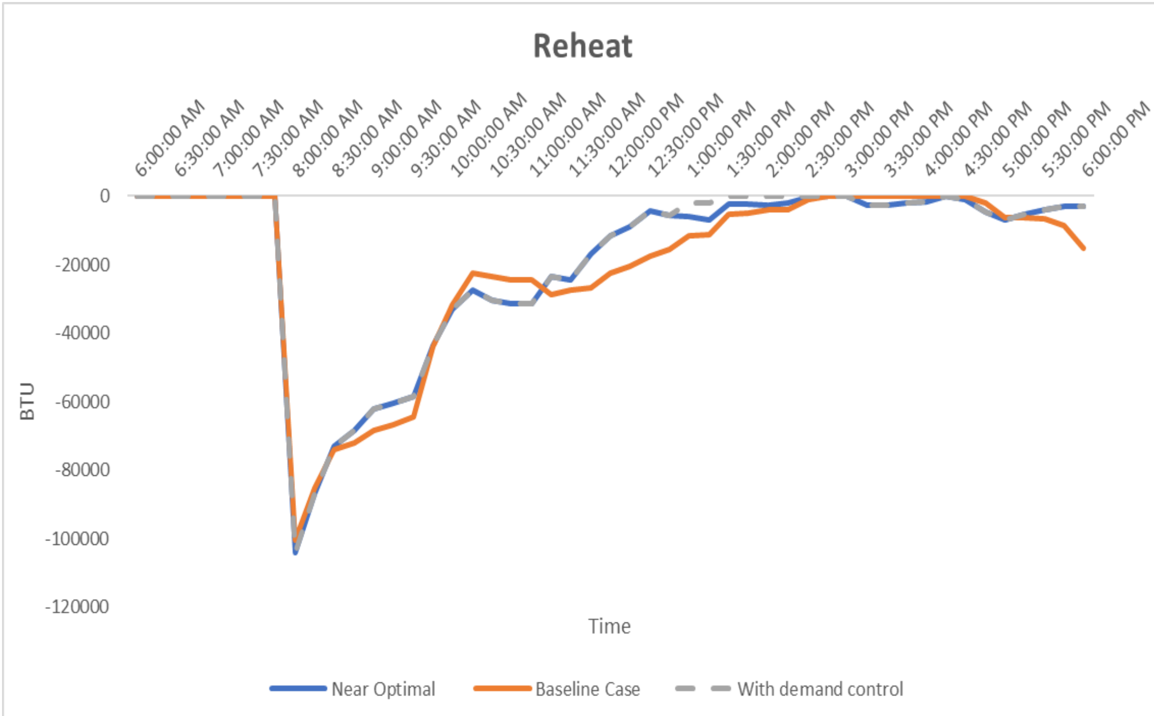

Figure 119. Reheat savings for October 10th. The total savings for the typical optimization case was 8.7%. While the total savings after implementing the demand control method increased to 10.7%.

APPENDIX I

Optimization process results

The following are the values for the system airflow rate for July 12th, represented in figure 72.

	Q_{sys} CFM		
Time	Near Optimal	Baseline Case	With demand control
8:00:00 AM	6335.3	4791.3	6335.3
8:15:00 AM	6611.3	4982.2	6611.3
8:30:00 AM	6830	5147.4	6830
8:45:00 AM	6243.3	5294.8	6243.3
9:00:00 AM	6414.2	5440.5	6414.2
9:15:00 AM	6239	5586.2	6239
9:30:00 AM	6401.4	5728.2	6401.4
9:45:00 AM	5860.2	5825.6	5860.2
10:00:00 AM	5926.8	5926.8	5926.8
10:15:00 AM	6008.6	6008.6	6008.6
10:30:00 AM	6095.2	6095.2	6095.2
10:45:00 AM	6143.6	6168.4	6143.6
11:00:00 AM	6230.9	6230.9	6230.9
11:15:00 AM	5791.9	5791.9	5791.9
11:30:00 AM	5820.8	5820.8	5820.8
11:45:00 AM	5898	5898	5898
12:00:00 PM	5986.3	5986.3	5986.3
12:15:00 PM	6548.9	6548.9	6548.9
12:30:00 PM	6643.7	6643.7	6643.7
12:45:00 PM	6735.5	6735.5	6735.5
1:00:00 PM	6875.7	6875.7	5978.9
1:15:00 PM	7041.8	7041.8	6123.3
1:30:00 PM	7206	7206	6266
1:45:00 PM	7290.5	7290.5	6339.5
2:00:00 PM	7336.8	7336.8	6379.8
2:15:00 PM	7373.3	7373.3	6411.5
2:30:00 PM	7391	7391	6426.9
2:45:00 PM	7526	7526	6544.4
3:00:00 PM	7714.7	7714.7	6708.4
3:15:00 PM	7258.2	7258.2	7258.2
3:30:00 PM	7450.6	7450.6	7450.6
3:45:00 PM	7837.5	7837.5	7837.5
4:00:00 PM	7926.6	7926.6	7926.6
4:15:00 PM	7772.3	7772.3	7772.3
4:30:00 PM	7712.7	7712.7	7712.7
4:45:00 PM	7674.2	7674.2	7674.2
5:00:00 PM	7644.3	7644.3	7644.3
5:15:00 PM	6956.8	6956.8	6956.8
5:30:00 PM	6834.4	6834.4	6834.4
5:45:00 PM	6778.4	6778.4	6778.4
6:00:00 PM	6734.4	6734.4	6734.4

APPENDIX G

Optimization process results

The following are the Supply air temperature reset calculations used to determine the supply air temperatures used for the baseline case at each timestep, as shown in figure 87.

Time	T_{out} in C°	RH%	T_{out} in F°		
10/10 07:00:00	7.2	80	44.96		
10/10 07:15:00	7.75	79.25	45.95	T_{out}<55	Then T_s =65
10/10 07:30:00	8.3	78.5	46.94		
10/10 07:45:00	8.85	77.75	47.93		
10/10 08:00:00	9.4	77	48.92		
10/10 08:15:00	10.375	75	50.675		
10/10 08:30:00	11.35	73	52.43		
10/10 08:45:00	12.325	71	54.185		
10/10 09:00:00	13.3	69	55.94	T_s=	62.03
10/10 09:15:00	13.875	66.75	56.975	T_s=	61.5125
10/10 09:30:00	14.45	64.5	58.01	T_s=	60.995
10/10 09:45:00	15.025	62.25	59.045	T_s=	60.4775
10/10 10:00:00	15.6	60	60.08	T_s=	59.96
10/10 10:15:00	16.275	58	61.295	T_s=	59.3525
10/10 10:30:00	16.95	56	62.51	T_s=	58.745
10/10 10:45:00	17.625	54	63.725	T_s=	58.1375
10/10 11:00:00	18.3	52	64.94	T_s=	57.53
10/10 11:15:00	18.575	51.25	65.435		
10/10 11:30:00	18.85	50.5	65.93		
10/10 11:45:00	19.125	49.75	66.425		
10/10 12:00:00	19.4	49	66.92		
10/10 12:15:00	19.7	47.75	67.46		
10/10 12:30:00	20	46.5	68		
10/10 12:45:00	20.3	45.25	68.54		
10/10 13:00:00	20.6	44	69.08		
10/10 13:15:00	20.725	43.25	69.305		
10/10 13:30:00	20.85	42.5	69.53		
10/10 13:45:00	20.975	41.75	69.755		
10/10 14:00:00	21.1	41	69.98		
10/10 14:15:00	21.375	40.25	70.475		
10/10 14:30:00	21.65	39.5	70.97		
10/10 14:45:00	21.925	38.75	71.465		
10/10 15:00:00	22.2	38	71.96	T_{out}>65	Then T_s =55
10/10 15:15:00	21.925	38.25	71.465		
10/10 15:30:00	21.65	38.5	70.97		
10/10 15:45:00	21.375	38.75	70.475		
10/10 16:00:00	21.1	39	69.98		
10/10 16:15:00	20.975	39.5	69.755		
10/10 16:30:00	20.85	40	69.53		
10/10 16:45:00	20.725	40.5	69.305		
10/10 17:00:00	20.6	41	69.08		
10/10 17:15:00	19.75	43.75	67.55		
10/10 17:30:00	18.9	46.5	66.02		
10/10 17:45:00	18.05	49.25	64.49		
10/10 18:00:00	17.2	52	62.96		

APPENDIX H

MATLAB

The following are the scripts developed for the integrated two-level optimization process using MATLAB.

Editor - C:\Users\rand_\Desktop\PhD degree\PhD thesis work\Thesis work after proposal\Optimization\MATLAB optimization\HVACSimulationModel.m

HVACSimulationModel.m | OptimizationProcess.m

```
function [Total,ChillerPower,FanPower,Reheat,Reheatz,qht,PowerPenalty,Constraint,Qz,DesignZone,Qo,Qv,Qsys,Tm]=HVACSimulationModel(Variables)
% Enter the loads qt, qs, ql for the number of zones
Loads=[-22267.15293 -12267.15293    -10000
-5120.646592    -13086.85605    -2000
-6359.469571    -8682.019879    -1200
-12258.48221    -16732.86704    -2000
-9693.55484 -8493.55484 -1200];

  % Enter Outside air conditions To, tw, td
OCond=[31.64,28.94,24.62];
DesignZone= [
   7.5000e+01   7.2000e+01   3674.624444   10588  50   6.0000e-02   5.0000e+00   1.0000e+00
   7.5000e+01   7.2000e+01   1937.609758   2232   10   6.0000e-02   5.0000e+00   1.0000e+00
   7.5000e+01   7.2000e+01   1426.535636   1413  6  6.0000e-02   5.0000e+00   1.0000e+00
   7.5000e+01   7.2000e+01   1412.67893   2232   10  6.0000e-02   5.0000e+00   1.0000e+00
   7.5000e+01   7.2000e+01   1630.106012  1413   6   6.0000e-02   5.0000e+00   1.0000e+00
   ];

% Enter design system parameters: Eff, C, Psd, Chillerdesign, L= % L pipe lenght ft, e=0.00015;
% %Pipe Roughness e it is 0.00015 for Steel, % N=10; %number of
% elbows/tees, DPch=4; %pressure drop across the chiller, Pipe Diameter,
% Gmax (Flow GPM),Water Diffrential Loop Pressure
DesignSystem=[
   7.0000e-01
   8.0000e-10
   2.5000e+00
   10.000e+01
   9.0000e+01
   1.5000e-04
   1.0000e+01
   4.0000e+00
   6.0000e+00
   5.0000e+02
   2.0000e+01];
% Those need to chnage based on each run
```

Editor - C:\Users\rand_\Desktop\PhD degree\PhD thesis work\Thesis work after proposal\Optimization\MATLAB optimization\HVACSimulationModel.m

HVACSimulationModel.m | OptimizationProcess.m

```
% Gmax (Flow GPM),Water Diffrential Loop Pressure
DesignSystem=[
   7.0000e-01
   8.0000e-10
   2.5000e+00
   10.000e+01
   9.0000e+01
   1.5000e-04
   1.0000e+01
   4.0000e+00
   6.0000e+00
   5.0000e+02
   2.0000e+01];
% Those need to chnage based on each run
```


```
S3=1;
Schedule=[
     100     1     S3
     100     1     S3
     100     1     S3
     100     1     S3
     100     1     S3
   ];

MinFlow=Variables(3:7);
DesignSystem(2)=4.5/(sum(DesignZone(:,3)))^2;
[FanPower,Reheat,Reheatz,qht,qct,Qw,Twr,PowerPenalty,Constraint,Constraintz,Qz,Qo,Qv,Qsys,Tm]=VAVSystemModel(Variables,Loads,OCond,Schedule,De
format shortE
[FanPower,Reheat,qct];
Tw=45;
Tc=85;
[~,ChillerPower,~]=ChillerModel(qct,Tw,Tc,DesignSystem);
F=0.4; % FACTOR from gas to electric equivalent
Totalcost=(ChillerPower+FanPower)*0.10+((abs(Reheat)+abs(qht))/100000)*0.85+PowerPenalty;
Total=Totalcost/0.10;
end
```

Editor - C:\Users\rand_\Desktop\PhD degree\PhD thesis work\Thesis work after proposal\Optimization\MATLAB optimization\OptimizationProcess.m

HVACSimulationModel.m | OptimizationProcess.m

```
function OptimizationProcess()
var=7;
%%----------Generation G=10 65 2.5 0.3 0.3 0.3 0.3 0.3       55 2.5 0.2 0.2 0.2 0.2 0.2
options = gaoptimset('Generations',2500,'PopulationSize',1000);
[x,fval1,exitflag,output,population]=ga(@HVACSimulationModel,var,[],[],[],[],[59 0.2 0.2 0.2 0.2 0.2 0.2]',[65 2.5 0.3 0.3 0.3 0.3 0.3]',[],opti
[Total,ChillerPower,FanPower,Reheat,Reheatz,qht,PowerPenalty,Constraint,Qz,DesignZone,Qo,Qv,Qsys,Tm]=HVACSimulationModel(x);
MinFlow=Qz'./DesignZone(:,3);
MinFlow(Reheatz'>=0)=0.99;x
OutputsEnergy=[Total-PowerPenalty,ChillerPower,FanPower,Reheat,qht,PowerPenalty,Constraint]
OutputsPerformance=[Qz,Qo,Qv,Qsys,Tm]
end
```